

POLITECNICO DI MILANO
FACOLTA' DI INGEGNERIA DEI SISTEMI
CORSO DI LAUREA SPECIALISTICA IN INGEGNERIA GESTIONALE



**Control Gap analysis in an assembly system
using Remote Laser Welding**

Relatore: Chiar.mo Prof. Tullio Tolio

Candidati: Valentina Menegatti 734161
Silvia Sadocco 736121

Anno Accademico 2009-2010

Alle nostre mamme, papà, sorelle.

Abstract

Dimensional variations of zinc coated sheet metal parts is a relevant problem in manufacturing process, especially during the joining operation with a Remote Laser Welding system. This issue requires a tight part-to-part gap control to ensure a good quality of final product. The remote laser technology needs for constricted tolerance limits in the gap between overlapped parts: in fact the lower tolerance is aimed to avoid porosity problem, caused by the zinc vapour escape during the welding, meanwhile the upper limit must be respected to obtain the metal fusion between parts. This work presents a methodology about the Selective Assembly, in which parts are previously selected and coupled, in order to reduce the gap problem. The proposed approach to evaluate the goodness of part-to-part joining is mainly based on a criterion to determine the easiness of parts' fitting. A Similarity Analysis is a valid solution to find the best predictor of a good joining. After a robust assessment about a set of indicators chosen for the analysis, the best one is applied to classify parts in different groups; the obtained clusters will be used for the selective assembly strategy.

The research about the similarity analysis has been carried on in the International Digital Laboratory of Warwick University (UK). A typical sector affected by this matter is the Automotive: remote laser welding is widely used in car components assembly line. A collaboration with Fiat-Comau and CRF (Centro Ricerche Fiat) allowed the real case treatment through a development of the complete approach on Cassino assembly line.

Sommario

Il seguente lavoro di tesi è finalizzato all'implementazione di un metodo per la risoluzione del problema di giunzione tra due parti metalliche bi-zincate attraverso un sistema di saldatura laser remota.

La saldatura laser remota è una recente applicazione introdotta in diversi settori, tra cui principalmente nell'automotive, nel navale e nell'aerospaziale. Infatti tra i principali vantaggi che tale tecnologia offre è la capacità di lavorare a distanza sulle parti, oltre alla flessibilità delle lavorazioni, accessibilità ai componenti e riduzione dei tempi di lavorazione e dell'ingombro spaziale nel layout di stabilimento. La sua principale applicazione risiede nella saldatura di componenti di veicoli automotive, come i diversi sottogruppi costituenti una portiera dell'autoveicolo.

In questo caso la saldatura non sarà effettuata in continuum lungo un'intera direttrice di saldatura lungo tutta la lunghezza dell'aletta del componente, difatti saranno presenti degli "stitches" sulla parte saldata, ovvero tratti di massimo 2cm in cui avviene la fusione del metallo tra due lamiere. La qualità di saldatura tra due componenti verrà quindi valutata ispezionando la buona fusione di materiale nei giunti, valutando visivamente l'apparenza del giunto e testando la resistenza dello stesso sottoponendolo ad una prova di distruzione. Spesso il giunto (lo stitch) può presentare difetti superficiali diversi e difetti di tenuta.

Infatti, un rilevante limite apportato dal suo utilizzo per ottenere una saldatura ottimale tra due lamine è la richiesta di un elevato controllo della distanza tra due parti sovrapposte che devono essere saldate. Tale controllo consiste nel rispetto di limiti di tolleranza molto ristretti che determinano la qualità del prodotto finale in termini di buona saldatura. Infatti, è necessario garantire il limite inferiore per evitare problemi di soffiatura e porosità, causate dall'evaporazione dello strato di zinco, determinato dalle elevate temperature in gioco durante il processo di saldatura stesso. Dall'altro lato la tolleranza superiore deve essere monitorata, affinché avvenga la fusione del metallo tra le due parti nei punti di giunzione. La soluzione a questo problema è attualmente

studiata e analizzata attraverso la progettazione del sistema di fissaggio e la selezione dei parametri tecnici proprio della tecnologia laser remota.

Per quanto riguarda il primo aspetto, l'ottimizzazione del sistema di fissaggio è 1 fase onerosa in termini di tempo, quindi sarebbe ottimale la sua flessibilità al variare dei diversi lotti di produzione che arrivano alla fase di saldatura senza apportare continue modifiche e aggiustamenti ad esso, con preventivo studio e analisi della particolare situazione una volta che questa si presenti. Per quanto fondamentale sia il sistema di fissaggio nella sua funzione di bloccare e tenere unite insieme le due lamiere da saldare, non sempre è possibile garantire che tra 1 tassello e l'altro del sistema di fissaggio il "gap" tra le parti sia contenuto nell'intervallo di accettazione mentre nei punti in cui i tasselli esercitano una pressione di bloccaggio, in quell'area precisa si può osservare il sicuro anche se forzato rispetto dei limiti di tolleranza.

Tale problema si manifesta principalmente a causa della variabilità di forma che le parti presentano dopo il processo manifatturiero (stampaggio e lavorazioni successive ad esso), che introduce difetti e scostamenti del profilo dal nominale. Le parti in esame saranno parti non perfette, anche se conformi alle specifiche di stampaggio. La loro variabilità influisce soprattutto nell'accoppiamento di due componenti da assemblare che, presentando andamenti dei profili diversi, possono comportare delle zone in cui la distanza tra loro sia fuori dai limiti di tolleranza richiesti, quindi troppo ampia per permettere la saldatura o troppo ristretta affinché questa avvenga con le corrette proprietà meccaniche.

Su codesta casualità da cui sono affette le lamine metalliche si potrebbe agire ottimizzando i parametri del processo di stampaggio. Ma una valida ed intelligente alternativa può esser rappresentata dalla minimizzazione della casualità dell'accoppiamento tra due parti processate. Il modo e la frequenza d'arrivo delle parti al sistema è del tutto casuale, quindi potrebbero presentarsi accoppiamenti la cui saldatura è buona e accoppiamenti casuali il cui accoppiamento porti a una scarsa qualità di saldatura.

Quindi una valida alternativa al controllo della variabilità sul profilo delle parti è rappresentata dal monitorare il processo d'arrivo delle parti e creare a priori degli accoppiamenti in grado di soddisfare un buon livello di qualità di saldatura da inserire nella cella del Remote Laser Welding. In questo modo si forza il sistema a saldare parti già definite e prestabilite come buoni accoppiamenti prima dell'entrata nella cella. Questo ovviamente viene effettuato a regime analizzando il profilo delle parti in arrivo alla fase di saldatura.

L'idea principale, su cui è basato questo lavoro, è quella di agire quindi anche a monte della fase di fissaggio, in quanto in caso contrario si richiederebbe una riconfigurazione

poco flessibile e onerosa in termini di tempo.

Una buona strategia può essere rappresentata da un approccio di Selective Assembly per ridurre la variabilità negli accoppiamenti casuali che si creano all'esterno della cella di saldatura. Tale approccio permette infatti di suddividere i componenti da assemblare in diversi gruppi, ognuno caratterizzato da una precisa specifica di forma; in questo modo, parti appartenenti alla stessa classe, possono essere selezionate insieme per poi essere accoppiate e conseguentemente assemblate.

La classificazione delle parti ha richiesto l'utilizzo di un metodo in grado di discriminare la caratteristica geometrica del profilo che descrive le diverse parti. Sono state analizzati a tale proposito due set di misurazioni appartenenti a due tipologie di parti diverse : in particolare i dati a disposizione si riferiscono a 12 misurazioni superficiali relative a 6 componenti metallici chiamati Plates (piatti, lamine lineari come barre metalliche) e di 6 componenti chiamati C-Shaped Channel (parti metalliche a forma complessa di "C").

Tali misurazioni, disponibili presso lo stabilimento UK della Warwick University in Inghilterra, sono state acquisite tramite uno strumento di scansione ottica in grado di rilevare una nuvola di punti x,y,z della superficie da analizzare. Tali parti rappresentano dei "tester" su cui sviluppare e applicare la classificazione basata sulla caratteristica del proprio profilo.

Per determinare un criterio di classificazione adeguato basato sulla forma della superficie dei componenti metallici è necessario considerare un indicatore in grado di *quantificare la similarità* tra due parti, in modo da predire la bontà di saldatura. Con tale assunzione, parti da saldare come un Channel e un Plate simili tra loro nel loro andamento di forma avranno una buona probabilità di saldatura in quanto il "good fitting" tra questi due sarà più semplice da ottenere rispetto a due parti con profili poco accoppiabili.

Il vantaggio principale che dovrà apportare lo studio degli indici è una **quantificazione** della similarità tra due profili da accoppiare. Un set di indicatori è stato quindi valutato presso l'International Digital Laboratory della Warwick University (UK): da tale analisi è emerso il più adeguato a tale proposito e utilizzato per lo studio di similarità , volto alla classificazione delle parti. Una volta selezionati gli indicatori più opportuni al nostro caso di studio, individuati i relativi principi base di funzionamento, i vantaggi e i limiti di ognuno di essi, questi sono stati applicati sulle misurazioni dei profili delle parti.

Dall'applicazione degli indici sul set di dati sono stati ottenuti dei risultati quantitativi. La validità e la bontà di ciascun indicatore è stata valutata confrontando i risultati

in output di ciascuno di essi con un altro set di dati a disposizione, sempre relativi alle medesime parti analizzate, ma contenenti un'altra tipologia di informazione : la misura del "Gap" tra le diverse parti accoppiate (ogni plate accoppiato con ogni channel) per un totale di 36 combinazioni. Questa misurazione sperimentale del Gap reale esistente tra le parti lungo la loro intera lunghezza è stata necessaria per valutare se quanto calcolato dall'indice in termini di "goodness of fitting" fosse rispecchiabile nella realtà .

Tramite quest'analisi è stato possibile effettuare una scrematura degli indici affidabili o no valutando l'esattezza dei risultati, da qui la possibilità di selezionare l'indicatore più robusto, attraverso cui successivamente sarebbe stato possibile implementare la classificazione delle parti in cluster diversi.

L'indicatore selezionato in quanto coerente con i risultati sperimentali, riesce a decomporre la superficie di ciascuna parte analizzata in un insieme di forme d'onda coseniche modulate diversamente in ampiezza. Ovviamente l'applicazione dell'indicatore non viene effettuata sull'intera parte ma solamente sulla limitata zona su cui agirà il fascio laser.

Attraverso tale analisi modale delle parti stesse si caratterizza la decomposizione del profilo in forme d'onda semplici e periodiche chiamate "modes". La comunanza di una certa percentuale di modes presenti in una coppia di parti, se considerata soddisfacente, ne determina il valido accoppiamento e quindi la classificazione delle stesse parti nello stesso gruppo. Parti classificate nello stesso storage, se accoppiate tra loro, portano ad ottimi accoppiamenti per cui il valore qualitativo di saldatura risulta elevato. Tramite tale indicatore quindi è stato possibile discriminare le coppie ottimali e accoppiamenti da evitare.

Per stimare l'efficacia del metodo nel individuare i buoni dai cattivi accoppiamenti è stata instaurata una collaborazione con il Centro Ricerche Fiat, grazie al quale è stato possibile simulare il comportamento e il ritorno elastico delle parti saldate analizzando tutti i possibili accoppiamenti sul set di dati UK, tramite un'analisi agli elementi finiti (FEM) sviluppata dal Centro stesso.

A fronte della suddivisione in classi ottenuta, una valutazione qualitativa sull'effettivo miglioramento della qualità di saldatura raggiunto post-classificazione è stata effettuata rispetto al caso base. Questo risultato è stato raggiunto tramite una ricerca iterativa euristica, valutando ad ogni step l'incremento percentuale qualitativo raggiunto dettagliando in modo sempre maggiore la classificazione in un maggior numero di sotto-classi.

Successivamente questo lavoro di ricerca è stato implementato in un vero caso industriale, considerando la linea di assemblaggio di componenti automotive presso lo

stabilimento di Fiat-Comau (Cassino). In particolare è stata analizzata la linea di laminazione portiere dell'impianto di COMAU, concentrando l'analisi sulla fase di saldatura dei sottogruppi costituenti tali portiere.

Dopo un'accurata analisi delle metodologie utilizzate in COMAU per ovviare i problemi presenti nella saldatura di lamine bi-zincate, è stato applicato tale approccio di Selective Assembly utilizzando la Similarity Analysis su un set di scansioni relative a due tipici componenti delle portiere delle automobili. Sono stati selezionati questi due precisi elementi in quanto il loro accoppiamento in saldatura risulta particolarmente critico e soggetto al problema del controllo del Gap.

A tale proposito sono state recuperate 8 misurazioni di ciascun componente studiato, sempre sotto forma di nuvola di punti, appartenenti a lotti diversi prodotti in turni di lavorazione differenti e l'applicazione dell'algoritmo sarà limitata alle zone di saldatura delle parti.

Successivamente allo stesso modo verrà presentata la classificazione in cluster di tali componenti automotive dopo la valutazione iterativa del miglioramento qualitativo indotto dall'introduzione di classi maggiormente dettagliate, e verranno proposte le eventuali modifiche di cui tener conto nella cella di saldatura per applicare la Selective Assembly strategy.

Contents

1	Problem Statement	1
1.1	Generality	2
1.2	Selective Assembly for parts	6
1.3	Similarity analysis between parts	7
1.4	Assembly System Reconfiguration: a case study	8
1.5	Aim of the analysis	9
1.6	Summary of the work	10
2	Introduction to Remote Laser Welding	13
2.1	Remote Technology evolution	13
2.2	History and Definition	14
2.3	System Technology	15
2.3.1	Physical Principles of Laser Radiation	15
2.3.2	Intention and Benefits of Remote Technology	18
2.3.3	Remote Processes	21
2.4	Applications	25
2.4.1	Automotive sector	26
2.4.2	Other sectors	27
2.5	Literature review for Remote Laser Welding	27
3	Similarity Analysis	31
3.1	Aim of the analysis	32
3.2	Experimental Data	33
3.2.1	Gap Measurements	34
3.2.2	The output of the gap analysis	38
3.2.3	Surfaces Measurements Data	39
3.3	Similarity analysis for the part-to-part control gap in a RLW	46

3.3.1	Similarity analysis methods	47
3.3.2	Similarity index based on RLW algorithm	48
3.3.3	Index descriptions	55
3.3.4	Consideration from the analysis	56
3.3.5	Correlation Index	60
3.3.6	Shape Distribution Index	65
3.3.7	SMA index	71
4	Statistical modal Analysis based on Discrete Cosine Transformation	73
4.1	Purpose of the SMA	74
4.2	SMA method	76
4.3	Index Visual Interpretation	79
4.4	Discrete Cosine Transformation	80
4.4.1	DCT and DFT methods	82
4.5	The SMA indicator	87
4.6	Results and Index Assessment	91
4.7	Parts Classification through SMA Analysis	99
4.7.1	Classification through Shared Modes	103
4.7.2	Final classification configuration	107
4.8	Non parametric Test	109
4.8.1	Sample data	109
4.8.2	Kolmogorov-Smirnov Test	110
4.8.3	Power test of Kolmogorov-Smirnov	112
4.9	FEM Analysis	112
4.9.1	FEM modeling	118
5	Selective assembly	121
5.1	Selective assembly for mating parts	122
5.2	Literature review for matching parts	123
5.2.1	The optimal binning Strategies	124
5.2.2	When distributions differ by a scale parameter	126
5.2.3	Non equal partition probabilities	127
5.2.4	Conclusion	127
5.3	Classification of parts	128
5.3.1	Analysis of results	135

6	Case study: COMAU	137
6.1	COMAU	137
6.2	COMAU products	138
6.2.1	3D remote laser welding system : AGILASER and SMARTLASER	140
6.3	COMAU process	148
6.4	COMAU-CASSINO productive site organization	149
6.5	COMAU Assembly system	150
6.6	The SMARTLASER application: Car doors steel bodywork	152
6.6.1	Door car loading sequence in FIAT-COMAU Group	152
6.7	Part-to-part gap control method	156
6.7.1	Dimpling design	157
6.7.2	Fixture design	160
6.8	Laser welding quality control	165
6.8.1	Visual Exam	165
6.8.2	Micrographic exam	167
6.8.3	Unbottomed test	167
6.8.4	Welding stitches locations	172
6.9	Aim of the work	174
6.9.1	Similarity Approach on COMAU System	175
6.9.2	Selected components for the case study	175
6.10	Similarity Analysis application on Comau parts	179
6.10.1	SMA results	182
6.10.2	The iterative classification for COMAU components	194
6.10.3	Conclusions	195
7	Conclusions	197
7.1	Future works	198
A	SMA code	203
B	Results correlation analysis	209
C	Results from shape distribution analysis	211
D	COMAU iterative classification	215
E	Results from FEM analysis by CRF	219

List of Figures

- 1.1 Remote Laser Welding (RLW) system 3
- 1.2 Requirements of the gap tolerance 5

- 2.1 Guideline for the system technology in remote applications 15
- 2.2 Reduction of the focal diameter and enlargement of the focal length by
increasing the beam quality 16
- 2.3 beam deflection by a tilting mirror and displacement of the focus spot . . 19
- 2.4 Heat induced distortions at remote laser cutting; thermal camera and
distortion measurement: unoptimized (left) and optimized (right) 20
- 2.5 Load optimized weld pattern 20
- 2.6 Remote laser beam welding of parts with limited accessibility to the pro-
cessing zone 21
- 2.7 Remote laser production unit: Segregation of the optics and the shielding
gas supply 22

- 3.1 Testing parts shapes 33
- 3.2 Gap Representation 35
- 3.3 Parts Reference System for Gap Measurements 35
- 3.4 Clamps positioning on the right side 36
- 3.5 International Digital Lab of University of Warwick clamping system . . . 37
- 3.6 Reference axes used for measurement data and surfaces shape 40
- 3.7 Axis origin 42
- 3.8 The deformation of the corner not considered for the welding area delim-
itation 43
- 3.9 Frontal profile of parts affected by typical deformations impressed by
shearing 44
- 3.10 Frontal profile of parts affected by typical deformations impressed by
shearing 45

3.11	Imperfection of parts causing the gap	47
3.12	Alignment of parts: (a) not comparable points, (b) comparable points . . .	49
3.13	Scheme of transformation permitted by interpolation	50
3.14	Synthesis for the measured points	51
3.15	Balance approach	54
3.16	A sketch of result table (a)	58
3.17	A sketch of result table (b)	59
3.18	Variation problem of the correlation	61
3.19	G/T Ratio Gap Measurements	62
3.20	Correlation values for the best and worst combinations	63
3.21	Absent correspondence between correlation index and Gap measurements	64
3.22	best couples between UK-parts	70
3.23	Worst couples between UK-parts	71
4.1	Pareto diagram	78
4.2	Error Modes Creation	79
4.3	The original sample is moved of half period on late and the total of the mirrored samples are doubled.	84
4.4	Efficiency representation of signals for FFT and DCT	85
4.5	Mean error square between DFT and DCT	86
4.6	Recomposition of part through modes in fft and dct	87
4.7	frequency output example	88
4.8	Positive and negative phase example	89
4.9	Single modes and sum of them	89
4.10	Sum of modes and part plot	90
4.11	Profiles with different signs and same value	91
4.12	Profiles with equal sign and different magnitude	91
4.13	Profiles with similar magnitude module value and different sign	92
4.14	the 7 best pats coupling combinations (blue-coloured)	93
4.15	6 worst combinations	95
4.16	P1-C5 couple, one of the most promising one confirmed by SMA index and Gap Measurements Analysis with G/T Ratio value equal to 1 (number of points with distances inside the tolerances)	96
4.17	The worst coupling P2-C6 with G/T ratio value equal to 0,26666	97
4.18	P1-C1 coupling having G/T ratio equal to 1 (best value)	98
4.19	Final SMA complete table	99

4.20	Presence of a lot of modes at the same importance	100
4.21	Presence of one dominant mode and other negligible modes	101
4.22	Evidently different shape distribution	101
4.23	Similar shape distribution	101
4.24	Plate 2 elimination from the analysis	104
4.25	Plate 2 elimination from the analysis	105
4.26	The only two parts having as secondary dominant mode C(1,2): Plate 6 and Channel 1	106
4.27	The only two parts having as secondary dominant mode C(3,1): Plate 6 and Channel 3	106
4.28	Parts with C(5,1) as second dominant mode	107
4.29	Parts with C(2,1) value characterizing more than 70% of the part surfaces	108
4.30	Classification in Buffer for the 12 sample parts	108
4.31	STL data format for the channel	113
4.32	STL data format for the plate	113
4.33	P1-C5 fitting estimated through SMA	115
4.34	P2-C6 fitting estimated through SMA	115
4.35	Plate 1- Channel 5, FEM spring-back range [0,612; -0,3541]	116
4.36	Plate 2- Channel 6, FEM spring-back range [1,012;-2,359]	117
4.37	Parts' variation in C-shape channels	120
4.38	Parts' variation in bottom plates	120
5.1	Scheme of the iterative method to determine the number of groups	129
6.1	Simple scheme of COMAU activities	139
6.2	Application fields of laser spring	140
6.3	Workspace of typical CO ₂ laser system	141
6.4	AGILASER system head welding and fixturing system	142
6.5	Peculiar parameters of the motors which let the AGILASER optical sys- tem components make translations and rotations(focusing lent and second mirror)	142
6.6	End-effector translations along X, Y,Z axis, mobile-mirror rotation around X axes and translation of the optic along Z axes	143
6.7	Functioning scheme of a typical AGILASER station	144
6.8	Laser source outline	146
6.9	Optical components(optic n ^o 1 and n ^o 2)	147
6.10	Work volume described using both the possible scanning mirror rotations	147

6.11 Comparison between two different quality beams generated by two different laser source	148
6.12 Layout of the assembly door in Cassino (Italy)	150
6.13 Car's door inner frame loaded by an operator	153
6.14 Reinforces and components mounted on the geometrical gripper	154
6.15 components door loaded on a geometrical gripper for positions maintaining	154
6.16 Scheme Operation 4	155
6.17 Scheme Operation 5	155
6.18 zinc steam pouring out during the zinc-covered steel welding	156
6.19 Air bubbling along welding stitch	157
6.20 Dimples representation	158
6.21 Dimpling process	159
6.22 Front Door Fixture System (a)	160
6.23 Front Door Fixture System (b)	161
6.24 Front Door Fixture System of Agilaser	161
6.25 Front Door Fixture Scheme	162
6.26 Door Fixture System symmetric for the left and right front door	162
6.27 Parts mating through plugs of clamping system	163
6.28 settled sheets pack considering the gap and the two parts thickness	164
6.29 Fusion area: 1 is the fusion area, 2 is the altered thermal zone	165
6.30 Acceptable stitch	166
6.31 Accettable stitch because the length of defects is lower than 30%	166
6.32 Non acceptable stitch	166
6.33 Principal geometrical variations: p = fusion depth, l = width of the stitch, s = thickness of sheet metal	167
6.34 Acceptable welding	168
6.35 Marginal incision: non acceptable welding	168
6.36 Non acceptable hollow welding	168
6.37 three planned quality checking points	169
6.38 fixed coordinates of quality points	170
6.39 Distance tolerances and single quality points measures	170
6.40 Process Capability	171
6.41 Total number of welding stitches on a car door	172
6.42 Welding stitches between inner frame and all reinforces	173
6.43 Welding stitches between inner frame and waist reinforce	173
6.44 Car's door components	176

6.45	Laser Dimples and Laser Welding Process	176
6.46	Laser Dimples and Laser Welding Stations	177
6.47	Synthetic description of part process	177
6.48	inner frame Internal view	179
6.49	inner frame welding area view	180
6.50	Waist Reinforce CAD	180
6.51	Waist Reinforce shape CAD	181
6.52	Matching view between reinforce and inner frame	181
6.53	stitches position planning between the two considered parts	182
6.54	stitches position planning between the two considered parts	183
6.55	Inner Frame welding area	184
6.56	Waist Reinforce welding area	185
6.57	SMA analysis on Comau parts	186
6.58	Reference batch, period batch and ID-name of COMAU parts	187
6.59	Best matching analysis based on reinforces belonging to the same batch	188
6.60	Parts classified through fundamental <i>mode C(1,2)</i>	189
6.61	Composition of <i>CLASS C(1,2)</i>	190
6.62	Composition of <i>CLASS C(1,2) & C(1,3)</i>	191
6.63	R4-B, the reinforce without possible couplings	191
6.64	Composition of <i>CLASS C(1,3)</i>	192
6.65	Parts affected by C(1,3) as dominant and C(1,5) as secondary and com- position of <i>CLASS 3 C(1,3) & C(1,5)</i>	192
6.66	Exceptional coupling	193
6.67	Final buffer creation	193
6.68	Step 4, Final buffer iteration	195
B.1	Link or Recurrences between correlation index and Gap Measurements	209
D.1	"As is" case car's components	216
D.2	Step 1 of the iterative classification	217
D.3	Step 2 of the iterative classification	218
D.4	Step 3 of the iterative classification	218
E.1	Plate 1 - Channel 1, spring-back range [0,8336;-0,611]	220
E.2	Plate 4 - Channel 1, spring-back range [0,573;-1,215]	221
E.3	Plate 5 - Channel 6, spring-back range [0,709;-1,333]	222
E.4	Plate 6 - Channel 3, spring-back range [0,448;-0,428]	223

E.5	Plate 6 - Channel 6, spring-back range [0,981;-0,913]	224
E.6	Plate 3 - Channel 1, spring-back range [1,355;-2,385]	225
E.7	Plate 3 - Channel 2, spring-back range [1,293;-0,882]	226
E.8	Plate 2 - Channel 2, spring-back range [1,299;-0,903]	227

List of Tables

- 3.1 Complete combinations 38
- 3.2 Possible set of combinations 38
- 3.3 7 best combinations after the fixture design 39
- 3.4 7 worst combinations after the fixture design 39
- 3.5 Norm_1, Norm_2, Norm_inf for the best-worst matching (a) 68
- 3.6 Norm_1, Norm_2, Norm_inf for the best-worst matching (b) 69

- 4.1 data for non parametric test 111

- 5.1 "as is" case 132
- 5.2 Quality matching parts with one class 133
- 5.3 Quality matching parts with two classes 134
- 5.4 Quality matching parts with three classes 134

- 6.1 Technical specifications of doors 178

Chapter 1

Problem Statement

In this chapter a general introduction to the thesis work is given.

The work is based on a research study on the remote laser welding technology, focusing the attention mainly on one of the main problems checked during joining operations with this system : the *tight control of the gap between parts* during welding process.

To be assembled, two steel metal sheets must be overlapped. In this situation, if parts present a reciprocal distance, called *GAP* outside the tolerance limit, the welding process will cause a non perfect finite part. It has to be precise that this problem occur especially in case of zinc-covered metal sheets because of the chemical composition of the zinc. The entire problem will be explored in detail in following sections.

Nevertheless the fixture design the problem of the gap is permanently present also at present, although fixture have the function to block parts and hold them in position through a calibrate pressing force which in some case can constraint parts each other to maintain the required Gap (mainly in areas affected by clamps). Nowadays there is a branch of research, basing several studies on the fixture design problem (Ceglarek et al., 2004). However, the possibility to reduce the problem of the gap up stream the clamping of parts is not yet considered.

An improvement to this limit can be overcome by acting to the system and not directly by a technological change (like laser parameters optimization). A research study of a method about constraining the welding system in selecting best couples between parts could be the correct way to solve the problem. With this solution the system will weld no more casual parts coming directly from stamping system, because in this case the variational shape of parts is unknown and the coupling happens randomly. The aim is to force the system in processing pre-imposed parts matchings through a Selective Assembly strategy, explained in followings sections. The aim to obtain perfect previously

fixed couplings is possible only having a good control and knowledge about welded part shapes, in order to mate together parts looking like similar in shape profile. For this reason there is the necessity to find a method, a shape-based-indicator able to classify parts in different groups.

Surely the maximum advantage could be obtained in developing a method able to ensure a good coupling between parts and reduce the gap before the fixture placement. What is called "*goodness of fitting*" between two parts could be a valid way to have a good predictor and then improve the quality of the joint operation. In particular this goodness of fitting can be evaluated through a shapes-similarity quantification between two surfaces. The idea of a selective assembly is correlated to the parts' clustering, in this work will be presented a study about the similarity between parts oriented to a following classification of them. Once classified, parts belonging to the same cluster can be selected to be welded together. Parts will be stored in dedicated storages, similar to "logical buffers", based on the own characteristic class; when two parts belonging to the same class are ready, then they can be put in the assembly system to be joint. After all, a quality control of the final product will be compared with the "as is" case.

The research study of the indicator for predicting a good welding has been developed through a collaboration between Politecnico di Milano and the International Digital Laboratory of Warwick University (UK), while the study of the selective assembly has been carried on in collaboration with COMAU and Fiat.

Section 1.1 provides a rapid description of RLW, principal impacts in a welding process, advantages, limits and in particular the problem of the gap during the joining operation will be underlined. In section 1.3 the research part is described, then will be presented motivations and causes of the evaluation of methods predicting the gap between two parts, which represent the main problem of the RLW process. After that, section 1.4 describes a real case study and an application of the research part in an automotive assembly system. The objective of the work is resumed in section 1.5.

1.1 Generality

In the last years market has been characterized from a shorter product lifecycle, high customization and a high demand variation. In this contest firms have to reduce time answer to be competitive: for this reason flexibility has assumed an important role in manufacturing systems.

In fact, a production system requires the possibility to reconfigure and change radically the volume and the mix of productions, with no long time and relevant investments.

From this configuration the flexibility must be present by Flexible Manufacturing Systems (FMS).

In automotive sector, in which a short cycle life of product is effective, the possibility to have flexible systems is the best way to be more competitive. In this way Remote Laser Welding (RLW) has been a cornerstone in automotive sector. Thank to the ability to be "remote", it permits to group a lot of advantageous in a single machine.

Remote Laser Welding (RLW) is emerging as a promising joining technology for sheet metal assembly of steel and aluminium parts in vehicle manufacturing. By having the laser optics embedded into the robot, laser is supervised by a scanning mirror head as end-effector, RLW can easily create joints in different locations on the product through simple robot repositioning and laser beam redirection (see figure 1.1).

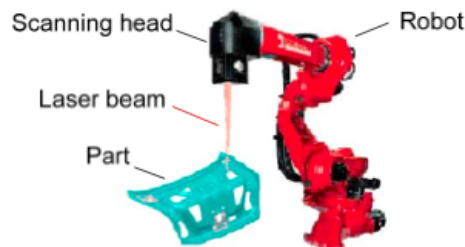


Figure 1.1: Remote Laser Welding (RLW) system

In a RLW system the laser beam is focused over the workpiece from a distance of about 0,5 mm until few meters. A combination of mirrors and mechanical movements of the laser delivery mechanism results in very fast beam positioning. For example, the repositioning for a welding operation may be less than 50 milliseconds. This is more efficient than traditional spot welding or more recent laser welding involving just robot motion because the seconds needed to move the robot from one to another are now eliminated. In some instances, the time it takes to move the robot from one weld position to the next it takes up to 90 % of the production cycle time.

Although the initial investment costs for a RLW system are higher than for a traditional resistance spot welding (RSW), RLW is faster than resistance welding and has lower operational costs as production volumes grow. For those applications requiring a large amount of spot welds on one assembly, RLW cells make a lot of sense.

Comparing RLW with other welding technologies (Resistance Spot Welding, Self Piercing Riveting, etc...), it has different advantages:

- Reduction of Processing Time from 50% to 75% to create a similar join as other

joining methods;

- Reduction of floor space and the total equipment until the 50% necessary to assembly a product;
- Possibility to make welding joint without adding material;
- Possibility to eliminate mechanical finish manufacturing post process;
- Reduction in energy use of 60%;
- Single sided accessibility for the laser beam and no contact operation;
- Tooling flexibility;
- RLW requires 50% less part's overlap at the joining area helping to reduce part's weight;
- Laser is mature and reliable technology (99,9% availability);
- RLW permits using fewer and lighter reinforcement components and parts;
- Shortening assembly lines help to reduce ramp up and changeover time due to the reduction in the tooling and equipment that has to be installed and calibrated.

All these points could bring big opportunities to automotive industry to be more competitive. In fact RLW has introduced a new way to assembly systems thanks to all these advantages. Consequently it provides an opportunity to improve and shape current product and process by improving system reconfigurability that reduces ramp up time or create mix product in a single line for example.

- The need for a high precision for the positioning between laser beam and point with tight tolerance limits for the distance and lateral deviation;
- The need for tight tolerance limits to guarantee a good joint;
- The high reflection and heat conductivity could affect the joint between different parts;
- High investment costs;
- The risk of porosity for the emission of gas during the joining operation.

However, the application of RLW is limited because there is a lack of information about its applications, which covers the process design & control to the product and process systems. Testing the RLW work is based nowadays on a **trial and error** approach because there is a lack of systematic methodologies too. This approach represent a limitation on the automotive processes and it is also time consuming, without any kind of specific experimentation. Currently the main challenge is the accurate part-to-part control gap between parts during the joining operation. This problem must be maintain under control in order to ensure join quality, specifically the mechanical integrity, leak tightness and craftsmanship of the weld. The gap between parts varies due to parts' dimensional and geometrical variation (caused during part manufacture). In fact, when two parts must be assembled, they are clamped and fixed together in order to minimize the distance between them. The laser welding requires a tight gap between parts mainly for two reasons: if the gap is less than minimum tolerance the zinc causes porosity with the emission of CO_2 of laser beam because made with galvanized steel parts, meanwhile overtaking the upper limit the fusion couldn't be done. The idea is represented in the figure 1.2.

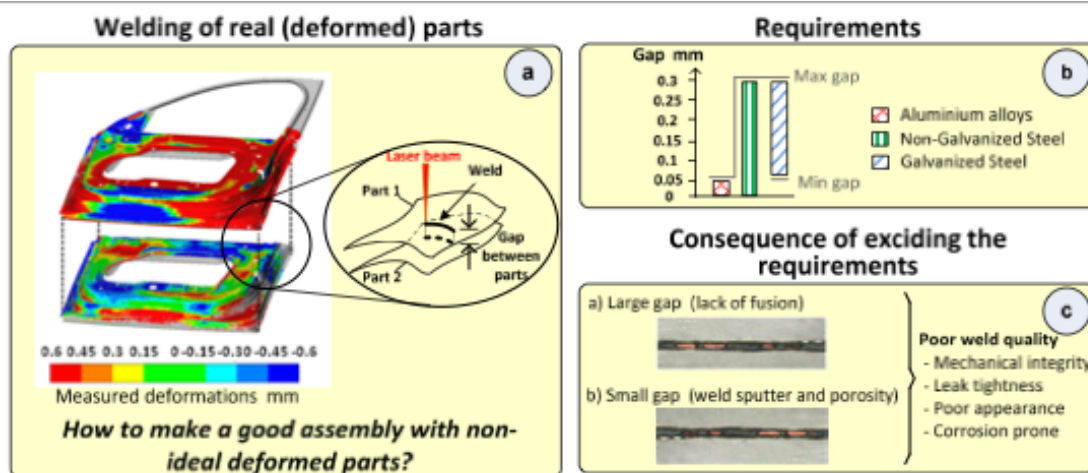


Figure 1.2: Requirements of the gap tolerance

The figure shows the necessity to maintain under control the gap, that is different for material (0.05 mm for aluminium and 0.3 mm for steel). Currently, the design and control of RLW assembly fixtures is based on a trial- and-error approach too, that is time consuming and suboptimal.

Resolving this problem, different steps can be done during the process, from the fix-

ture design to the laser parameter selection, which are case studies currently in progress.

The current work proposes the possibility to reduce the gap between parts before the fixture design and a valid approach is the selective assembly. In fact, selective assembly permits to divide parts in different storages, based on the most appropriate method. Nowadays, the correction of the manufacturing variability is based on the compensation of the error between two parts to assembly. The proposal of the work is estimation of the similarity between two profiles. Parts subjected to a remote laser welding are lap joint and the analysis of the surface is the best way to assess the weldability.

In particular, the similarity analysis approach will be implemented with the Statistical Modal Analysis (SMA). The SMA is based on the Discrete Cosine Transformation (DCT): the method divides part in cosine functions, which sum is a detailed description of the profile. Each cosine function is called mode. In fact, before fixture process, parts can be categorized by own modes; based on the presence of same modes, two parts can be matched and then welded. If the profile follows a match profile, then a constant distance is present along parts and the gap could be consider inside the tolerance limits. Under a certain limit, the similarity analysis can guarantee a good welding joint, reducing non perfect parts. In the next section a description of selective assembly approach is done.

1.2 Selective Assembly for parts

Parts, after manufacturing process, usually present errors and variability on their shape form. Since non perfect parts have a big impact during the assembly process, their shapes need to be analyzed in order to control a possible Gap between them (once overlapped). Selective assembly is used whenever the tolerances which have to be allowed for the components are so large that the natural build up with random assembly will not satisfy functional requirement's¹. For a high-quality assembly products from a low accuracy of machining errors, there are mainly two strategies to apply for the assembly process: the corrective and selective assembly.

- Corrective Assembly reprocesses parts during the manufacturing process: if parts present a variation upper a target limit, are reprocessed or rejected. Anyway, this alternative is not feasible because it is expensive and onerous;
- Selective assembly corrects the tolerance using the same errors of the parts, minimizing the surplus between them, in which variance dimension is evaluated to

¹*Simplification of selective assembly*, Desmond, Setty, International Journal of Production Research, Volume 1, Issue 3 1961 , pages 3 - 18

compare errors of parts. The compensation of variance between parts reduces manufacturing error and costs.

The method implies the division of parts in different ways to categorize them and let the assembled product be better. An application is the classification of parts based on similarity value. The evaluation of the best coupling before a buffer allocation with similarity analysis is a good predictor of the gap because it points out the pattern of the profile and, the most similar parts' shapes are, the most likely will be the good parts coupling.

Selective assembly is a good way to correct the problem of the gap. In fact, parts will be divided in specific classes, based on similarity parameters, which are the interesting research study of this work. This case study allows to create groups of parts to be put in the same storage. After that, combination of parts is simplified, because the similarity study identifies the best couple of parts to assembly and a reduction of scraps during the assembly process is really reached. A threshold to value the goodness of the gap must be satisfied to have a good laser welding.

Selective assembly will be built on an heuristic method, which iteratively finds the best number of classes in order not to permit bad couples. The work focused on heuristic approach to quantify similarity because in literature there are not analytical methods to compare two parts profiles decomposition through a shared modes evaluation. So a lower it' is imposed a threshold based on experimental got measurements. The partition of classes is built on the similarity between parts. Next section will describe the approach.

1.3 Similarity analysis between parts

Because the control of the gap is the first obstacle, it must be solved up stream, that is before parts are fixed and joint.

Predicting parts variation based only on tolerances assigned by designers is not appropriate as manufacturing process simulations used during the design stage are not precise. Therefore, it is necessary to characterize the geometrical variation of the parts based on measurements of real parts. The measured data can be characterized by the Statistical Modal Analysis [8]. The main idea is to evaluate the similarity between parts that must be matched before the welding process.

In fact, parts are an output of a manufacturing process, so they are non perfect parts. The presence of errors on the welding surface causes a deformation, consequently a non constant contact between parts, even if they are fixed and clamped.

It is necessary to perform part variation characterization to identify all the possible error patterns. Part variation means the difference between the real parts manufactured by pressing process and the original model (the nominal part). It will be necessary to classify part variations according to measured data during the ramp-up period (pre-production). Then, during the real production, once a sample part from a batch has been measured, it should be possible to confirm that this batch belongs to a certain category of part variations. For part variation characterization several techniques (surface fitting, surface classification, similarity between two surfaces) are required. As to characterization of part variation, one method is to produce a discrepancy map, taking the difference between the ideal and the real surface as a Z-value and look for different patterns of errors in the domain. This requires picking faces from the CAD model, measuring the corresponding faces in the real part, fitting surfaces to the measured points and generating the point map.

The shape of the gap has a proportional effect to the joining parts, that is if parts are similar in its deformation, then the welding operation should be conform. This work proposes to search a method in order to analyze the similarity between two parts, especially we will deal with two test parts, a C shape channel and a bottom plate, that must be joint along two welding areas. The goodness of fitness will be evaluated with parts after the fixture process, in order to ensure the minimization of the gap is gain. In fact, the similarity analysis can be validated if, after fixture process, the real gap is inside the tolerance limit. If the one-to-one is unambiguous, then the method is able to predict a good coupling.

Because the analysis of the fixture design is a topic in progress (Ceglarek, 2004), in which the best position of clamping must be found, then the following step is the research of the best matching between parts before the fixture system.

Parts will be divided in classes, respect the output of the best significant method. The partition in groups permits to go on the next level, the selective assembly system.

1.4 Assembly System Reconfiguration: a case study

In the second part of the work the application of the work will be done. In particular COMAU and Fiat assembly system is the case study analyzed.

An existing assembly system architecture must be reconfigured to provide the opportunity to evaluate the RLW system in terms of its feasibility to perform all required assembly tasks. This will provide crucial information about the most similarity analysis value for matching parts to improve the quality of the final product, to reduce non per-

fect parts and consequently workstation level efficiency assessment. The result will lead to the creation of a self-selection of parts that must be matched for the welding process and add value to the new welding technology.

In an automotive assembly system parts present imperfections, after the pressing process. The possibility to predict good match subparts permits to select them with the similar parameter to be matched, in order to reduce the distance gap, because characterized by the same profile.

A final quality product must be evaluated constantly for analyzing a possible improvement respect the actual one. The joint consists of a series of laser welding stitches, which can present imperfections, caused by an out of tolerance distance between parts.

Additionally, it will be imperative to develop the evaluation methods of the overall performance, cost- effectiveness of the RLW. As is the case with any new technology development and implementation, RLW will involve up-front costs related to the installation of necessary equipments. This production cost model can provide the analysis of the cost-effectiveness of production quantity, above which RLW becomes profitable. Furthermore, it will be equally important to determine the optimal configuration of the assembly system that ensures the eco-efficiency and higher productiveness. This will require the simultaneous consideration of factors such as total energy consumption, flow efficiency, welding quality, production cost, and vehicle weight saving.

1.5 Aim of the analysis

The main purpose of the research part is to find a possible solution to the part-to-part Gap control through a Selective Assembly implementation, which let system process already. To obtain a selective parts classification in clusters, a set of Similarity Indexes are analyzed to find out which one is the best in predicting the quality of a welding joint between two parts.

We have analyzed some Indicators which are able to quantify the goodness of the welding joint, with the aim of selecting and choosing the most robust and meaningful one. An indicator is a way to measure, indicate, point out, point to and predict with more or less accuracy and precision; in fact in this case of study, all the following presented researches are based on looking for a valid methodology to anticipate properly what could subsequently happen when two parts are joint.

For this purpose the indicators during analysis phase are called "similarity index": a similarity index determines how closely the peculiarity and characteristics between a group of individuals/object are. This study can be very usefulness because this index

could foretell how the welding will be good before positioning and fixing with clamps the metallic parts one above the other, just analyzing the shape similarity of the parts studied.

The most significant request for a good laser-welding joint, in fact, is the part-to-part control gap between two parts, which must be matched. The gap must be within a tolerance limit very thin (0,05-0,2 mm): if the gap exceeds the upper limit, the joint creates empty spaces between the joint stitches points, meanwhile if the gap is under the lower limit, the joint causes porosity (only in case of zinc coated sheet metal).

This case study can be very usefulness because this index could predict the welding joint quality before positioning and fixing the parts one above the other, just analyzing the shape similarity of the parts studied.

Consequently, the visible quality of the laser stitch is important and the possibility to reconfigure the fixture design determines a series of improvements for the assembly process and the final product quality. A case study with COMAU for the assembly door of FIat Group will be analyzed.

In particular, a Markov chain method will be used to model the assembly system with dedicated buffer. Starting from the "as is" case, the number of dedicated buffers will be constantly added, until a threshold is reached. For each part an effective improvement of the quality joint between a inner frame and a waist reinforce of a door will be evaluated.

The purpose is to find the best buffer allocation to gain a visible improvement.

1.6 Summary of the work

The thesis work is divided in the following chapters:

- Chapter 2 introduces the Remote Laser Welding technology. It is based on the explanation of the beam sources, working and applications. Moreover, a brief paragrapher on literature review for RLW and state of art is present.
- Chapter 3 introduces the research work made in collaboration with International Digital Laboratory of Warwick (UK). In particular all the possible indicators for the prediction of the welding joint are outlined. Each indicator is explained and commented. The most significant indicator will be described in the following chapter.
- Chapter 4 describes the SMA model, the indicator for the evaluation of the part-to-part control gap between parts. The model is described and results are shown,

in comparison with experimental research work. Thank to this parameter, parts can be classified to make the best matings.

- Chapter 5 is devoted to the selective assembly approach. A brief literature introduction is done; then an application of iterative class dimension for parts is calculated. Based on the idea to incrementally add a groups for the division of components, an asymptote situation will be achieved, in which the addition of classes will not improve the quality.
- Chapter 6 introduces the problem and industrial case of COMAU: the products, processes, the site organization and the assembly line. The application of the similarity approach for two parts of the doors and the classification is done. The iterative classification of these is the next step to really evaluate an effective improvement for the final assembly product.
- Chapter 7 reports conclusions, with the corresponding limitations and results of the work.

Chapter 2

Introduction to Remote Laser Welding

In this chapter an introduction to remote technologies is shown.

The purpose is to give an overview about the remote technology, in terms of laser use, beam sources and principles; then a section for citing the remote applications is present, in particular the automotive sector, because of interest for the thesis work. Consequently a description of the main problem affecting remote laser technology will be explained and at the end a resume of the principal solutions about this limit is argued.

At the end, a literature review for Remote Laser Welding is done: the main problem of the joint between parts with a remote technology has open the branch of research especially in

Laser beam welding technology has been widely used to weld automobile components, especially for taylored blank welding, that is steel metal sheets welding of different thickness. [42], [3], [6].

2.1 Remote Technology evolution

In this section the developments in remote laser material processing with highly brilliant laser beam sources are reviewed. Its history and the system technologies, i.e. laser beam sources and optical components, are presented. The remote laser beam welding and the two remote laser beam cutting processes as well as current research topics and application areas are described. Finally, the impact of the remote technologies on the industrial production is discussed.

2.2 History and Definition

The steady improvement of beam quality and the increase of optical output power of laser beam sources are a strong point in the field of laser material processing. Since the 1990s high power laser beam sources with high beam quality have been available. Thank to these features the focal length has gain high results for its applications without the need for large and therefore hardly manageable lenses to reach the threshold intensity of welding and cutting processes.

The first advance of the technology began with the development of high power lasers able to generate beams focusable to a small spot that assured sufficient power density at the workpiece for keyhole welding from a significant distance, that is the ability to maintain the beam in focus, however the gap between work surface and laser tool.

An early contribution to development of RLW came from John Macken [34], founder of Optical Engineering (Santa Rosa, CA), whose unique 4kW laser allowed the welding of sheet metals from a previously unseen distance. The first experimental analysis of keyhole welding application is described in *Remote laser welding* by him (1996), which it describes the behavior of the laser beam with long focal length up to 1600 mm. This article is acknowledged in several patents and publications as the cornerstone in remote welding applications.

The first industrial RLW designed primarily for the automotive industry was built in 1999 as a result of a partnership agreement between Aetna Industries Inc. and Rofin-Sinar. This was made possible because of the availability of Rofin's laser with first-rate beam quality and the comprehension that this solution could be applied in the automotive industry.

The Aetna-Rofin system adopted transmissive optics for beam focusing, as opposed to reflecting mirrors. Further development of this system resulted in full industrial application of RLW when Utica Enterprises and Optical Engineering introduced its system to Chrysler manufacturing plant.

Another application area of remote laser processing is the laser beam cutting. First application were made in 1990s. The fundamental motivation for remote cutting was the constricted access to the processing zone, as it can for example be found in the dismantling of nuclear reactors.

In general remote laser application can be defined as laser beam material processing with focal length larger than in conventional processes. Due to the longer working distance small movements of the mirror or an optics manipulator effect fast and large deflections of the laser beam focus on the workpiece.

High brilliant laser beam sources are used in order to reach the threshold intensities to start and keep running the processes, which differ in general from their related non remote process [42].

2.3 System Technology

One of the assets of remote technology is the capacity of laser beam to work from a distance to the workpiece. Scope of this section is to outline the needful principles to this technology. The section introduces a brief description about physical principles (see 2.3.1). In addition the system technology regarding the beam generation, the optics manipulation, the beam forming and the beam guidance will be discussed, as outlined in figure 2.1. To get together the topic, the challenge of laser safety for remote applications will be addressed [3].

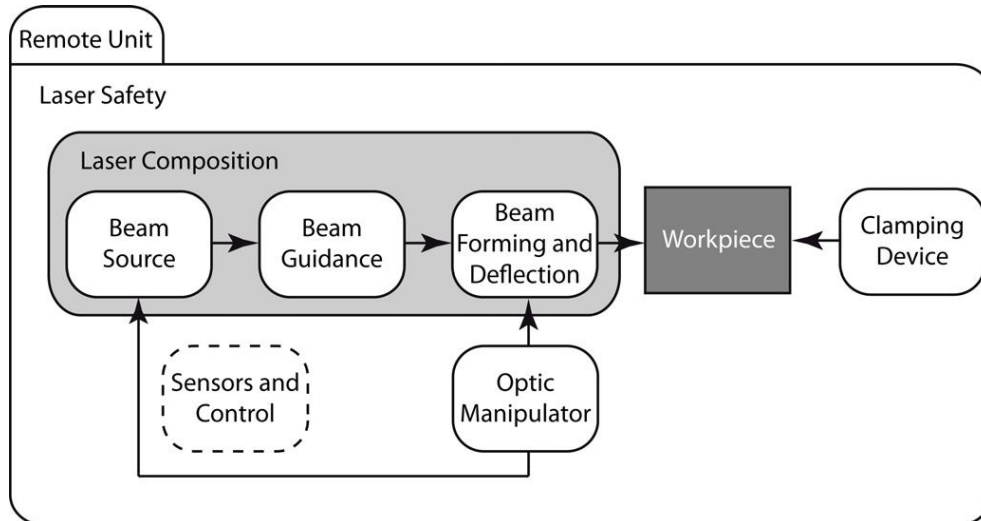


Figure 2.1: Guideline for the system technology in remote applications

2.3.1 Physical Principles of Laser Radiation

The radiation emitted by a laser device is purely artificial. It is formed by a tight band width and an uniform direction of propagation. The energy is emitted periodically in pulses or constantly as a continuous wave (cw), it depends on the type of laser. For pulsed laser systems the lengths of the single pulses are reflected in the nomenclature of those devices. For example ultra short pulse lasers are called femto or pico second

lasers, since their emitted pulse length is located in that scale. To quantify the quality of a laser beam, a characteristic number was found to compare the focusability and the beam spread of different systems.

That number is called beam parameter product BPP and is defined as the focal diameter d_f in the beam waist multiplied by the divergence angle.

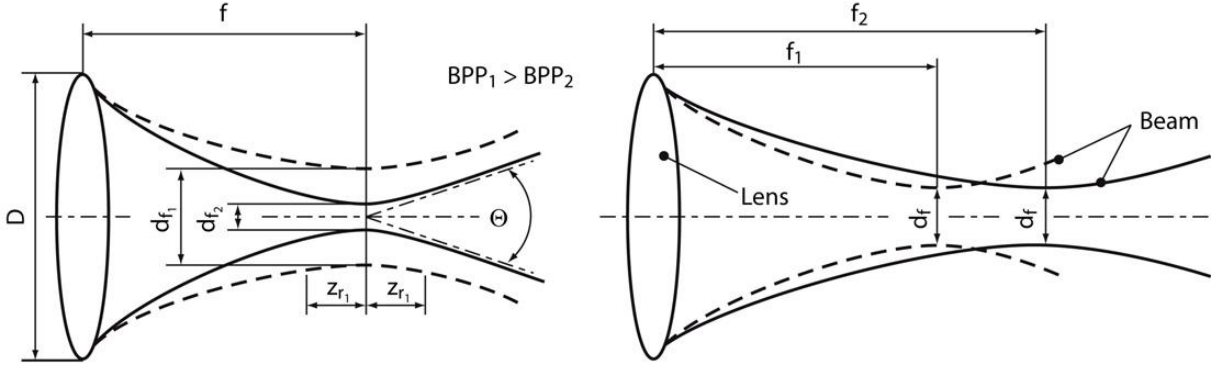


Figure 2.2: Reduction of the focal diameter and enlargement of the focal length by increasing the beam quality

Smaller is that value, better can the beam be concentrated on one spot for a given focus length f and a fixed diameter of the laser beam on the focusing lens D . On the other hand larger the distance between the optics and the processing zone can be set for a given spot diameter d_f and a fixed diameter of the laser beam on the focusing lens D , if all other parameters are constant (see figure 2.2). Since the remote technology deals with long focal distances, a small BPP is very important for those applications. Another aspect of a good beam quality is an enlarged depth of field. The length until the irradiated laser beam area is doubled and the intensity is halved due to the beam divergence is called Rayleigh-length z_r . Within this range it is considered, that the laser beam maintains a sharp projection on the workpiece. Longer the Rayleigh-length, more tolerant the process appears in terms of misalignments of the optics and the workpiece or in terms of focus shifting due to lens heating.

Along the quality of the radiation, the quantity of the emitted power and the intensity of the radiation are of importance, too. The beam quality and the quantity of the emitted power together form another characteristic which describes the laser beam, the brightness B . Higher the output power and smaller the BPP is, higher is the brightness

of the laser beam.

As already mentioned a laser device emits a central wavelength with a narrow band width. This wavelength is characteristic for the type of laser and its laser medium. Depending on the wavelength, the laser radiation can be guided from the beam source to the optics either by complex mirror systems or by fibers. Especially fiber guided solutions are a flexible, robust, easy and cost-efficient solution to transport the power from the laser to the processing zone. Solid state lasers hold this advantage since the fibre material is transparent for the wavelength [3], [6].

Beam Sources

The beam source can be present in three different states: gas, liquid and solid state. Because the liquid state sources are principally used in medical field, the most important sources are the CO_2 for the gas and $Nd : YAG$ for the solid state.

Despite the different state, the properties of the radiation are set as well as and affect all following considerations. The most important characteristics of a laser beam, concerning the remote laser beam welding and cutting applications, are the wavelength, the beam parameter product and the maximum output power. Both gas lasers and solid state lasers can perform the desired small BPP below 10 mm·mrad and optical output power in the multi-kilowatt range.

As just mentioned, the only representative of the gas lasers in the high power material processing is the CO_2 laser with a wavelength of 10,6 μm . The quantic efficiency of CO_2 is only of the $\mu_{CO_2}=38\%$, with a global efficiency of 10%. This limit is linked to the disposal capacity of the generated heat. In fact, adding the temperature the gas mix decay, with a consequent diminution of the efficiency and output power.

It has been the first system that combines a high output power and a high beam quality, up to the point of diffraction limited focusing. In order to guide the beam from the beam source to the processing zone a complex mirror system is necessary.

Besides gas lasers, the solid state beam takes on a more important role for remote laser applications. The active medium is the neodymium ion (Nd^{3+}), which are welcomed in YAG crystals. The energetic pumping is made by a light beam and it is optic type. The solid state laser is able to emit radiation at a wavelength of about 1 μm with high output power rates and high beam qualities. The efficiency is 49%, higher than CO_2 source. Nevertheless, the global efficiency attests about 10%. The quality of the beam is worse than CO_2 source.

While dealing with BPPs of about 25 mm·mrad in the recent years, the systems are now emitting radiation with a beam quality of less than 4 mm·mrad for multi mode

lasers and of 0,4 mm·mrad for single mode lasers.

To choose the best laser beam source for the remote application, both technical and economic aspects must be taken into account.

For this reason another parameter to consider is the economical aspect. The wall plug efficiency (WPE) of laser beam sources is another aspect of economic considerations. It is defined as the emitted optical power P_{out} divided by the incoming electrical power P_{in} ; typically refers to the effectiveness of converting electrical to optical power and it is defined as:

$$WPE = \frac{P_{out}}{P_{in}} \quad [3]$$

The WPE depends mainly on the conversion of electrical current to monochromatic radiation. This conversion is done directly with diode lasers or stepwise via pump light with Nd:YAG lasers or high-frequency fields in CO_2 lasers. Therefore the fewer steps are needed to generate the laser radiation and better the single efficiency of the conversion from one step to the next is, better is the overall plug efficiency [3], [6].

Beam Forming and Guidance

Transport system for the beam are essentially two: a series of oriented mirrors, which form an optic chain, and a wave guide denominated fiber optics.

The first solution with a mirror way is applicable both for CO_2 and $Nd : YAG$ laser sources. The way must be formed by linear stretches, with a mirror in each angle.

Scanner optics extends that approach by an active beam guidance unit to position the focus freely within the scan field. Generally it is done by a scan unit consisting of one or two rotating mirrors. Those mirrors deflect the beam into the processing zone.

In figure 2.3 the beam inclination by a tilting mirror is displayed.

The optic fiber is made by a cable with a circle section in transparent material to laser beam filled in an external cover. The aspect and the flexibility is similar to an electrical cable. The fiber working is based on the internal total reflection of the light [3], [6].

2.3.2 Intention and Benefits of Remote Technology

Today, remote technology is used in various industrial applications, like laser beam welding or marking.

Realizing the spot displacement with scanners or scanner-less approaches, high focus velocities can be achieved on the workpiece. This results in minimized non-productive

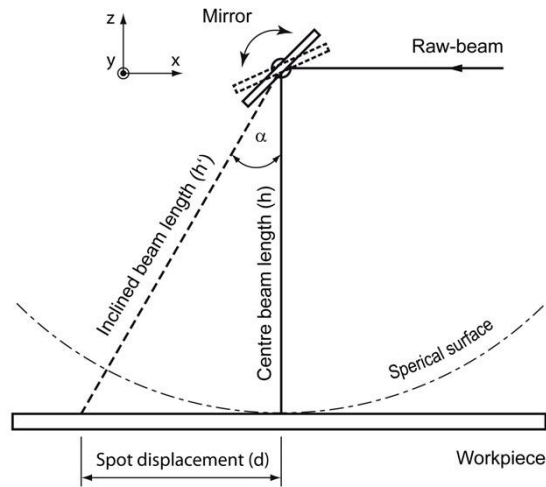


Figure 2.3: beam deflection by a tilting mirror and displacement of the focus spot

times since the jump movement between one processing zone and the next is done in milliseconds.

The resulting cycle time is thereby defined by the process itself: having such little laser-off times, the productivity increases in comparison to conventional laser beam welding processes and is equivalent to an optimization of the cycle time.

In addition to that, the high jump velocities from one processing zone to the next (with more than 5 m/s) hold the possibility to optimize the part quality. At the remote laser welding or cutting for instance, the sequence of the seams and edges applied on the workpiece affect the development of heat induced distortions. By optimizing that sequence, the thermal energy is inserted in a homogeneous way without building up internal tensions.

In figure 2.4 the heat induced distortions at the remote laser cutting is shown. The left picture shows a unoptimized cutting with a heat concentration at the right side of the workpiece, indicated by the white areas. Below the thermal camera picture, the measured surface distortion is displayed. It is obvious that there is a winding in the workpiece caused by induced tensions effected by an inhomogeneous heat distribution.

On the right hand the same part is processed with an optimized strategy for the laser exposition. By changing the sequence of the processed contours the distortions are reduced to a minimum, as can be seen in the diagram below, although the cycle time remains the same.

Since the resulting contour on the workpiece arises from the tilting of the scanning

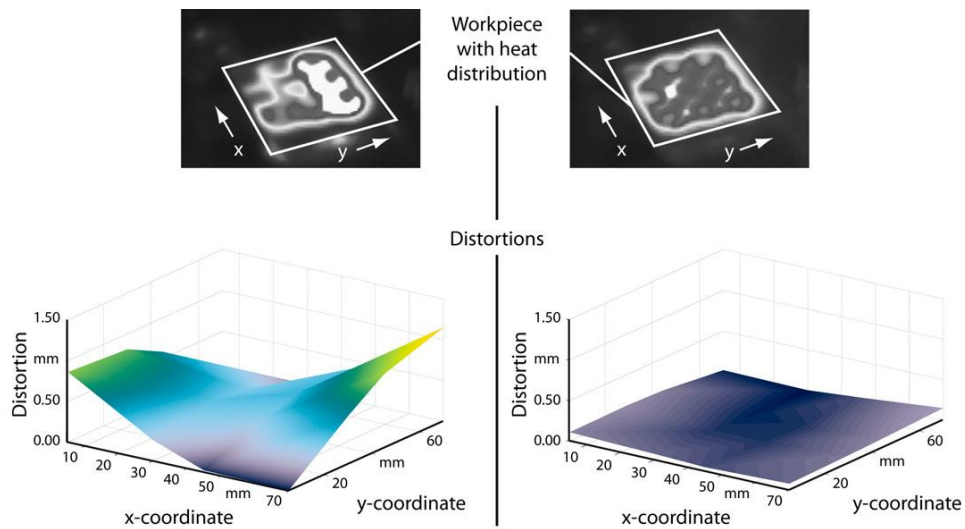


Figure 2.4: Heat induced distortions at remote laser cutting; thermal camera and distortion measurement: unoptimized (left) and optimized (right)

mirrors and is not bound to the geometry of the tool (like die cutting or resistance spot welding), there are almost unlimited possibilities to design welding seams, cutting edges or markings within the scan field. An example for that is shown in figure 2.5.



Figure 2.5: Load optimized weld pattern

So called weld patterns, load adapted seams, are used in lap configuration welding. Depending on the load in the flange the pattern can be optimized for the geometry and the applied load.

Dealing with long focal lengths in the scale of 300 to 1600 mm, the remote technology enhances the accessibility of the laser beam to the processing zone. Since the optics is not directly above the workpiece, angled designs are no longer interfering and parts with cavernous processing areas can be treated (see figure 2.6). The long focal length has another advantage regarding the system technology. Plume and particularly spatters, emerging from the processing zone, are barely reaching the optical elements and do not obstruct cover glasses.

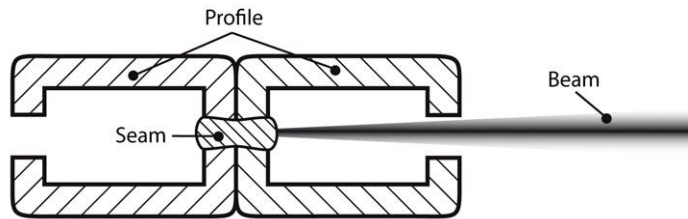


Figure 2.6: Remote laser beam welding of parts with limited accessibility to the processing zone

For the processes carried out with remote technology these benefits mean an advance in terms of production speed and flexibility. To deal with the question whether it is a revolution or evolution, a deeper look into the processes is necessary [3], [6].

2.3.3 Remote Processes

Remote laser welding has two major advantages over traditional laser welding with short focal length optics. First the high speed of the weld beam movement, which contributes to a significant reduction of the cycle time. Also, the long stand-off of the focusing head permitting access to areas not accessible with short focal length welding. The principal applications are in cutting and welding processes. A brief description is reported in the next subparagraphs [3], [6].

Remote Welding

The remote laser welding (RLW) is basically a laser beam deep penetration welding process. In order to generate a keyhole, the intensity of the focused laser beam on the workpiece must exceed the threshold value of 10^6 W/cm^2 .

Generally, a lot of the knowledge can be transferred from the conventional laser beam welding to the RLW. In addition to the process parameters known from near field welding (e.g. laser beam power, spot diameter, traveling velocity), remote specific aspects have to be considered. One aspect is the inclination angle of the laser beam achieve the workpiece. In the basic research, effects of big inclination angles are studied (G. Tsoukantas et al., 2006) concerning the change in keyhole position and shape. In applied research the exact limits of the process windows are objects of attention, as the results are needed as input for the robot path planning algorithms at optics manipulation.

Another aspect is the study and optimization of the process in application fields where the laser beam welding has not been established before. An example is the welding of zinc coated sheets, used in the automotive industry. In this case the resistance spot welding is replaced by the remote laser welding. As the zinc starts to evaporate already at temperatures far below the melting point of steel, the zinc vapour disturbs the the melt bath and causes keyhole instabilities. The results are often porous welding seams and spatter formations on top the sheet surface as a result of melt ejection.

A solution in this context is a local shaping of the workpiece surface by laser radiation to produce a defined dimple. Due to this dimple the sheets are clamped with a little gap in between to enable the zinc to degas.

A successful implementation of remote laser welding requires a certain system technology regarding the clamping device, the shielding gas supply, the feeding of welding and the seam tracking. These functions are completely or partly integrated in a conventional laser beam welding head. However, this is per definition not possible in remote laser welding due to the fast beam displacement and the long focal length. Instead of that, the functions have to be integrated in a special remote laser welding clamping tool, which gets much more complex than its conventional counterpart (see figure 2.7).

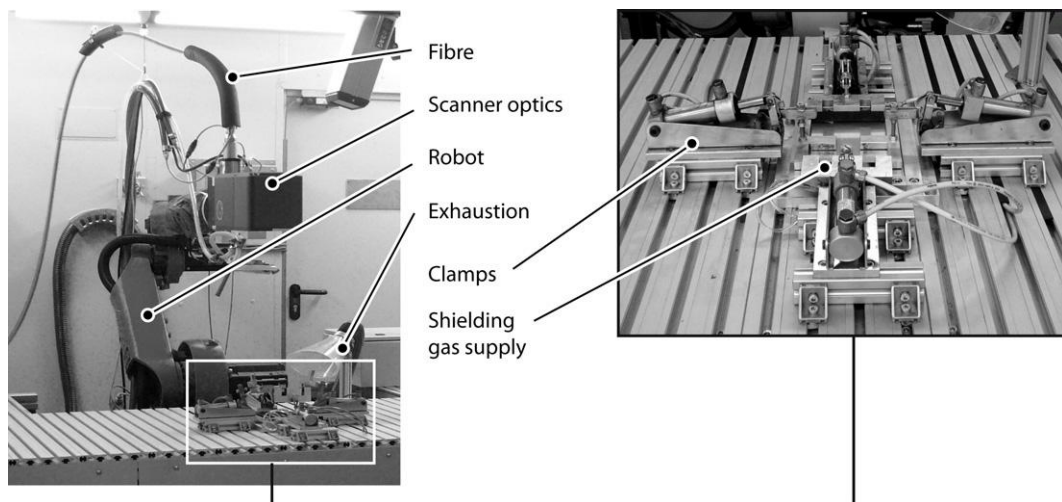


Figure 2.7: Remote laser production unit: Segregation of the optics and the shielding gas supply

The shielding gas performs two tasks in laser beam welding. The first is the protection of the workpiece against oxidation by the displacement of the environment oxygen. The second task is the removal of metal vapour and particles from the laser beam path.

This is necessary to avoid laser beam absorption and defocusing in the plasma which is ignited by CO_2 laser sources and to avoid the scattering and absorption of the laser beam by the plume when using solid-state lasers. If the surface quality of the welding seam plays a inferior role, the first task is not required necessarily. It is shown how to perform the second task with compressed air instead of shielding gas. Otherwise the shielding gas supply has to be integrated in the clamping device. As the gas nozzle does not move with the process zone, a shielding gas feeding device is needed for weld seam on the workpiece. The whole joining zone is flooded with process gas. Especially at high welding velocities, more than one nozzle must be open simultaneously, as they cannot be switched fast enough within the short repositioning time of the laser beam from one welding spot to the next one. So the cost of shielding gas supply increases due to an increasing number of gas nozzles and a higher shielding gas consumption.

Regarding the clamping, no forces can be applied to the joining zone with the remote laser welding head. Thus normally for each welding seam one separate clamping has to be provided which is contrary to resistance spot welding as well as to conventional laser beam welding with special laser welding heads [47]. An alternative, especially for smaller parts, are clamping frames with openings for laser beam access [37]. Whether using clamping frames or single clamping tools for each weld seam, remote welding clamping devices are complex, due to the wider range of functions integrated. A further point is the trend, to profit from the increased accessibility of the laser beam and to perform as much welds as possible in one station.

An additional challenge is the seam tracking. Tactile systems, which are often used for fillet welds, cannot be utilized in remote laser beam welding. Up to now no broadly usable and efficient optical tracking system is available for remote laser welding applications. Lap joints need for a less accurate positioning of the laser beam on the workpiece than fillet welds. So lap joints are usually chosen instead of fillet welds. Two points impede to this day optical seam tracking and process monitoring in remote applications. The long working distance means a limitation either in the resolution or in the field of view of the system.

Remote laser beam welding is mainly applied in the mass production of flat assembly groups which are characterized by a high number of welding seams in many different points on the workpiece. Typically, 0.5 up to 4 mm thick metal sheets are welded in a two or three fold lap joints. Exemplary parts are the doors, the centre pillars, the rear shelf or the seats in car production, where it replaces resistance spot welding more and more [37]. In these cases the remote laser beam welding proves its superiority and replaces other welding methods, like the resistance spot welding. Cycle times can be

dramatically reduced due to a higher welding speed and a faster movement between the welding spots, which is described in chapter 3. The good accessibility, as mentioned in chapter 3, allows to weld more spots in one station or gives the engineer new degrees of freedom in the car design. Finally, the remote laser beam welding permits a flexible design of the welding geometries, as it is explained in chapter 3. Thus the welding seams can be suited to the flux of forces in the car components, so that the stability and the crash performance of the cars is improved [3], [6].

Remote Cutting

The most common way to separate metal sheets with a laser in industrial production are fusion and combustion cutting. These processes are characterized by melting the material and by expelling the melt respectively the oxide with an external processing gas jet, coaxial to the laser beam. Hence the expulsion needs a high gas pressure, the nozzle is positioned close to the processing zone with a stand off between 0.3 and 1 mm above the workpiece surface. Due to the cutting gas feeding, it is impossible to carry out the fusion and the combustion cutting with remote technology. Besides the material expulsion with external gas, there are cutting processes with self induced melt ejection. Specific effects within the processing zone accelerate and blow out the molten material and consequently form a cutting kerf in the workpiece. Today there are two different processes to perform remote cutting: remote ablation cutting (RAC) and remote fusion cutting (RFC).

For remote ablation cutting the force to eject the melt from the kerf is formed by partly vaporized matter. The material in the gas state expands, builds up a gas pressure and accelerates fused matter from the centre to the kerf walls.

Next to the remote ablation cutting there is a new approach to process meltable materials from the distance without external gas: remote fusion cutting. At the RFC the molten material is expelled from the processing zone to the opposite direction of the laser beam irradiation. With the removal of the material, the kerf is formed and the workpiece is cut without processing gas. The main difference to the ablation cutting is the kerf formation in one overscan [3], [6].

Conclusions

The new remote technologies have involved a lot of innovation system technologies like scanner systems or robot path planning, too. Due to specific advantages they have opened new application areas for high power laser applications. Today, the remote laser

technologies with highly brilliant beam sources comprise one welding and two cutting processes.

The remote laser beam keyhole welding is strongly related with the conventional laser beam keyhole welding. Therefore, the elongation of the focal length can just be seen as an evolutionary step. However, considering all the new research areas, that affect on the one side the process itself and on the other system technology, as well as the new application fields, it can be ranked as a revolution in the industrial production.

The two remote laser beam cutting processes differ strongly from the conventional laser beam cutting processes. The material ablation and the melt expulsion are completely different. Still a lot of research efforts are necessary to understand them in detail. Both the remote ablation and the remote fusion cutting have enormous potential for the industrial production. They allow for example a change from cutting to welding applications or vice versa in one station with the same system technology just by an alteration of the focal position or the machining speed. This is a real revolution. However, the remote laser beam cutting has only recently been established in the research and has only recently been implemented in the industrial production. Increasing cost pressure as well as the trend to more customer individual products and therefore decreasing batch sizes lead to more flexible production units in industrial production. The processes presented in this paper could be the solution for some of the future challenges. However, a real revolution is a combination of different processes in one system technology to carry out joining and cutting tasks as well as the workpiece marking for part tracing [3].

The remote technology holds the potential to realize that vision.

2.4 Applications

Laser welding process, and more in general laser technology, find employment in high number of applications in different sectors:

- Automotive
- Energetic
- Shipbuilding
- Aerospace
- Electromechanical

Some of these sections have an advanced experience with it and use the application in different ways, while others are completely inexperts, even if technology has been studied from some years.

2.4.1 Automotive sector

The automotive sector was the first one to use the technology with a sort of continuity and a high duty cycle to exploit in the best way sources and amortize costs of installation and running.

The first laser application was used for replacement soldering process for a synchronization of change gearing with a speed welding wipe; in this way gearing were not corrupted because temperature is restrained. Moreover the automatization of the process was ideal for the laser technology. Laser is utilized in other applications, for example for the welding clutch elements, anti vibration damping disks.

An important application of laser welding is in assembly systems of vehicles and semi worked for bodywork. Since over 12 years laser is applied in taylor blanks realization, sheet metal plates with drawing deep different thickness. The tendency is to move towards taylor blanks with curvilinear joint, where laser cannot be replaced with other technologies. Laser lends well to be used as technique of preparation and joint of tubular elements, or final frame assembly, and results an advantageous substitute of Resistant Spot Welding, because it is able to joint part only in one way, to improve through continuous welding crash tests and improve the productivity.

The typical application is the roof-flank and doors. The maximum application uses bi-zinc sheet metal, even if aluminium is worked too. One of the main problems correlated to the material to be weld, is the zinc covered, especially in case of lapping parts. In fact, zinc has the limitation to gain the gas status with a lower temperature than the fusion of metal: that's cause the presence of a gas between two parts that must escape before the completion of the welding. The presence of gas between parts causes lost of quality and continuity in the welding area, which is essential for the final quality of the product.

Remote laser welding system

In automotive sector flexible welding systems can be two typologies: *articulated robot* and *portal system*. The laser beam can be addressed on the working part through mirrors or optical fibers.

The time rate is low, for principally two reasons: the short time required for the

welding and the waist of time for repositioning the laser on the hand effector of robot between a stitch and the next one. In the way to eliminate this concept and reduce the waisting time the concept of remote laser welding system has been introduced. For remote system implies the capacity to work with high distances between the optical point and the working piece, with repositioning time under 100-150 ms.

Remote laser systems can be classified in two systems:

- Remote system CO_2
- Remote system $Yb : YAG$

The first family is characterized by a CO_2 source with high power and excellent quality. The beam is focused thanks to a mirror system, able to address it: the high focus length (1000- 1500 mm) let to have a long working distance.

2.4.2 Other sectors

A second sector, in which laser found good applications, is in energetic one, in particular in nuclear. The demand is principally for parts with medium-high thickness, that is 10-15 mm. With CO_2 laser source welding joint are possible until 15-20 mm, while with opportune joint preparations and welding procedure (multiple wipe), thickness over 50 mm have been done.

Often materials require require a pre-heating to avoid the creation of bunch during the solidification. In conclusion, in energetic sector, laser is occasionally used, because production is limited and it is not able to amortize costs.

A third sector is shipbuilding, which is showing increasingly interesting on the employment of laser for working small parts to be integrated in big components. The main problem of this sector is that the 25% of costs are caused by corrective interventions [42].

2.5 Literature review for Remote Laser Welding

In literature remote laser welding has been discussed in different point of views. The meaningful problems have been argued for the parameter selection and the fixture design.

The attention is particularly focused to the zinc covering and the gap control problem.

Zinc-coated steel materials are often used to form various structures, including automobile frames and bodies. While zinc provides excellent corrosion resistance to steel, it can also cause difficulties during welding. During this process, explosive zinc vapour can

form and cause undesirable spattering of the weld metal, as well as extensive porosity in the weld after solidification. The issue of porosity is more significant in certain types of welds, such as lap welds, which are a preferred welding method for automotive body fabrication (see the process of the door assembly in the chapter of COMAU). Thus, the scrap rate in this welding process is typically higher, forcing manufacturers to incur material losses to maintain certain quality standards. As such, manufacturers that weld zinc-coated steel materials would benefit from improved welding techniques and in-process quality control methods.

In the automotive industry, the use of zinc coated sheet steel is rapidly increasing as a result of consumer demand for improved corrosion resistance of automobile bodies. However, overlap laser welding of steels remains a difficult operation because of the low vaporizing temperature of the steel.

To prevent the weld pool from being destroyed by zinc vapour, various approaches have been investigated.

One of the first works was published by Baardsen in 1976¹, in which he proposed a method of welding galvanized steel: he introduced a layer for suppressing the evaporation of the zinc.

Pennington² patented in 1987a technique that involved to remove the zinc cover in the welding area and replace it with nickel coating, because it does not vaporize appreciably during the fusion process, and result is the lack of corrosion, that is porosity in the lapping welding. However the approach is an additional processing cost.

Others approaches focused on the creation of a gap to escape zinc gas after its vaporization. Akhter and Steen [40] proposed for the first time in 1990 the introduction to the dimpling process in the weld line, in order to guarantee the minimum gap in lapping parts to be welded. However, there is difficulty to maintain a constant distance between two parts, because for different factors, like the manufacturing variability and thermal distortions.

Piane et al. [41] investigated an altered joint geometry technique, laser welding sheet metal is protected by using low-vaporizing-temperature materials. Controlled channels between sheets are put to escape the zinc gas; the alternation of concave and convex geometry is created in the top sheet surfaces. Before being subjected to a laser welding beam along a weld area, two metal sheets are placed on top of each other in such a manner that at least one layer of the said protecting material is located between the sheets at the weld area and that the weld area communicates externally of the weld area

¹*Method of welding galvanized steel*, U.S. Patent N. 3969604, 1975

²US Patent N. 4642446, 1987

between the sheets and the created gas can go out from the welding area. The advantage of this approach is the weld quality is not sensitive to dimensional variation of sheets.

As a simpler solution, the welding process has been tried with pulsed lasers and it has been observed that the weld quality is improved but still the improvement is not up to the mark, i.e. some porosity has been found to be inevitable, which increases with the increase in the welding speed. Tzeng in 1999 examined the a mechanism to exhaust of zinc gas by pulsed Nd:YAG laser beam welding [31]. The method has more flexible in terms of parameter selection of the laser beam and a better energy coupling. Although results show good improvement, the Nd:YAG laser speed is lower than with CO_2 one.

An important progress was introduced by Mehmood and Awan, in which an alternative to the first work on the zinc coated welding were discussed. In fact, until their work, all the proposes were remained in R&D laboratories because onerous works to be applied. Mehmood and Awan found the simplest and cost-effective method for laser lap welding in a production line.

Mehmood and Awan [23] proposed in 2002 an alternative for the control of the zinc coated. Until now, all the solutions found to solve the problem of lapping welding, could not be accepted in production line, because expensive and difficult to implement. The solution adopted by Mehmood and Awan is a use of both laser beams sources (*Nd : YAG* and CO_2) to be used sequentially: a hybrid solutions combining CO_2 and Nd:YAG lasers. In both cases a CO_2 laser provides the keyhole that follows the Nd:YAG beam.

In one case authors suggested the Nd:YAG beam drilling micro-holes at an inclination to the surface to weld, in order to exhaust zinc vapours. Micro holes are drilled with a variable periodicity, accordingly to the weld path geometry, without limitation of their density. However this case study is very difficult to implement.

In the second approach the Nd:YAG beam cuts a slot to remove the zinc coating and to exhaust zinc vapours produced by the keyhole through the laser cut slot. This solution is more practical but more expensive. In order to ensure good edge quality the edge sides of the sheets to be lap welded are firstly trimmed with a laser beam, then joined. A procedure in economical terms is evaluated, since one of the main critics to this procedure has been on economical and not on technical terms. They try to compare this technique with competing techniques that use a second laser beam to delay the close-up of the keyhole, thus providing a way-out to the zinc-vapours.

The aim of the work was to extract from past research works keyholes and principal points, in order to guarantee the weld quality and a production process, in terms of cost effective too.

This method in fact establishes a new way to have a zero gap, but making a double

laser beam.

Another approach is to modify the lap joint configuration to allow for the release of vapour by using fillet lap joints and pre-stamping stand-off projections. Experimental results indicate that the former might not be successful in welding large free surface areas, while the latter is difficult and costly.

The idea of controlling the formation and interaction of the zinc vapour during welding by using various shielding gas combinations has also been investigated, but the effects are not significant. Some researches have even tried adding particles that would react chemically with zinc vapour and reduce the porosity. Unfortunately, this method is inconsistent.

As example, in 2007 Li et al. [10] proposed the addition of a substance to the welding environment to absorb and dissolve with the zinc, to create a chemical reaction. The introduction of small amounts of aluminum in the interested welding region permits to reduce welding with minimal effects on the lapping joint. The reaction causes an Al-Zn liquid to elevated boiling temperatures.

Despite all these research case studies, the problem of zinc coating is relevant and difficult to eliminate; moreover, the limit of galvanized steel is the necessity to maintain always a minimal distance between lapping joints.

However the limitation of a remote laser welding joint is the control of the upper limit of the gap, which must be maintained under control not to cause a lack of fusion.

Nowadays this problem has been solved with fixture designs. Li et al. were the first to study the fixture problem related to laser welding. They analyzed a case study of fixture design for laser welding, in which a reverse engineering model has been done. The behavior of clamps is subject to a finite element method for the output evaluation, in particular the position variation along the welding area [42].

Chapter 3

Similarity Analysis

In this chapter the work in collaboration with International Digital Laboratory will be explained.

The necessity to improve the quality of the welding joint brings the research to go on up stream from the fixture system, because nowadays non exhaustive results have been found to solve the problem. The similarity analysis between parts takes into account the pattern shape for each part, in order to foretell if the gap can be out of the tolerance limits. Even if the fixture system reduces effectively the distance between parts the method would study if the shape of the parts have a hugh effect on this limit, even if the clamping system can change the conditions.

The chapter introduces the main step for the improvement of the quality joint: the similarity analysis between parts, in order to evaluate the goodness of fitting between parts. The similarity analysis has been considered as a good indicator to evaluate the adjustment of profiles. In fact, because the problem is focused on the lapping joint, the pattern of profile directly affects on the gap during the joint and the addressed study on it is the best way.

As just mentioned in the problem statement, a similarity approach to evaluate the goodness of fitting between parts is a method, that could be able to predict a good welding quality joint, before the fixture process and the introduction to assembly line. To evaluate that, a set of indicators has been selected and analyzed with the International Digital Laboratory staff.

The similarity approaches will be analyzed with the same data set of parts and the analysis of results will be compared with experimental data, obtained by a real process of fixture system and described in section 3.2. Then, an outline of the selected similarity indicators follows the part and an exhaustive paragrapher with each description,

following limits and good points in every case.

3.1 Aim of the analysis

The main purpose of this first research part is to analyze a set of several *Similarity Indicators* to find out which one is the best in predicting the quality of a welding joint between two metallic parts, before the fixture process. In fact parts are not nominal and profile is affected by geometrical deformations, because output of a manufacturing process.

Some Indicators, able to quantify the goodness of the welding joint, were analyzed with the aim of selecting and choosing the most robust and meaningful one. An *indicator* is an application to measure, indicate, point out, point to and predict a specific result with more or less accuracy/precision; in fact in this case of study, all the following presented researches are based on finding a valid index to anticipate properly what could subsequently happen when two parts are joint.

For this purpose the selected indicators during all the analysis are called "Similarity Index": this typology of index determines how closely the peculiarity and characteristics between a group of individuals/objects are. This study can be very useful because this index could foretell how good the welding will be, before positioning and fixing with clamps the metallic parts one above the other and just analyzing the shape similarity of the studied parts. So basically all this indicators used are geometrical instruments which considered the pure and simple profile shape.

The most significant request for a good laser-welding joint, in fact, is the part-to-part control gap between two parts, which must be matched. The index must quantify the similarity between two profiles and compare this value with the gap value between them.

The parts analyzed in the following case of study are sample parts on which is possible to test the index. But since the technology (Remote Laser Welding) is used for component door's welding, the index must evaluate and treat the testing parts considering the characteristics of the sub-groups constituent a typical door. In the figure 3.1 the mentioned testing parts are illustrated.

Taking into account this aspect, the gap between two parts must be within a settled tolerance limit very thin (0,05-0,3 mm): if the gap exceeds the upper limit, the joint will not take place, meanwhile if the gap is under the lower limit, the joint can be affected by superficial faultiness (especially in case of using zinc metal steel or some other superficial treatments).

Basically the course in this work will firstly evaluate the goodness of all the considered

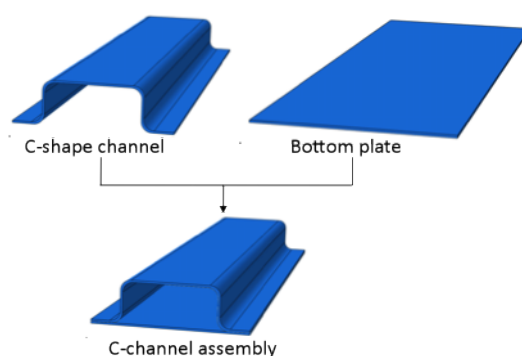


Figure 3.1: Testing parts shapes

indicators in predicting welding. All indicators will be applied on this set of sample metallic parts designed expressly for the indexes testing phase. For this reason these items are defined through simple shapes, for example parts with planar parts and bars, but referable approximately to components car doors.

Testing this index directly on real parts of the door could be very complicated and laborious, not for the application but rather for the interpretation and evaluation of results. For this reason there was the choice to test indicators on simpler parts, which however are affiliated to real metallic door components : this is explicable considering the shape of the welding area of real car parts. In fact two components of this typology usually are welded in specific zones (called for this reason *welding areas*) with planar profile, even if the whole part has a complex shape. The welding takes place in similar areas to linear bar, for this reason the evaluation of indicators can be used the simplified typology of elements.

3.2 Experimental Data

In order to conduce a meaningful index assessment, it's necessary evaluate if what they predict is approachable and comparable to the real situation of the data. The main idea is to supply two different kinds of data coming from the same sample of parts.

Testing parts were analyzed at the *IDL* International Digital Laboratory of the University of Warwick, Coventry (UK), where this research case of study is widely treated. The set of parts is constituted by 6 parts called **C-shaped channels** (upper parts with a shape like "C") and 6 other parts called **Bottom Plates** (lower parts with completely planar surface). Two different kind of data measurements from the same set of parts

were obtained.

A first data set is composed by the gap between all the couple of available metallic parts (in particular every C-channel mated with every possible Plate) clamped together and fixed, as if they were ready for the welding process. Data are representative of the goodness of the welding, because they are the result of the real gap, created after the fixture process.

The second group, always got from the available metallic part in the IDL, represents the whole top surfaces for each part express by the proper *points cloud* (several 3-coordinates points describing the surfaces as well).

1. Experimental gap measurements are fundamental to prove the index as a good estimator of the welding quality; in fact the gap after the fixture design is measured. The research of an indicator is evaluated on the most robust and significant in prefiguring the output of the joins, that is a univocal correspondence between these data and the output of an approach.

They were available for each part matching , so there is an explicative Gap value between the interval [0,1] for each of the 36 possible parts couples as a whole. They were got in the format of filler data (as explained in the next section).

2. Surface of parts : this is a set of 12 complete measurements of the six real metallic channels and the respective six plates of the case of study (see figure 3.1). They are scatter data typology, made of data sets composed by 3D coordinates points. For each part is available the complete surface measure formed by several (x,y,z) points. These data, getting from the survey of the real metallic parts, were necessary to the whole following analysis to calculate similarity indicators, because they are the input for every algorithm to extract the indicator output.

3.2.1 Gap Measurements

Gap Measurements are the result of a process of measuring the distance between two clamped parts using the *filler*: it is a measurement instrument, which using bars with different thickness value inserted into the aperture between parts, succeeds in estimating the gap value in millimeters.

The gap has been measured manually, positioning one by one the top parts (one of the six available C-shape channel) on the bottom ones (also present in the same number of the tops). It is clear the reason for which 36 gap values are present (one for each couple). Only one side of parts is fixed by clamps because only one side clamping system was



Figure 3.2: Gap Representation

available, but considering the present features, the orientation is always maintained. The next analyses are focused on the right side only because gap measurements are available for this side only. What is intended to be the right side is shown in figure 3.3.

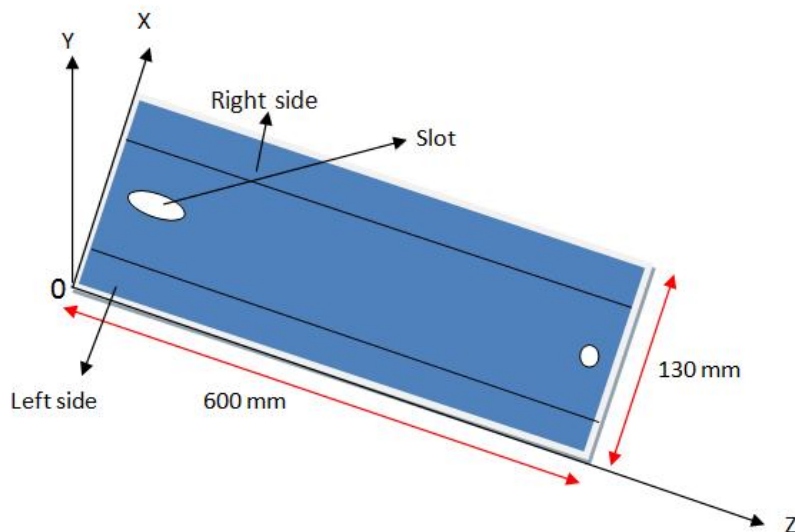


Figure 3.3: Parts Reference System for Gap Measurements

For simplicity, taking the local reference system at left edge than slot, the right side is exactly the opposite to the axis origin. So recalling the real global reference axis for a typical machine, the right side is a clear simplification to mean the side with X-Y coordinates forward. To fix the parts were used 6 clamps equidistant each other, and the measurement with the filler were taken in some precise and specific points. For the analysis of the gap were considered three points between every couple of fixtures, for a total of 15 points for the whole side (figure 3.4). Clamps are in contact with metallic parts through circular features characterized by a diameter of 9 mm. The distance between the circumference center of the first and the last clamp and edges is 15 mm.

The distance between two clamp centers are 115 mm.

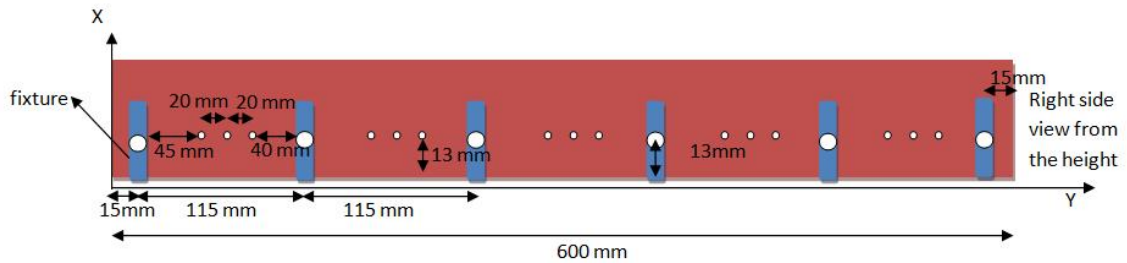


Figure 3.4: Clamps positioning on the right side

The measurements were taken only focusing the attention on selected points between fixtures, and they were obtained, once clamped the top with the bottom parts, placing fillers between the parts, and calculate the precise value gap. If the filler does not fit into the fissure, it will be changed with another thinner one to permit the penetration into the gap and the following measurement. On the contrary if one filler enters in the gap but with too much remaining tolerance space between its body and parts and so there can be observed the absence of friction force which avoid movements between the two surfaces, the thickness gauge must be changed with another a bit thicker one. The main idea is to find for each point the thickest filler which enter the gap, and go back up to the numerical value of the gap through the thickness value (mm) of the appropriate filler.

The clamping system is composed by 6 clamps, which are fixed on X and Z axis, but they can be moved on Y axis pressing force on this direction, and two steel stakes, in which hole and slot are filled in. In this way part cannot be rotated, because feature dimension for the hole and slot is different.

In the following image is reported clamping system used in the IDL for parts clamping (figure 3.5).

Considering the depth of the points in relationship to the edge, points have been measured more or less at half width of one welding area, so penetrating the gap for a filler length equal to the position of the points considering the X-direction. The measurements can be considered confident and certain, because they are the output of a design of experiment work, conducted in the International Digital Laboratory, several set of trials and repetitive measurements were taken, showing the same results for each experiment and backing up the property of results, the reliability and repeatability of



Figure 3.5: International Digital Lab of University of Warwick clamping system

the analyzed data. In the experimentation 15 points were measured for each pair of parts (36 total coupling), and once all the points were calculated for every possible couple, all these values were grouped into a matrix in input to a validated algorithm used to calculate the Good-to-Total Ratio for each pair of parts.

The G/T Ratio is an index representing the percentage of points studied by the filler satisfying the tolerances on the total number of points (the fifteen measures for each couple), having the gap value between 0 mm and 0,3 mm. For each point the value becomes a binary, it is 1 if the value is within the tolerance upper limit and 0 otherwise (upper than 0,3 mm).

The G/T Ratio Index can be also considered as a robust quality measure, because if the value is 1, it means that all the points measured stay into the tolerance, and so it is likely to have a good quality welding. The number of possible couple between the 12 parts is 36 (table 3.1).

One combination is meant to be a grouping of six couples. In one mating is impossible to have one Plate combined with more than one Channel. In this way the total number of existing combinations is $6! = 720$ (3.2).

It was possible to calculate the Average G/T Ratio value for each combination of six pairing, simply calculating the mean G/T Ratio value between the six couples belonging to the same combination, and this value illustrates overall how good-quality that specific welding can be. This value will be comprise between 0 and 1. Higher is the value of the

Table 3.1: Complete combinations

C1-P1	C2-P1	C3-P1	C4-P1	C5-P1	C6-P1
C1-P2	C2-P2	C3-P2	C4-P2	C5-P2	C6-P2
C1-P3	C2-P3	C3-P3	C4-P3	C5-P3	C6-P3
C1-P4	C2-P4	C3-P4	C4-P4	C5-P4	C6-P4
C1-P5	C2-P5	C3-P5	C4-P5	C5-P5	C6-P5
C1-P6	C2-P6	C3-P6	C4-P6	C5-P6	C6-P6

Table 3.2: Possible set of combinations

Combination 1:	C1-P6	C2-P4	C3-P2	C4-P3	C5-P4	C6-P5
Combination 2:	C1-P4	C2-P6	C3-P2	C4-P3	C5-P4	C6-P5
Combination 3:	C1-P1	C2-P3	C3-P6	C4-P5	C5-P2	C6-P4
...						

Average G/T Ratio, better will be the quality of the combination because there will be a major number of points with distances (gaps) within tolerances.

3.2.2 The output of the gap analysis

The code receives the matrix of all the gap values (15 points for each couple) for all the possible couple, 36 in total, so a [15x36] matrix as input. To this matrix is associated another one containing the correspondent G/T ratio Index for all the 15 points of any combination, collected so into another matrix with Boolean values (1 or 0). For each couple is easier to have only the average value of G/T ratio between all the 15 points measured for it. So in input at the code will be also the column vector of 36 value of average G/T value Index concerning the couplings. The code find out all the 720 possible sorted combinations of couple, the corresponding value of G/T ratio for each couple and the Average G/T Ratio value for each row(so for each combination). By sorting the Average G/T value , it's possible to single out the combinations with the highest value of average G/T ratio, and also the ones having lowest value. The 7 best and worst combinations obtained are respectively on table 3.3 and 3.4.

Analyzing the best combinations, it was possible to define the coupling which better satisfy the requirements, and so try to assemble those real parts which present this

P1	P2	P3	P4	P5	P6	G/Tr1	G/Tr2	G/Tr3	G/Tr4	G/Tr5	G/Tr6	G/T
C5	C3	C4	C2	C6	C1	1	0,6667	0,6	0,8	1	0,8667	0,8222
C5	C3	C2	C6	C1	C4	1	0,6667	0,6	1	1	0,6667	0,8222
C5	C3	C2	C1	C6	C4	1	0,6667	0,6	1	1	0,6667	0,8222
C5	C4	C2	C6	C1	C3	1	0,5333	0,6	1	1	0,8	0,8222
C5	C4	C2	C1	C6	C3	1	0,5333	0,6	1	1	0,8	0,8222
C5	C2	C4	C6	C1	C3	1	0,5333	0,6	1	1	0,8	0,8222
C5	C2	C4	C1	C6	C3	1	0,5333	0,6	1	1	0,8	0,8222

Table 3.3: 7 best combinations after the fixture design

P1	P2	P3	P4	P5	P6	G/Tr1	G/Tr2	G/Tr3	G/Tr4	G/Tr5	G/Tr6	G/T
C4	C6	C1	C3	C5	C2	0,8	0,2667	0,5333	0,733	0,6	0,6	0,5889
C3	C6	C1	C4	C2	C5	0,733	0,2667	0,5333	0,733	0,6	0,6667	0,5889
C2	C6	C1	C3	C5	C4	0,733	0,2667	0,5333	0,733	0,6	0,6667	0,5889
C3	C6	C1	C5	C4	C2	0,733	0,2667	0,5333	0,867	0,467	0,6	0,5778
C3	C6	C1	C2	C4	C5	0,733	0,2667	0,5333	0,8	0,467	0,6667	0,5778
C3	C6	C1	C4	C5	C2	0,733	0,2667	0,5333	0,733	0,6	0,6	0,5778
C2	C6	C1	C3	C4	C5	0,733	0,2667	0,5333	0,733	0,467	0,6667	0,5667

Table 3.4: 7 worst combinations after the fixture design

characteristic, and also to avoid the assemble of parts that matched together have the lowest G/T average value. This step of the analysis is fundamental above all to provide a comparison between all the similarity index analyzed and to evaluate which index is the most suitable to predict the welding quality before fixing and clamping the parts.

3.2.3 Surfaces Measurements Data

For each testing part (6 C-shape channels and 6 Bottom Plates), parts surfaces were scanned by 3D measurement system. This is a portable measurement platform calculating the coordinates of the points for all 3 coordinates values (x,y,z), in figure3.6.

3D laser scanning device

The only set of surfaces measurements, scattered data of the surfaces of all the single whole parts available through x,y,z point describing the surfaces, was got by a CMM

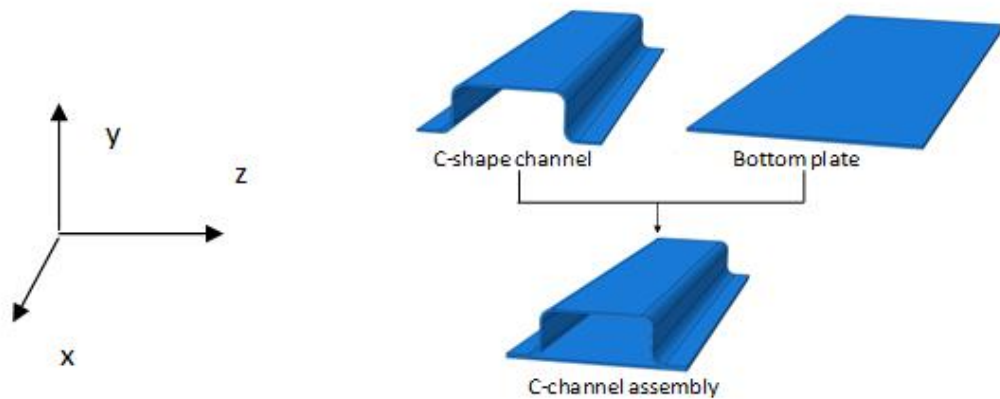


Figure 3.6: Reference axes used for measurement data and surfaces shape

instrument : CogniTens Optigo, a "fully featured 3D Shop Floor" non-contact measurement ¹.

Optigo, whose platform is purchased by Cognitens, is a product line of portable *optical 3D measurement* and digitizing system based on the unique white light stereo vision technology by CogniTens. As a manually operated device, Optigo provides high accessibility to small to large objects and is designed to withstand the demanding conditions of the engineering and manufacturing environments. It gives design, manufacturing and quality engineers fast and comprehensive metrology feedback on full surfaces, common manufacturing features, various edge types and other dimensions of interest.

The white-light system, which facilitates quality iterations and manufacturing-process corrections in real time, is commonly used for dimensional inspection and reverse-engineering applications.

The precision and reliability of measurements is comparable with existing CMMs, in fact this 3D scanner is a device that analyzes a real-world object or environment to collect data on its shape and possibly its appearance. The collected data can then be used to construct digital, three dimensional models useful for a wide variety of applications.

These devices are used extensively by the entertainment industry in the production of movies and video games. Other common applications of this technology include industrial design, orthotics and prosthetics, reverse engineering and prototyping, quality

¹www.hexagonmetrology.it/cognitens-optigo

control/inspection and documentation of cultural artifacts.

The principal functionality is usually to create a point clouds of geometric samples on the surface of the subject. These points can then be used to extrapolate the shape of the subject.

The precise Reliability value of the real system used is left out, but assuming the characteristic of this system like a CMM one and the recent advances in rangefinder technology, together with algorithms for combining and processing 3D, it's not a mistake to be confident in this product commonly available on market.

In particular, it should be verified:

- Accuracy = mean error of machine's position within the coordinate system.
- Repeatability = the variability of the measurements obtained by one person while measuring the same item repeatedly.
- Reproducibility = the variability of the measurement system caused by differences in operator behavior.

The precision of a measurement system is called Reproducibility & Repeatability, that is the degree to measure and get out the same results without changing conditions.

It should be remembered that many limitations in these kind of objects that can be digitized are still present even if the system is adequately calibrated: for example optical technologies encounter many difficulties with shiny, mirroring (like the available Metallic parts) or transparent objects. Laser scanners can send trillions of light photons toward an object and only receive a small percentage of those photons back via the optics that they use.

Many problems are caused by the reflectance of the metallic surface which makes it difficult for light projection or the insufficient accuracy of state-of-the-art scanning devices. This problem will be faced in followings section, considering the usual application of a known filter to solve this acquisition data problem.

Location of the axis origin

These scans have to be brought in a common reference system, a process that is usually called alignment or registration, and then merged to create a complete model. This whole process, going from the single range map to the whole model, is usually known as the 3D scanning pipeline.

From the reference axis origin point of view, the Cartesian local coordinates system is assumed to be in a different position from the Global one. Regarding to the location

of the origin used for the analytical studies, it's fixed in one corner during the data acquisition with the scope to have a sorted coordinates system. In this way x and y axis follow crescent value.

In the figure 3.7 is represented the axis origin.

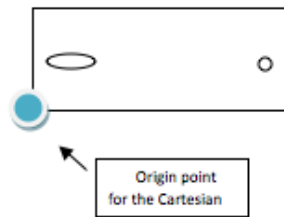


Figure 3.7: Axis origin

The global reference system of a typical machine is quite complicated to be used for some analysis, often it is associated and linked to a local reference coordinates system, easier to be used and more practical. For the acquisition of part surface measurements the local axes origin was placed in the corner even if this particular point is not a good one for an optical system and additionally it has no tolerances assigned, could be distorted and affected by errors. Furthermore it is not a representative and main feature of the parts like the hole- feature on both parts, perfect for the machine axis reference.

Welding areas delimitation

During the analysis, the selection of the joining area trimming like 2 mm from the edges and the bending is explained to the regions, which tend to be very noisy areas.

In fact some parts like the C-channel present a deflection of the metal to change suddenly its height.

Edges and bendings are usually affected by visible and important peaks or deformations. To avoid the inclusion of the noise in calculations, welding areas are considered starting at the distance of 4 mm from the central body of the parts, and 2 mm from the edge as in figure 3.8.

Not consider reduction of welding area is a well-advised action: first of all the real welding concerned with the most central zone, then, if considered obviously, it will compromise the analysis, because of its impossibility to be welded with a real metallic "planar-shape" sheet metal without deforming nastily the part.

For this reason it will not take place in our following analysis 3.8.

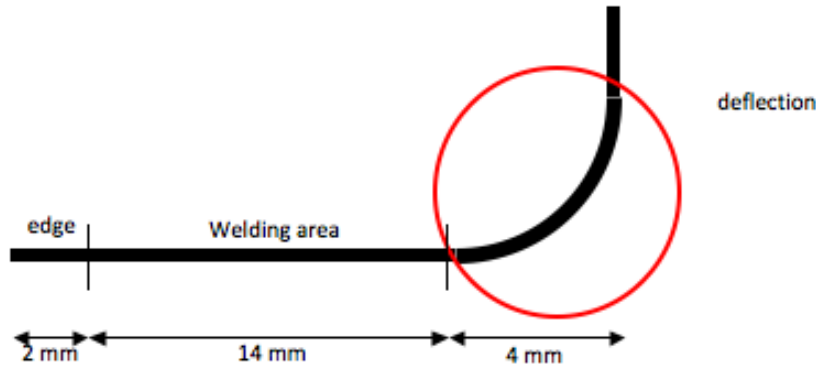


Figure 3.8: The deformation of the corner not considered for the welding area delimitation

In this analysis only a single welding area is studied and precisely what is called "right side" in the local coordinates system. It should be not considered the other one, because relating to the experimental fixture design of the lack of clamping system for the other side., all the experimental data are measured only to the X and Y forward side (right side).

The clamping system is composed by 6 clamps, which are fixed on X and Z axes, but they can be moved on Y axis pressing force on this direction, and two steel stakes, in which hole and slot are filled in.

In this way part cannot be rotated, because feature dimension for the hole and slot is different. For this reason the left side cannot be measured.

Welding areas check and screening

The edges of the components are critical features of the part. In fact usually edge presents a lot of smears caused by the manufacturing process of the part. In fact the real analyzed metallic parts are the output of a folding process starting from a sheet metal, and a following shearing (cutting) process, which lead to obtain borders. The second metalwork stresses hard the shape of parts and impresses deformation forces basically on the little lateral tab of the parts. Basically the most frequent huge deformation affecting the parts very seriously caused by the process of shearing are shown in the scheme on figure 3.10.

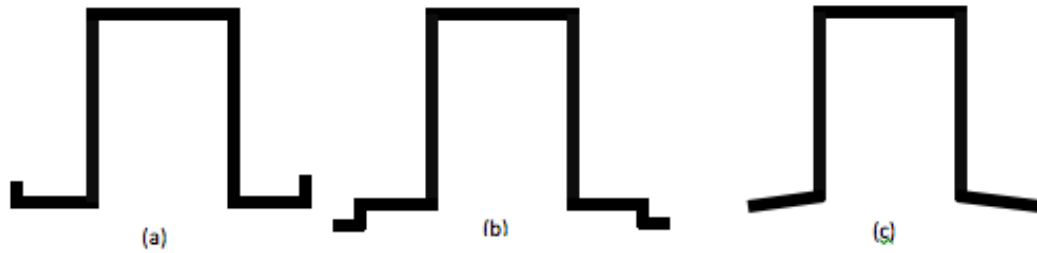


Figure 3.9: Frontal profile of parts affected by typical deformations impressed by shearing

If there is no intervention before the welding operation, situation (b) could be very compromising about the welding process, but, if singled out in time, the two protrusions on the borders can be removed, so it is possible to obtain a good welding joining the bottom part only with the most central area of the sides top part of the parts. Welding the part type (a) problems are not present during the welding process, on the contrary the final product will not be there two little tabs at the tips. Removing them through manufacturing work, the final product will be adequate.

Then, considering the shape of the sides and selecting appropriately the proper zone, it is possible to avoid peaks and huge deformations for a good quality final product. Situation (c) could not impair the welding joint after the fixture usage, but it is not removable through a second manufacture.

If one of the three welding area's behaviors is present, it will be diagnosed during the use of similarity indices, as mentioned previously.

The welding areas are collocated in the two sides represented below (3.10), so it is visible that they do not include external edges and internal bending.

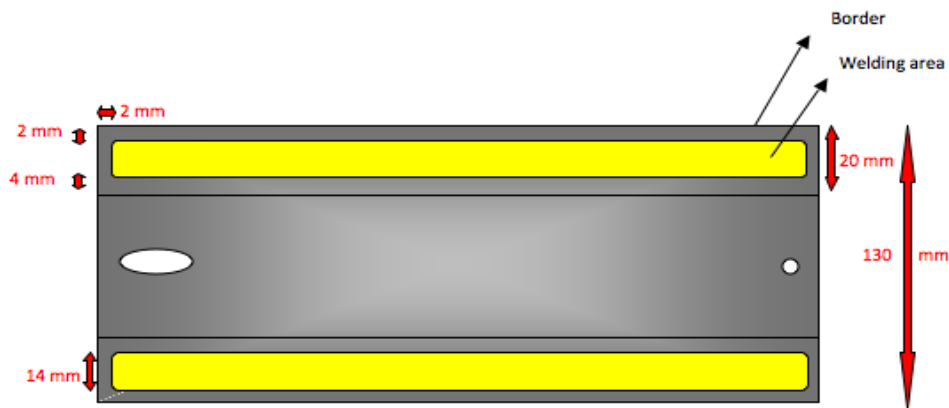


Figure 3.10: Frontal profile of parts affected by typical deformations impressed by shearing

Necessity of a 2-D median filter

The process of data capture is always full of noise because the reflection of this typical acquisition data system causes error during the calculation of coordinates values, especially on z-coordinate. In fact surfing parts (Error Maps), it can happen that some huge peaks are visible mostly on the edges.

These getting data systems are used to create noise during measurement phases, visible in high frequencies affecting parts.

For this problem the use of common high frequencies filters on data set is usual, in order to smooth parts and let them be affected by their real low frequencies deformations. To smooth image the use of several filters from image processing toolbox were possible.

Some mean filters like **fspecial**, **filter2** which can be applied to intensity images (2D matrices), **imfilterand** applied on multi-dimensional images (RGB images or 3D matrices), could be helpful.

All smoothing techniques are effective at removing noise in smooth patches or smooth regions of a signal, but adversely affect edges. Often though, at the same time as reducing the noise in a signal, it is important to preserve the edges.

Some other existing filters have a quite heavy impact on signals, because of their excessive smoothing power which create a loss of information. These common filters usually remove both high and low frequencies. Anyway the suggested one is the **medfilt2**, the 2-D median filtering offered by Matlab:

filter established: $B = \text{medfilt2}(A, [m \ n])$

This filter performs median filtering of the matrix A in two dimensions. Each output pixel contains the median value in the m -by- n neighborhood around the corresponding pixel in the input image. **medfilt2** pads the image with a vector of 0 on the edges, so the median values for the points within $[m \ n]/2$ of the edges might appear distorted.

Median filtering is a nonlinear operation often used in image processing to reduce "salt and pepper" noise. A median filter is quite effective when the goal is to simultaneously reduce noise and however preserve edges without losing data. So it consider low frequencies and do not remove them. The two advise parameters (m,n) for the filter application were already optimized and selected by a research work in IDL (UK):

$[Zc]=\text{medfilt2}(Zc, [4 \ 30])$

The values of $m = 4$ and $n = 30$ were an output of a set of trial and error experiments and attempts which pay attention to not smooth so much the parts deleting the deformation searched for, so maintaining intact the low frequencies and smoothing enough to not have anymore huge noise. The filter is used for the scatter data after the fundamental preprocessing phase.

3.3 Similarity analysis for the part-to-part control gap in a RLW

Objective of the work is to find an indicator in order to predict a good welding joint between two parts in a Remote Laser Welding assembly.

Parts are non perfect because always outputs of manufacturing processes, causing dimensional variations in excessive part-to-part gaps error.

Non perfect parts must fit perfectly, especially in remote laser welding, to improve a good coupling and minimize the gap between them.

To quantify the "goodness of fitting" between two general surfaces a part-to-part similarity study an be settled. Similarity analysis is conducted through some methods, partially developed in IDL.

Figure 3.11 presents some effects of imperfections on the gap error. Some possible deformed shapes of the channel's flange, all inside the tolerance range, can present different welding results. Depending on a flange's shape, the number of part-to-part gaps, their location, size and shape will be very different. If both parts are welded

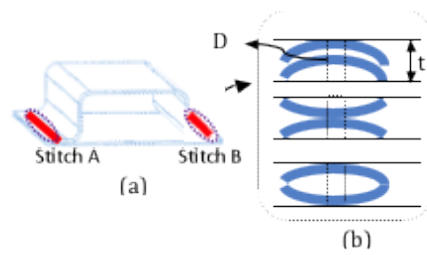


Figure 3.11: Imperfection of parts causing the gap

at location C, then the effort to close the gap will be dependent on the flange shape variation; hence, the importance of part's shape error similarity in the joining areas.

Usually, to evaluate the distance between two clamped parts which must be welded together, the resultant gap will be measured through filler, once forced by fixture pressure. So it's clear that, if gap assessment takes place before clamping, its value could be different than the one in the post-clamping situation because of fixture pressure. So the results about the welding areas weldability will be weak. In fact in automotive welding process clamping systems and their impact is relevant in holding parts with an acceptable distance between them.

The goal of the work is to avoid gap evaluations through filler after fixing parts by fixture positioning, predicting if they can be welded only analyzing their geometrical shape before clamping.

In this way the purpose is considered as a trial to predict the goodness of welding through some indicators, which can quantify the fitting between parts. The welding process will be foresee through a similarity analysis between the part's geometrical shapes; similarity usually is based on graphical analysis, so there is the necessity to find some indicators able to quantify how similar two parts are.

For this reason the indicators explained and used in the following analysis will be called "*Similarity index*" because of their peculiar characteristic to consider part's shape.

The fitting problem is relevant and every similarity index has the objective to quantify the goodness of the joint between two parts.

3.3.1 Similarity analysis methods

The following criteria proposes to develop a methodology to evaluate the goodness of fit between all the possible surfaces of parts matching taking into consideration their dimensional and geometrical variability. The proposed method will focus on evaluating

the degree of similarity between parts and use the resulting information as a criterion to determine the easiness of parts' fit.

1. Similarity index based on RLW algorithm
 - Hausdorff distance
 - Information Index
 - Entropy
2. Correlation
3. SMA analysis
 - Error Modes for each part
 - Frequency and Percentage of Error Modes shared between parts
 - Modes Magnitude
4. Shape Distribution

For each method will be presented a brief description of the work, the results obtained from the analysis and the encountered criticality with a judgment on the goodness of the indicator.

3.3.2 Similarity index based on RLW algorithm

The main idea of this work is to use an algorithm, developed in Warwick University, which takes the (x,y,z) points of surfaces for the parts to be welded and evaluates quantitatively the possible future welding through some index giving an idea of the fitting.

Consequently it is necessary to confirm if this index is properly and which one is the most robust and meaningful comparing them with gap measurements.

The first problem was to define a grid data, in order to standardize the reference system. This preprocessing phase is fundamental because it creates a matrix, both for all plates and all channels. If matrix will not be transformed, they cannot be put in comparison, otherwise a comparison for each point with the same coordinates can be done.

In fact the principal limit was that part surface measurements, which were not directly usable, because of their type and their big size. To be more precise, data came directly out from the acquisition of the scanner, a matrix representing the x,y,z coordinates in each column and 700.000 rows about, representing for each rows a precise (x,y,z) point, with a total of 700.000 points about.

The interpolation function must create 12 data matrices, one for each part available: measured points got during the acquisition were casually relieved on parts. Their (x, y) coordinate positions were not prefixed, but randomly distributed along the parts, so not always they are comparable. To calculate the distance between two points on two different surfaces they must respect the same collocation. The Transformation of this matrix into another matrix by fixing (x, y) coordinates and increasing only the value of z (error) was the way to sort the error affecting a surface (Gap Map).

In this way is possible to compare two parts and for example calculate the distance between one point on one surface and a second point on another surface. They must be aligned and refer to the same little area/section of the part.

First of all this code takes the value surfaces points coordinates of one plate and one channel, and it positions the top part on the bottom one through several rotation and translation of the top part only, but before using this main code was necessary to create a previous preprocessing phase to transform input data in a different required format.

In this case the algorithm used required some simple matrices in Gap Map format (which concerned only with the Z coordinates value). The original matrices were transformed into other matrices with (x, y) fixed and memorized by two vectors created and only the value of z (height) represented into the matrix, that is what is mean to be the error affecting a surface (Gap Map).

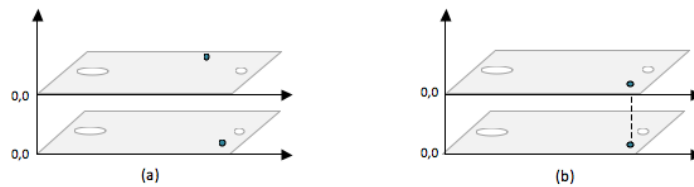


Figure 3.12: Alignment of parts: (a) not comparable points, (b) comparable points

Without the precise and established grid it's impossible to be confident in create a relationship between the two metallic part, because there is the risk to study the distance between two not corresponding points, which returns a failed results.

So it was clear the necessity of use a reference grid of data to make the points comparable and usable. The parts measurements were got all in the same way using the same reference axis even if the points got in one part can be different and allocated in some x, y position missing (not got) respect to the other part. Furthermore the number of points for each part is numerically very impressive and superfluous because some points are redundant e overlapped.

The grid was useful also for this secondary problem of points-selection and cloud-points filtering.

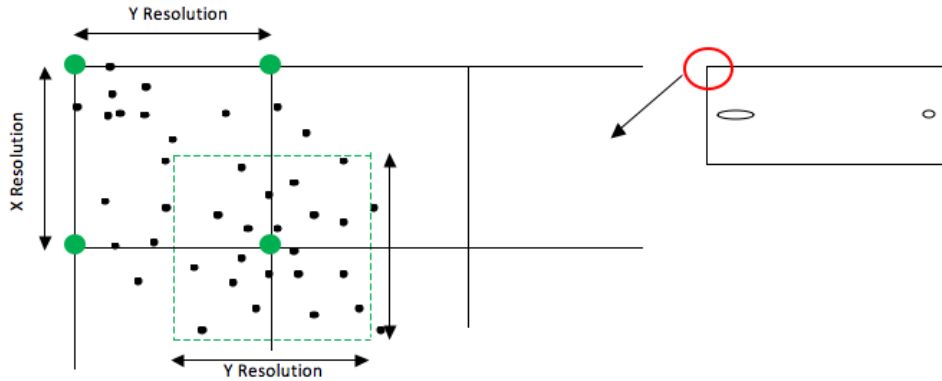


Figure 3.13: Scheme of transformation permitted by interpolation

The grid procedure is about defining the fixed incremental steps of X-Y resolution representing the size of one cell containing a group of casual disordered data. The grid is the distance between each x and y coordinate.

Referring to the image 3.13 scattered data are represented by the little black point, the gridded final point are the green ones. To lead black points to the green big point located at the intersections of the grid lines an interpolation function was used to transform the data in the right format.

The second step is focused in approximating all the points into a fixed selected area around the green point on one vertex of the grid interpolation. The selected areas have the grid points as center and their size and extension is defined by the resolution of the grid. Once fixed the Resolution, it was possible to know all the X-Y coordinates values for each gridded point, while the Z value is calculated interpolating all the Z values of the black points closed into the zone selected around the green one. The interpolation gives as result a mean value of all the Z coordinates value in the same zone.

Input to the Interpolation function: data.xyz for all the parts.

Output to the Interpolation function: "Synthetic parts", which is the error of the parts, called also "Error Map" because a reduced matrix with all the Z gridded values, while the X and Y coordinates are memorized in some other different reference vectors used every time. It's necessary to use the Synthetic part . Surfing the whole Synthetic part, it's possible to see this kind of figure representing the parts:

OUTPUT: Z_{Real} which represents the **ERROR MAP(EM)** of the parts, the gap

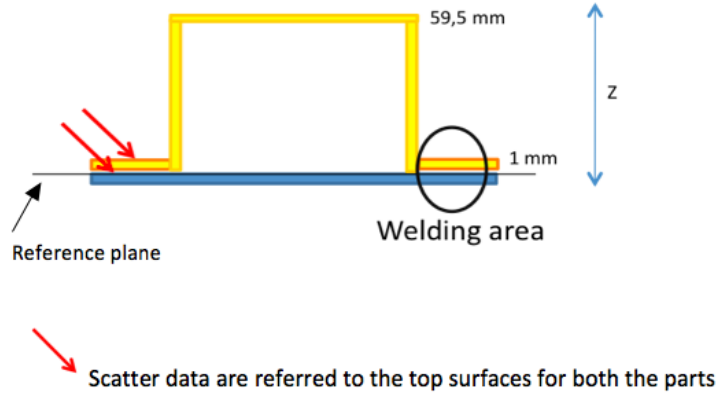


Figure 3.14: Synthesis for the measured points

between the measures of nominal and real parts. This transformation was necessary not only for the similarity indexes depending on the Master code, but also for the following SMA analysis and for the Shape Distribution Function, because input data for each algorithm are GMs. The grid used put X Resolution and Y Resolution value firstly equal to 1 mm, then reducing this value to 0.5 mm. In the first case there is the possibility to transform a matrix of (700.000 rows) x (3 columns) in another matrix of 600 rows and 130 columns of Z values, visibly and computationally easier to use.

A relaxing hypothesis was introduced: no variations in the thickness value of the parts, always considered constant and equal to 1 mm.

For the plates, data measured can be used directly, because the nominal plate has Z at the top surface equal to zero because perfectly on the reference plane:

$$ERRORMAP \rightarrow EM(plate) = Z_{Real} - Z_{nominal} = Z_{Real}$$

Once assumed constant thickness, for the channel is needed a sort of first not-real translation along Z axes of -1 mm, assigning the data obtained to the under surfaces of C-channel. The nominal channel under surfaces has Z equal to zero within the welding areas, 58.5 in the central section.

$$EM(channel) = Z_{Real} - Z_{nominal} = (Z_{Real} - 1) - Z_{nominal} = (Z_{Real} - 1)$$

Once obtained EM (plain) and EM (channel) it is possible to use some sections of the Master code developed in UK, an algorithm which places the top part above the bottom to calculate the value of the Similarity Indicators, returning their value as outputs.

The code will be run 36 times (for each possible couple).

Problems of the algorithm

As mentioned before, real data are affected by noise, visible on surfing parts. This noise is represented by peaks entering in contact with the other surfaces, increasing distances between parts and returning probabilities to have points satisfying requirements equal to zero.

Using the filter already mentioned, results are improved, but there is a big limit on this code: the allocating points are near each other. They appear in a little zone of the parts, putting in contact just one side or one edge of the parts and causing a deep distances on the other. That's because it is based on a geometrical model, which considers only the shape and geometry, but not the specific weight and mass of part.

A possible solution is to find three points of contact, and verify if the center of gravity is within the triangle of points: if it is not there, then should be useful to find the forth nearest point based on a generic angle and rotate the part along the side of triangle along the axis. The process will be repetitive until center of Gravity does not lie into the region of the selected points. A possible problem could be the loop, in which it can run because there is not any kind of solution. The problem could be solved introducing the center of mass gravity, but it's a very difficult approach and it would require to develop another entire work on this way (out of work). But without considering the specific mass, it will be impossible to reach the stability in the solution. A possible problem of penetration in parts must be considered and solved.

Alternative for the part balance problem

There are a lot of huge peaks at the part's edge which enter in contact with the other surface.

Using the already mentioned filter results were improved, but there is a big unsolvable limit on this code: when it finds the three points of contact, all of them are near each other. They appear in a little zone of the parts, putting in contact just one side or one edge of the parts and causing a deep distances on the other. It's a limited geometrical model, which considers only the shape and geometry, but not the specific weight and mass of part.

The three points of contact have been forced to be in three different zones along part. The algorithm acts in these steps: if the first point is placed in the first welding area the second one is constrained to follow in the second one, and vice versa. But to avoid the following situation which leads however to a big Hausdorff distance in case the third point was indifferently near one of them, also the last point of contact was obliged to

stay in a precise zone.

This method is quite invasive because it forces the code to find some points in specific area, otherwise the points without constraints are naturally falling in some others zones of the part which have the minimum distance.

Forcing the presence of contact points in specific areas, it's likely to have a possible problem of co-penetration within the parts after the third point of contact. Interferences between parts must be absolutely avoided because it's not physically possible and it's very dangerous from the good-quality of welding point of view.

Eliminating this risk, after the third point of contact is calculated the minimum distance between parts (the minimum gap), and if its value is negative it means there is a penetration between two parts, so in this case a translation of the top part on the bottom is done. The part is translated on the other one in order to have the minimum distance equal to zero.

Validation of the code

The code for the interpolation function is composed by Matlab function already optimized (Meshgrid and Griddata), so there was not necessary to validate and test it. While for the validation the similarity index was useful the creation of two non perfect parts (two plates) with known shape (identical) and dimensionally comparable, so the results of the index were already expected and well-known. For this agreed parts the Master code were used, and Indexes results were compared with their manual calculations on Excel.

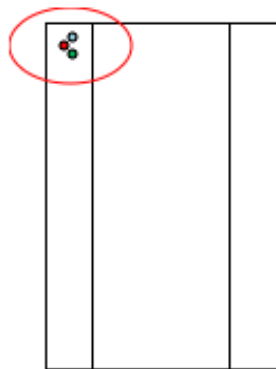
Going into detail:

- **Probability Map** calculation : if every distance for each couple of points satisfies the requirements ($GM < 0,3$), then put the point probability equal to 1, otherwise 0. The Probability has been calculated as the sum of the value of all the point probabilities divided by the total.

$$Dist_i = \begin{cases} 1 & x \leq 0,3 \\ 0 & otherwise \end{cases}$$

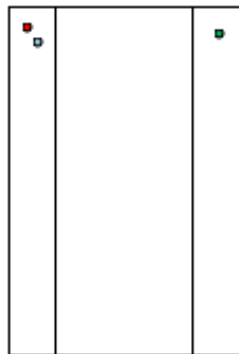
- **Correlation** has been calculated with excel *CORREL* function between the two stripes representing the same side.
- **Hausdorff distance** has been calculated as the maximum gap:

$$Max(distance) = max(GMvalues)$$



STARTING PROBLEM OF THE ALGORITHM:

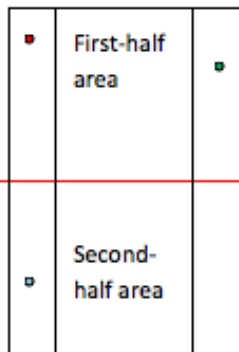
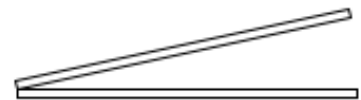
All the points are grouped in a small zone in the same welding area (left or right is the same), so the parts are completely not in balance (matlab plot)



The second point of contact between parts is forced to fall in the opposite welding area as regards the first one.

The third must be constrained only in this cases in which it appear near one of the previous two, otherwise the parts are not in contact on one side.

The typical situation presents the parts in contact on the border near the zone containing the points, and far on the other.



To fix the third point of contact was necessary the division of the parts in 2 half-areas, the first half starting from 0 to 300 mm and the second half from 300 to 600 (the whole length of the part). If the first and second points are in the same half-area, the third is forced to be in the other half area.

On the contrary, if the first two points are already in different half-areas and different welding areas, the third point is free to fall wherever, because the parts are already balanced on the opposite vertices.

Figure 3.15: Balance approach

- **Entropy Index** has been easily calculated as :

$$probability * Information\ index$$

because if the probability for each point can be 1 or 0, then the $\log(p)$ in case $p=0$ can give some problems. It's better to take the global probability for the welding area.

Results of the code and of the validation index calculations are the same. Concluding the output of the code is confident. All the code part-positioning functions, used before calculating the four indexes, have been calculated in the International Digital Laboratory of Warwick, owner of the whole RLW code.

For the aim of this work just some sections of that code was selected and used. Every run of the code load two set of data, the *Syntheticpart₁* (C-Channel) and a *Syntheticpart₂* (Plate), and after positioning the top part on the bottom one finding the three points of contact, the code calculates analytically the values of all these indexes for all 36 possible couplings.

3.3.3 Index descriptions

For each part couple were considered four indicators:

Hausdorff index (maximum distance)

The maximum gap at a given joining surface can be determined based on the Hausdorff distance between two EMs, and it is calculated as:

$$h(E_i^1, E_i^2) = \max(f(E_i^1, E_i^2), (E_i^2, E_i^1))$$

where in a general

$$f(A, B) = \max_{\forall a \in A} \min_{\forall b \in B} \|a - b\|_2$$

The similarity indices and the Hausdorff distance are complementary and provide a good description regarding how alike the joints' surfaces are, and which gap level can be expected. The most little are the gap value between two surfaces, the welding between the two parts is likely to be better quality [1].

Information Index

The analysis of the GM's content can be performed by borrowing tools that have been developed in the field of information theory. In particular, it is proposed first to determine the Information (I) contained on a GM. This can be calculated for the i -th GM as:

$$I_i = \log_2(p_i)$$

where p_i represents the probability of satisfying the joining requirements in the i -th GM. This can be estimated as the ratio between the numbers of points in a GM satisfying the joining requirements over the total number of points of the GM. The closer I is to zero, the more likely that the parts can be joined in that particular surface [1].

Entropy of the gap

The entropy (H) for a complete assembly having N number of joining surfaces can be calculated, following Shannon's definition, as:

$$H = \sum_{i=1}^n p_i I$$

The entropy of an assembly reflects the probability level of successfully joining the parts. On one hand, values of entropy close to 0 reflect cases where either all the joining surfaces satisfy or do not satisfy the tolerance requirements. On the other hand, entropy values close to the maximum 0.5 reflects that the near half of the surfaces satisfy the requirements [1].

3.3.4 Consideration from the analysis

Focusing the attention on the most meaningful output similarity index, which is the probability in predicting welding joint, is frequent to find mean-low probability value for one side and values equal to zero for the other even if the parts are balanced the one on the other.

That's because to avoid the co-penetration after the third point of contact found, a translation takes place and gets parts far the one from the other. Parts remain in contact in the point of maximum co-penetration, that is the smallest distance between points, but all the rest of the surface has no other points in common with its coupled.

As it's visible from the analysis, results are not promising. Most of the probability of welding quality are low values, but the worst aspect is the value zero quite frequent in matching parts (figure 3.16 and figure 3.17).

This problem reflects the physical limit of the algorithm, the missing of mass and specific weight of parts, because it is a geometrical model.

In fact this similarity index cannot be considered robust and reliable because of this main two aspects: the constraint of two points of contact and the leave out of the mass gravity centre.

Moreover putting in comparison those results obtained from the run of the code with the experimental data, there is not an evident and clear correlation between the two data sets, so this index is not the best indicator to predict a good quality welding at the moment, it requires some adjustments and revisions.

resY=1

resX=1

COUPLES	Hausdorff Distance		prob		Information index		Entropy Index	
	left	right	left	right	left	right	left	right
C1-P1	1,2219	1,9101	0,2617	0	1,9342	INF	0,50618014	NO VALUE
C1-P2	1,6316	0,6647	0,0158	0,3780	10,2216	1,4037	0,16150128	0,5305986
C1-P3	1,3082	1,7926	0,2717	0	1,8798	INF	0,51074166	NO VALUE
C1-P4	1,3216	1,7803	0,2282	0	2,1319	INF	0,48649958	NO VALUE
C1-P5	1,1674	1,8801	0,2247	0	2,1540	INF	0,4840038	NO VALUE
C1-P6	1,0898	2,0831	0,2239	0	2,1593	INF	0,48346727	NO VALUE
MEAN	1,2901	1,6852						
C2-P1	2,1459	1,8025	0,1156	0,0853	3,1131	3,5512	0,35987436	0,30291736
C2-P2	3,5392	2,3241	0	0,0620	INF	4,0121	NO VALUE	0,2487502
C2-P3	1,9940	1,2322	0,2883	0,1336	1,7941	2,9035	0,51723903	0,3879076
C2-P4	1,9286	1,8078	0,0296	0	5,0806	INF	0,15038576	NO VALUE
C2-P5	2,3221	2,1019	0,0627	0,0437	3,9955	4,5172	0,25051785	0,19740164
C2-P6	2,0223	1,6915	0,0997	0,0777	3,3268	3,6869	0,33168196	0,28647213
MEAN	2,3254	1,8267						
C3-P1	2,5341	4,5997	0,0915	0	3,4496	INF	0,3156	NO VALUE
C3-P2	1,4243	0,7853	0	0,3277	INF	1,6095	NO VALUE	0,5274
C3-P3	2,2409	4,1569	0,1969	0	2,3442	INF	0,4616	NO VALUE
C3-P4	2,1627	3,9011	0,2154	0	2,2152	INF	0,4772	NO VALUE
C3-P5	2,2105	4,1357	0,1112	0	3,1694	INF	0,3524	NO VALUE
C3-P6	2,5404	4,6130	0,0777	0	3,6869	INF	0,2865	NO VALUE
MEAN	2,1855	3,6986						

Figure 3.16: A sketch of result table (a)

resY=1

resX=1 COUPLES	Hausdorff Distance		prob		Information index		Entropy Index	
	left	right	left	right	left	right	left	right
C4-P1	0,5005	1,2794	0,7985	0,0292	0,3246	5,0982	0,2591931	0,14886744
C4-P2	2,0729	1,6019	0	0,0483	INF	4,3707	NO VALUE	0,21110481
C4-P3	0,6703	1,5667	0,3982	0	1,3285	INF	0,5290087	NO VALUE
C4-P4	0,592	1,1859	0,835	0,0054	0,2601	7,5371	0,2171835	0,04070034
C4-P5	0,4421	1,2533	0,9226	0,0136	0,1162	6,1961	0,10720612	0,08426696
C4-P6	0,4662	1,3343	0,6674	0,0279	0,5834	5,1648	0,38936116	0,14409792
MEAN	0,7907	1,3703						
C5-P1	1,1695	2,014	0,3693	0	1,437	INF	0,5306841	NO VALUE
C5-P2	1,4628	0,8706	0	0,3975	INF	1,3311	NO VALUE	0,52911225
C5-P3	1,1287	1,856	0,452	0	1,1455	INF	0,517766	NO VALUE
C5-P4	1,2767	1,9115	0,2931	0	1,7704	INF	0,51890424	NO VALUE
C5-P5	1,1807	1,9114	0,2212	0	2,1764	INF	0,48141968	NO VALUE
C5-P6	1,2308	2,2816	0,2286	0	2,1288	INF	0,48664368	NO VALUE
MEAN	1,2415	1,8075						
C6-P1	0,3791	1,0157	0,9982	0,1016	0,0026	3,2993	0,00259532	0,33520888
C6-P2	2,4980	1,5802	0	0,0962	INF	3,3779	NO VALUE	0,32495398
C6-P3	0,6442	0,9589	0,8308	0,0573	0,2674	4,1251	0,22215592	0,23636823
C6-P4	0,5306	0,7727	0,9178	0,3257	0,1237	1,6185	0,11353186	0,52714545
C6-P5	0,1878	0,9142	1	0,0956	1	3,3869	1	0,32378764
C6-P6	0,2456	1,1433	1	0,1176	1	3,0879	1	0,36313704
MEAN	0,7476	1,0642						

Figure 3.17: A sketch of result table (b)

3.3.5 Correlation Index

An important and useful index could be the correlation between same sides for each couple of parts (36 pairings). This index must be calculated before any kind of positioning data, it should be applied directly on the matrix of data, once has been selected the welding area.

The similarity between the EMs can be determined based on the correlation between them, and it is calculated for maps containing m elements or points represented as:

$$R_i = \frac{\sum_{k=1}^m (E_{ik}^1 - \bar{E}_i^1)(E_{ik}^2 - \bar{E}_i^2)}{\sqrt{\sum_{k=1}^m (E_{ik}^1 - \bar{E}_i^1)^2} \sqrt{\sum_{k=1}^m (E_{ik}^2 - \bar{E}_i^2)^2}}$$

where E_i^1 and E_i^2 stand for the mean of the i -th EM on the respective part. Values of R_i closer to 1 reflect higher levels of correlation, hence the similarity between the EMs. Additionally, values of R_i closer to -1 reflect that the EMs have similar shape but in the opposite direction (reflected or mirrored shapes).

Even though the correlation between two EMs determines how similar or dissimilar two EMs are, it is not sufficient to properly characterize the goodness of fit between the two joining surfaces, however. The reason is that the correlation does not capture any scaling relationships between the EMs. As an example, if one EM is the scaled factor of the other, then the value of R will be 1 for all values of the scaling factor. However, the gap or gaps between the maps can be very different. Such differences may even prevent a successful joining to take place [1].

Therefore, it is necessary to characterize the gap between the EMs by analyzing the information content in the GMs. Such analysis should provide an insight on the likelihood that the parts can be joined on each surface.

Values of Correlation closer to 1 reflect higher levels of correlation, so also the similarity between the Error Maps. Values of Correlation close to -1 reflect that the EMs have similar shape but in the opposite direction (reflected or mirrored shapes).

The correlation does not capture any scaling relationships between the EMs. If two parts have high values of correlation, it's likely they have the same trend (increasing or decreasing), but without the value of standard deviation any approval can be done, in this case the gap or gaps between the maps can be very different.

However this index could be helpful to understand the relationship between the assembly quality and part error, but only in a superficial and first analysis.

For example these two shapes ((a) and (b)) could have correlation index value near to 1, because they have the same trend. In reality their shape is not so similar because

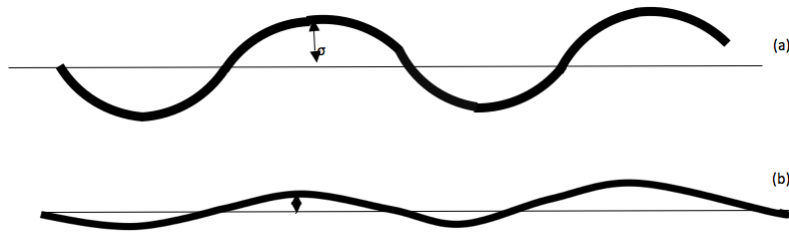


Figure 3.18: Variation problem of the correlation

the mean trend is the same, but the variation is very different. Only parts with mean and standard deviation equal can be considered similar. In this case so we just can see if the parts have the same trend, but it's hard to confirm they are similar through correlation.

- when Correlation value between parts is near to 0 : the probability of welding is quite low, so the parts cannot be considered similar, it's likely they will not be grouped in the same class;
- when Correlation value between parts is near to 1 and positive : the probability of welding is high and near to the value 1 (very high) so parts can be matched together;
- when Correlation value between parts is near to -1 (negative): the probability of welding should be quite lower because of opposite shape of parts in the areas considered. In this case parts will not be grouped. Considering this aspects, there will be grouped only parts having positive correlation value close to 1, visible and reflected also in the value of Probability.

So correlation can be indicative of how similar parts are, but just a rough estimation of the similarities among the parts. However, this index is not enough to explain the matching among the parts as it does not include the actual gap that has been taken into consideration while determining the correlation index which is vital for part weld ability.

In figure 3.19 and 3.20 results from case study.

The table 3.20 represents the correlation index values for the 36 possible coupling between parts and the G/T Ratio value only for the best and worst couples visible into the 7 best and worst cases of combinations. Established that a good quality probability is represented by Good to total Ratio value equal or bigger of 0,6 for a single mating, is possible to classify some couples in some clusters (in figure 3.20):

7 BEST COMBINATIONS												
P1	P2	P3	P4	P5	P6	G/T r1	G/T r2	G/T r3	G/T r4	G/T r5	G/T r6	Between the best combinations all couples could be acceptable from the G/T Ratio value point of view, only the one in the red profile have low value (less than 0.6). The same is reported for the 7 worst combinations, in which there are coupling to be avoided into the red profiles.
C5	C3	C4	C2	C6	C1	1	0,6667	0,6	0,8	1	0,8667	
C5	C3	C2	C6	C1	C4	1	0,6667	0,6	1	1	0,6667	
C5	C3	C2	C1	C6	C4	1	0,6667	0,6	1	1	0,6667	
C5	C4	C2	C6	C1	C3	1	0,5333	0,6	1	1	0,8	
C5	C4	C2	C1	C6	C3	1	0,5333	0,6	1	1	0,8	
C5	C2	C4	C6	C1	C3	1	0,5333	0,6	1	1	0,8	
C5	C2	C4	C1	C6	C3	1	0,5333	0,6	1	1	0,8	
7 WORST COMBINATIONS												
P1	P2	P3	P4	P5	P6	G/T r1	G/T r2	G/T r3	G/T r4	G/T r5	G/T r6	
C4	C6	C1	C3	C5	C2	0,8	0,2667	0,5333	0,733	0,6	0,6	
C3	C6	C1	C4	C2	C5	0,733	0,2667	0,5333	0,733	0,6	0,6667	
C2	C6	C1	C3	C5	C4	0,733	0,2667	0,5333	0,733	0,6	0,6667	
C3	C6	C1	C5	C4	C2	0,733	0,2667	0,5333	0,867	0,467	0,6	
C3	C6	C1	C2	C4	C5	0,733	0,2667	0,5333	0,8	0,467	0,6667	
C3	C6	C1	C4	C5	C2	0,733	0,2667	0,5333	0,733	0,6	0,6	
C2	C6	C1	C3	C4	C5	0,733	0,2667	0,5333	0,733	0,467	0,6667	

Figure 3.19: G/T Ratio Gap Measurements

- The violet couples are the most promising between all the matching presented into the 7 best combination of couple obtained from gap measurements;
- The blue couples are the less promising between the 7 best combinations because of their value lower than 0,6;
- The orange couples contain the worst G/T Ratio value couples present into the 7 worst combinations, so they are coupling to be avoided during for the welding process.

It's quite clear that high G/T Ratio values coupling should be characterized by correlation index near to 1. But what is observed is different: some of them have very low correlation value, also near to zero in some cases even if they refers to a very promising couple from the welding point of view.

And some matching, like Plate1-Channel5 have definitely low correlation value to represent one of the strongest best one. Also the situation of the matching Plate4-Channel1 reveals this incongruity in terms of having the highest G/T Ratio value associated to a nearly zero value correlation.

		correlaton INDEX	G/T ratio			correlaton INDEX	G/T ratio
plate1	channel1	0,5493		plate4	channel1	-0,0178	1
plate1	channel2	0,7952		plate4	channel2	0,4416	0,8
plate1	channel3	0,562		plate4	channel3	0,3469	
plate1	channel4	0,6783		plate4	channel4	0,3366	
plate1	channel5	0,4659	1	plate4	channel5	0,3823	
plate1	channel6	0,4882		plate4	channel6	0,1964	1
plate2	channel1	0,9277		plate5	channel1	0,3145	1
plate2	channel2	-0,3689	0,53333	plate5	channel2	0,1701	
plate2	channel3	0,7246	0,66667	plate5	channel3	0,3418	
plate2	channel4	0,7658	0,5333	plate5	channel4	0,306	0,4666
plate2	channel5	0,047		plate5	channel5	0,3716	
plate2	channel6	0,59	0,267	plate5	channel6	0,2904	1
plate3	channel1	0,1843	0,5333	plate6	channel1	0,8887	0,8667
plate3	channel2	0,1154	0,6	plate6	channel2	-0,61	
plate3	channel3	0,0747		plate6	channel3	0,4446	0,8
plate3	channel4	0,3616	0,6	plate6	channel4	0,599	0,66667
plate3	channel5	0,1125		plate6	channel5	-0,2118	
plate3	channel6	0,3014		plate6	channel6	0,4084	

Figure 3.20: Correlation values for the best and worst combinations

This cases of inconsistency are several, so it's clear the absence of meaningful connection between the correlation indicator and what is the real situation of the case.

Weakness of index

This index cannot be considered a strong method because in the sphere of application. If Correlation index values and experimental filler data are compared, any conclusion can be done, because they are got under different system conditions. Correlation values are got before fixing the parts with clamps and without any positioning of the top part on the bottom one. On the contrary filler data are measured fixing the parts, so deforming them through the application of the clamps forces. In this second case it's likely the part in the welding area, under the stress impressed by the pressure, change its shape. So we don't necessarily expect to find high positive value of correlation in those real combination in which the G/T ratio is very high. This index therefore will be not considered very robust to predict the welding quality.

Conclusion of results

Comparing results of correlation analysis and experimental data study, the relationship between the different results is quite absent. It seems to miss the link between what observed in one and what is explained by the other, and this result is definitely clear and visible analyzing some possible existing relationship between them, which is lacking.

In figure B.1 every blue colour row represents some combinations composed by six parts coupling each. For each couple in every line, the found correlation value is reported. Every correlation value is compared with the G/T Ratio value, which should be linked and influenced to the correlation. Checking the situation, there is the lack of any link between the indicator and the real situation.

In the figure 3.21 the complete lack of linkage between correlation index values and experimental data is clear because their correspondence is totally random.

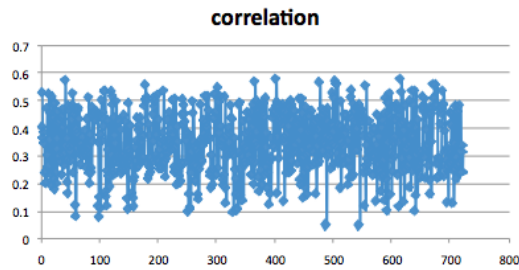


Figure 3.21: Absent correspondence between correlation index and Gap measurements

As blatant from this last graph and from the correlation values of the best combination, it's clear the less of relation between the analysis conducted on real parts and scattered data. For this reason this index is also excluded from the following analysis on selective assembly.

3.3.6 Shape Distribution Index

This is a method which finds the shape distribution of the parts for every single side of all channels and plates studied and then it calculates the distances between a couple of distributions based on the differences between their features and/or their spatial relationship.

Determining the similarity between 3D shapes is a fundamental task in shape-based recognition, retrieval, clustering and classification. Its main applications have traditionally been in computer vision, mechanical engineering and molecular biology. However, due to recent developments, 3D model databases will become ubiquitous and the applications of 3D shape analysis and matching will expand into a wide variety of other fields [12].

The proposed method is not only fast and simple to implement, but it also provides useful discrimination of 3D shapes and thus is suitable as a pre-classifier for a recognition or similarity retrieval system.

The key idea is to represent the signature of an object as a shape distribution sampled from a shape function measuring global geometric properties of an object [12].

The primary motivation for this approach is to reduce the shape matching problem to the comparison of probability distributions, which is simpler than traditional shape matching methods that require pose registration, feature correspondence, or model fitting.

Many previous approaches have difficulty with 3D polygon soups because they invariably require a solution to at least one of the following difficult problems: reconstruction, parameterization, registration or correspondence. The motivation behind this index is to develop a fast, simple and robust method for matching 3D polygonal models without solving these problems.

The approach is about representing the shape signature for a 3D model as a probability distribution sampled from a shape function measuring geometric properties of the 3D model. This generalization of geometric representation is called shape distribution.

Once the shape distributions for two objects is computed, the dissimilarity between the objects can be evaluated using any metric that measures distance between distributions (e.g., LN norm), possibly with a normalization step for matching scales

To briefly review, prior matching methods can be classified according to their representations of shape: 2D contours, 3D surfaces, 3D volumes, structural models, or statistics. The vast majority of work in shape matching has focused on characterizing similarity between objects in 2D images. Unfortunately, most 2D methods do not extend directly to 3D model matching and their main problem is boundary parameterization.

The key idea of this approach is to transform an arbitrary 3D model into a parameterized function that can be compared with others easily and thus this index can be used for similarity queries [12].

Shape Function selection

The first and most interesting issue is to select a function whose distribution provides a good signature for the shape of a 3D polygonal model. Ideally, the distribution should be invariant under similarity transformations and tessellations, and it should be insensitive to noise, cracks, tessellation, and insertion/removal of small polygons. In general, any function could be sampled to form a shape distribution, but we focus on purely geometric shape functions based on simple measurements [12].

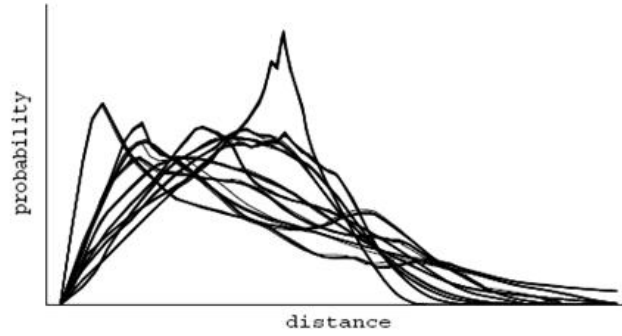
Specifically, the following shape functions have been experimented:

- A3: Measures the angle between three random points on the surface of a 3D model.
- D1: Measures the distance between a fixed point and one random point on the surface. The centroid of the boundary of the model method is used as the fixed point.
- D2: Measures the distance between two random points on the surface.
- D3: Measures the square root of the area of the triangle between three random points on the surface.
- D4: Measures the cube root of the volume of the tetrahedron between four random points on the surface.

All of these function are invariant to tessellation of the 3D polygonal model, since points are selected randomly from the surface. They are insensitive to small perturbations due to noise, cracks, and insertion/removal of polygons, since sampling is area weighted.

The one called D2, represents the distribution of Euclidean distances between pairs of randomly selected points on the surface of a 3D model. Samples from this distribution can be computed quickly and easily, while the hypothesis is that the distribution describes the overall shape of the represented object. In each plot, the horizontal axis represents distance, and the vertical axis represents the probability of that distance between two points on the surface.

The image below represents D2 shape distributions for seven variants of ten models.



Having constructed the shape distributions for two 3D models, the task of comparing them is remained to produce a dissimilarity measure. There are many standard alternatives of comparing two functions. In this implementation, dissimilarity measures are based on LN norms of the probability density functions (pdfs) and cumulative distribution functions (cdfs)

- PDF L_N : Minkowski L_N norm of the pdf $D(f, g) = \int |f - g|^N)^{1/N}$ [12]
- CDF L_N : Minkowski L_N norm of the cdf $D(f, g) = (\int |\hat{f} - \hat{g}|^N)^{1/N}$ [12]

PDF L1 norm performed the best for comparing shape distributions [12]. In general, the pdfs did better than the cdfs, possibly because peaks and valleys of pdf curves are easier to discriminate using LN norms than the steep areas and plateaus of cdf curves. L2 and L1 norms performed worse than the L1 norms.

Applying the validated properly shape distribution algorithm on UK parts, the results coming out from all the 36 coupling are the following table 3.5.

		PDF			CDF		
		Similarity Norm			Similarity Cumulative		
		Norm_1	Norm_2	Norm_inf	Norm_1	Norm_2	Norm_inf
plate1	channel1	26,9822	4,18	0,86	1696,7	198,8	25,8
plate1	channel2	6,0087	1,241	0,4171	68,97	9,6253	2,404
plate1	channel3	9,9494	2,0022	0,7376	512,6134	66,6	9,5019
plate1	channel4	8,84	1,9114	0,705	458,67	59,15	8,1941
plate1	channel5	6,4817	1,292	0,3959	279,35	39,88	6,3407
plate1	channel6	5,909	1,17	0,5254	56,22	7,59	1,9876
plate2	channel1	25,7184	3,8346	0,866	1645,6	192,6	25,3
plate2	channel2	10,1395	1,9778	0,7475	81,8087	14,3317	4,7
plate2	channel3	9,1829	1,7217	0,5566	461,53	61,0379	8,99
plate2	channel4	7,8915	1,5649	0,535	407,599	53,373	7,68
plate2	channel5	9,4532	1,8611	0,719	252,12	36,3152	5,8319
plate2	channel6	6,4074	1,2	0,6322	35,45	5,345	2,0417
plate3	channel1	25,0403	3,7489	0,766	1453,6	168,3	22,6
plate3	channel2	8,2533	1,6621	0,7179	227,827	29,5946	5,1
plate3	channel3	8,417	1,54	0,502	169,58	34,87	6,182
plate3	channel4	8,586	1,5455	0,478	215,65	28,2397	5,6553
plate3	channel5	5,9708	1,26	0,5101	68,3691	8,8265	1,696
plate3	channel6	6,3683	1,327	0,6322	202,56	28,1869	4,5756

Table 3.5: Norm_1, Norm_2, Norm_inf for the best-worst matching (a)

Established that a good quality probability is represented by Good to total Ratio value equal or bigger of 0,7 for a single mating, is possible to classify some couples in some clusters: the violet couples are the most promising between all the matching presented into the 7 best combinations of couples obtained from gap measurements study .

This couples are the less promising between the 7 best combinations because of their value lower than 0,7. This cluster contains the worst G/T Ratio value presents into the 7 worst combinations, so they are coupling to be avoided during for the welding process.

In figure 3.5 and figure 3.6 green and red values are the minimum distance values for a fixed plate coupled with all the six channels between all the other value along the column for that precise plate.

The value is green colored if what predicted by the shape distribution index is the same of what appears in the gap measurements (violet couples), so if a couple is the best matching (which minimize the distances between two distributions) for both the approaches. Otherwise, the value is red painted.

		Similarity Norm			Similarity Cumulative		
		Norm_1	Norm_2	Norm_inf	Norm_1	Norm_2	Norm_inf
plate4	channel1	28,315	4,4316	0,914	1772,5	208,5	27,3
plate4	channel2	3,882	0,9149	0,4381	106,5012	15,1228	2,41
plate4	channel3	11,4025	2,5324	0,86	588,4155	76,868	10,718
plate4	channel4	11,05	2,4719	0,8843	534,47	69,484	9,9888
plate4	channel5	7,8434	1,7968	0,7651	355,26	49,658	7,5568
plate4	channel6	4,4211	0,8995	0,5418	126,84	15,86	2,9
plate5	channel1	30,8313	4,6764	0,9726	1912,1	226,5	30,1
plate5	channel2	5,5612	1,408	0,6201	230,5961	34,1845	5,451
plate5	channel3	14,0792	2,828	0,9517	728,0122	95,7358	13,7552
plate5	channel4	12,83	2,71	0,9321	674,07	88,18	12,4474
plate5	channel5	10,61	2,19	0,7612	494,75	68,931	10,594
plate5	channel6	6,519	1,1392	0,517	266,43	34,424	5,09
plate6	channel1	24,21	3,5736	0,7453	1499	175,6	23,3
plate6	channel2	11,2191	2,05	0,712	181,53	26,06	6,1897
plate6	channel3	11,5901	2,1632	0,6588	344,5	46,1933	6,928
plate6	channel4	10,13	2,0133	0,6338	290,3	38,4418	5,62
plate6	channel5	11,9621	2,1833	0,6835	207,18	26,59	4,0766
plate6	channel6	5,84	1,25	0,6238	146,81	18,5	9,377

Table 3.6: Norm_1, Norm_2, Norm_inf for the best-worst matching (b)

Between the six indicators belonging to this family, the most robust seems to be the probability density function using the infinite norm, because for almost each considered plate, the minimum distance value corresponds to the top part pointed out also from gap measurements. There is clearly a sort of parallelism. All the other five pointers are not able to predict a good mating between all the parts. In this analysis must be also considered the fact that the promising index Similarity Norm inf can predict with the minimum value just one good-fitting matching for a plate choosing the best channel to be pair with. But if more than one channel to be well-welded with a plate is present, it will be not signaled clearly by the indicator. In fact often the lower value after the minimum one does not belong to the others good couples suggested by gap results.

To understand more from this index is necessary to study the distribution differences between two parts. Analyzing the shape distributions for all the most meaningful parts couples the best couples are represented in figure3.22.

Going into detail, it is possible to analyze specifically all the couples showing G/T

P1	P2	P3	P4	P5	P6	G/T r1	G/T r2	G/T r3	G/T r4	G/T r5	G/T r6	Average G/T ratio
C5	C3	C4	C2	C6	C1	1	0,6667	0,6	0,8	1	0,8667	0,822222222
C5	C3	C2	C6	C1	C4	1	0,6667	0,6	1	1	0,6667	0,822222222
C5	C3	C2	C1	C6	C4	1	0,6667	0,6	1	1	0,6667	0,822222222
C5	C4	C2	C6	C1	C3	1	0,5333	0,6	1	1	0,8	0,822222222
C5	C4	C2	C1	C6	C3	1	0,5333	0,6	1	1	0,8	0,822222222
C5	C2	C4	C6	C1	C3	1	0,5333	0,6	1	1	0,8	0,822222222
C5	C2	C4	C1	C6	C3	1	0,5333	0,6	1	1	0,8	0,822222222

Figure 3.22: best couples between UK-parts

Ratio value equal to 1, representative of highest welding quality value. The optimal couple **P1-C5** presents in all the best combinations of couples shows a similarity in shape distributions of the two involved parts (figureC). In the same way also the couple **P4-C6** and **P4-C1**, ten **P5-C6** and **P5-C1** with very high G/T ratio value. Also the other less representative couples like P4-C2, P6-C1 and P6-C3 are promising seeing their shape distributions. Optimal coupling seems to be always well represented by similar distributions.

Analyzing the medium-low level G/T Ratio value couples belonging to best combinations, they are described by almost different distribution characterized by different and singular features present in just one of the distributions, like the peaks shown in P3, P2 and again in P6.

Analyzing now the 7 worst combinations, it is evident and clear the situation of mostly three couples:

P2-C3 distributions appear different and are explained by the low G/T Ratio value.

P3-C1 distributions are most near in their trend, and this similarity is seen also through the little bit higher G/T Ratio value of this couple.

In comparison with P3-C1, the **P5-C4** couple has a variety between distribution more important and visible, explained through the lower G/T Ratio value.

All the possible combinations are visible in the next tables linked in the appendix C at the end of the work, the first column figuring P1 and P2 with all the possible plates, the second one P3 and P4, the third P5 and P6.

P1	P2	P3	P4	P5	P6	G/T r1	G/T r2	G/T r3	G/T r4	G/T r5	G/T r6	Average G/T ratio
C4	C6	C1	C3	C5	C2	0,8	0,2667	0,5333	0,733	0,6	0,6	0,588888889
C3	C6	C1	C4	C2	C5	0,733	0,2667	0,5333	0,733	0,6	0,6667	0,588888889
C2	C6	C1	C3	C5	C4	0,733	0,2667	0,5333	0,733	0,6	0,6667	0,588888889
C3	C6	C1	C5	C4	C2	0,733	0,2667	0,5333	0,867	0,467	0,6	0,577777778
C3	C6	C1	C2	C4	C5	0,733	0,2667	0,5333	0,8	0,467	0,6667	0,577777778
C3	C6	C1	C4	C5	C2	0,733	0,2667	0,5333	0,733	0,6	0,6	0,577777778
C2	C6	C1	C3	C4	C5	0,733	0,2667	0,5333	0,733	0,467	0,6667	0,566666667

Figure 3.23: Worst couples between UK-parts

3.3.7 SMA index

Statistical Modal Analysis (SMA) based virtual assembly method was usually applied to simulate product and process error into a nominal part, but in this case of study it has been used as similarity index to predict the quality of the welding before parts are clamped. The SMA analysis offers a discrete-cosine-transformation (DCT) decomposition method, whose aim is to extract the dominant modes from the measurements of error represented by the Error Map, and model this form error. In this way the error field (the whole surface of the part) is entirely decomposed into a series of independent error modes (called also normal modes).

The purpose of incorporating DCT in SMA is to take advantage of some of the characteristics of the measured data so that the energy of the transformed data is localized into a small number of coefficients associated with the dominant modes [16]. In fact *compression*, which ensures a compact model, is achieved by correlation reduction or mode truncation based on good energy compaction property of DCT. The transformation has been proven to be equivalent to least square regression with 2D cosine-base for modeling of part variation pattern. Estimation of these parameters in the model has also been developed [8]. The proposed method was applied to model and evaluate assembly and stamping errors at one of the US stamping plant.

Through this function, the part error related to assembly process (rigid body modes) and part distortion during manufacturing (deformation modes) can be separated and identified [8].

Because this method showed an optimal prediction of experimental data, the explanation of the complete index is proposed in the next chapter.

Chapter 4

Statistical modal Analysis based on Discrete Cosine Transformation

In a manufacturing system, the presence of a different complexity for a part can be present and the current parameterized tolerance techniques confront great difficulties.

For example, in automotive industry the body is comprised of hundreds of sheet metal parts. Reducing the geometric variation of an auto body is particularly important not only for functionality (proper functioning, avoidance of water leak, wind noise, aesthetic), but also for manufacturability and suitability for assembly [8].

Dimensions due to geometric part complexity cannot simply define the specifications of most of these parts.

Current tolerance models are not yet satisfactory in simulating the effect of the manufacturing process on part geometry. It is an enormous challenge to develop a model, which conforms to the tolerance zone suggested by standard and helps to generate instances statistically to simulate part manufacturing process statistics for tolerance analysis [8].

In this contest, it could be useful to be able in predicting the quality of the final product as soon as possible. More the control is supervised up stream, less errors are added during the production cycle.

The following chapter will introduce the complete description of the method used for the similarity analysis between parts. The discrete cosine transformations are a good method to be able to evaluate the goodness of fitting between two parts. Until now, DCT has never been used

4.1 Purpose of the SMA

The application of SMA in this work looks ahead, because the aim is to apply the approach with real part, which are non perfect, to predict the quality of the welding joint. In fact this Analysis offers the use of a **discrete cosine transformation** (DCT) decomposition method, whose aim is to extract the dominant modes from the measurements parts error represented by the Error Map and model a form error following the profile of the part.

In this way the error field (the whole profile of the part) is entirely decomposed into a series of independent error modes (called also normal modes).

Usually DCT is used in manufacturing processes to automatic inspection of shape defects using this specific image filtering strategy. In fact to describe and control form error, the main step is to be able to define it.

In order to work on surfaces a mathematical model is needed to identify and compare part by part: to have a correct form defect study only, useless information must be removed from measurement signal. Firstly an interpolation, as mentioned in section 3.3.2, in specific points must have been made, in order to remove the most relevant errors, caused by the capture of part and standardize the coordinates set, to have an equal grid. But the fundamental step is the removal of waviness and roughness defects as well as CMM (coordinates measurement machine) uncertainties. This can be done by filtering data points got after measurement operation, because CMM introduces randomly errors around the surface on every node of the grid (every millimeter).

DCT is used for filtering errors because a decomposition of part in more frequencies would find more sense: the different defects can be classified by their wavelength, and suppressing high frequencies cosine function is possible to remove roughness defects to let the profile with only the desired form defect.

The DCT method is usually well-known for its implementation in data compression in image processing or for profiles-surfaces decomposition from a technological point of view, helping to find defects origin along a manufacturing process in order to reduce global form error and interview on the process introducing errors. Differently in this work DCT is proposed from a new point a view : it will be used for a wave profile decomposition in order to identify a shape similarity between couples of parts, so it will be considered for the shape similarity study between two profile in order to classify parts based on their differential geometry. The basic theme of the work is focused on the selective assembly strategy, but to classify adequately and cleverly parts in different classes it's needed an indicator able to distinguish different parts characteristics and

later classify them to permit an efficient selective assembly implementation.

Another way to describe free-form surfaces is based on the use of parametric surfaces as **NURBS** or **BSpline** surfaces, which can be considered valid methods to describe surface, if a sufficient number of nodes is used in order to obtain a significant surfaces representation [33] [20]. The problem in using this kind of methods is given to their impossibility in bringing an easy way to *filter* measured data in order to extract different errors forms from the global part surface, so for example it won't be possible to distinguish singularly and separate defects like waviness, roughness and measurements uncertainties. For this reason is supposed to be more adequate the use of a statistical modal surfaces description [7]

The goal of this work is to use an indicator developed on a mode-based decomposition technique to create an error representation. This technique provides a basis for establishing a surface-based variational model, which is suitable for implementation in statistical geometric tolerances. This index has the objective to solve the limit how to describe the statistical properties of the part form error field by developing unified math model with minimum number of independent variables. Form error field in this model is defined as the difference of actual and nominal surface feature.

Two hypotheses are introduced to simplify the modeling process:

Smoothness assumption : form error field signal has sufficient smoothness such that the high spatial frequency components (short wavelength error such as surface roughness and waviness) are small and can be ignored. This assumption implies that form error is highly spatially correlated [8].

Height field assumption: the form error of a part feature (surface) can be represented as a height field function $f(x,y)$ defined in 2D domain, which is a stationary random field process [8].

In general, part form error field can be sampled as discrete space signals by CMM measurements.

In order to minimize the number of parameters in describing this form, the correlation reduction technique, such as orthogonal transforms commonly used in digital image processing, can be applied [8].

The sampled error data set $f(n,m) = f(n\Delta(x), m\Delta(y))$, where n and m represent sample size in two axes, is transformed into spatial frequency domain [8].

The used transformation has the property of selecting number of transform coeffi-

cients in the model to reduce correlation between error data points. For typical *smooth* error field a large amount of *signal energy* is expected to be concentrated in a small fraction of the transform coefficients [8].

Let \vec{v} represents the measurement of the deformed part, where, $\vec{v} \in R^{m \times l}$ [1].

Then the *error mode* can be determined using the following equation:

$$\tilde{C}(u, v) = \sqrt{\frac{2}{m}} \sqrt{\frac{2}{l}} \sum_{i=0}^{m-1} \sum_{j=0}^{l-1} \alpha_i \alpha_j \cos\left[\frac{\pi u}{2m}(2i+1)\right] \cos\left[\frac{\pi v}{2l}(2j+1)\right] \vec{v}(i, j) [1]$$

where

$$\alpha(\xi) = \begin{cases} \frac{1}{\sqrt{2}} & \text{if } \xi \geq 0 \\ 0 & \text{otherwise} \end{cases} [1]$$

$C(u, v)$ represents the **amplitude** of the cosine wave with frequency $k=u, v$, and approximately behave as gradient of the data. Thus, $C(u, v)$ gives the rough approximation of the overall deformation of the part. The SMA decomposes these part deformations into few error from deformed modes defined by DCT (discrete cosine transformation) kernels used in the algorithm [1].

4.2 SMA method

The SMA model is based on the *discrete cosine transformation*, a function expressing a sequence of finitely many data points in terms of a sum of cosine functions oscillating at different frequencies. DCTs are important to numerous applications in science and engineering, from lossy compression of audio and images where small high-frequency components can be discarded, and in spectral methods for the numerical solution of partial differential equations.

The use of cosine rather than sine functions is critical in these applications: for compression, it turns out that cosine functions are much more efficient, whereas for differential equations the cosines express a particular choice of boundary conditions [2].

In particular, a DCT is a Fourier-related transform similar to the discrete Fourier transform (DFT), but using only real numbers. DCTs are equivalent to DFTs of roughly twice the length, operating on real data with even symmetry [2].

The discrete cosine transformation of a sequence $x(n)$ of length N , is a sequence $X(k)$ of length N , defined by:

$$X(k) = \sqrt{\frac{2}{N}} \alpha(k) \sum_{n=0}^{N-1} x(n) \cos \left(\pi \frac{k(2n-1)(k-1)}{2N} \right) \quad [30]$$

with:

$$\alpha(k) = \begin{cases} 1/\sqrt{N} & \text{if } k = 1 \\ \sqrt{2/N} & \text{if } 2 \leq k \leq N \end{cases} \quad [30]$$

while the *inverse discrete cosine transformation* of a sequence $X(k)$ of length N , is a sequence $x(n)$, of length N , defined by :

$$x(n) = \sqrt{\frac{2}{N}} \sum_{k=0}^{N-1} \alpha(k) X(k) \cos \left(\pi \frac{k(2n-1)(k-1)}{2N} \right) \quad [30]$$

where:

$$\alpha(k) = \begin{cases} 1/\sqrt{N} & \text{if } k = 1 \\ \sqrt{2/N} & \text{if } 2 \leq k \leq N \end{cases} \quad [30]$$

This transformation is similar to the Fourier transformation, with the difference that the cosine transformation does not consider the sine frequency. The development of only the cosine sign is possible if only the Fourier transformation is real pure, that is the sign is equal (symmetrical around the 0).

The principal properties of DCT transformation are:

- *Decorrelation* : the principle advantage of image transformation is the removal of redundancy between neighboring points. This leads to uncorrelated transform coefficients which can be encoded independently. Hence, it can be inferred that DCT exhibits excellent decorrelation properties [22].
- *Energy Compaction*: efficacy of a transformation scheme can be directly gauged by its ability to pack input data into as few coefficients as possible. This allows to discard coefficients with relatively small amplitudes without introducing visual distortion in the reconstructed image. DCT exhibits excellent energy compaction for highly correlated data and it is perfect for the aim of this work. In fact through this function is possible to obtain **low high-frequencies**: they are the most representative manufacturing deformation on a part, while low frequencies can be omitted because not representative for similarity studies.

The DCT contains impulses with amplitudes proportional to the weight of a particular frequency in the original waveform [22].

- *Symmetry and Separability* :the property known as separability has the principle advantage that $C(u, v)$ can be computed in two steps by successive 1-D operations on rows and columns of an image. The arguments presented can be identically applied for the inverse DCT computation. Another look at the row and column reveals that these operations are functionally identical. Such a transformation is called a symmetric transformation [22].

There are eight standard DCT variants, about which four are common. The most common variant of discrete cosine transform is the type-II DCT, often called simply "the DCT". The DCT, and in particular the DCT-II, is frequently used in signal and image processing, especially for lossy data compression, because it has a strong "energy compaction" property ¹: when applying the DCT to a signal, a higher ratio of the energy is concentrated in a smaller number of coefficient relative to the Fourier transformation, approaching the Karhunen Loeve transform (which is optimal in the decorrelation sense) for signals based on Markov processes. As shown in the graphic 4.1, the firsts four modes cover more than 98% of energy compaction.

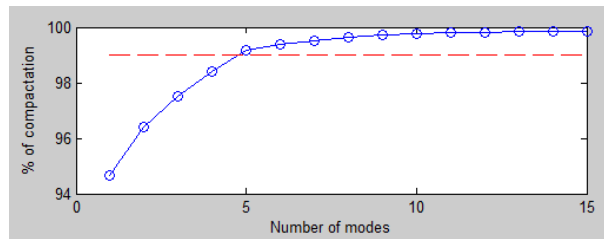


Figure 4.1: Pareto diagram

¹www.wikipedia.com

4.3 Index Visual Interpretation

The form error surface or field is represented as a combination of a series of mode components as illustrated in figure 4.2.

Each mode can represent various manufacturing error patterns. For example, the rigid body mode (Mode 1) can represent assembly fixturing positioning error; deformation mode (Mode 2 or 3 or the others) can represent part distortion (bending) during stamping operations [8].

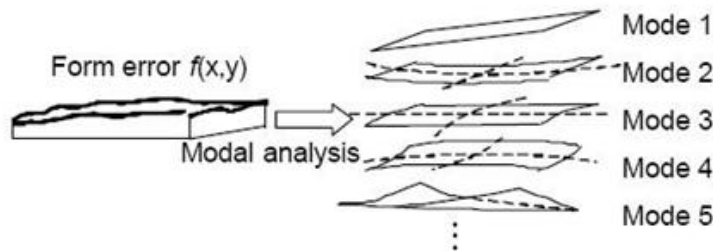


Figure 4.2: Error Modes Creation

Coefficients of DCT and corresponding modes can provide easy-to-interpret illustration of the part of subassembly error field. The superposition of the first modes approximately represent the rigid modes of the form error field. These coefficients provide the information of the significance of each individual mode's contribution to the total form error.

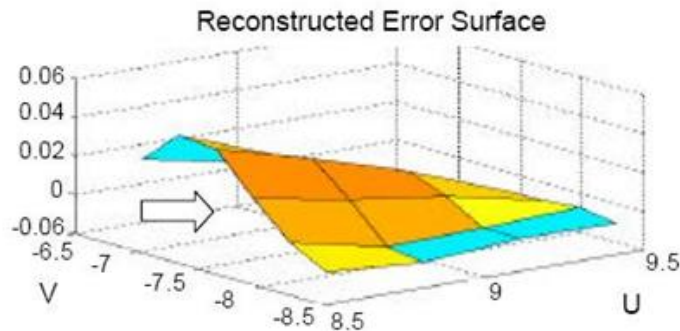
Compression, which ensures a compact model, is achieved by correlation reduction or mode truncation based on good energy compaction property of DCT. Fewer significant modes are required to represent the error surface thereby, establishing more compact representation [8].

The real revolutionary aspect is that mode shape, orientation and its significance (coefficient) provide more error pattern information than raw data.

The form error surface was obtained by calculating the differences between the measured by CMM parts and nominal data in Z direction (Gap Map as already mentioned).

Figure 4.3 presents reconstruction of the surface error field by using the DCT model, summing all modes in which part is decomposed.

The form error surface is represented as a combination of a series of mode compo-



nents. The orthogonality of these modes ensures the independency of their coefficients, a fundamental prerequisite for statistic geometric tolerance analysis. Fewer significant modes are required to represent the error surface thereby, establishing more compact representation [8].

4.4 Discrete Cosine Transformation

A discrete cosine transform (DCT) expresses a sequence of finitely many data points in terms of a sum of cosine functions oscillating at different frequencies.

In particular, a DCT is a Fourier-related transform similar to the discrete Fourier transform (DFT), but using only real numbers. DCTs are equivalent to DFTs of roughly twice the length, operating on real data with even symmetry [2].

Most of the signal information tends to be concentrated in a few low-frequency components of the DCT, approaching the Karhunen-Loeve transform (which is optimal in the decorrelation sense) for signals based on certain limits of Markov processes. As explained below, this stems from the boundary conditions implicit in the cosine functions².

Like any Fourier-related transform, discrete cosine transforms (DCTs) express a function or a signal in terms of a sum of sinusoids with different frequencies and amplitudes. Like the discrete Fourier transform (DFT), a DCT operates on a function at a finite number of discrete data points. The obvious distinction between a DCT and a DFT is that the former uses only cosine functions, while the latter uses both cosines and sines (in the form of complex exponentials). However, this visible difference is merely a consequence of a deeper distinction: a DCT implies different boundary conditions than

²www.wikipedia.com

the DFT or other related transforms. In fact the DFT, like the Fourier series, implies a periodic extension of the original function. A DCT, like a cosine transform, implies an even extension of the original function ³.

The most important property of the presented one is that of **energy compaction**, "the most energy (information) of the sampled data can be represented by a small number of the transformation coefficients $T(u,v)$ " [8], that furthermore allows us to discard many coefficients or to truncate many trifling modes without seriously affecting the error field information.

In fact one of the advantages of the DCT transformation is that there is a fast algorithm available as in Discrete Fourier Transform (DFT), which allows high efficient computations. The DCT can be obtained from the DFT by mirroring the original N -point sequence to obtain a $2N$ -point sequence. Furthermore, DCT outperforms DFT in energy compaction, because DFT block or segment-based transforms will lead to discontinuities at block boundaries [8].

All these problems will be explained in next subsections.

All transformations used presently in image processing are *orthogonal*, so the energy preservation holds between frequency domain and error field pixel domain (space domain represented by sampled measurement data). In fact the orthogonality of these modes ensures the independency of their coefficients, a fundamental prerequisite for statistic geometric tolerance analysis [8].

Thus, based on this property a mode "truncation criteria" can be developed. The significance of each mode can be identified as magnitude of the parameter $T(u,v)$ and expressed as the level of signal energy represented by that mode. The ratio of the energy expressed by selected number of significant modes to the total energy of the signal (sampled data) can be used to characterize the energy compaction of the model [8].

Another advantage of the method is the ability to separate and identify error pattern sources, since the most significant modes have an intuitive and easy to explain physical interpretation. The modes are related to the manufacturing process error sources such as part positioning error (lower order modes), part twisting, spring back, wrinkling and other etc., (higher modes) [8].

Calculating for each selected welding area of each part the model is able to put out a sorted list of modes names affecting it (from the most representative to the less one), the Pareto diagram which explained the cumulative value of percentage contribution of

³www.wikipedia.com

all the modes, the value of magnitude and the error on surfaces (RMS).

The aim of the SMA analysis was to obtain a finite number of the most meaningful frequencies representing the profile decomposition, and associated to own representativity through a system of weights revealing the importance of a single frequency respect the total. For this purpose DCT appears a good method, even if imaginary part of complex number giving the phases value is lost. However, the phase information is present and it is explained in section 4.5.

To maintain the frequency and phase information was obviously necessary the DFT (Discrete Fourier Transformation), but first of all it implies that the limited fragment analyzed is an interval of a periodic infinitely extended signal; and the inverse function of DFT can reproduce the entire time domain only if the original function in input is "periodic". Using the DFT in this case through the `fft2` function, the number of frequencies increase exponentially in an impressive way, and every frequency is characterized by complex numbers often negative and very low in module value, and not very expressive because as complex number, they cannot be performed easily ad a percentage value.

4.4.1 DCT and DFT methods

It is important to mention the superiority of DCT over other image transforms. More specifically, we compare DCT with two linear transforms:

1. The Karhunen- Loeve Transform (KLT);
2. Discrete Fourier Transform (DFT).

Both the function decompose profiles in different frequencies and transform signal from the time domain to frequencies, but DFT is a signal development based on sine and cosine, while DCT is forced to characterize the signal only through amplitude cosine.

Familiarity with Discrete Fourier Transform (DFT) has been assumed throughout this document. The DFT transformation kernel is linear, separable and symmetric. Hence, like DCT, it has fixed basis images and fast implementations are possible [22]. However, the DFT is a complex transform and therefore stipulates that both image magnitude and phase information be en coded. In addition, studies have shown that DCT provides better energy compaction than DFT for most natural images [22].

Furthermore, the implicit periodicity of DFT gives rise to boundary discontinuities that result in significant high-frequency content. Both the function decompose profiles in different frequencies and transform signal from the time domain to frequencies, but DFT is a signal development based on sine and cosine, while DCT is forced to characterize the

signal only through amplitude cosine. Its characteristic to preserve only low frequencies and not high ones (representing the detail of the profile), do not lead to loss of notable information.

Maintaining the frequency and phase information of the signal was obviously realizable through the DFT (Discrete Fourier Transformation), but with some limitations: first of all it implies that the limited data analyzed is an interval of a periodic infinitely extended signal; then the inverse function of DFT can reproduce the entire time domain only if the original function in input is "periodic" ⁴.

Using the DFT in this case through the `fft2` function, the number of frequencies increases exponentially and every frequency is characterized by complex numbers often negative and very low in module value, and not so much expressive because, as complex number, they cannot be interpreted easily as a percentage value. The problem of implementing FDC transformation is the automatization of the process, because FDC finds out frequencies and phases for each column of the data matrix, and is very difficult estimating the highs and amplitudes of picks. While DCT succeeds in decomposing the profile in a sequence of sorted MODES described only by a cosine function each. Those modes are not properly frequencies, they are different amplitude cosine wave characterized by matrix of points representing the basic sinusoids composing the profile. In synthesis the algorithm finds out iteratively all the proper modes that, once summed, delineate the general parts profile shape. Furthermore the FDC or FFT are function proper for audio-video signals, while for the image treatment usually is used DCT for its better properties.

However studies have shown that DCT provides better energy compaction than DFT for most natural images and the implicit periodicity of DFT gives rise to boundary discontinuities that result in significant high-frequency content.

Resuming the principal differences between DCT and DFT are:

- DCT does a better job of concentration energy into a lower order coefficients than does the DFT for image data;
- DCT is purely real, DFT is complex;
- A DCT operation on a block produces coefficients that are similar to the frequency domain coefficient produced by a DFT operation.

⁴www.wikipedia.com

- It is a real transform with better computational efficiency than DFT which by definition is a complex transform;
- It does not introduce discontinuity while imposing periodicity in the time signal. In DFT, as the time signal is truncated and assumed periodic, discontinuity is introduced in time domain and some corresponding artifacts is introduced in frequency domain. But as even symmetry is assumed while truncating the time signal, no discontinuity and related artifacts are introduced in DCT.

It is possible to develop any sign only in cosine series if the domain is multiplied through the symmetry around the 0 of the same sign. Moreover, it is possible to develop any signal in cosine series if the domain is doubled through a symmetry around 0 of the same signal (show in figure 4.3) [30].

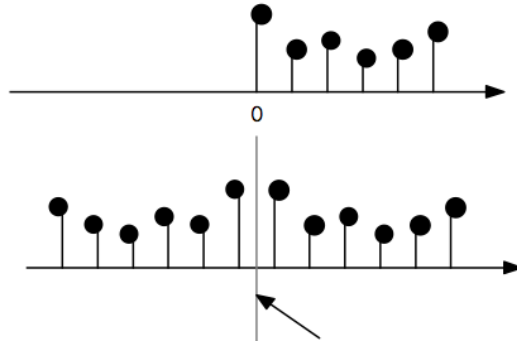


Figure 4.3: The original sample is moved of half period on late and the total of the mirrored samples are doubled.

Starting from these observations, the expression of the DCT is derivable to DFT and equally for the IDCT to the IDFT.

In fact, defined $x_2(n)$ the mirrored sequence balanced on 0 the DCT of $X(k)$ of the sequence $x(n)$ of N samples is equal numerically with the DFT $X_2(k)$ on $2N$ points of the sequence, symmetric on $x_2(n)$, multiplied with a late term, equal to the half period of sampling of the sequence $x(n)$ [30], that is:

$$X(k) = e^{-j\pi k/(2N)} X_2(k) \quad [30]$$

which permits a fast computation of the DCT of N samples through algorithms FFT on $2N$ points.

The discrete cosine transformation (DCT) is better than the fast Fourier transformation (FFT) for data compression because it has a better energy compaction property: when applying the DCT to a signal, a higher ratio of the energy is concentrated in a smaller number of coefficient relative to the Fourier transformation, approaching the Karhunen Loeve transform . That is resumed in the possibility to use less frequency to represent the signal. Moreover, the validity of the representation through DCT coefficient consists on the capacity to represent in a compact way (just few bits) development's coefficients. Frequency distribution on FFT is uniform all over N data. So there is not much scope for quantization and hence compression. FFT also has a boundary conditions (see figure 4.4) [30].

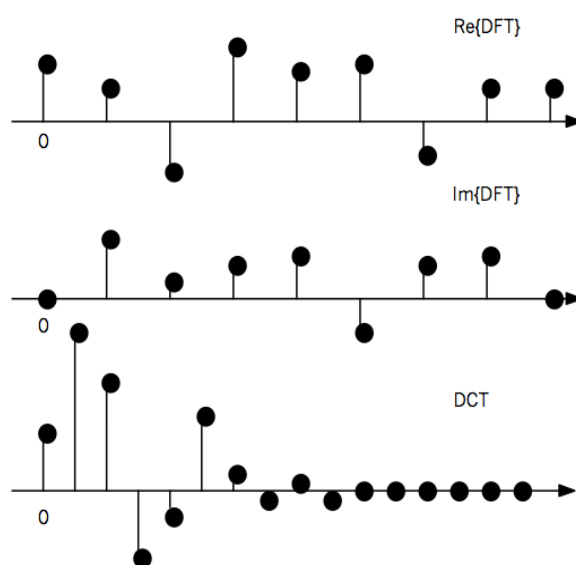


Figure 4.4: Efficiency representation of signals for FFT and DCT

Deciding to transmit only the half or a quarter of coefficients, the cutting off error would be insignificant for the DCT, while important for the DFT.

Note how the energy of the error is equal for 0 and N omitted coefficients in both cases using DFT and DCT. In fact, both functions are complete basis for the representation of signals or imagines. The difference is in the efficiency of representation, considering only the subgroup of developed coefficients.

In fact, a lot of coefficients DCT can be quantized to zero and then omitted in the transmission, saving a big bit quantity [30].

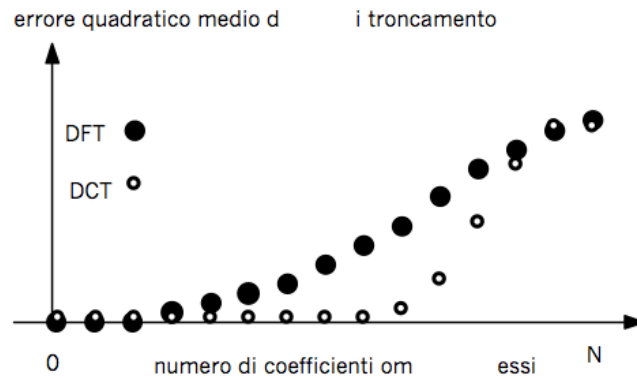


Figure 4.5: Mean error square between DFT and DCT

The Karhunen-Loeve theorem is a representation of a stochastic process, analogous to Fourier series representation of a function on a bounded interval. Because this technique is closely related to the Principal Component Analysis. KLT permits to reduce the number of correlated variables into an uncorrelated ones.

The main difference with PCA is that KLT is based on a combination of orthogonal functions, analogous to the Fourier series. While the Fourier series has real numbers like coefficient and the expansion basis is a sinusoidal function, KLT has random variables and the which basis is determined by the covariance function of the process ⁵.

Furthermore in signal processing using DFT, *aliasing* is a phenomenon that can turn up and compromise the signal decomposition ⁶. As we can see in figure 4.6, the recomposition of the part through the inverse function for respectively fft and dct is evident:

Sinusoids are an important type of periodic function, because realistic signals are often modeled as the summation of many sinusoids of different frequencies and different amplitudes (with a Fourier series or transform). Understanding what aliasing does to the individual sinusoids is useful in understanding what happens to their sum ⁷.

It's important to take care of this outstanding loss of information to analyze prudently the results, always considering the fact that the information returned by this code are not wrong, but also not complete at all.

⁵www.wikipedia.com

⁶www.wikipedia.com

⁷www.wikipedia.com

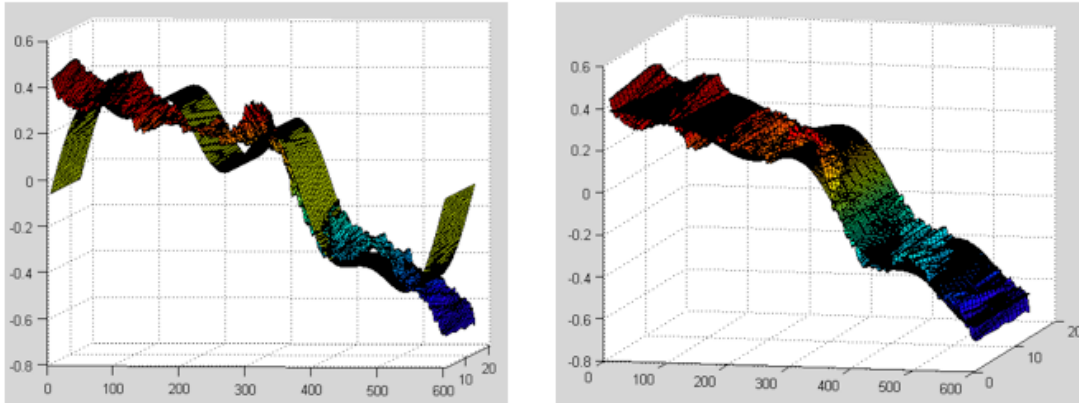


Figure 4.6: Reposition of part through modes in fft and dct

Processing with the SMA analysis all the single parts and then considering the best couples obtained from the gap measurements, the analysis one by one is the following.

4.5 The SMA indicator

The SMA model is a sequence of steps based on the DCT function and its inverse (IDCT).

First of all, the indicator receives in input the welding area of the single part. The input data is a matrix containing the profile of the welding area, that is Z value matrix. Please note the importance to have the profile because containing the error of the part, that is the surface which will have to contact the other part.

Calculating for each selected welding area of each part the model is able to put out a sorted list of modes names affecting it (from the most representative to the less one), the Pareto diagram which explained the cumulative value of percentage contribution of all the modes, the value of magnitude and the error on surfaces (RMS).

After having positioned the welding area in the centre of 0, the DCT function is applied to part. The need to position in the centre the part is because it must be symmetrical to a point, the centre of the part.

The DCT returns the output based on this function:

$$X(k) = \sqrt{\frac{2}{N}} \alpha(k) \sum_{n=0}^{N-1} x(n) \cos\left(\pi \frac{k(2n-1)(k-1)}{2N}\right) \quad [30]$$

Now the most significant frequencies, which represent the 99% of the energy compaction, are found. Doing that, cosine transformation values are sorted in decrescent order (from the highest value to the lowest), each frequency gives a percentage of representation, calculating as the ratio between the own value and the total of them. As we can see in figure 4.7, the low frequency represents alone the 90% of the energy compaction, following the high ones with smaller percentage.

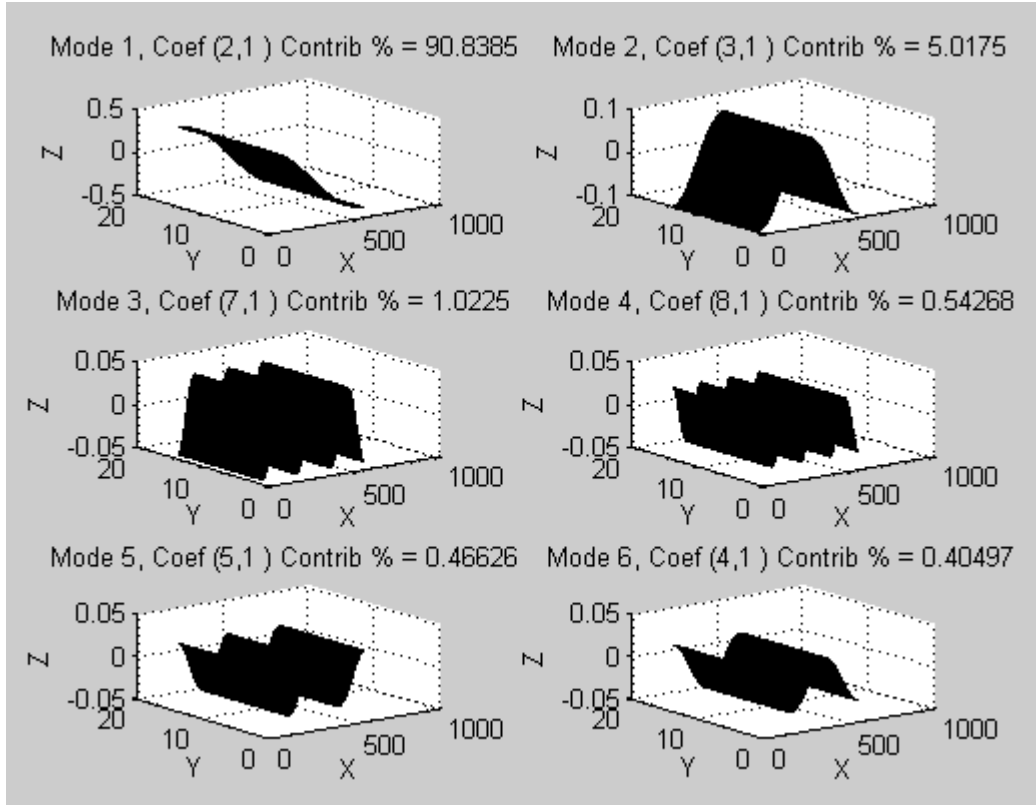


Figure 4.7: frequency output example

At this moment the Karhunen Loeve theorem (KLT) is applied. Until the sum of the significant frequencies is less than energy compaction, the research of the most representative frequencies goes on.

Each modes is described by the percentage of significance (figure 4.7) and phase. Because the discrete cosine transformation, the phase can only be present in 0 or π value, because the presence of the real number undoes the possibility to have a phase on sine axis. The phase is visible observing the sign of the cosine in the first column of the mode matrix: if it is positive, the mode starts to 0, otherwise to π . As it is visible

in figure 4.8, the phase is different, though the same mode.

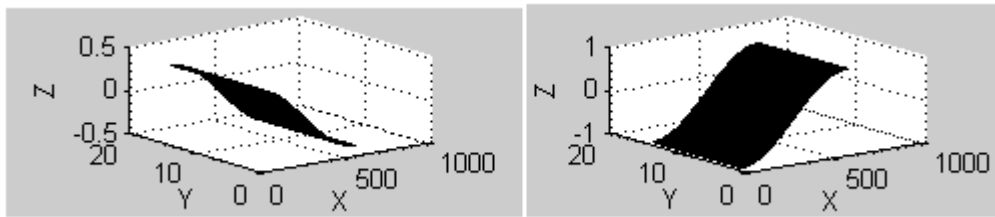


Figure 4.8: Positive and negative phase example

When the energy compaction can be designed for each selected frequencies, than the inverse of the discrete cosine transformation can be obtained. The sum of these modes gives in output a surface similar to the input welding area, but more simplified (figure 4.9) and with the absence of uncertainties of CMM.

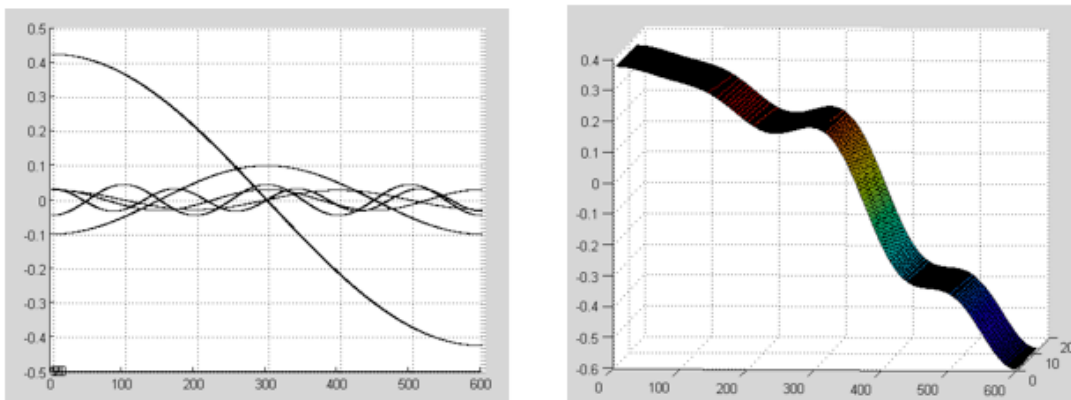


Figure 4.9: Single modes and sum of them

Assuming signal is a realization of a stationary process having a correlation, because of that between samples, the KLT should be able to compress the signal data significantly ⁸.

As in the figure 4.10, the sum of the modes follows the surface.

The output of the code was the description of different modes affecting the parts characterized by several factors: coefficient name, value, magnitude value for each mode

⁸ww.wikipedia.com

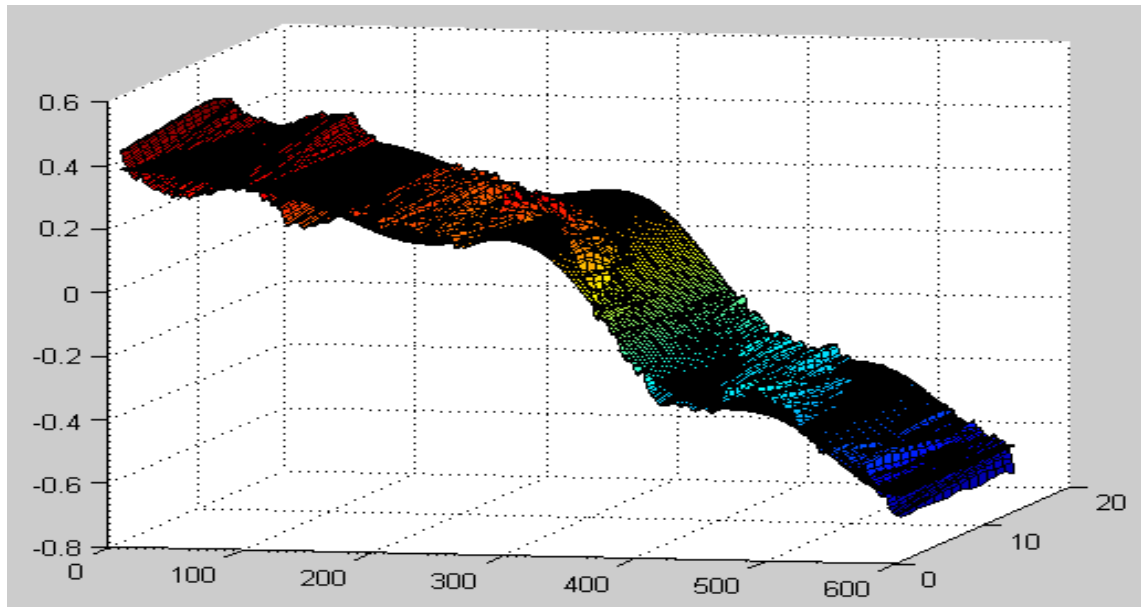


Figure 4.10: Sum of modes and part plot

and value of RMS:

- **MODE NAME:** it explain the typology of the mode, with the "number of wave" u and v along X and Y axis on parts surfaces. From its value is possible to obtain an assessment of the wavelength for each mode.

If the u and v value is low, the part is affected by a faint and light deformation. Frequency values bigger then 5 can be considered quite high and disturbing, unless they are present in little percentage, so they can be leave out.

- **CONTRIBUTE:** this indicator explain the significance and the importance of every mode on the total of them. In this way a distinction came out between Dominant Modes and Not Dominant ones. If a considered mode has contribute value bigger then 70% and all the other modes present value very low (like 2%), the first mode is dominant. But some cases present a sequence of not-dominant modes. In this situation all the modes have more or less the same weight, so the part is affected simultaneously by different modes of the same importance.
- **MAGNITUDE:** is mainly the "amplitude" of the wave and it also explain the

concavity or convexity of the mode considered. The same mode with magnitude equal in absolute value but with different sign, has symmetric shape as in figure4.11:

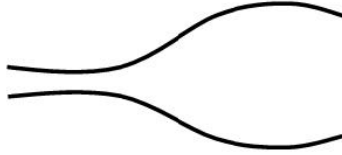


Figure 4.11: Profiles with different signs and same value

If the same mode has equal sign of magnitude but is very different in absolute value, the concavity and the bending is very different between the two samples. For example as in figure4.12 if the MODE1 has magnitude 10,2 in the top part and 2,2 in the bottom one:



Figure 4.12: Profiles with equal sign and different magnitude

This means that, if two different parts have the same dominant mode, in agreement with the sign but very different in the absolute value, there will be a not high-quality fitting between them, especially if the difference between their absolute value is quite big. Otherwise if two parts with magnitude values different in sign but not so distant in difference value between modules, they are likely to be joined with a good-quality welding because the gap between them will be lower (figure 4.13).

Magnitude is also a good indicator of phase, which can assume positive value (if $phase = 0$) or negative (if $phase = \pi$)

4.6 Results and Index Assessment

First of all is required a recall to experimental data about Gap measurements between all the possible couples of the 12 available parts, imposing the mating of each plate with



Figure 4.13: Profiles with similar magnitude module value and different sign

every C-Shaped channel. Considering the 7 combination with higher values of Good to total ratio (number of points of two parts with distances between fixed tolerances), the perfect couples between the best combinations are the one having G/T ratio equal to 1:

- Plate1-Channel 5 \Rightarrow G/T ratio = 1

- Plate 2-Channel 3 \Rightarrow G/T ratio = 0,66667
 Plate 2-Channel 4 \Rightarrow G/T ratio = 0,53333
 Plate 2-Channel 5 \Rightarrow G/T ratio = 0,53333

- Plate 3-Channel 3 \Rightarrow G/T ratio = 0,6
 Plate 3-Channel 4 \Rightarrow G/T ratio = 0,6

- Plate 4-Channel 1 \Rightarrow G/T ratio = 0,8
 Plate 4-Channel 2 \Rightarrow G/T ratio = 1
 Plate 4-Channel 6 \Rightarrow G/T ratio = 1

- Plate 5-Channel 1 \Rightarrow G/T ratio = 0,8
 Plate 5-Channel 6 \Rightarrow G/T ratio = 1

- Plate 6-Channel 1 \Rightarrow G/T ratio = 0,86666
 Plate 6-Channel 3 \Rightarrow G/T ratio = 0,8
 Plate 6-Channel 4 \Rightarrow G/T ratio = 0,66667

Figure 4.14 the 7 best parts coupling combinations (one combination corresponds in 6 coupling between the 12 parts) between some other good sorted ones.

RIGHT SIDE	P1	P2	P3	P4	P5	P6	I1	I2	I3	I4	I5	I6	G/T Ratio average
	5	3	4	2	6	1	1	0,667	0,6	0,8	1	0,867	0,822222222
	5	3	2	6	1	4	1	0,667	0,6	1	1	0,667	0,822222222
	5	3	2	1	6	4	1	0,667	0,6	1	1	0,667	0,822222222
	5	4	2	6	1	3	1	0,533	0,6	1	1	0,8	0,822222222
	5	4	2	1	6	3	1	0,533	0,6	1	1	0,8	0,822222222
	5	2	4	6	1	3	1	0,533	0,6	1	1	0,8	0,822222222
	5	2	4	1	6	3	1	0,533	0,6	1	1	0,8	0,822222222
	5	3	4	6	1	2	1	0,667	0,6	1	1	0,6	0,811111111
	5	3	4	1	6	2	1	0,667	0,6	1	1	0,6	0,811111111
	5	3	2	4	6	1	1	0,667	0,6	0,733	1	0,867	0,811111111
Best combinations	4	5	2	6	1	3	0,8	0,667	0,6	1	1	0,8	0,811111111
	4	5	2	1	6	3	0,8	0,667	0,6	1	1	0,8	0,811111111
	4	3	5	2	6	1	0,8	0,667	0,733	0,8	1	0,867	0,811111111
	1	5	4	2	6	3	1	0,667	0,6	0,8	1	0,8	0,811111111
	1	3	5	2	6	4	1	0,667	0,733	0,8	1	0,667	0,811111111
	4	2	5	6	1	3	0,8	0,533	0,733	1	1	0,8	0,811111111
	4	2	5	1	6	3	0,8	0,533	0,733	1	1	0,8	0,811111111
	1	4	5	2	6	3	1	0,533	0,733	0,8	1	0,8	0,811111111
	4	3	2	5	6	1	0,8	0,667	0,6	0,867	1	0,867	0,8
	1	3	2	5	6	4	1	0,667	0,6	0,867	1	0,667	0,8
	5	4	3	2	6	1	1	0,533	0,6	0,8	1	0,867	0,8
	5	2	3	6	1	4	1	0,533	0,6	1	1	0,667	0,8
	5	2	3	1	6	4	1	0,533	0,6	1	1	0,667	0,8
	5	1	4	2	6	3	1	0,6	0,6	0,8	1	0,8	0,8
	4	3	5	6	1	2	0,8	0,667	0,733	1	1	0,6	0,8
	4	3	5	1	6	2	0,8	0,667	0,733	1	1	0,6	0,8
	2	5	4	6	1	3	0,73	0,667	0,6	1	1	0,8	0,8

Figure 4.14: the 7 best pats coupling combinations (blue-coloured)

Analyzing the 7 worst matching between parts, the worst coupling to avoid during the assembly process are:

- Plate 2-Channel 6 → G/T ratio= 0,2666
- Plate 3-Channel 1 → G/T ratio= 0,5333
- Plate 5-Channel 4 → G/T ratio= 0,46667

The other worst coupling are however above the threshold probability supposed equal to 0,6 about. So even if their union has the lower quality value among all the possible mating, this value allows to have a good welding:

- Plate 1-Channel 2 → G/T ratio= 0,7333
 Plate 1-Channel 3 → G/T ratio= 0,7333
 Plate 1-Channel 4 → G/T ratio= 0,8

- Plate 4-Channel 2 → G/T ratio= 0,8
 Plate 4-Channel 3 → G/T ratio= 0,7333
 Plate 4-Channel 5 → G/T ratio= 0,8667

- Plate 5-Channel 2 → G/T ratio= 0,6
 Plate 5-Channel 5 → G/T ratio= 0,6

- Plate 6-Channel 2 → G/T ratio= 0,6
 Plate 6-Channel 4 → G/T ratio= 0,6667
 Plate 6-Channel 5 → G/T ratio= 0,6667

Blue values in figure 4.15 represent Channels IDs (for example in the first line Channel 4 is combined with Plate1). This analysis was used to observe mostly the boundary cases: couples with very high G/T Ratio value , for example equal to one, which are composed by parts obliged to match together during the welding process and couples which must be avoided because of the dreadful G/T Ratio value which can have serious consequences on the non conformity percentage in the system throughput analysis.

These two kinds of couples (best and worst) should present in the SMA some repetitions or some evident special differential aspects not present in any other couple and which distinguish them . The SMA should discriminates and recognize when a coupling is very good or very bad fitting without any doubts.

Is quite hard to predict from the SMA the precise level of quality welding value, for example it's very difficult to discriminate and quantify through SMA if a couple has G/T ratio equal to 0,6, or 0,5 or 0,7 and so on. This because the output is not quantitative and must be interpreted. So was find a numerical indicator taking into consideration, the sum of all minimum of the two values of the same coefficient shared between two parts coupled, only to give an idea of how similar(in percentage) parts can be through their shared modes.

But if the welding is predicted to be perfect or very bad, it should be clearly visible.

The couples of parts presented in the following images are all the possible coupling, the green ones representing the best, and the red one representing the worst. For each

RIGHT SIDE	P1	P2	P3	P4	P5	P6	I1	I2	I3	I4	I5	I6	G/T ratio average
	4	2	1	3	5	6	0,8	0,533333	0,533	0,733	0,6	0,53	0,622222222
	3	4	1	2	5	6	0,73	0,533333	0,533	0,8	0,6	0,53	0,622222222
	3	6	1	5	2	4	0,73	0,266667	0,533	0,867	0,6	0,67	0,611111111
	2	6	1	5	4	3	0,73	0,266667	0,533	0,867	0,47	0,8	0,611111111
	2	1	6	3	4	5	0,73	0,6	0,467	0,733	0,47	0,67	0,611111111
	6	2	1	3	4	5	0,73	0,533333	0,533	0,733	0,47	0,67	0,611111111
	3	2	1	5	4	6	0,73	0,533333	0,533	0,867	0,47	0,53	0,611111111
	2	5	1	3	4	6	0,73	0,666667	0,533	0,733	0,47	0,53	0,611111111
	2	6	1	4	5	3	0,73	0,266667	0,533	0,733	0,6	0,8	0,611111111
	2	6	1	4	3	5	0,73	0,266667	0,533	0,733	0,73	0,67	0,611111111
	3	2	1	4	3	5	0,73	0,533333	0,533	0,733	0,6	0,53	0,611111111
	2	4	1	3	5	6	0,73	0,533333	0,533	0,733	0,6	0,53	0,611111111
	5	6	1	3	4	2	1	0,266667	0,533	0,733	0,47	0,6	0,6
	4	6	1	3	2	5	0,8	0,266667	0,533	0,733	0,6	0,67	0,6
	3	6	1	2	5	4	0,73	0,266667	0,533	0,8	0,6	0,67	0,6
	4	6	1	3	5	2	0,8	0,266667	0,533	0,733	0,6	0,6	0,588888889
	3	6	1	4	2	5	0,73	0,266667	0,533	0,733	0,6	0,67	0,588888889
	2	6	1	3	5	4	0,73	0,266667	0,533	0,733	0,6	0,67	0,588888889
	3	6	1	5	4	2	0,73	0,266667	0,533	0,867	0,47	0,6	0,577777778
	3	6	1	2	4	5	0,73	0,266667	0,533	0,8	0,47	0,67	0,577777778
	3	6	1	4	5	2	0,73	0,266667	0,533	0,733	0,6	0,6	0,577777778
worst	2	6	1	3	4	5	0,73	0,266667	0,533	0,733	0,47	0,67	0,566666667

Figure 4.15: 6 worst combinations

couple are reported the personal modes, with the percentage of incidence and the magnitude. Near each couple there is also the G/T ratio value. These results referred to a 99% energy compaction.

The side analyzed was only the right one as in all the others function because G/T ratio values were available only for that particular side, so the comparison with real experimental data could be possible only operating in this way.

In figure 4.19 is reported the final SMA general table in which are shown all available metallic parts with the proper SMA decomposition. For each part is explained the ordered sequence of modes with the related coefficient values and percentage contribution.

To pick out the goodness of this indicator only the most significant and important couples results are reported, for example only some revealing sample of best and worse couples.

As far as best couples are concerned, SMA results follow clearly what underlined by Gap measurements. Some samples are reported in figures 4.16,4.18 and 4.17.

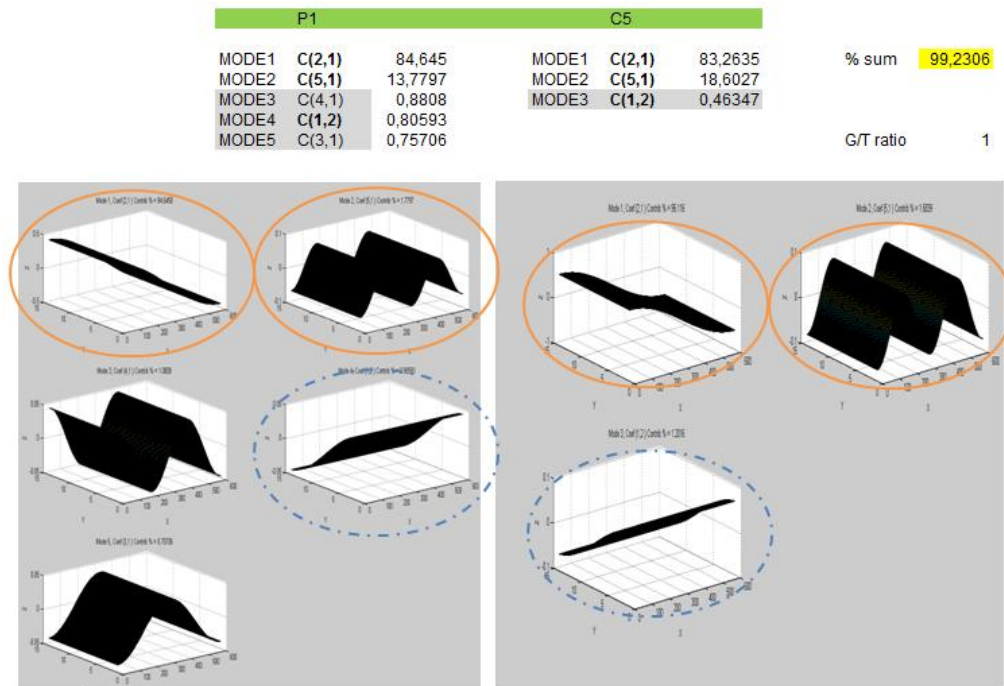


Figure 4.16: P1-C5 couple, one of the most promising one confirmed by SMA index and Gap Measurements Analysis with G/T Ratio value equal to 1 (number of points with distances inside the tolerances)

Even if all couples are composed by C(2,1), which will be called the *fundamental MODE* because of his presence in every part, best couplings usually are constituted by parts with a very high percentage value of representativity (more than 80%), so their shape is mostly owing to the fundamental mode as is shown for Plate1 and Channel 5. These two parts for example have in common three modes, but only the firsts and the second one will be take into account because both with a higher representative value than the others.

A mode is considered a bit representative if his percentage is higher than 8 – 9% on the whole surfaces. All modes under this threshold will be not considered so relevant, so during the analysis they will be discarded. Usually a so low value would not be considered as meaningful, but in this specific analysis the lower modes have coefficient equal to 0,8 – 1% or 2%, distancing themselves quite a lot from secondary modes value, that, for this reason, will be take into account.

During this analysis it is also necessary and logical consider the phase of the modes in common. For example as in figure 4.17, the *fundamental mode* $C(2,1)$ is shared between plate2 and channel 6, but phase's mode is completely opposite in one case respect the other. In fact in P2 $C(2,1)$ has phase 0, while in C6 is π , completely symmetric respect y-axis. So the fundamental mode, even if shared, cannot be considered as the same mode preset in both parts but the situation can be faced as this mode appears in a different way in some parts, so like it would not be the same shared mode between them. For the mode $C(1,2)$ it is always the same reason.

In figure 4.17 $C(4,1)$ and $C(3,2)$ are the only shared with phase in agreement, an so the analysis can consider only them which give a very low shared-compaction value.

Its low sum-compaction value is given by the having in common only secondary low-value modes which are not able to describe most of the profiles.

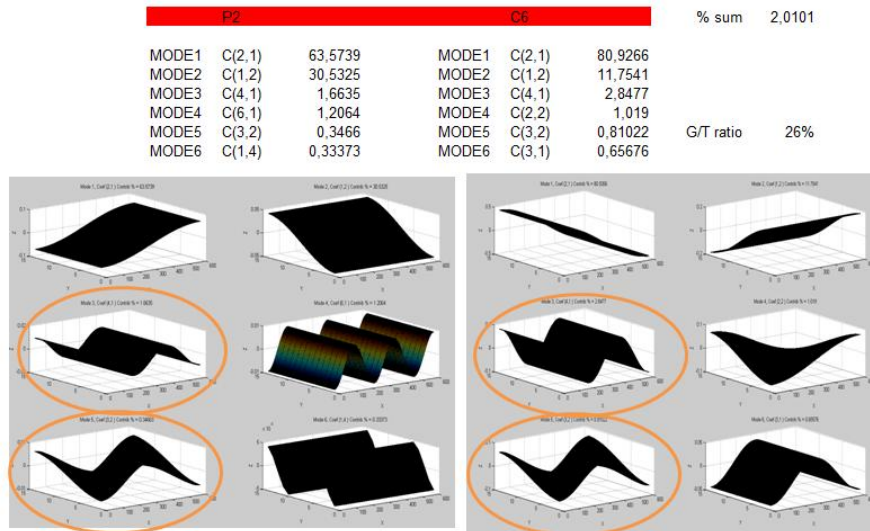


Figure 4.17: The worst coupling P2-C6 with G/T ratio value equal to 0,26666

In figure 4.18 representing Plate 1 and Channel 1, their shared-compaction value appears high (strengthened by high G/T ratio value) mostly thank to the fundamental mode shared with high representation value, even if the also shared $C(4,1)$ has opposite phase so will be not considered as shared in the *% sum* value (*% sum* is the sum of the minimum compaction value of the shared modes).

In all these graphics are reported *% sum* and G/T Ratio values to compare and show if the index is valid and reflect gap measurements.

Even if this analysis is based on geometrical study of surfaces, as the already mentioned Correlation Index, this indicator presents coherent results with gap measurements. That's because while correlation looks at global similarity of the singular shape and it is not able to detect roughnesses and uncertainties, caused by acquisition data system, the SMA succeeds in decomposing and isolating them. In conclusion, using correlation it can happen two surfaces having the same dominant mode in a relevant percentage appear different in correlation value, because it takes into account higher different frequencies, which have marginal weight.

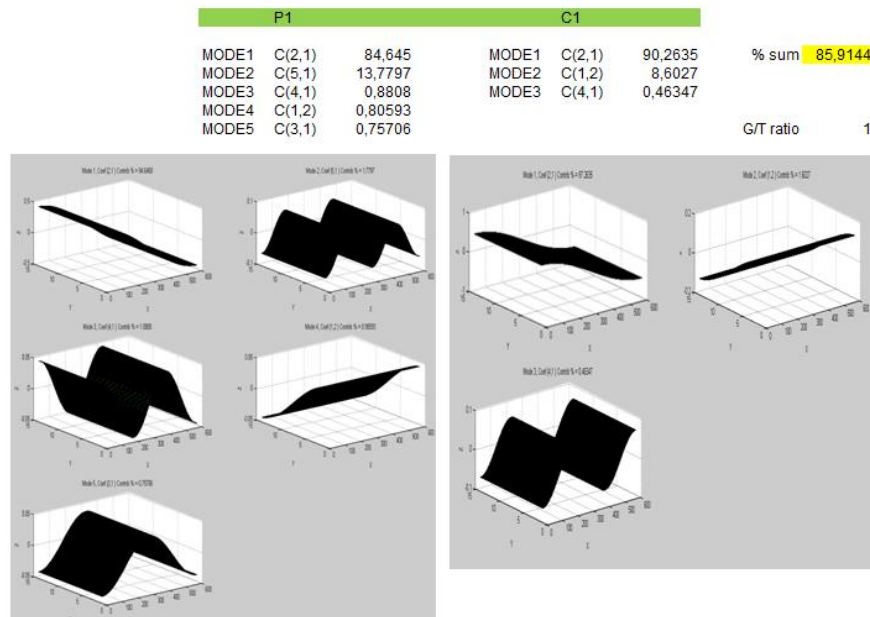


Figure 4.18: P1-C1 coupling having G/T ratio equal to 1 (best value)

PART	SIDE	RANK	MODE NAME	CONTRIBUTION %	PART	SIDE	RANK	MODE NAME	CONTRIBUTION %
P1	side2	MODE1	C(2,1)	84,645	C1	side2	MODE1	C(2,1)	90,2635
		MODE2	C(5,1)	13,7797			MODE2	C(1,2)	8,6027
		MODE3	C(4,1)	0,8808			MODE3	C(4,1)	0,46347
		MODE4	C(1,2)	0,80593					
		MODE5	C(3,1)	0,75706					
P2	side2	MODE1	C(2,1)	63,5739	C2	side2	MODE1	C(2,1)	66,723
		MODE2	C(1,2)	30,5325			MODE2	C(5,1)	21,844
		MODE3	C(4,1)	1,6635			MODE3	C(1,2)	5,6258
		MODE4	C(6,1)	1,2064			MODE4	C(7,1)	1,2727
		MODE5	C(3,2)	0,3466			MODE5	C(4,1)	1,161
		MODE6	C(1,4)	0,33373			MODE6	C(9,1)	0,8887
P3	side2	MODE1	C(2,1)	51,89	C3	side2	MODE1	C(2,1)	69,7
		MODE2	C(5,1)	20,9089			MODE2	C(3,1)	15,0175
		MODE3	C(4,1)	15,787			MODE3	C(7,1)	10,0225
		MODE4	C(3,1)	2,875			MODE4	C(8,1)	0,54268
		MODE5	C(6,1)	0,34997			MODE5	C(5,1)	0,46626
				MODE6	C(4,1)	0,10497			
P4	side2	MODE1	C(2,1)	91,5782	C4	side2	MODE1	C(2,1)	56,52
		MODE2	C(3,1)	4,9733			MODE2	C(5,1)	18,5396
		MODE3	C(5,1)	1,961			MODE3	C(6,1)	16,6375
		MODE4	C(4,1)	0,77566			MODE4	C(3,1)	5,8932
				MODE5	C(7,1)	1,0195			
				MODE6	C(3,2)	0,9085			
P5	side2	MODE1	C(2,1)	98,2103	C5	side2	MODE1	C(2,1)	83,2635
		MODE2	C(4,1)	1,035			MODE2	C(5,1)	18,6027
						MODE3	C(1,2)	0,46347	
P6	side2	MODE1	C(2,1)	63,2472	C6	side2	MODE1	C(2,1)	85,9266
		MODE2	C(4,1)	14,8375			MODE2	C(1,2)	4,7541
		MODE3	C(3,1)	12,6011			MODE3	C(4,1)	1,0977
		MODE4	C(1,2)	9,2274			MODE4	C(2,2)	1,019
		MODE5	C(8,1)	0,30688			MODE5	C(3,2)	1,81022
				MODE6	C(3,1)	1,65676			

Figure 4.19: Final SMA complete table

4.7 Parts Classification through SMA Analysis

Parts Segmentation in different class was possible through mainly the SMA analysis which offers the most meaningful similarity index between the previous mentioned. The shape distribution index was valid too, but essentially it's not enough alone, it needs to be put side by side with another indicator more reliable and robust because it's not able to quantify "how" similar parts are.

The only index giving similar and correlated output to Gap measurements one is

the SMA. The division took places considering first of all Gap Measurements properly, provided by measuring the gap between real metallic parts in the considered side.

Experimental data provided through repeated gap measurements can be considered to match together one casual plate with a casual channel, so we can select the best combinations of matching parts between all the possible 720 combination. Considering the 7 combination with the highest values of good to total ratio, which are the perfect matching between parts related to previous section, the matching having the maximum value **1** are characterized by:

- shape distribution very similar
- considering SMA index, usually these couples have most of dominant modes in common having magnitudes in agreement (both positive or both negative) and furthermore very similar in absolute value(usually this happened for the most dominant between the modes in common) with dominant modes having very high percentages (like 80%) and all the others very low like in figure 4.20. In fact on the contrary the pareto dyagram for some other couples decreases in a constant and slow way, showing the important modes as equal in percentage (for example the fist mode is the 25%, the second is the 20%, the third is the 16% and so on).

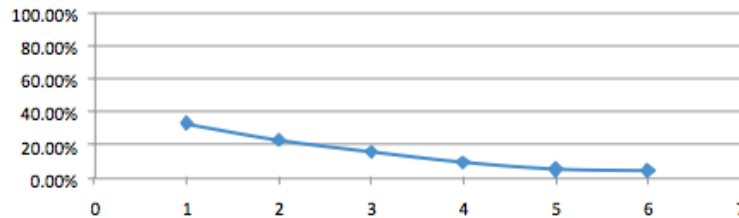


Figure 4.20: Presence of a lot of modes at the same importance

Considering shared modes between two parts, and ensured the correspondent magnitudes have the same sign, the most similar the magnitude absolute value modes are, higher is the value of the G/T ration.

If between the dominant modes of two parts no one is shared, usually of course the G/T Ratio value will be very low, otherwise if two parts have the same dominant modes which represent also a big percentage (more than 80 %) with magnitude almost similar, of course their shape distributions could not be so different, and G/T value is always high.

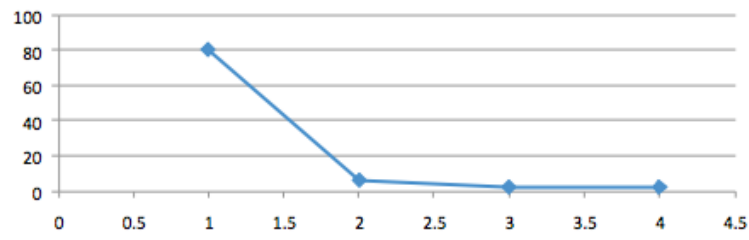


Figure 4.21: Presence of one dominant mode and other negligible modes

In figures 4.22 and 4.23 it is possible to see what is meant to be a similar or very different shape distribution, using two examples.

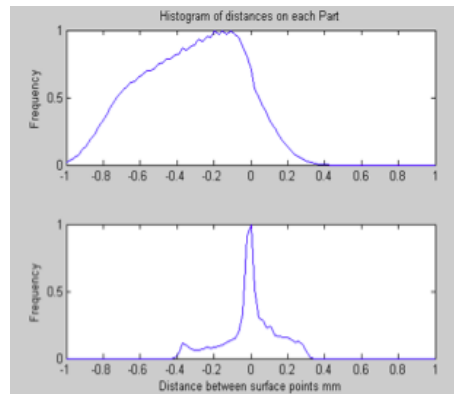


Figure 4.22: Evidently different shape distribution

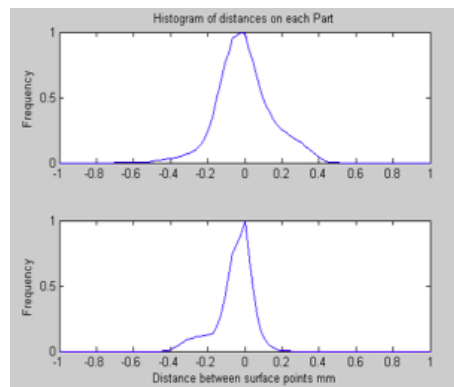


Figure 4.23: Similar shape distribution

Through the SMA and Shape Distribution analysis some circumstances are visible to be disadvantageous to a good quality of the welding, in fact in the following statements the low values of the G/T ratio stand for low-quality welding.

- no modes in common between the parts.
- if the modes present in both the parts are not in a dominant position (the dominant ones are different modes) and their values of magnitude are in agreement for each couple but quite different in absolute value, the G/T value will tend to be low.
- on the contrary if the shared modes are in a dominant position but with very different value of magnitude (in sign and value) the G/T value will be definitely very low, because even if the modes are the same, their convexity and concavity in shape will not match together.
- if one part has a big portion of modes in common with another on the total number of modes it presents (for example all or 5 on a total of 6 modes), than the G/T value will be likely to increase.

Summarizing the most important characteristics which can lead to a peculiar G/T ratio value, it's important to take into account:

- number and reciprocal position of modes in common between parts

The G/T ratio is likely to increase if the number of modes shared is higher and if they have dominant percentage value of impact on parts.

- shape distribution distance

If the two shapes are similar, the distance between the distributions will be less, so the G/T value will be better, but it's not a critical aspect as the similarity between the modes, because, sometimes also parts with very different shape seems to be a good matching.

- value and sign of magnitudes of shared modes between parts

The same modes present in both the parts and having similar numerical value and same sign are very representative of a good quality matching, especially if they are dominant and if numerically they are several. It's definitely better having two magnitude values not in agreement but very with low absolute value (for example +1,04 and -0,8) than having the same sign but absolute value quite different (like -3 and -9).

4.7.1 Classification through Shared Modes

An interesting partition of parts in different clusters can be guided by shared dominant modes, describing parts profile. The idea to classify parts before welding can be helpful in optimizing quality welding value, favoring best parts matching and constraining the RLW system to interview on already defined good couplings.

This issue has a strong industrial importance, because with few modes and simpler geometrical analysis through DCT transformation is possible to have a huge improvement on parts matching.

In this section the clusterization will be applied on the 12 sample parts available through the Warwick University with the aim to enforce this method also to an industrial reality, like the study of car-doors components supplied by Fiat COMAU (Torino).

A first "skimming phase" can be obtained analyzing step by step all the first dominants modes and rejecting all the others with percentage contribute less than 10%, which do not bring more useful information.

Most of the 6 Channel and 6 Plates are characterized by the dominant fundamental modes $C(2, 1)$ constituted by very low frequencies and representing the whole general shape profile. The first partition is given focusing the whole process on phase value.

In fact parts represented by the same mode can be mated only if the that mode's cosine wave has the same phase in both parts, otherwise the mating turn out to be really hard to be obtained.

Analyzing all Plates and all Channels through DCT transformation, the cosine wave are represented with phase equal to 0 (in this case the first column of the matrix has positive values) or π (first column of the matrix with negative values). Magnitude represent the amplitude wave evaluation for each mode, and its values is strictly linked to phase information: if phase is equal to zero, amplitude has a positive value, otherwise negative.

Phase and magnitude give more or less the same information about the wave trend, but the magnitude explain also the convexity or concavity direction of waves and their amplitude (how waveless or flat they appear). See that for one modes the magnitude module value are quite similar for a specific modes in several parts having them (for example for modes $C(2,1)$ changing from the value of 26 to 31 about) and this situation is visible for all the other modes present in more parts, this information will be neglected and the analysis will consider only phase information.

Fundamental Mode: C(2,1)

Analyzing this main cosine wave, a first result is reached (figure 4.24).

All sample parts have C(2,1) with phase equal to zero, less Plate 2 and Plate 3, which have opposite value (π). P2 and P3 in this case can be removed from the classification, because their fundamental mode representing most of their profile, is not in agreement with any other channel.

P2 and P3 can be seen as a sort of "scrap" because their welding with any other channel will be disastrous from the welding point of view and the consequences can be also seen through G/T Ratio values, always lower the requirement limits. An exception is P3 and C5 coupling, the unique couple having no correspondence between experimental results and SMA indicators.

PART	SIDE	RANK	MODE NAME	CONTRIBUTION %	phase
P1		MODE1	C(2,1)	84,645	0
P2		MODE1	C(2,1)	63,5739	3,141593
P3		MODE1	C(2,1)	51,89	3,141593
P4		MODE1	C(2,1)	91,5782	0
P5		MODE1	C(2,1)	98,2103	0
P6		MODE1	C(2,1)	63,2472	0

Figure 4.24: Plate 2 elimination from the analysis

P1, P4 and P5 have very high C(2,1) contribution value, so, if coupled with channel with the same characteristic (high C(2,1) value quantitatively more than 70%), their welding will be promising, because more than 70% of their profile is explained by the same mode, and it's likely the parts will be similar in profile shape.

On the contrary P6 has C(2,1) value lower than the established threshold, so in this specific part, this mode alone is not able to guarantee the good quality of the welding. In this case is visible the necessity to deepen the analysis getting down to the just lower dominant modes and classify parts according to them subsequently.

Analyzing Channels, the actual situation is the following (figure 4.25):

In the Channel case, all parts are in phase, so there is no risk to exclude any metal sheets from following analysis. Also in this situation is necessary go into a detailed analysis and consider lower secondary modes, because classify parts through only the

PART	SIDE	RANKMODE	NAME	CONTRIBUTION %	phase
C1		MODE1	C(2,1)	90,2635	0
C2		MODE1	C(2,1)	66,723	0
C3		MODE1	C(2,1)	69,7	0
C4		MODE1	C(2,1)	56,52	0
C5		MODE1	C(2,1)	83,2635	0
C6		MODE1	C(2,1)	85,9266	0

Figure 4.25: Plate 2 elimination from the analysis

first mode is not always possible.

In fact parts like C1, C5 and C6, characterized once again by high C(2,1) value, if coupled with a plate with also high, they can be defined as good couples with only one mode in common, because its percentage value satisfy completely welding requirements.

In the same way C2, C3, C4 need more analysis on the other dominant modes to be classified correctly, because their percentage contribution value is not enough alone to make sure the welding quality guarantee.

Secondary Dominant Modes: C(1,2), C(3,1), C(5,1)

Analyzing the presence of other dominant modes, there is a smaller percentage in parts of another modes, like C(1,2), C(3,1), C(5,1) which are present in them for about the 10% of contribution, which is not a very relevant value, but if compared with all the other around 1% or 0%, they can be considered as modes really affecting parts.

Considering firstly **C(1,2)**, it is present in a dominant contribution value only in two specific parts, P6 and C1, which in this way can characterize a first define group (figure 4.26). This couple guarantees a joining value equal to 0,876 (G/T Ratio) and a shared contribution of 72,4746% and it represent a cluster in which can be sent all parts of C1 type and P6 type having C(1,2) as relevant secondary mode.

Taking **C(3,1)** into account, this is another secondary dominant mode present only in two parts, P6 and C3, which define another cluster in which all parts having C(3,1) as dominant can be contained. Also other parts are composed by C(3,1) and C(1,2), but

Secondary dominant mode group C(1,2)				
PART	SIDE	RANK	MODE NAME	CONTRIBUTION %
P6		MODE4	C(1,2)	9,2274
C1		MODE2	C(1,2)	8,6027

Figure 4.26: The only two parts having as secondary dominant mode C(1,2): Plate 6 and Channel 1

in a very low percentage, so they will be not considered.

Secondary dominant mode group C(3,1)				
PART	SIDE	RANK	MODE NAME	CONTRIBUTION %
P6		MODE3	C(3,1)	12,6011
C3		MODE2	C(3,1)	15,0175

Figure 4.27: The only two parts having as secondary dominant mode C(3,1): Plate 6 and Channel 3

This coupling has G/T Ratio value equal to 0,8, and the sum percentage contribute of the share modes is 76,25327%. As it's visible, the percentage contribution is strongly representative of G/T ratio. This mode unify P6 with C3 for the 12%.

Since P6 is present in both groups, it's possible to unify and create a unique group containing P6 (which has both the characteristics of the two groups), C1 and C3 and this cluster will contain all parts having their same formation.

The last cluster is determined by **C(5,1)**, common as dominant weight between several parts. Taking into account only the parts in which it's relevant, the outcome is illustrated in figure 4.28.

The couplings P1-C2 and P1-C5 have G/T value 0,7333, while P1-C4 has 0,8 G/T Ratio value. All of them belong to the set of best combinations, so if parts characterized by C(5,1) as dominant merge in this same cluster, this classification leads to good quality welding performances.

As far as all other remaining parts are concerned, P4 and P5, not included in previous groups, are characterized by very high fundamental modes value C(2,1) exactly like C6. There will be set another buffer containing this three parts and the other existing ones

Secondary dominant mode group C(5,1)				
PART	SIDE	RANK	MODE NAME	CONTRIBUTION %
P1		MODE2	C(5,1)	13,7797
C2		MODE2	C(5,1)	21,844
C4		MODE2	C(5,1)	18,5396
C5		MODE2	C(5,1)	18,6027

Figure 4.28: Parts with C(5,1) as second dominant mode

having C(2,1) with the same peculiarity (value greater than 70%).

So in this last buffer can enter also parts already classified in the other secondary modes groups, like C5, C1 and P1 because these two parts have both the correct qualifications to be classified in more than one cluster because of their particular constitution made of C(2,1) very high values (more than 70%) and second mode relevant.

In figure 4.29 are reported all the six parts between the 12 initial ones with surfaces explained mostly through C(2,1). The first three parts are comprises in some other groups recorded in the second column of the grid.

This cluster guarantee the perfect matching between this parts, because if one casual plate is mated with an also casual channel, the joining has high probabilities to be good, because both parts are simplified by C(2,1) mode explaining their profile for the most and because the joining has they present a more than 80 % common contribute if mated.

For this reason it will be likely to see some parts, like C1, C5 and P1, directed towards more clusters.

4.7.2 Final classification configuration

This clusterization of parts in different group will lead to a best quality welding, because parts will be no more welded casually with the risk of face with bad joining situations. Obviously for each group will correspond a specific Buffer in a manufacturing system, in which will be contained only parts having the precise features required to access to it. Once parts are scanned and analyzed by SMA index, they will be addressed to the several buffer created based on their typical deformation modes (with the exception of P3 and P2, not included in the analysis):

Fundamental mode group C(2,1)				
PART	other groups	RANK	MODE NAME	CONTRIBUTION %
C1	C(1,2)	MODE1	C(2,1)	90,2635
C5	C(5,1)	MODE1	C(2,1)	83,2635
P1	C(5,1)	MODE1	C(2,1)	84,645
P4		MODE1	C(2,1)	91,5782
P5		MODE1	C(2,1)	98,2103
C6		MODE1	C(2,1)	85,9266

Modes already present in clusters created through secondary modes

Modes never included in previous groups defined

Figure 4.29: Parts with C(2,1) value characterizing more than 70% of the part surfaces

CLUSTER 1 [C(3,1) & C(1,2)]	
P6	C1
	C3

CLUSTER 2 [C(5,1)]	
P1	C2
	C4
	C5

CLUSTER 3 [C(2,1)]	
P1	C1
P4	C5
P5	C6

Figure 4.30: Classification in Buffer for the 12 sample parts

4.8 Non parametric Test

Non parametric statistic covers all possible techniques that do not rely on data belonging to a particular distribution, because the assumption of data following a particular distribution function is not required. The non parametric test must be implemented for the validation of the SMA index. In fact, SMA results come from a geometrical model, while comparing data

To evaluate the equality of two results, the Kolmogorov- Smirnov test is effectuated. The Kolmogorov-Smirnov test (KS-test) tries to determine if two datasets differ significantly. The KS-test has the advantage of making no assumption about the distribution of data. In statistics, the Kolmogorov-Smirnov test (K-S test) is a form of minimum distance estimation used as a non parametric test of equality of one-dimensional probability distributions used to compare a sample with a reference probability distribution, or to compare two samples. In the case analyzed we will use the two sample K-S test. The Kolmogorov-Smirnov statistic quantifies a distance between the empirical distribution functions of two samples. The null distribution of this statistic is calculated under the null hypothesis that the samples are drawn from the same distribution.

4.8.1 Sample data

Two sample data sets are the results from the experimental data and SMA analysis. Each value is the result corresponding to the value of every possible couple made of a C-shape channel and a bottom plate, for a total size of 36 data.

For experimental data set the G/T ratio is used, that is the percentage of points within the interval limit.

For the second data set a combination of cumulative energy compaction of the common modes between two parts is calculated. In fact, every part presents for each mode a percentage of representation in the shape of profile, therefore if a part has more than 60% for a single mode of representation it is "strong", meanwhile if it presents only a value like 4%, then it is not representative in the part: in this case, a common mode with a high percentage is better than one with a low value, because is more representative in the part. Because it means that mode is hardly affecting both parts, every couple of parts presents different common modes, each of which characterizes parts with different values (the magnitude and the energy compaction presence). For each coupling, the sum of the common energy compaction mode has been considered, in particular it takes into account of a shared mode the minimal value between two parts, for example, if two parts have the same mode with 57% and 70% of representation, then only the first value

will be included in the cumulative value of energy compaction. The sum of common modes gives the percentage of similarrity representation.

Two data sets are shown in table 4.1.

4.8.2 Kolmogorov-Smirnov Test

Considering two data sets: X_1 are result from G/T ratio, X_2 are from SMA analysis.

$$H_0 : X_1 = X_2$$

$$H_1 : X_1 \neq X_2$$

X_1 represents G/T ratio results, X_2 SMA data. The main intention is not to reject the null hypothesis, because the null distribution of this statistic is calculated under the null hypothesis that the samples are drawn from the same distribution.

The test is based on the calculation of:

$$D_{n,n'} = \sup_x |F_{1,n}(x) - F_{2,n'}(x)|$$

where $F_{1,n}(x)$ and $F_{2,n'}(x)$ are the empirical distribution functions of the first and the second sample respectively and n is the sample dimension.

The null hypothesis is rejected al level α when:

$$\sqrt{\frac{nn'}{n+n'}} D_{n,n'} \geq K_\alpha$$

The test value is a $p - value = 0,6585$.

As it is visible both results of the test and in the table 4.1, data present a similar cumulative distribution and then the possibility to reject the null hypothesis is low.

For this reason, we cannot refuse the hypothesis for which populations are not equal, so the predictor can be consider good, because the two data sample come from the same population.

It's possible to evaluate the univocal correspondence with the quality threshold too: the minimal percentage doorstep of points inside the tolerance limit, considered as satysfing is fixed at 70% based on the comparison with gap measurement outputs, than a binomial value can be assigned for each element.

$$x = \begin{cases} 1 & \text{if } x \geq 0.7 \\ 0 & \text{otherwise} \end{cases}$$

If the application of this binomial condition is implemented in both data sets, there is only a case in which the correspondence is not confirmed, that is P5-C3 coupling. For

Table 4.1: data for non parametric test

Plate	Channel	G/T ratio	SMA
P1	C1	1	0.859144
P1	C2	0.7333	0.821894
P1	C3	0.7333	0.708924
P1	C4	0.8	0.710568
P1	C5	1	0.992306
P1	C6	0.7333	0.721766
P2	C1	0.6	0
P2	C2	0.5333	0
P2	C3	0.6667	0.004
P2	C4	0.5333	0
P2	C5	0.6667	0
P2	C6	0.267	0.0201
P3	C1	0.5333	0.5189
P3	C2	0.6	0.54765
P3	C3	0.6	0.671247
P3	C4	0.6	0.606582
P3	C5	0.733	0.54765
P3	C6	0.467	0.54644
P4	C1	1	0.915782
P4	C2	0.8	0.8
P4	C3	0.733	0.7554
P4	C4	0.6	0.634543
P4	C5	0.867	0.852245
P4	C6	1	0.88359
P5	C1	1	0.902635
P5	C2	0.6	0.67758
P5	C3	0.6667	0.701
P5	C4	0.6	0.5652
P5	C5	0.6	0.698
P5	C6	1	0.869616
P6	C1	0.867	0.724746
P6	C2	0.6	0.63034
P6	C3	0.8	0.7625327
P6	C4	0.667	0.624132
P6	C5	110.667	0.6371
P6	C6	0.533	0.69099

the other coupled parts the boundary condition is satisfied both in real and experimental data. This result confirms the capacity of the DCT to carefully predict the percentage of points inside the tolerance limit, consequently is possible to have an idea about the portion ratio of the stitch respecting welding requirements.

4.8.3 Power test of Kolmogorov-Smirnov

Statistical power is defined as the probability of rejecting the null hypothesis when it is false and should be rejecting, this is the Type II error β . The calculation of the power can be done using a Monte Carlo simulation methods ⁹.

Generally the power of Kolmogorov-Smirnov test is high, around 95% for samples of small size, while it is around 99% with big samples (over 30 of dimension). In [5], the author guarantees the powerful of the Kolmogorov-Smirnov test using Monte Carlo simulation.

This work however simulates the power of the test using other two random sample populations, coming from the same distribution but in one of them there is an error, that must be known. In this case two populations coming from a normal distribution with the same mean and standard deviation have been created, with the difference that in one population an error has been added to the mean.

Evaluating the power of the test, it guarantees a power of 100% only with a little error for the normal distributions, meanwhile for the gamma population the power is 91,52%, the permutation of the mean of only a unit (from 0 to 1). This means power test is robust to find errors.

Thank to this simulation the result of the Kolmogorov Smirnov test can be considered strong.

4.9 FEM Analysis

The Finite Element Method (FEM) is a numerical technique for finding approximate solutions of partial differential equations as well as integral equations. A variety of specialization of mechanical engineering disciplines (such as aeronautical, biomechanics and automotive industries) commonly use integrated FEM in design and development of their products.

FEM allows detailed visualization of where structure bend or twist if subjected to stress through proper simulation software. Before the simulation and the application

⁹Statistical power of non-parametric tests: A quick guide for designing sampling strategies, P.J. Mumby.

of forces on parts, their surfaces must be discretized in several triangular or polygonal areas to analyze specifically some section and focus the attention on the more stressed and deformed zone.

The FEM analysis was conducted by CRF (Fiat Research Center) on the available surfaces measurements in STL format (figure 4.31 and figure 4.32) about 6 Bottom plates and 6 Plates of the Warwick University to make the SMA indicator stronger and to give additional prove of the goodness of the indicators used during the Similarity Analysis.

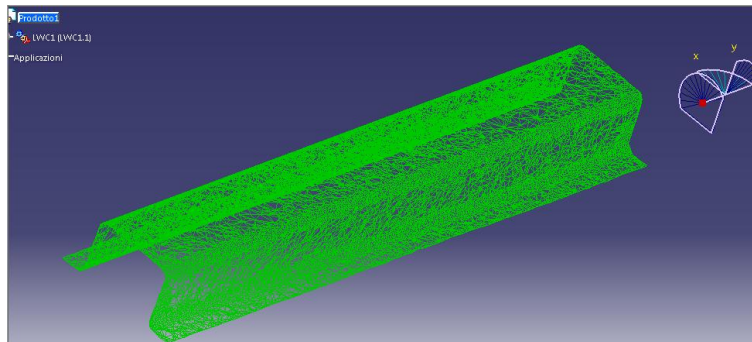


Figure 4.31: STL data format for the channel

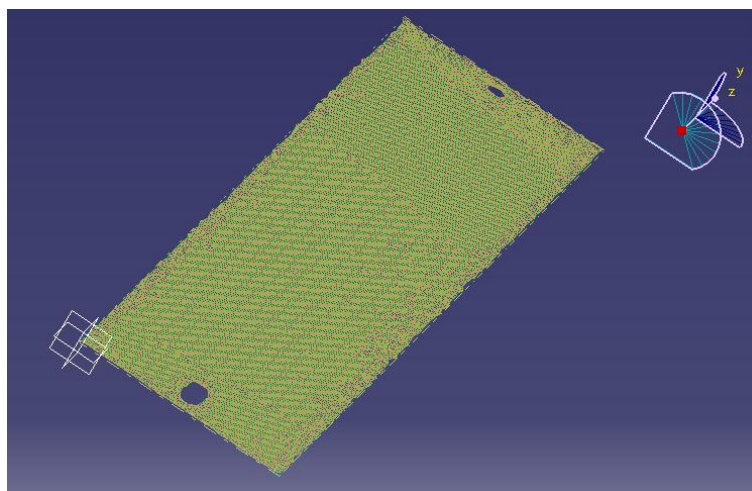


Figure 4.32: STL data format for the plate

In fact its aim is to stress UK part, once coupled, simulating UK clamping system forces, and to obtain deformation and the sprinback visualization. In fact parts will be mated following all 36 possible combinations, a fixture system and a spot welding process

is simulated. Once parts are released from clamps' pressure, the final assemble release tension stored in the profile during the coupling. When parts are no more forced they will point out the material sprinback on the final product shape. This aspect depends mostly on the elastic properties of the used materials.

FEM analysis was used to evaluate the reaction of some parts couples under fixture stress: if two parts are very similar, fixture can hold them in position without a huge impressed deformation because their profiles are likely to fit easily.

While if two parts are very dissimilar in their shape profiles, it will be difficult to constraint their fitting, because even if clamps are used, the shapes of the two parts will change but not radically, especially if clamps are considered as attachments, not as punch presses twisting and distorting completely parts shapes. In this case the tensional residual stress of final assembled product will be evident and wide.

If two sample parts are mate and their profiles present no modes in common, forcing the clamping system in some specific points, the parts are constrained to be joint together in that precise points so they will enter in contact each other in those. But the huge deformation caused by the variability in their profile and imposed to bond parts surfaces is reflected in the evident *Springback* effect after the release of parts from clamps. Otherwise, if the most dominants modes in both situation are the same for most of parts, their shapes are likely to be very similar, so clamping only hold parts in position and push them together without deforming impressively them.

The obtained spingback in this case will be surely more uniform and less accentuate.

This aspects is often retrieved in a correspondence between experimental data and what declared by the FEM analysis.

For example this two very similar couples are likely to fit immediately and with very promising quality-welding results, like the already mentioned couple P1-C5.(Figure 4.33).

On the contrary this other couple in figure 4.34 is very difficult to show good quality output value, even if hold and lightly deformed, because the distortion is quite huge.

The collaboration with CRF let to obtain some important outcome. Most of them are reported in the proper appendix section, but some significant ones must be considered in a relevant way.

The figure 4.35 presents one of the best couples. During the analysis of this FEM study, only the right welding area will be considered because it's the only zone sensible to the welding process, like the UK problem statement is concerned.

After parts are released by fixture, it's necessary a careful analysis of these particular areas and their metal spring back effect.In fact the overall tensional state on welding

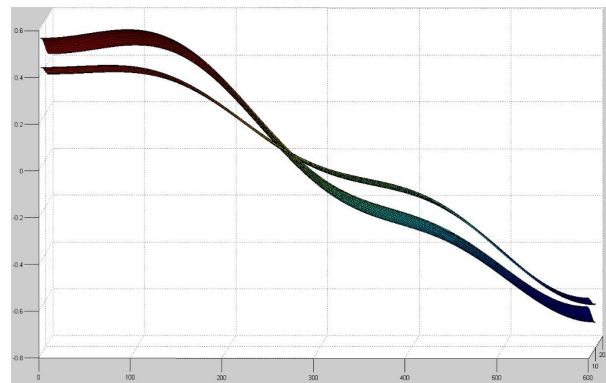


Figure 4.33: P1-C5 fitting estimated through SMA

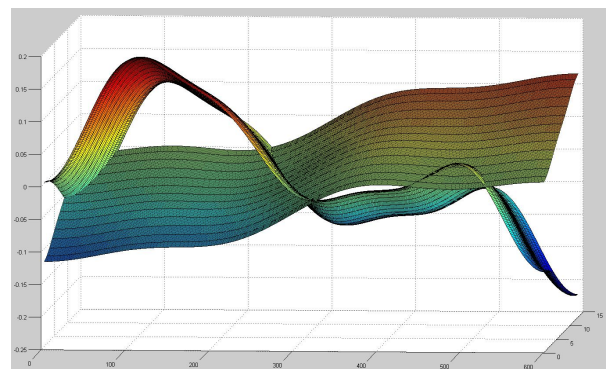


Figure 4.34: P2-C6 fitting estimated through SMA

areas must be contained inside a range $\pm 0,8$ for the final product welded, otherwise tensions affecting the assembled part are relevant and dangerous for the final quality.

Most the welding area uniform and homogeneous is, less will be the value of spring-back effect, because the material of a surface will be stressed by a softer effort to follow the other surface profile which is mated with.

To obtain a correct analysis, first of all it's necessary to check the maximum and minimum value on the column at left side in every figure, showing the sorting of all the tension values affecting parts.

If the lowest and the highest values are inside the tensional tolerances, the part is always a good matching for the right side because of the similarity of welding areas profile. On the contrary it's necessary to verify if those values are affecting the joining zone or the rest of the part, because in this case it won't affect the welding.

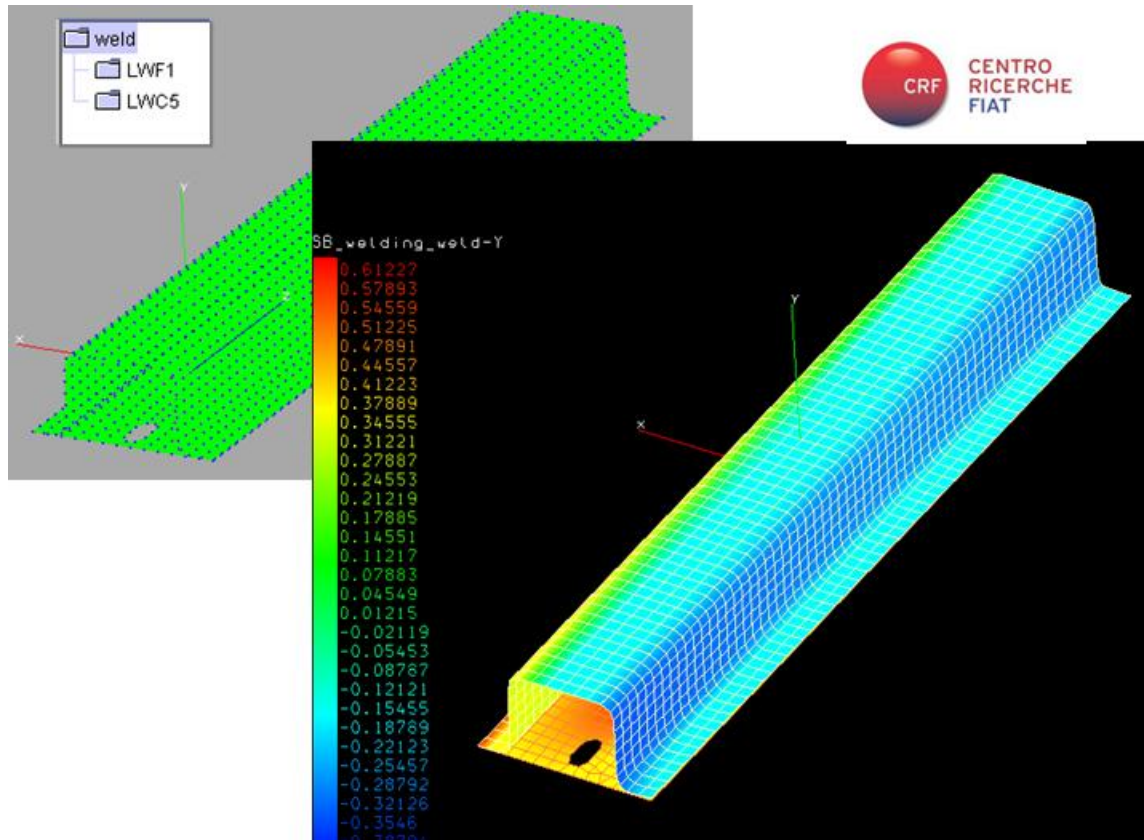


Figure 4.35: Plate 1- Channel 5, FEM spring-back range [0,612; -0,3541]

For example most of the lowest values of springback (blue colored) are often present on the top of some Channels as a dip, but the analysis is circumscribed to welding areas only. The tensional spring-back can interest one part only (the plate or the channel) or both of them at the same time.

In figure 4.35 for example present welding areas very uniform and with low spring-back value on the Channel, as for the Plate as well. The extreme values are inside the tolerance limits for acceptable springback values.

While figure 4.36 shows one of the worst couplings : the welding area is not homogeneous in its color, and the maximum and minimum values are outside the tolerances $\pm 0,8$.

The blue problematic tension affect as already explained the top of the Channel as it was a dip, but the red highest value is present on the analyzed welding area on one edge.

This important help deriving from CRF to get our analysis robust is deeply supporting results found through SMA analysis on the 26 couples, as another additional proof of the goodness of the developed indicator.

The link between the two analysis is immediate and intuitive and CRF analysis was really useful to show how the spring-back can act if parts are not similar in their shape forms and how residual tensions can return if two different profile are pair.

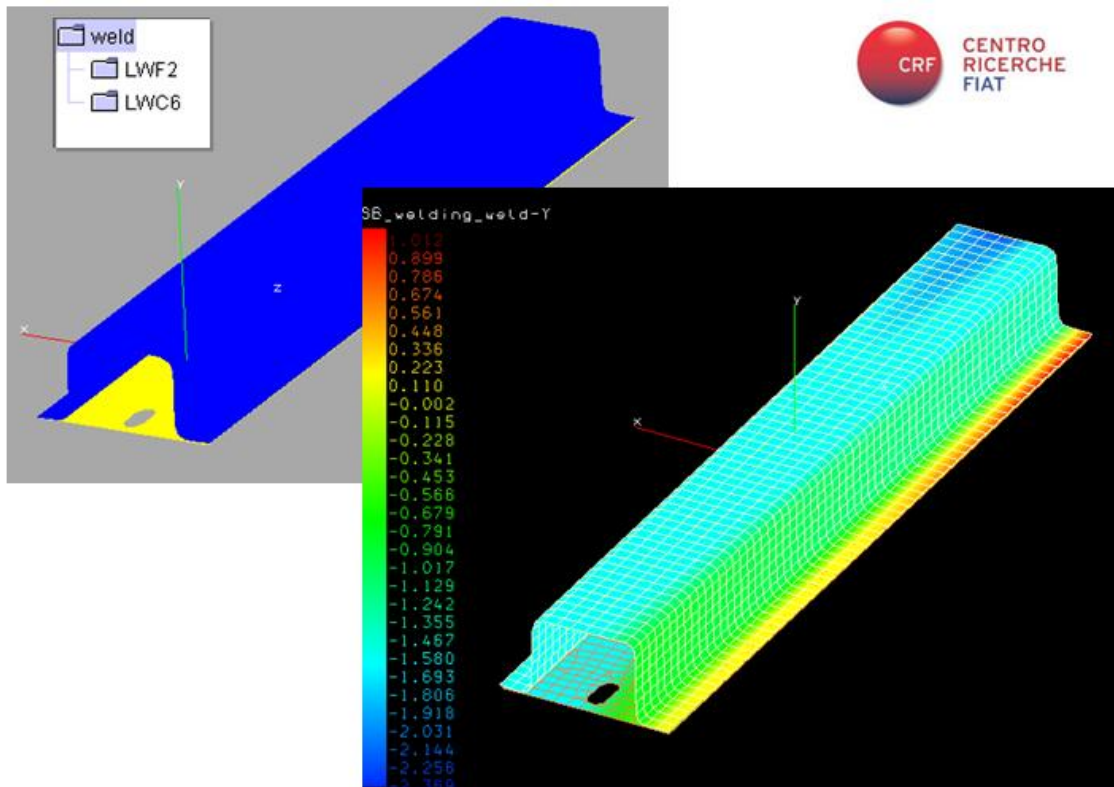


Figure 4.36: Plate 2- Channel 6, FEM spring-back range [1,012;-2,359]

It could be interesting to obtain the complete deformed profile of separated standing-alone parts once subjected to clamps pressures and use the SMA algorithm on them, to see how modes affecting parts change and to evaluate if the most distorted parts after the clamping with another one are actually constituting the worst couples. This analysis was not possible to be implemented using the prototype FEM simulator developed by CRF.

Another possible valuable analysis concerning fem analysis but not conducted by CRF because of their prototype software limits, is about the gap measures for each

couple of parts, as another confirm supporting gap measurements obtained in UK plant.

4.9.1 FEM modeling

The FEM processing was made in collaboration with CRF (Centro Ricerche Fiat).

The analysis has calculated all 36 combinations between plates and C shape channels. Input parts were .stl files; because the necessity to have regular meshes, surfaces were remeshed regularly.

Parts were positioned in the space isostatically, considering the features on the parts (the hole and the buttonhole).

The used welding simulator is a valid software, internally created and validated by CRF. The simulator was created for spot welding applications, nevertheless the output of the analysis is the tension of deformation of parts, so the kind of welding is not a significative variable.

Input variables are:

- coordinates of clamping closure points;
- coordinates of welding points;
- clamping load= 0,3 KN each;
- Poisson coefficient= 0,3;
- Young module= 210 GPa;
- yield point= 0,39 GPa.

The tools, used for the simulations, were:

- HyperWorks 10, a computer aided engineering (CAE) simulation software platform;¹⁰, to realize the mesh map for every single part;
- Prototypal tool Pre Processing, developed by CRF for processing FEM modeling development;
- LS Dyna, a solver code for the simulation phase calculation; in particular it is characterized for the crash test.

¹⁰www.altairhyperworks.com

The output variable is the FEM result of the clamping state for every combination between the C shape channel and the bottom plate. Result shows the deformation of the assembly respect the initial value, before the clamping process. For each couple a scale between the maximum and minimum gap is present and every interval values has a different representative color. Parts are colored by the state of deformation in each part, letting to see the variation.

Two important assumptions have been considered during the FEM simulation: the springback and non intersection. The first one is related to the elastic return of material, subjected after the clamping action. Because steel is an elastic material, its component tightens itself after the stamping process. The output of the analysis includes this consideration. The other aspect is related to the impossibility between two parts to make a co-penetration each other. In fact, because physically channel leans on the plate, there are some points of contact, but any kind of intersection.

The processing simulation visualizes movements respect the original position. In particular, the gap on the Z values were calculated, because the interesting axis reference. A positive gap was visualized in red (over the nominal reference point), a negative one in blue.

The tolerance specifications of a single piece is 0,5 mm, while the assembly must be 0,8 mm.

As shown in figure 4.37 and 4.38, parts present different geometries, which confirms the variability in the manufacturing process respect the nominal mathematic of the part.

This variability is the same output of the SMA model, because the representative modes are different in every case, and moreover the energy compaction value is different, giving different weights.

Analysis results

Results show parts with a more or less various states of deformation. All results are present in appendix E.

Comparing results with experimental data set, the interval variation is smaller in parts with similar modes than parts with no common modes.

End of proof, low quality welding matings present a bigger interval of tensional deformation than parts with a good coupling. Highest and lowest values are "touched" by the worst too, a confirm of the non satisfied common modes threshold.

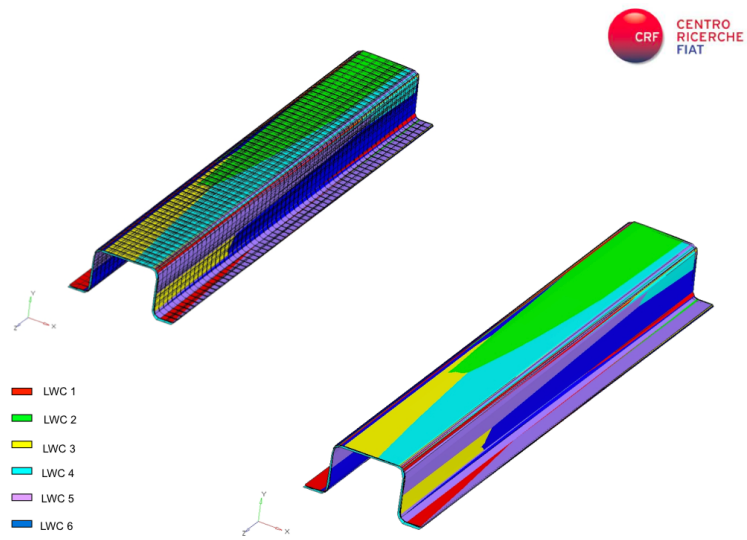


Figure 4.37: Parts' variation in C-shape channels

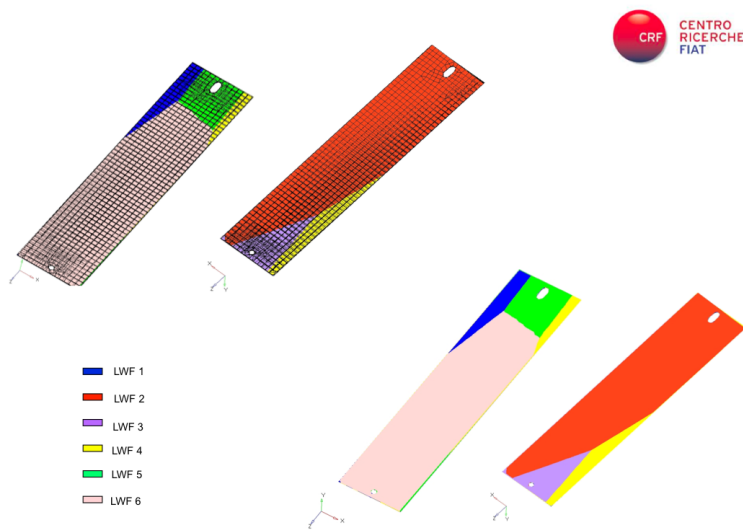


Figure 4.38: Parts' variation in bottom plates

Chapter 5

Selective assembly

In an automotive assembly system the control of dimensional variation of parts is important, in order to have a good final product. Dimensional and geometrical variation accuracy can cause problems during the assembly process, in which a lot of parts must be joint. In fact the sum of the individual component tolerance weights upon the quality of the final product.

In particular, the most critical challenge preventing the systematic application of Remote Laser Welding in automotive sector is the tight control of gap between parts (part-to-part gap) during the joining operations. This is a requirement that must be controlled to have good final mating parts. The part-to-part gap is the most critical requirement of the assembly because it presents tight limits and the quality of the joining operation depends on the distance between parts. The gap is a consequence of dimensional and geometrical error of the parts caused during manufacturing and shipping handling, for this reason a variation from the nominal value is common and real. If gap between parts exceeds limits, then a defective weld is created and parts must be rejected.

Selective assembly allows to address components in appropriate buffers to meet the required specifications as closely as possible. In fact, buffers are reserved for each class of error, based on the variation of parts.

After that, a combination of parts is selected based on their similarity, in order to be assemble.

The main idea is to evaluate the process, in terms of maximization of the production rate within the tolerance limits of the final part. In fact, the most critical parameter to maintain under control is the gap between parts. If the gap is outside limits, part must be rejected.

The classification of parts based on SMA model permits to improve the final product

quality, because the gap is controlled thanks to a flow rate partition.

The proposed classification in the previous chapter describes a clustering of parts which ensure at least 70% of energy compaction in common. Because the classification was based on the minimal value to satisfy the quality requirements, it's now possible to iterate the classification based on modes. Basing on the number of representative modes, an iterative classification can be done. The addition of classes claims the growth of dedicated storages.

The intention of chapter is to briefly analyze the state of art of selective assembly study in section 5.1; in section 5.3 to describe the idea of iteration for the classification of parts based on the research case study; then an evaluation of the proposal to verify the real improvement this approach can bring to the final product quality, in section 5.3.1.

5.1 Selective assembly for mating parts

In a manufacturing process, parts could present imperfections, caused by machining error. In an assembly process, the sum of different errors could present a large variance dimension, that can be in conflict with the tolerance of the final product.

For a high-quality assembly products from a low accuracy of machining errors, there are mainly two strategies to apply for the assembly process: the corrective and selective assembly. The first one reprocesses parts in machine, if the error is upper a certain tolerance limit; sometimes machines are different based on the error to correct. The selective assembly corrects the tolerance of the final product using the same errors of the parts, minimizing the clearance between them.

The reprocess of parts during manufacturing is expensive and onerous, for this reason a selective assembly of parts is an alternative, in which variance dimension is evaluated to compare errors of parts. The compensation of variance between parts reduces manufacturing error and costs.

Before applying a statistical selective assembly, several criteria must be met before, for example an inspection of part before the assembly process, or an increase in inventory to classify components. The selection of component, instead of a random assembly, is an economical and strategic way for a high- precision final product.

5.2 Literature review for matching parts

One of the first cases was argued by Mansoor in 1961¹, who classified the selective assembly problem as a resolution for the natural process tolerances.

The case study was discussed by Iyama and Mizuno in 1992 [38], in which a matching method must have been considered to produce high-quality elements efficiently. This paper deals with modeling of material flow in the system where the assembly stage considers "matching", and analyzes the effects of the machining accuracy of elements produced in the machining stages and the buffer capacity on the line efficiency. From the numerical results, buffer storage for matching part, which is selected in the assembly stage, is more useful for improving the line efficiency than the buffer storage for the part which selects the matching part, and that the difference in the accuracy distribution of the parts between machining stages has an important effect on line efficiency.

Pugh, in the same year, analyzed the effect of the dissimilar variance in parts [39]. Results were not satisfactory, for this reason he presented a limited solution, in which showed parts with high variances should be truncated, so that the resulting component variances could be rendered equal to each other. In fact, he leaned on the consideration that parts should have the same variance.

A new algorithm for minimizing the surplus parts in selective assembly was developed to Fang and Zhan in 1994 [35]. They proposed a new algorithm to group mating parts with the same probability but different tolerance limit to be in the same group. This method permitted to consider the imbalance of mating parts and a lower machining accuracy requirements, especially on the dimensional distributions of the mating parts. In fact, two principles were assumed: the first confirmed that the probabilities of holes and shafts expected in the corresponding group must be the same; the second one was introduced because limits of fit properties must be agreeable with the design specifications in each group with unequal tolerance range.

However, though Fang and Zhan proposed an approach better than the traditional one because the difference of tolerance limit, the algorithm was tested with normal distribution data. Only in 1998, Chan and Li [32] proposed a method that considered dissimilar distributions of parts. In particular, this method consented to couple parts through the cumulate distribution, in order to compensate the clearance specification and minimize the surplus part.

Nevertheless, none of these research was focused on the error measurement.

In 2001, a new grouping method to minimize the surplus part of selective assembly

¹*Selective assembly with components of dissimilar variance*

was proposed by Kannan e Jayabalan [29], in which parts are divided by the clearance specification to minimize the surplus parts. This approach was tested with a normal distribution, even if authors confirms that it can be extended to a non-normal one.

In the same year, Mease and Nair defined a different approach for selective assembly. First of all, they criticized the constraint on the number of bins, which is fixed; for this reason they proposed number of groups was not fixed, then for each part the cumulative distribution was calculated. For minimizing the difference between two parts, the number of groups to divide each of both must be the same. Because the algorithm to define the number of bins comes from a heuristic approach, it is resumed in section 5.2.1.

An heuristic method was defined, in order to find the best interval for each group of similar part. This algorithm confirms the optimal solution, only if parts follows a normal distribution. The approach permitted to define the number of groups (bins) iteratively and no more fixed. This approach was mentioned by Matsuura and Shinozaki [4], because they disapproved the idea of having used normal distribution, in fact in a non normal distribution case, the global optimum is not confirmed and the best solution could not be the global one.

They assumed to arrive at the precise interval expected value as Mease and Nair, in order to minimize the sum of error loss square.

In 2007, Iyama investigated a dynamic matching technique to estimate the measurement error, after that parts could be selected and allocated [9].

A corrective assembly method using buffer in a high precision machining assembly production system was developed. The main revolution was the introduction of reworking part (Iyama et al., 2010) but this approach is difficult to implement for essentially two motivations: one is that measurement errors confound the knowledge about each part's dimension, moreover the part's reprocess is complicated, especially if each machine is dedicated for a precise error.

5.2.1 The optimal binning Strategies

Until the last ten years, the number of groups to store parts were defined. Mease and Nair [18] proposed an iterative process to define the number of bins and interval variation for each interval, in order to find a convergent point with an heuristic approach based on equal area and equal width. They assumed both cases in which only one component and both of them are binned.

In selective assembly, after the manufacturing process, parts are put in different bins, the final assembly is made by matching parts from corresponding bins, because the clearance between the parts is yet estimated, before the joining operation. Mease and

Nair considered the case to reduce the clearance between $Y - X$ between part Y and X, while some cases consider the sum of X and Y.

The design for an optimal selective assembly model considers a lot of statistical and optimization variables. They assumed, as the early works, a normal distribution for both parts. This limitation will be jumped on by Matsuura and Shinozak, especially because in the work different cases were analyzed (as the non equal partition limit for the bin allocation, or a presence of a coefficient that differs by a scale parameter) apart from the non normality of the distribution of parts.

By the way, let's consider the case in which both parts must be binned to explain the model.

Let X and Y be a continuous random variables, refer to the dimensions of the two respective components. Variables are:

- $n =$ number of bins;
- $(x_0, x_1, \dots, x_n) =$ partition limits for X;
- $(y_0, y_1, \dots, y_n) =$ partition limits for Y;
- $p_i^x = P(x_{i-1} \leq X \leq x_i)$;
- $p_i^y = P(y_{i-1} \leq Y \leq y_i)$;
- $X_i = (x_{i-1}, x_i]$, that is the random variable for X conditioned to the interval;
- $Y_i = (y_{i-1}, y_i]$, that is the random variable for Y conditioned to the interval;

The case study is frowned to minimize the sum of the error loss function. The squared error loss is:

$$\sum_{i=1}^n E(Y_i - X_i)^2 p_i$$

To minimize this function, calculate the present terms:

$$\sum_{i=1}^n E(Y_i - X_i)^2 p_i = E(Y^2) + E(X^2) - 2 \sum_{i=1}^n E(Y_i X_i) p_i$$

The first two terms don't depend on the partition, for this reason the unique terms it must be maximize is the covariance between parts. Because X and Y are iid, so the calculation is equivalent to $\sum_{i=1}^n [E(X_i)]^2 p_i$.

Considering the density of X with f , while the cumulative function is defined by F , we can rewrite as:

$$\sum_{i=1}^n \frac{(\int_{x_{i-1}}^{x_i} x f(x) dx)^2}{F(x_i) - F(x_{i-1})}$$

The iterative algorithm used by Mease and Nair is useful for determining the interval for each group. Anyway, the value to calculate as the following iteration:

1. Begin with an initial set of partition limits $(x_0^0, x_1^0, x_2^0, \dots, x_{n-1}^0)$
2. Using these initial partitions, compute the conditional means $E(X_1)^0, E(X_2)^0, \dots, E(X_n)^0$.
3. Compute

$$x_i^1 = \frac{E(X_i)^0 + E(X_{i+1})^0}{2}$$

4. Go back to step 2 using $(x_0^1, x_1^1, x_2^1, \dots, x_{n-1}^1)$ in place of $(x_0^0, x_1^0, x_2^0, \dots, x_{n-1}^0)$ and iterate until converge.

Results demonstrate that the solution is not necessarily unique, so the global optimum is not guaranteed. In fact solution could correspond to a local minimum. For this reason, they established a condition for determining if the solution is the global optimum one.

If the density f is positive in an interval (A, B) where $-\infty \leq A \leq B \leq \infty$ and:

$$\frac{\int_t^{t+h} x f(x) dx}{\int_t^{t+h} f(x) dx} - t$$

is non increasing in $t \in (A, B)$ for all h in $(0, \infty)$, then only one global solution exists.

While if the density $f(x)$ is strongly unimodal, then the density above is non increasing in t for all h in $(0, \infty)$.

5.2.2 When distributions differ by a scale parameter

In the paper, Mease and Nair extended the case in which one distribution differs to the other by a coefficient, maintaining the same scale, so $P(Y \leq y) = P(X \leq \sigma y)$, with $\sigma \geq 0$. Rewriting the expected value considering this relation, we can find:

$$\sum_{i=1}^n E(Y_i - X_i)^2 p_i = E(Y^2) + \sigma^2 E(X^2) - 2\sigma \sum_{i=1}^n [E(Y_i)]^2 p_i$$

Because the first two terms do not depend on the partitions, we have to minimize the third one. Considering the effect of the σ , we can minimize that:

$$\sigma = \frac{\sum_{i=1}^n [E(Y_i)]^2 p_i}{E(Y^2)}$$

The value is not necessarily equal to 1, so the distribution are not the same for the optimal value. Pugh analyzed the case in which variance could change between parts, but results were unsatisfied, so he truncated parts with a high variance. Actually this result doesn't confirm this thesis.

5.2.3 Non equal partition probabilities

Let's try to relax the assumption to have the same probability for both part: $p_i^x \neq p_i^y$. In fact, when you have only one part to be binned and cost is relatively cheap, than it is no more so compelling. They go on considering the minimization the expected value, but now the partition limits for one part must be fixed before.

For example, fixing $(x_0, x_1, x_2, \dots, x_n)$ the value of X will be function of Y. The value is now:

$$E(Y - X_{\delta(Y)})^2$$

where $\delta(Y)$ is equal to i when $y \in (y_{i-1}, y_i]$. Then δ will minimize:

$$E(Y - X_{\delta(Y)})^2 | Y = y = (y - E(X_{\delta(y)}))^2 + var(X_{\delta(y)})$$

Moreover, when y is equal to

$$\frac{E(X_i) + E(X_{i+1})}{2} + \frac{var(X_i) - var(X_{i+1})}{2E(X_i) - 2E(X_{i+1})}$$

then:

$$(y - E(X_i))^2 + var(X_i) = (y - E(X_{i+1}))^2 + var(X_{i+1})$$

5.2.4 Conclusion

The variation of parts is a problem that must be controlled during the joining operation. Selective assembly is a method which permits to define the best combination between them, in order to minimize the clearance of mating parts. The division in bins for components is a good way to control this problem, even if the cost is proportional to the number of bins for stocking parts and the quality of assembly for a more detailed

measurement of them. The trade-off could be controlled by a fixed number of bins: in fact, if it is yet defined, then the heuristic method permits to reduce variation.

On the other hand, the approach doesn't consider an asymmetric loss function and an overall tolerance constraint. Moreover, the buffer capacity is not limited. At the end, as other works, the problem of measurement errors is not considered.

5.3 Classification of parts

Until now, the branch of research about the selective assembly has always looked for methods directed to the compensation of the error. Because the following work is based on the joint of lap parts, proposed methods are not workable. A better way is the similarity analysis: the shared pattern between two parts it's a methodology to maximize the common part progress and reduce the error map.

The heuristic method mentioned in section 5.2.1 finds a solution to decide the optimal number of bins and minimize the error in the final product. The intention of this work is to be able on finding the optimal number of classes, in which divide parts and so maximize the quality of the joint. The main difference in the approach is the decision-making variable: meanwhile the paper of Mease rests on the partition of the distribution of parts and try to minimize the error between two parts, in this work the decomposition of a part in modes which define the profile is the principal variable.

In fact, each part is categorized by the kind of modes, with the corresponding phase and percentage of energy compaction. Based on modes, the work proposes a partition of parts on the cosine discretization. As seen in chapter ??, modes are representative of the profile and they are significant in an coupling if the percentage of shared modes is high.

The starting number of classes is defined by the principal modes, because they are the main characteristic of the part. So, evaluating the main modes affecting each part, if in percentage greater than 60%, they can be considered fundamental. A first subdivision of part in class will be obtained, the total number of them is equal to the fundamental modes between more than two different type parts.

In this way a series of unuseful steps are removed. From this point, step by step a secondary mode is added from each group, until the number of non conforming matings are removed.

Once found the fundamental characterization for every part, then other groups can additionally divided into some other subclasses defined by secondary modes. In this phase, the iteration will be implemented mode by mode, considering one of them at the

step. Evaluating the improve in obtaining a fewer number of bad couplings.

The idea to make iterative the number of groups is justified with the research of an improvement in quality step by step. For each iteration the mode which reduces the number of bad couplings is selected and a class based on that mode is created.

Then another mode is found and so on, until the non good matings are no more possible. In fact, in each class both parts are inserted and all possible combinations must be evaluated.

A scheme of the iteration is represented in the figure 5.1.

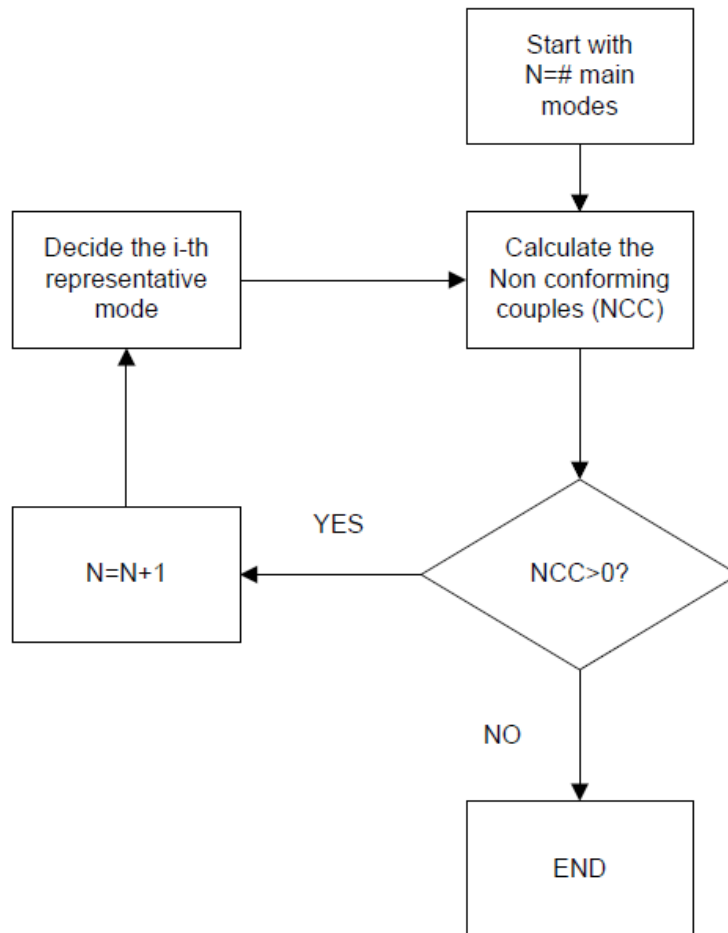


Figure 5.1: Scheme of the iterative method to determine the number of groups

Starting from the parts of the research case study, the iteration of the groups has been done.

The idea of an iterative classification starts from the incrementation of the welding quality of couplings and the reduction of the defective final products, because the addition of groups permits step by step to mate parts in a more detailed way. In fact, adding groups, parts are selected with more specific modes, that leads to a more number shared modes. Bigger is the number of common modes (with magnitude in agreement) and the cumulative energy compaction, more parts can be consider similar, that is the goodness of joint.

Each pairing is evaluated by the cumulative energy value of the same modes: if the sum is over the limit requirement (70%) the welding joint will be good, otherwise no. The decision to impose the threshold of this percentage is because the energy compaction represents the weight of each modes present in the profile: if for each common mode between parts the minimal value of energy is considered and the sum of all is done, then it is presumable as a good value from the similarity point of view.

An heuristic approach sets up limits and constraints like decisional variables. The choice to use this approach is because any analytical has never been used to identify the similarity between two objects, based on modes; moreover any analytical function has not been found to compare parts through modes in manufacturing process was never used and a threshold on the common modes was never considered until now. For this reason, comparing experimental data with the results from the SMA analysis, the limit to 70% was defined.

The iterative classification is based on the idea to classify parts starting from a unique class ("as is" case), in which no selection is done, step by step adding a group until a quality improvement is not present. For each class both plates and channels must be included. Once classes are defined by modes, then parts are selected and address to the most appropriate group. When parts are in the same class, all possible combinations are made and an evaluation of which matings are good or not is done.

Making some preliminary remarks, the classification of parts is based the fundamental mode, which in this case is C(2,1) mode, the most present with an energy compaction more than 50%.

From the output of the SMA model, each part is represented by a certain number of modes with the corresponding energy compaction and phase.

The intention of classification is to reduce non good welding, in order to improve the final product quality. The elimination of the scrap ratio before the assembly line, let the line work only with perfect part matings. The division of parts has been set up to minimize the wrong couplings.

Considering this assumption the following states are found:

1. **"As is" case**, in which all parts are not analyzed and random couplings are made.
2. **First partition**, in which parts sharing the same fundamental mode are put in the same storage and a first reduction of some worst couplings is gained.
3. **Second partition**, in which parts are divided principally in two flows.
4. **Third partition**, the ideal case.

Suppose that both channels $C_i, i = 1...6$ and plates $P_i, i = 1...6$ with $i \neq 2, 4$ put in the same class, the evaluation of the coupling is done.

"As is" case

The "as is" case is the basic situation, which doesn't present any classification, so all combinations are possible, because parts arrive at the assembly line randomly. In the actual state, P2 and P3 are considered, because there is not possibility to analyze parts, they are not considered as scraps.

In this case, all the possible 36 combinations are made:

The 67% of couples is not a good mating, only the 33% could guarantee a good welding joint (see table 5.1).

First partition

Calculating all the possible matings, there is a 54% of non perfect couples, while a 45% is conformed to a good quality joint.

This division is based on the most relevant mode C(2,1) (see section 4.7.1). Parts having an energy compaction for this mode greater than 70%, can have a good quality mating with parts having the same peculiarity, otherwise no. Because P2 and P3 have phase π , they are rejected, in fact any channel has the same phase π and they can't have a good couplings.

As it is visible from the table 5.2, the percentage of possible low quality weldings is high, more than half combinations and a correction of part to reduce the defect must be done. For the correction another class must be added.

As we can see in the table 5.2, C2, C3 and C4 don't satisfy singularly the threshold for the minimal value of energy compaction, considering only the most relevant mode C(2,1). In fact all combinations between plates and these parts are not good.

The addition of another mode (the secondary one depends on the first chosen) to classify parts will be taken into account in the next division.

Table 5.1: "as is" case

Good Welding	Non good Welding
P1 C1	P1 C2
P1 C5	P1 C3
P1 C6	P1 C4
P4 C1	P2 C1
P4 C5	P2 C2
P4 C6	P2 C3
P5 C1	P2 C4
P5 C5	P2 C5
P5 C6	P2 C6
P6 C1	P3 C1
P6 C3	P3 C2
	P3 C3
	P3 C4
	P3 C5
	P3 C6
	P4 C2
	P4 C4
	P5 C2
	P5 C3
	P5 C4
	P6 C2
	P6 C4
	P6 C5
	P6 C6

Table 5.2: Quality matching parts with one class

High quality class 1 C(2,1)	Low quality class 1 C(2,1)	C(2,1) phase π
P1 C1	P1 C2	P2
P1 C5	P1 C3	P3
P1 C6	P1 C4	
P4 C1	P4 C2	
P4 C5	P4 C3	
P4 C6	P4 C4	
P5 C1	P5 C2	
P5 C5	P5 C3	
P5 C6	P5 C4	
P6 C1	P6 C2	
P6 C3	P6 C4	
	P6 C5	
	P6 C6	

Second partition

In case of two different classes, a significant improvement is present. In fact, a selection of P6, C1 and C3, which are the best channels to be assembled with this plate, are addressed in a different buffer in order to reduce the number of possible combinations between the plate 6 and the other channels. These parts are characterized by the secondaries modes C(3,1) and C(1,2). Then, parts presenting these modes, are put in a different class separated the rest of other parts, which not present them.

In this way a reduction of non perfect matching is achieved:

The percentage of non perfect couples is reduce from 54% to 40%; in the first class C(3,1), C(1,2) there is no possibility to have a "bad" mating.

The division of these parts is on the partition to the characteristic mode of the channel C1 and C3. In the other class C(2,1) non perfect matings are the combinations of P1, P4 and P5 with C2 and C4. In the next division this separation will be done.

Table 5.3: Quality matching parts with two classes

High quality class 1 C(3,1) C(1,2)	Low quality class 1 C(3,1) C(1,2)	High quality class 2 C(2,1)	Low quality class 2 C(2,1)
P6 C1 P6 C3		P4 C1 P1 C5 P5 C6 P5 C5 P4 C5 P4 C6 P5 C1	P4 C2 P4 C4 P5 C2 P5 C4 P1 C2 P1 C4

Three classes

In this last case the worst cases will be avoided by an additional specified classification, in order to obtain the best case in which no faults are introduced in the assembly line. The introduction of the mode C(5,1) permits to separate P1 and C2, C4. In particular, these channels caused a bad mating with P4 and P5. Thank to this separation, non good coupling are no more present.

Table 5.4: Quality matching parts with three classes

High quality class 1 C(3,1) C(1,2)	Low quality class 1 C(3,1) C(1,2)	High quality class 2 C(2,1)	Low quality class 2 C(2,1)	High quality class 3 C(5,1)	Low quality class 3 C(5,1)
P6 C1 P6 C3		P4 C1 P4 C5 P4 C6 P5 C1 P5 C5 P5 C6		P1 C1 P1 C2 P1 C4 P1 C5 P1 C6	

The division in three classes allow to have only the best fitting couples, which guar-

antee a good quality of welding.

Four classes

Surely another partition of the flow can be carried on, nevertheless the efficiency and the improvement is not present, if not for only a best sophisticated matching. The possibility to detail more dedicated buffers permits to divide further parts, in order to add the common energy compaction, that is the more similar surface. This approach implies not a satisfaction of the quality limit, as much an improvement of the quality of the final product. In fact, instead of guaranteeing a joint with the 70% of gap points inside the tolerance limit, a bigger percentage can be satisfied.

However, the objective of the work is to get better the quality of the final product, that is a reduction of non quality welding; the result is reached if the total length of the laser stitch has a gap under the upper limit greater than the 70% of total. This condition doesn't distinguish a laser joint from another, if the respect of the limit is obtained.

Of course, it's reasonable try to have always the laser joint stitch inside the tolerance in all its length, but it is as much true that a guarantee of a perfect joint is not always possible to be guaranteed, because during the joining operation other variables play an important role to the quality, like the choice of laser parameters, the fixture design and the variability of the process.

5.3.1 Analysis of results

In terms of quality, this approach shows efficiency because laser stitch requirements are very tight, however the potential addition of buffers and selective flow parts is expensive and a guarantee to have always a couple of parts available is not always determined. Because the pressing cycle time is less the welding process, a cumulative queue of parts is present. It's supposed that at steady state all parts can have the correspond other one to constitute a matching, but in ramp-up phase can not always be happen.

The achievement of results is a consequence of the SMA analysis use, that permitted to classify parts in a simple way. In fact, the only limitation of this approach is a prior analysis of a parts' sample, in which profile is taken and points cloud are the output. After having the matrix of points, the indicator can be applied. Afterwards an analysis about the possible classification of parts must be evaluated.

Computationally the method is fast and simple. Moreover the process to scan parts and address them in dedicated buffers is judged to stay in the assembly cycle time, in this way the introduction of the selective design doesn't cause a bottleneck condition in

the line.

If a good matching parts is not available, then another selection of parts is done.

The flow rate ensures the continuous presence of parts in storage and there are not situations of starvation for the remote laser welding.

Chapter 6

Case study: COMAU

COMAU Body Welding & Assembly is a global leader in the supply of advanced production systems for vehicle full body, body components manufacturing, and complete turnkey body shops worldwide.

In this chapter the intention is to briefly describe in section 6.1 a generality view of Comau. The description of the productive site organization and assembly line brings a detailed representation of the firm.

This problem of controlling the upper limit permits to similarity index to find the best combination between parts, in order to eliminate the process of tweak and reduce cycle time, improve quality of the joint and automate the fixture process. The chapter goes on studying the similarity of Fiat doors. The application of the SMA method and the classification of parts is done thank to a collaboration with Fiat. The data acquisition from real manufactured parts has permitted an analysis of the modes present in them and consequently the best partition and accomplishment is found.

The aim of this part is to apply the method to a real case, in order to evaluate the unvisible variety between parts and let the matings best quality. In fact, if parts present different modes, then a selection is necessary to the reduction of defects and the getting quality requirements.

6.1 COMAU

COMAU is the leader of the Fiat group in production systems sector, in particular its specialization is robotics, and it's also the worldwide leader in the automatized welding machines field.

Comau is divided in four sectors: Aerospace Production Systems, Body Welding &

Assembly, Powertrain Machining & Assembly and Robotics & Maintenance Services.

The activity of Fiat in this area started in 1935, during the desire of verticalization during that period, on the will of the founder Giovanni Agnelli to realize all the production machines on his own "behalf".

In 1973 a group of companies managed to combine together to form a consortium called COMAU (CONsorzio MACchine Utensili), whose president was Sergio Rossi, with the purpose to realize a common establishment in the ex- Soviet Union. In 1977 this consortium became a firm, giving life to the Comau Industriale S.p.a, which evolved into Comau Finanziaria S.p.A in 1978. The society was controlled by Fiat from the beginning of this period.

With 26 locations in 15 countries, and more than 40 years of experience, Comau takes pride in being a global leader in the industrial automation field, while providing the highest level of localized support. Its products consistently exceed the needs and expectations of its customers in industry segments such as automotive, aerospace, heavy industry, military, and recreational.

Currently COMAU is a big multinational company and can be supported by different placements in all the EU, from Italy to Germany and France or Spain, but it's also an important presence in USA where, after the acquisition of PICO society, show a complete presence in all sectors.

Recently was realized the Chinese location, where planning activity takes place, and the south-Africa placement, where the core-activity is the production.

The activities developed by COMAU are multiple and concern two main aspects: the product planning and assembly system projection.

6.2 COMAU products

Considering the product COMAU, in particular its engineering division UTS, starting from design activity, takes care of car body shell planning, modeling and components structural analysis. In Figure 6.1 a brief list of COMAU activities is represented.

Between the most important COMAU productions there are RoboGate and Open-Gate systems for the body shell assembly, which are body-framing systems. But basically the core-products are remote laser welding systems like *Agilaser* and *SmartLaser* and, car doors assembly systems characterized by very high values of repeatability and flexibility

In the last years COMAU, in collaboration with **CRF (Centro Ricerche Fiat)** in Turin, Italy, spent most of the time and money on the laser welding problem because

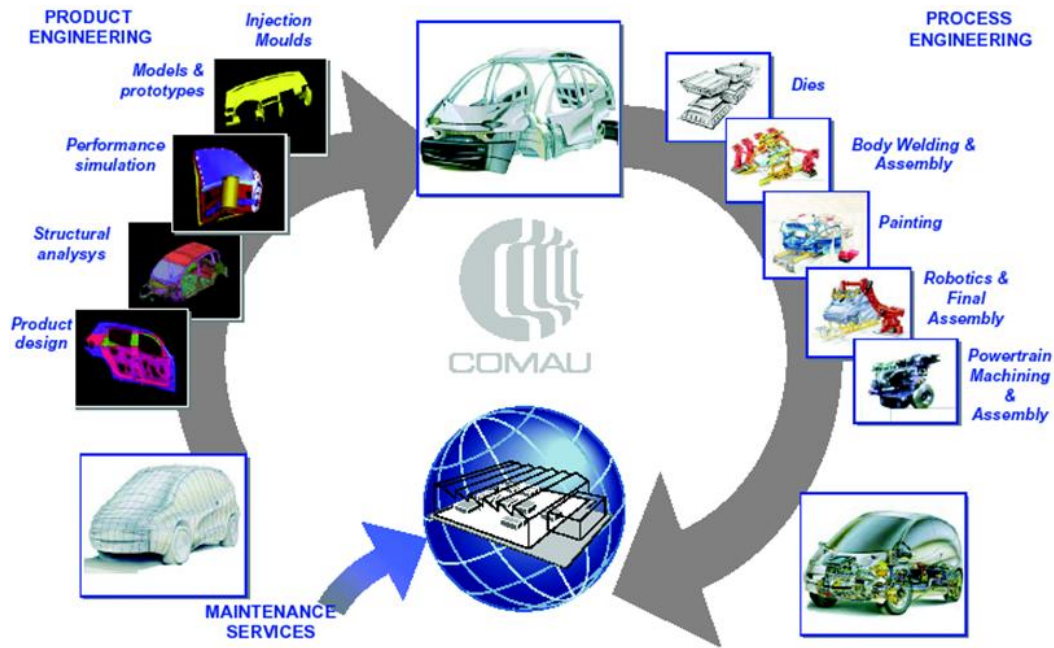


Figure 6.1: Simple scheme of COMAU activities

this kind of welding obtained several approvals. On one side the possibility to realize welding speed very performing respect to all the others techniques, on the other side the high aesthetic value joints and at the end the reachable flexibility, made the laser welding one of the most appreciate joining techniques in the automotive field.

At the beginning developed only for mechanical components and then extended to sheet metal work applications, with the research progress COMAU introduced in 2000 a new concept of welding through the birth of the first remote laser welding system 3D, the **AGILASER**. The particularity of this system was the facilitate accessibility to the parts and the possibility to realize joints without any contact or interaction between the part and the optic. In fact traditional systems oblige to locate welding joints in easily accessible areas for the anthropomorphic robot movement; The idea of remote welding solved completely this problem through the use of non conventional focusing optics. This optics, with a focal distance more than 1000 mm, permit the realization of welding stitch in zones not-reachable before.

In figure 6.2 all the application fields for the several laser spring with the power and beam quality variation are reported.

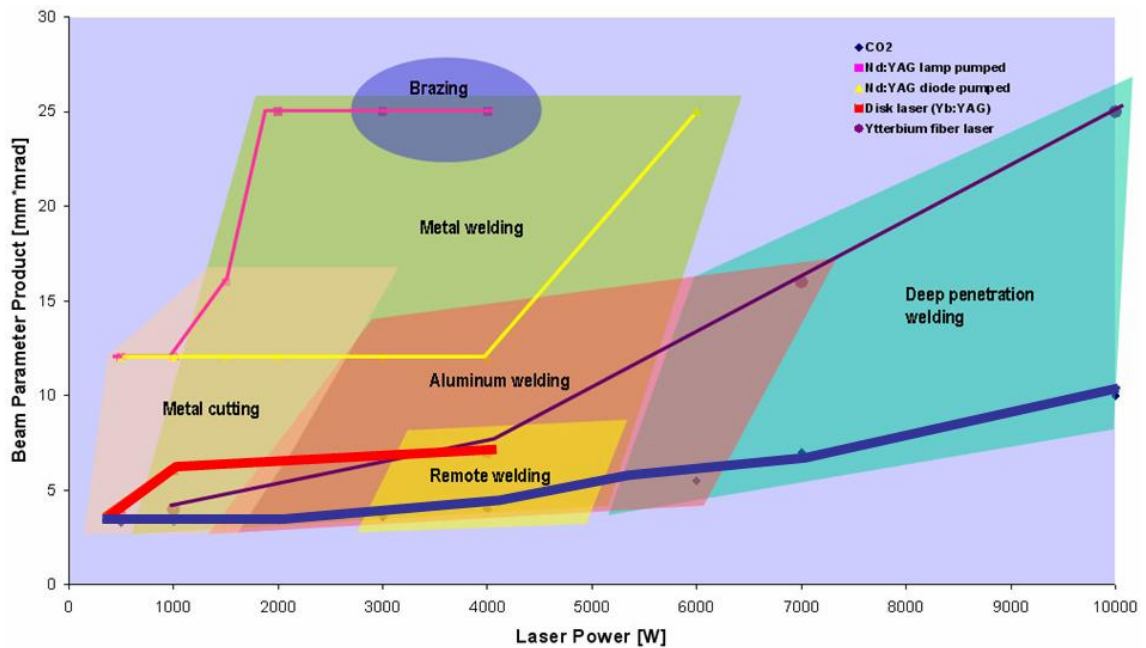


Figure 6.2: Application fields of laser spring

6.2.1 3D remote laser welding system : AGILASER and SMART-LASER

AGILASER system

In the classical CO_2 laser system, described in Chapter 1, the beam is carried towards the part through a mirroring system. The high focal length of the focusing lens (1000 ÷ 1500 mm) let to have a huge distance for the work.

The laser beam created by the source is carried through little mirrors and then guided to the head of the robot where is focused through a specific lens.

The focused beam is reflected by an inclined mirror, which allows two rotation respect two axis perpendicular each other.

Through the focusing lens movement and the fixed mirror the system is able to describe a work volume shown in figure 6.3. Thanks the capacity of the head to move along all the axis and thanks the mobile mirror able to rotate around x axes, the system can guarantee an optimal work volume.

This CO_2 laser solution, characterized by elevated dynamics, allows the reduction of the re-positioning time between a welding stitch and the following one, increasing as a

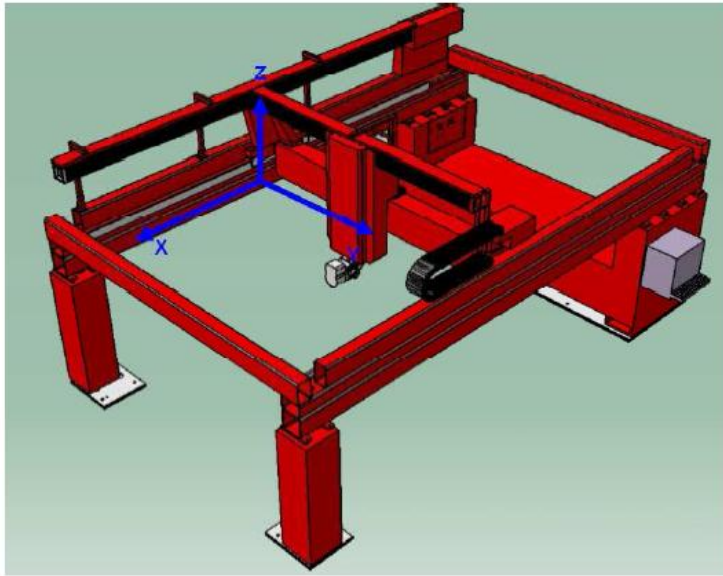


Figure 6.3: Workspace of typical CO_2 laser system

consequence the *duty cycle*, the ratio between the time of effective use of laser welding and total time required to complete all the process; this technology is able to increment the number of weldings of a factor between 5 and 10 in a precise cycle time. But this laser typology are affected by some limitations:

- Dimensions work-volume are quite restricted for a typical car component;
- Welding on the vertical plane was not realizable;
- The welding feasibility was limited also because of the angles between the incident laser beam and the perpendicular/normal coming out from the laser stitch.

These problems were overtaken by COMAU introducing a new integrated remote laser welding system : AGILASER. (figure 6.4)

AGILASER is a laser welding portal composed by a high dynamics scanning head installed on the 3-axis portal. The 3D portal structure was projected with the aim to obtain high precisions. The portal structure give to the scanning head 3 degrees of freedom, in particular the movement on X,Y,Z axis (figure 6.3).

This remote system is basically composed of a CO_2 slab source, the 3D portal and a focusing head.



Figure 6.4: AGILASER system head welding and fixturing system

Differently from typical CO_2 remote laser system described previously, the laser beam is carried to the Z axes of the portal. Here the laser, once collimated, meets the focusing lens mounted on a linear axes which permits the focal point translation. The focused beam hits the first fixed mirror inclined of 45° , which reflects it towards the second mobile mirror able to rotate around two axis perpendicular each other, describing two arches respectively of $\pm 120^\circ$ and $\pm 30^\circ$ (for a maximum angle of 240°).

Lens Movement (L axis)	
Stroke	480 mm
Speed	2 m/s
Acceleration	50 m/s ²
Mirror Rotation (B axis)	
Stroke	± 120 degrees
Speed	22 rad/s
Acceleration	150 rad/s ²
Mirror Rotation (S axis)	
Stroke	± 15 degrees
Speed	22 rad/s
Acceleration	100 rad/s ²

Figure 6.5: Peculiar parameters of the motors which let the AGILASER optical system components make translations and rotations(focusing lens and second mirror)

The optical system is a relevant component of the portal structure of the robot. Characteristics described above allow to reach every point inside the volume 4500(X)x2500(Y)x920(Z)

mm^3 with high values dynamics. All the axis of this system work in a particular coordinated way permitting the re-positioning time covering. The choice to adopt a Cartesian robot was necessary at the beginning because only through this configuration could be obtained high precision level to move the beam laser.

The volume of work is reported in figure 6.6.

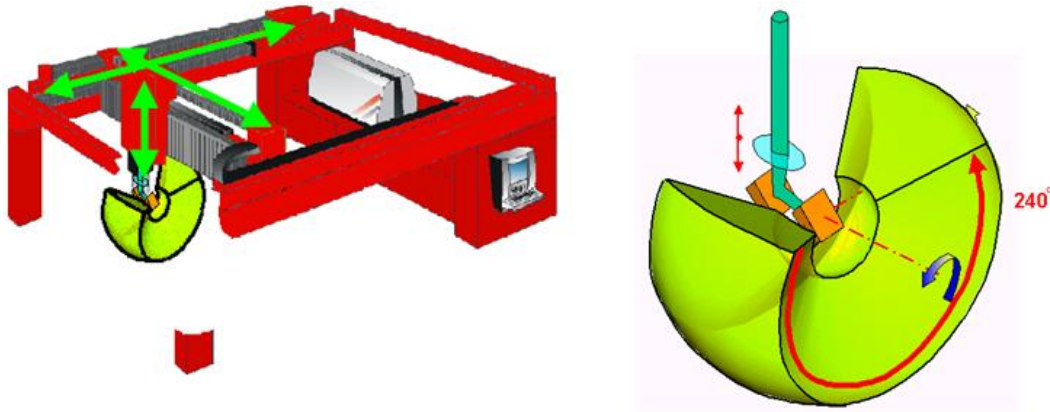


Figure 6.6: End-effector translations along X, Y,Z axis, mobile-mirror rotation around X axes and translation of the optic along Z axes

AGILASER is a very flexible system. As we can see in figure 6.7, a welding end-effector free to move along X,Y,Z axis, and two input/output zones for parts are present in the station. During the manufacturing process, components are positioned on rotating supports, and they are held in the correct geometry through special fixture and blocking system. The use of routing supports allows a noteworthy cycle time reduction, because it is possible to load parts outside the station while into the station the previous manufacturing process is happening. Revolving bearings permits the unloading of the manufactured in the same side in which is introduced parts to be manufactured.

The double input/output areas and their corresponding rotating supports offer the possibility to realize different parts on two sides of the station, using the welding head movement capacity. This last aspect was particularly appreciated by automotive firms which decided to adopt the system for both front doors and rear doors (left and right) belonging to the same model. manufacturing them in the same station.

The AGILASER is nowadays used for the production of Fiat Bravo assembly door in Cassino plant.

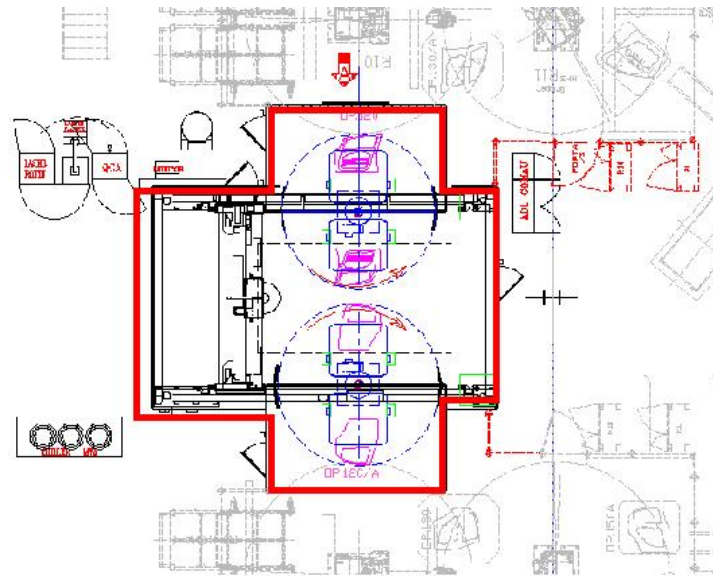


Figure 6.7: Functioning scheme of a typical AGILASER station

SMARTLASER system

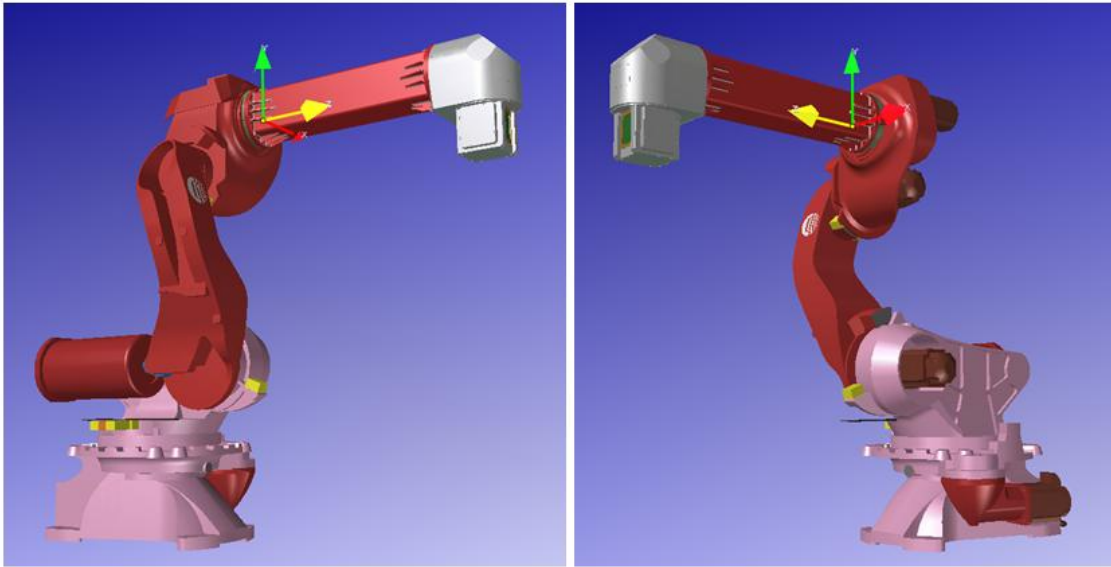
The availability of rigid dish laser source with high focus and the willing to realize a remote laser system quite versatile pushed COMAU to develop a 3D anthropomorphic remote laser welding: the **SMARTLASER**.

The SMARTLASER belongs to the second family (Yb:YAG system) and represents the new borderline for remote laser welding systems. In the next paragraph all the analysis are referred to the SMARTLASER present in the Cassino establishment, that in the moment is dedicated for the assembly of Giulietta Alfa Romeo and Lancia Delta door.

The robot used in Cassino plant (Italy) is composed by a 3D articulate robot with 4 axis, coming out from the COMAU standard of the SMART NH1 with C4G control, on which is installed a focusing scanner module. This scanner module receives inside the optical fiber coming from the solid state source: *laser disk HDL 4002*, produced by TRUMPF.

In the following outline all the parameters characterizing the laser source used in the establishment are reported.

- Wave length radiation \Rightarrow 1029nm
- Minimum Power \Rightarrow 40 W



- Maximum Power \Rightarrow 4000W
- Beam quality \Rightarrow 8 mm mrad

The issued laser radiation from the source is very high quality beam and is characterized by a wave length near the infrared. The scanner module also contains several lens composing the focusing optic system.

Through the possibility of carrying with optical fiber the beam laser generated by the already mentioned Yb:YAG source, and through the adoption of an optical dimensionally small-size zoom, it is possible to obtain a focal length similar to the AGILASER one but moved through the first 4 axis of the robot (like in *COMAU SMART NH1*).

Two important characteristics of SMARTLASER system are time sharing and back up. The time sharing is the possibility to use at the same laser source for more working stations, while the back up is the possibility to use in the same position a second laser in case of failures of the used one. SMARTLASER presents some advantages like repositioning time reduction which generally causes an higher duty time. That means a more intensive use of the source, granting a more rapid amortization of laser costs.

Another relevant step reached through this system was the realization of a remote welding solution exploiting as most as possible standard components, with consequent advantages in terms of cost reductions and better reliability of the final product.

The typical advantage of this solid state source Yd:YAG than the traditional Nd:YAG,

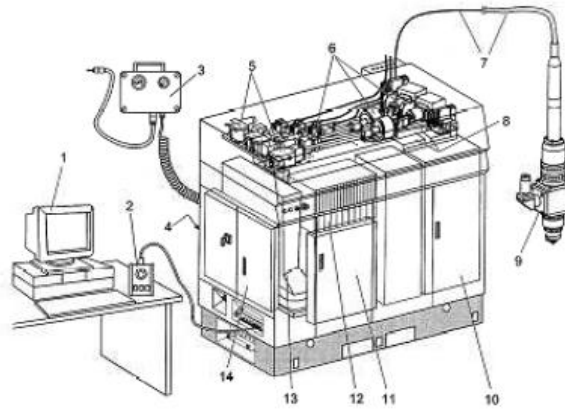


Figure 6.8: Laser source outline

pumped by lamps, is represented by the visible higher efficiency (10 % for Yd:YAG and 3 % for Nd:YAG) which permits a meaningful reduction of the dimension of the external water cooling engine, called chiller, very cumbersome for Nd:YAG source.

The consequence is a reduction of both occupied space and energy consume.

This system presents a series of positive aspects like also respect to CO_2 remote systems:

- the possibility to transport the laser beam through fiber: through this systems there is the possibility to carry the fiber till the 4^o axes, while in case of AGILASER is necessary to carry the beam through a mirrors chain very unwieldy.
- a better coupling efficiency between YAG laser radiation and the metallic parts.

The high work volume is another important aspect. In fact this volume is given by the sum between the work volume of the movement of lens placed inside the scanner module ($1,5m^3$) and the characteristic inner robot work volume. The total work volume is represented in figure(6.10).

The most common SMARTLASER applications are parts manipulation, assembly, spot welding, laser welding and protective, sealant, sticky applications. The robot can be linked to a control unit called $C4G$ created for the simple, efficiency and multi-functional management of a working cell. This 3D remote laser welding can operate also on big dimension objects like body shell and car chassis, mobile car parts.

The objectives prefixed by COMAU in these kind of systems planning are the minimization of the system time repositioning between two welding stitches and the following

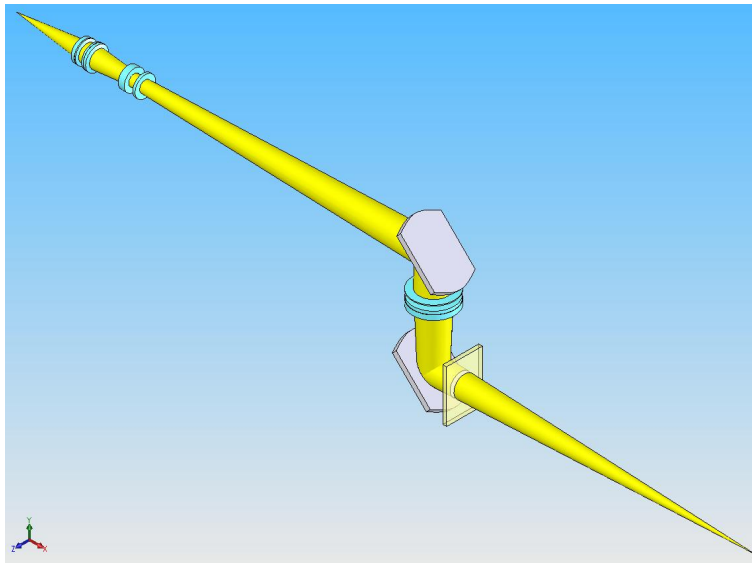


Figure 6.9: Optical components(optic $n^{\circ}1$ and $n^{\circ}2$)

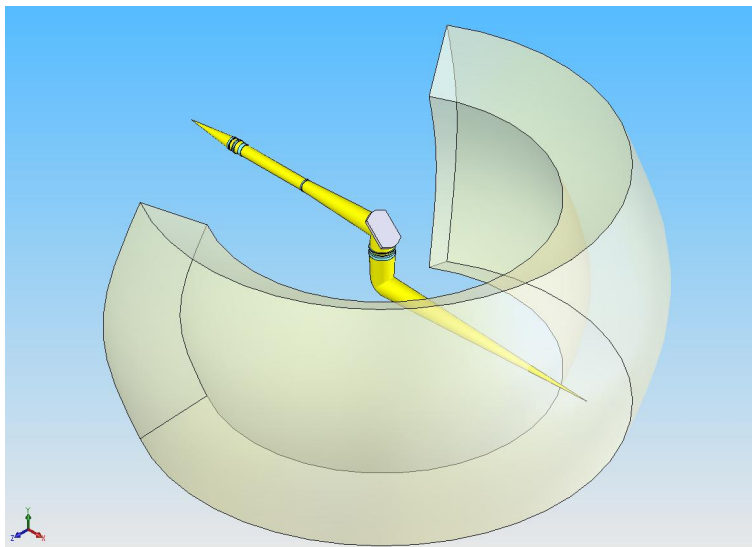


Figure 6.10: Work volume described using both the possible scanning mirror rotations

maximization of the laser source use.

To reach these objectives were necessary a very high quality beam laser realization and an important laser power use, assisted by a performing optical components movement system (high speeds and accelerations). In fact using the same optical system the diameter of the focused spot appear smaller in case of better beam quality, while fixing the same spot diameter, with an higher value beam quality possible to work with bigger distance from the part, with a definitely major space depth. (figure6.11)

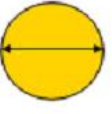
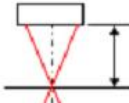
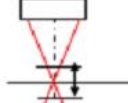

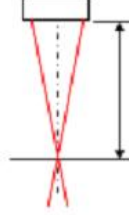
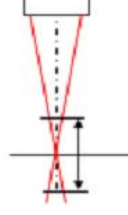
Laser beam quality	Focused spot diameter	Work distance	Depth of field
25 mm x mrad (Nd:YAG lamps)			
8 mm x mrad (Yb:YAG disk)			
	The same focusing optic	The same focused spot diameter	

Figure 6.11: Comparison between two different quality beams generated by two different laser source

6.3 COMAU process

Concerning to the process, the activity of COMAU is focused on the planning, realization and installation of specific fixture and machines for the cars steel bodywork, painting, mechanical sub-group manufacturing and final vehicle assembly.

Here is placed the *COMAU Body Welding and Assembly sector* which develops assembly system for car body shell: under body shell , doors, body and car-sides assembly technologies, which are composed by systems able to maintain the correct geometry of the assemblage or welding machines.

6.4 COMAU-CASSINO productive site organization

PRESS-WORK PROCESS

The press-work is the deep-drawing process for metal sheet. Through this process is possible to obtain hollow and bent bodies maintaining the initial thickness, starting from planar parts. Not always the manufacture can be done with only one wipe, so in many cases is visible an off-hand diameter reduction, inducing excessive residual tensions in the material. Another important factor causing part deformations is the control of the matrix ray edge: if too small can induce extreme extensions, if too big can provoke creases and folds during the turning away of the sheet-press. Usually in automotive industry the sheet metal press-work takes place in special purpose pressing centres inside the plant. The choice of machines typology depends on installed productive capacity: for high production series (more than 600 series/day) usually firms recourse to multi-station mechanical presses characterized by elevated rate. In this situation is necessary to have an optimal efficiency and high productivity because fixed costs are definitely considerable.

Moreover there is the need to optimize the sheet metal use, minimizing the scraps quantity and recycling them.

Usually the production of pressed parts take places in batches. So produced elements are optically examined by operators to guarantee a high superficial quality on the 100 % of the production. Furthermore a geometrical quality control takes place, but in this case is used an automated and statistical control.

PAINT WORK PROCESS

Painting process is necessary to guarantee three vehicles fundamental aspects: *protection, aesthetic properties, sound-proof deafening*.

First of all is necessary to eliminate all the previous operations residuals. In fact in different moment during the vehicle painting, some furnaces occur to bring the body shell to a defined temperature for a settled time period and then they provide also to body shell cooling. The utility of this oven is to purify vehicle parts from residual gases of the painting.

FINAL ASSEMBLY

After steel bodywork and painting processes, the body frame is ready for the final

assembly along a main line in which are merged components and sub-group produced in secondary lines. In the sub-groups converging to the main line three fundamental areas are noticeable:

- the mechanical area, including the motor, the gear level, the tank, the radiator and the starter
- the steel bodywork area of car doors
- the windows area

6.5 COMAU Assembly system

The door assembly line presents two symmetric lines, for the front and rear door respectively. For each of them the line is specular for the left and right door and some workstation are shared (figure 6.12). Because the symmetry, we will describe only the flow line for a type of door.

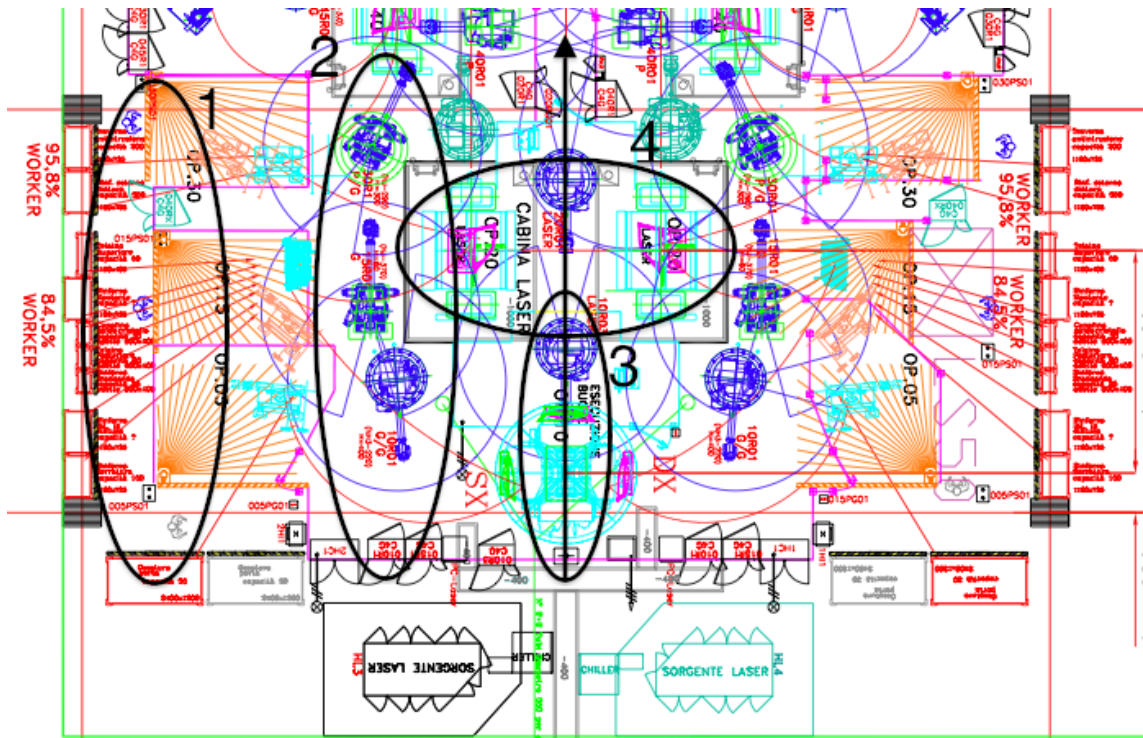


Figure 6.12: Layout of the assembly door in Cassino (Italy)

The door is formed by seven subgroups and all of them arrive from the pressing process. A precise description of layout will be presented in this section, based on the illustration in figure 6.12:

Section 1

After the pressing process, all parts arrive at the assembly line and a buffer allocation for each of them is present. The assembly line presents two input doors: one is dedicated only for the inner frame and the other for the rest of subparts. That is because in its cycle the frame presents the dimpling manufacturing before the joint between all other components and this process has been added for correcting the problem of the minimum distance between parts during the laser welding joint. For this reason the inner frame is loaded by stand alone operator, singularly the other subparts are loaded together in the same proper device: the geometrical gripper.

Section 2

A series of robots is dedicated for pallet handling. All of them are anthropomorphic. One robot is completely dedicated to the pallet of the inner frame, while the robot above is for the other components pallet. Robots are the unique transports in the flow line.

Section 3

After parts are loaded, the inner frame is pushed inside the line and a robot moves the part in the laser workstation, a rotating table let the pallet to be laid down, then it brings the part to the laser tool through a rotation and the part is worked for the dimpling process. This phase is important for the creation of the dimples, which guarantee the minimal distance for the escape of the gas, caused by the over heating of the zinc after the laser welding (next workstation). In fact dimples are nothing else then circles in relief: the minimal high of the dimple will constraint the subparts not to have a direct contact with the inner frame. The problem of porosity caused by the zinc is solved. The dimpling process requires 0,125 seconds each and it requires exactly the half time for a stitch welding, that's why the dimpling workstation is shared for the right and left door and the work time is inside the cycle time.

After the processing is finished, part goes out through another rotating table (the output is shared between right and left inner frame) and it is drawn by another robot (in the middle of the arrow in the picture), which allocates part in the input table for the RLW. The part is now ready to be joint with the other subparts.

Meanwhile the inner frame is completing the processing, the other subparts are loaded

together by another operator on the gripper which hold components in right final position for the welding, then another robot in front of the input door takes the part and loads it on the rotating table, input of the RLW.

Section 4

The remote laser welding produces joining between all parts, spending 0,25 seconds for a single laser stitch, with a total of 55 stitches on the complete door.

After that, part is put out and moved towards the clipping processing, in which the door covering is put on.

The remote laser welding owns an external source, so in case of failure a connection to the other source permits to the machine not to block the process. Instead the laser machine for dimpling process presents only a source. In fact it requires the half of the time for a single operation (0,125 versus 0,25 seconds); moreover in case of failure, the dimpling process on the inner frame can be removed and another control for lower limit between part is used.

6.6 The SMARTLASER application: Car doors steel bodywork

From the SMARTLASER application point of view, the car doors sheet of metal work is the most significant process. In fact SMARTLASER was created to obtain a more flexible welding system than traditional engines. SMARTLASER seems to be suitable for little-size subgroup body shell realization and also for the whole side of a car. In fact the typical application of RLW in automotive sector is the door assembly, which is a process standing for joining the inner frame with the subparts to obtain the final door.

The choice follows to this kind of application properly because laser welding lends itself perfectly to sub-group realization.

In addition, the car doors steel bodywork process presents lots of criticality during the welding activity.

6.6.1 Door car loading sequence in FIAT-COMAU Group

The following steps sequence is about the loading parts succession in the car doors steel metal work in the COMAU plant.

OPERATION 1 : the inner frames are loaded by the operator on the positioning devices robot, from the outside of the welding cell.

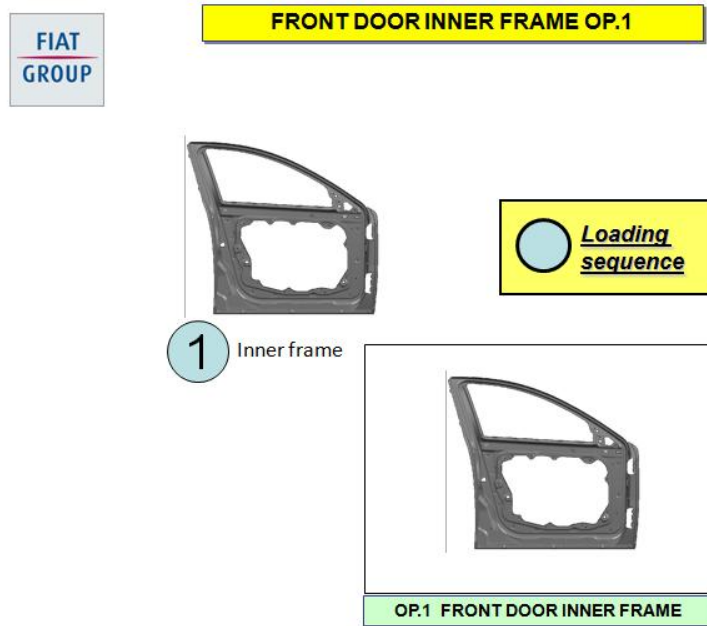


Figure 6.13: Car's door inner frame loaded by an operator

OPERATION 2 : outside the welding cell in an another separate area, the 5 reinforces are loaded on a geometrical gripper, which maintain the correct geometrical position and references between components (figure 6.14). The 5 sub-groups are introduced together in the cell, and they are usually positioned under the inner frame. After the clamping activity which hold in position inner frame and sub-groups, the welding process takes place through the RLW system, joining parts hitting directly the inner frame located above the 5 sub-groups.

OPERATION 3 : obtained the door internal structure, is necessary to add some other 3 reinforces to be overlapped on the reinforces loaded in op.2 to increase the robustness and the strength of some door sections (figure 6.15).

OPERATION 4 : in this operation auxiliary and secondary components are mounted, with sound-proof functions, external protection covering and heat-treatment solutions like presented in figure 6.16.

OPERATION 5 : Adding at the and the external covering of the car door, the whole door is now ready for the painting process and then for the final assembly (figure 6.17).

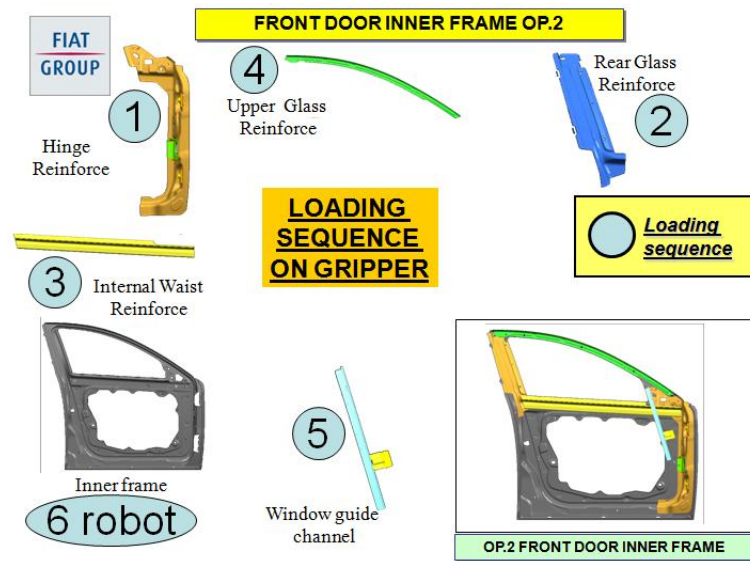


Figure 6.14: Reinforces and components mounted on the geometrical gripper

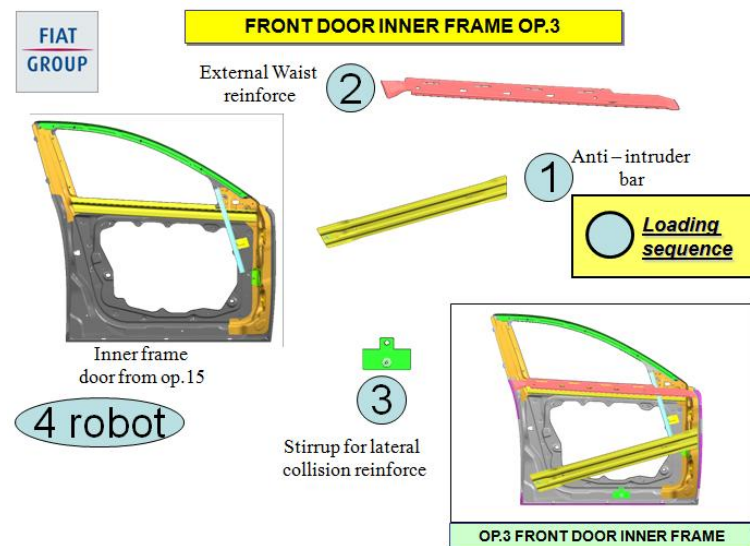


Figure 6.15: components door loaded on a geometrical gripper for positions maintaining

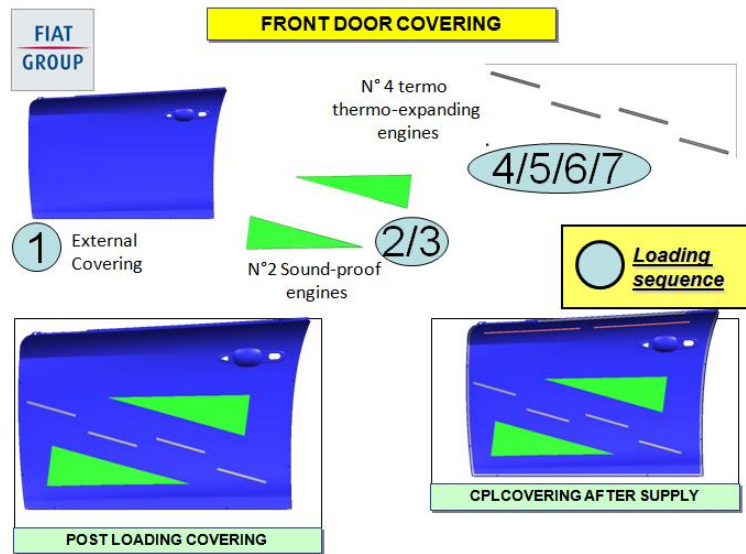


Figure 6.16: Scheme Operation 4

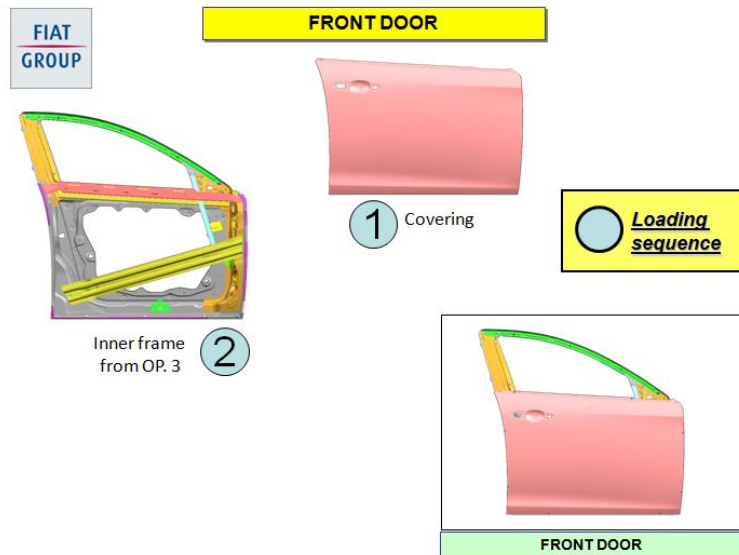


Figure 6.17: Scheme Operation 5

6.7 Part-to-part gap control method

Currently, in Cassino plant, a RLW in every flow line for each door is present. The door is made by different materials, even if every steel used as component is zinc-coated sheets because of their promising performance. This is a relevant information, because this way needs to characterize the welding system with an important variable: the gap between metal sheets.

The gap takes a fundamental rule because working with two sides zinc-coated steels, during their overlapping the consideration of *escape route* is critical for the zinc steam, which is formed during the process. The zinc coating between two steels is a low-boiler material and during its fusion imperfection and air bubble along the welding stitch can be present.

In automotive sector, for a major stiffness of the body shell and a more performing in corrosion resistance.

In case of zinc-covered steel closed as pack, to avoid the mentioned problem is needed a case-for-case study depending on the zinc-coating thickness and parts thickness to develop the best solution for the steam escape (figure 6.18).

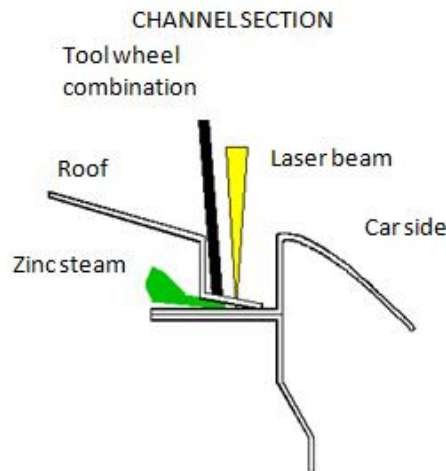


Figure 6.18: zinc steam pouring out during the zinc-covered steel welding

As just worked on, RLW requires a tight control of the gap, in both tolerance limits, in order to guarantee a good laser welding joint. The objective imposed for parts in Comau is to maintain an optimal gap of 0,2 mm between parts, because if the gap is upper than tolerance limit (0,3 mm) the welding will be not realized, in contrary case

the problem of porosity will be present in the stitches if the gap is less than 0,15-0,2 mm.

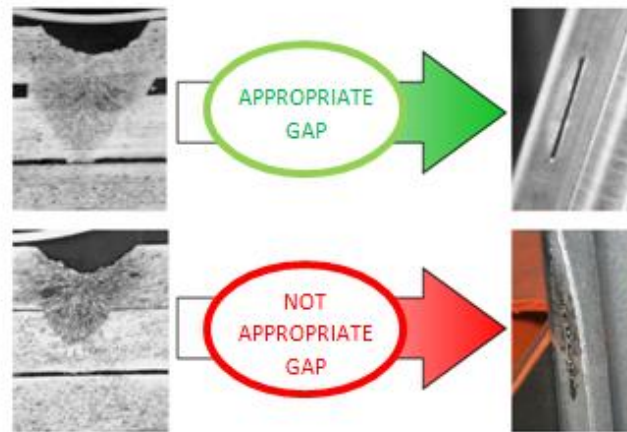


Figure 6.19: Air bubbling along welding stitch

A possible porosity it's likely to appear if zinc-coated parts are used, because of the low zinc vapourization temperature (906°) against the high steel melting pot (1500°). During the welding joint, high temperatures let the zinc atoms evaporate, for this reason it's necessary to have a minimum gap greater than zero to let it go out, otherwise it creates blowing during the overlapping joint, that is a non perfect part.

The control of the gap is subject to the dimpling and the fixture design.

6.7.1 Dimpling design

The dimpling process is an adjustment for the gap control introduced for the lower tolerance limit, which can causes porosity in matching parts. Sheet metal is covered by zinc and it is important during the press work process. When this element gets high temperatures, it converts in gas. This gas is formed during the welding process and it requires to go out. The possible porosity it's likely to appear if zinc-coated parts are used. During the welding joint, high temperatures let the zinc atoms evaporate, for this reason it's necessary to have a minimum gap greater than zero to let the gas escape, otherwise it creates the blowing, that is a non perfect part. This problem has been solved introducing a machine, which produces dimples on the main sheet bodywork of the door. These dimples ensure the lowest distance two parts have to.

The optimal gap which Comau tries to maintain is 0,2 mm. To preserve the optimal

gap some dimples are put on the inner frame before the welding phase with the other subparts of the door. The purpose of the dimples is to maintain the minimal gap along the stitch zones; in particular, for each stitch two dimples are foreseen as in figure 6.20.

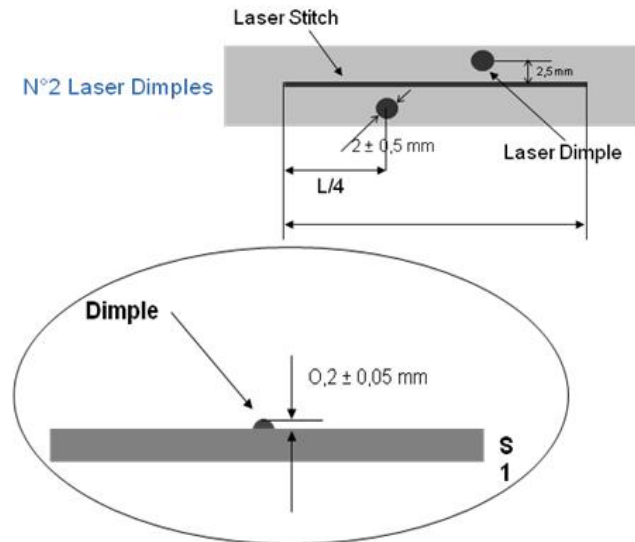


Figure 6.20: Dimples representation

Dimples are produced on the metallic parts by impulses generated by a SmartLaser System.

The time consumed for one dimple is 125 milliseconds, while for each stitch 250 milliseconds are required. This time is exactly the half time spent for the stitch welding production, in order to guarantee the dimpling process is not a very time consuming activity and the it stays within the cycle time, without causing bottlenecks.

Nowadays dimpling process is the most used technique to obtain welding requirements and to control the gap in automotive systems. Usually the sheet pack is studied: to control the gap both parts thickness and the upper tolerance limit of 0,2 mm must be considered. Because parts are not nominal and their thickness is variable along the profile, hence the necessity to maintain the distance between them as homogeneous as possible.

The problem to avoid gap between parts more than the upper limit requirement, a fixture system is introduced to position correctly parts. The aim of the clamping system is not to deform and stress parts pressing them to achieve forcedly requirements. In fact it just blocks parts and refers them each other, because if it would have a pressing function and it would force parts in staying in a not natural position, the final obtained

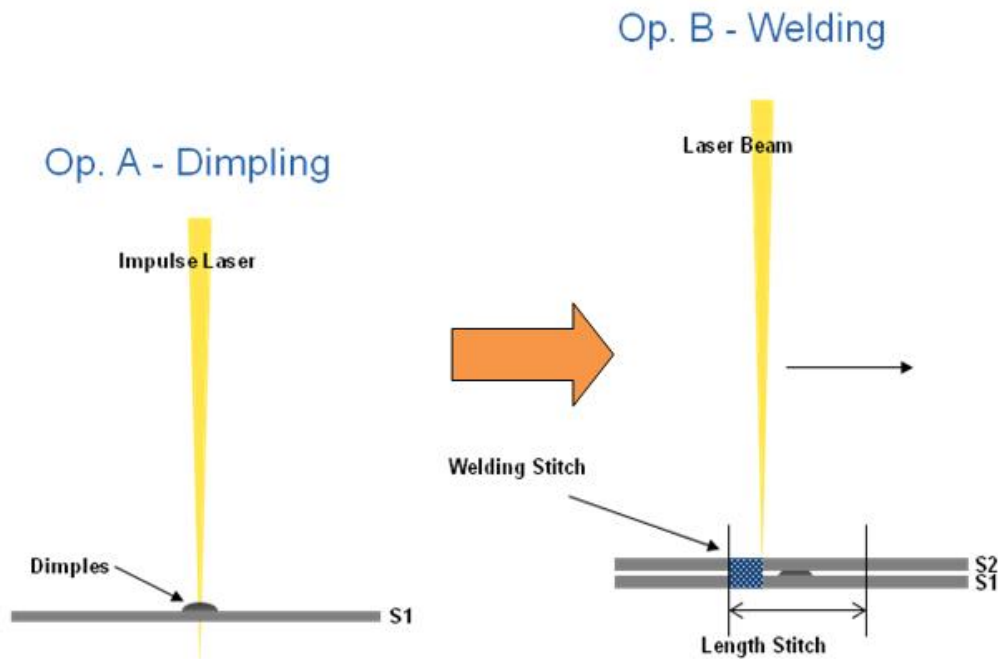


Figure 6.21: Dimpling process

product could present some tensional states and is likely to observe a parts geometry loose.

Anyway the activity is quite expensive, because must be introduced a special purpose laser machine in the system. For not zinc-covered parts dimples are not required at all, because parts can be welded with distance equal to zero, that is in contact each other.

In the past, when in Comau was produced a non perfect part because out of the tolerances, its deformations were studied and this part, called master; was the reference to produce the other family of parts to be welded with the one analyzed. In fact the master is representative of a product family affected by the same kind of errors on the shapes. The solution to this problem was to project ,before manufacturing process, the shape of the complementary families to be joint with the master in order to compensate the error. A pressing re-process of parts were done. But basically this solution was more expensive than the dimples method and long time consuming. For this reason Comau, as a lot of other automotive firms, developed the dimple idea.

6.7.2 Fixture design

Another way of the gap control is by fixture design, which have the aim to control the upper limit. The aim of the clamping system is not to deform and stress parts pressing them to achieve forcedly requirements. In fact it just blocks parts and refers them each other, because if it would have a pressing function and it would force parts in staying in a not natural position, the final product could present some tensional states and is likely to observe a parts geometry loose; moreover the sensibility of the laser joint risks not to survive in a unbottomed quality control, that we will discuss consequently. The two selected parts are welded in the zones affected by the fixture in which there is the coupling between them.

The clamping system considered is the complex front door Fixture Design of Fiat Bravo developed by COMAU.



Figure 6.22: Front Door Fixture System (a)

In the following illustration the coupling and the clamping mechanism for the considered parts (inner frame and waist reinforce) before the welding joint is shown. Parts are welded in the zones adjacent the fixture (considering the parts profile, they will be welded only along the fixture disposition but between them). The non planar inner frame is coupled with the box-shape reinforce, which is a closed-profile part and for

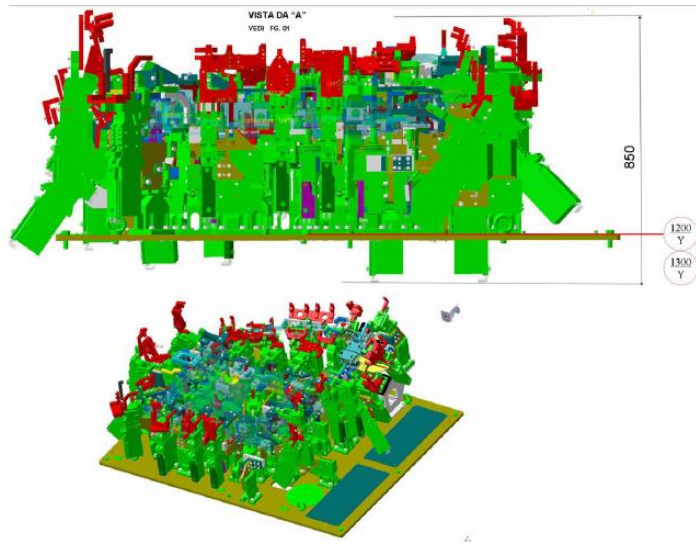


Figure 6.23: Front Door Fixture System (b)

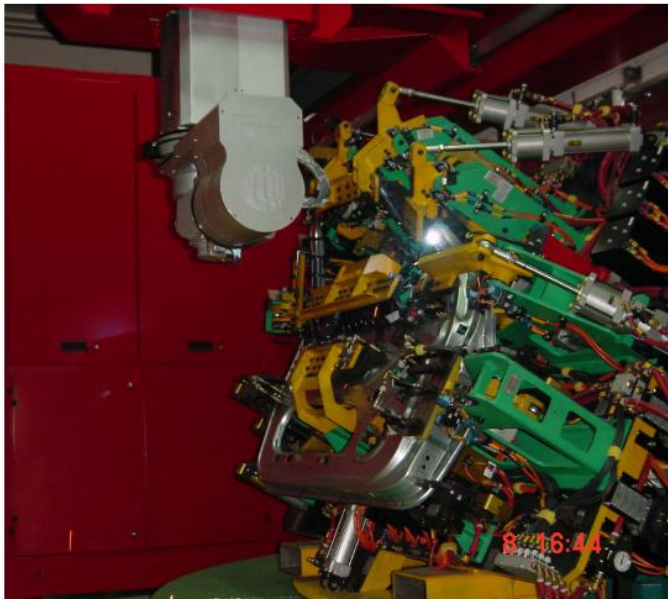


Figure 6.24: Front Door Fixture System of Agilaser

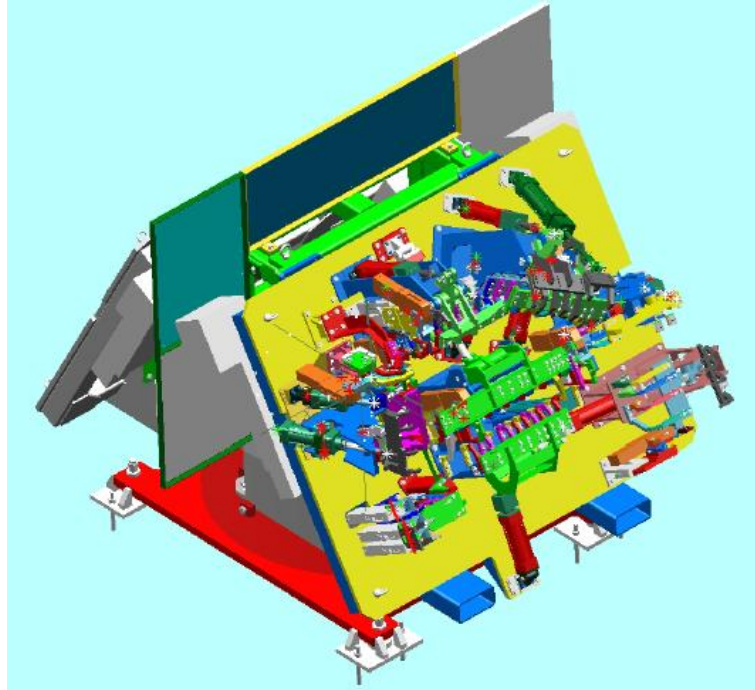


Figure 6.25: Front Door Fixture Scheme

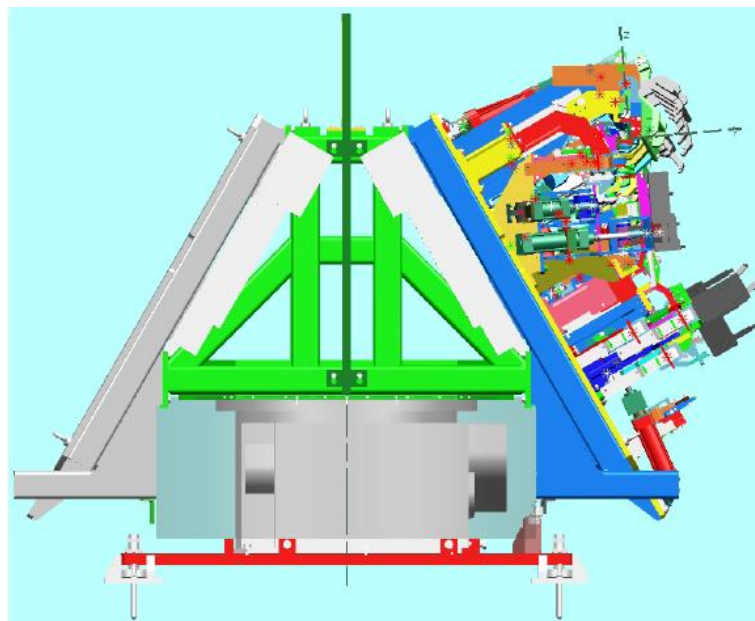


Figure 6.26: Door Fixture System symmetric for the left and right front door

this reason quite complicate to be managed and controlled. In fact, as it's visible, the welding surfaces of the waist reinforce is 3-thickness stratus, not so deformable with fixture forces. The plugs pressing on the box-shape area of the reinforce (reference point X=1400, Z=652,5) will not modify the geometry of the part, because this fixture is just fixing and holding a quite tick parts difficult to be deformed.

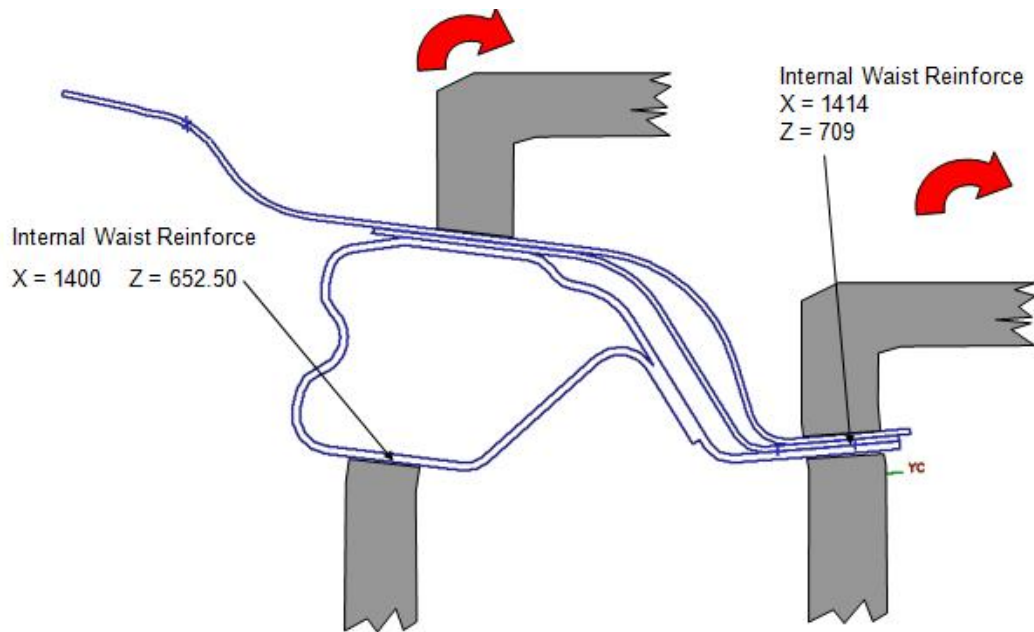


Figure 6.27: Parts mating through plugs of clamping system

To control the minimum gap COMAU usually use the dumpling strategy; on the contrary this strategy cannot be useful to restrain the maximum gap. To grossly solve upper limit gap problem COMAU developed some targeted interventions on the clamping system: the *sheet metal pack creation* and *fixture fine tuning*.

Sheet metal pack consideration is used to maintain constant distance between parts which must be widen to avoid the creation of huge deformations in part's profile. Plugs are calibrated in way of impress a settled force (30 kg per plug) in way of taking into account the two thickness of the parts and the optimal gap 0,2 mm between them, trying to uniform the global distance between the inner frame and the reinforce. So in general the fixture adjustment take place only to guarantee the elements closure. The presence of welding stitches in areas adjacent to the geometrical clamps imposes pressure regulating with not complete closure of the elements. All the present plugs respect the

optimal sheet pack, in this way sheets areas between the fixture are constrained to have maximum distance equal to 0,2 mm. If the distance in this zones is lower than the optimal gap value, this does not entail a problem because parts will be welded in zones between two clamps through short stitches. So the real criticality is to control the parts gap between one fixture and another, where variability of parts can lead to a gap value greater than 0,3 mm.

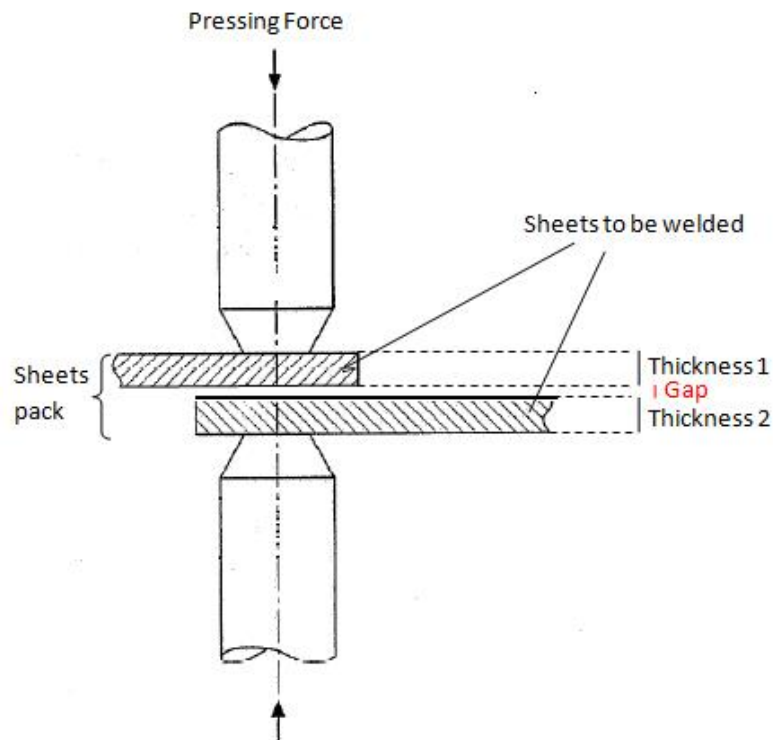


Figure 6.28: settled sheets pack considering the gap and the two parts thickness

In some cases the control of the gap between parts requires the fine-tuning of the clamps, that is a manual movement of the fixture points to reduce the gap. Sometimes, in fact, the gap exceeds the upper tolerance limit (0,3 mm) and operator has the task to delete this problem.

The fine-tuning is time consuming process that should be automate. In fact, the fine tuning is a process that is analyzed and corrected during a research project: if a better fixture design for a particular door (both front and rear one) is found, then the fixture design is corrected.

Technological constraints for overlapped joints

Usually the influential processes on the final quality of the welding are:

- Product Definition
 - joint typology
 - dimensions and tolerances
 - materials involved and surfaces treatment
- Pressing Process
 - Pressing tolerances
- Sheets Bodywork Process
 - reference method (geometry of the sub-goups)

6.8 Laser welding quality control

The applied norms for testing the joint quality is verified on the overlap between the inner frame and the other subparts, both for zinc covered or zinc-covered parts.

The welding joint must present as indicated in the figure 6.29.

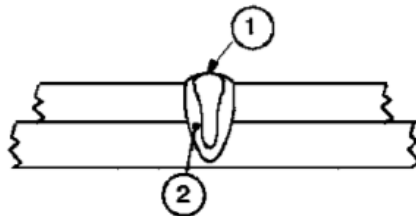


Figure 6.29: Fusion area: 1 is the fusion area, 2 is the altered thermal zone

The quality control can be done in 3 different methods: a visual exam, a micrographic exam and an unbottoming test.

6.8.1 Visual Exam

The visual exam differs from the upper to lower surface. The surface must be homogeneous, without burrs. Any kind of breaking is allowed.

For the upper control the visual exam contains 3 different kinds of defects:

- Top sheet metal breaking: the length of single defect must be less than 20% than total length of stitch (figure 6.30);
- Porosity, blowing: the sum of defective lengths must be less than 30% of total stitch lengths;
- Marginal incision: the sum of defective lengths must be less than 30% of total stitch lengths (figure 6.31).



Figure 6.30: Acceptable stitch

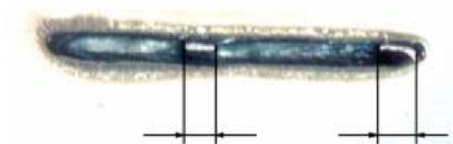


Figure 6.31: Acceptable stitch because the length of defects is lower than 30%



Figure 6.32: Non acceptable stitch

The lower part is testimonial of a correct fusion depth:

- Missed fusion: the missed breaking at the beginning or at the end of the stitch must be less than 50% of the total length. If in the middle is not present a fusion but at the extremes of the stitch it is, then the fusion can be considered acceptable.

6.8.2 Micrographic exam

The test must be done on a sample for each welding examination. Samples must be taken at the half of a cross section of the joint, or near an evident defect.

In the figure 6.33 the principal geometrical variations are represented.

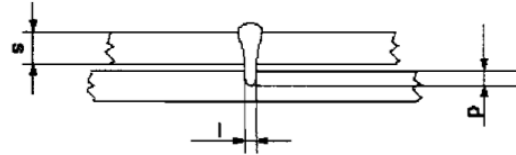


Figure 6.33: Principal geometrical variations: p = fusion depth, l = width of the stitch, s = thickness of sheet metal

The welding joints are considered acceptable (figure 6.34) only if they are conformed to the following lower limits:

- Fusion depth (p): it must be $\geq 30\%$ of the sheet metal thickness;
- Stitch width (l): it must be upper or equal to the thickness of the thinnest sheet metal;
- Hollow welding: the depression of the welding must be $\leq 30\%$ of the sheet metal thickness (figure 6.36);
- Marginal incisions: it must be $\leq 20\%$ of the sheet metal (figure 6.35);
- Porosity: admitted.

6.8.3 Unbottomed test

The test consists in running the stitch welding through the tensil/cutting stress until the separation of the lapping parts.

For unbottomed test understands the breaking on one of the two sheet metals cross the stitch, which underlines on one plate a protrusion, meanwhile on the other a fissure.

The welding joints must be considered acceptable if the protrusion of material is $\geq 70\%$ of the total length of the stitch.

These 3 tests must be applied for each turn on the last 5 samples, as the norm explains. If all these tests have good outcome, the pressing process can go on without

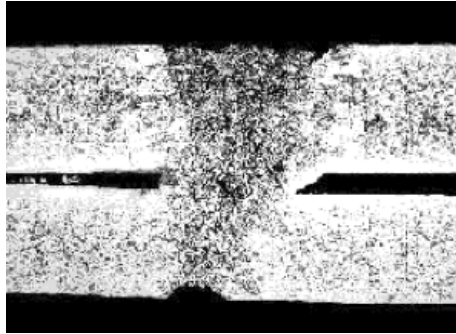


Figure 6.34: Acceptable welding

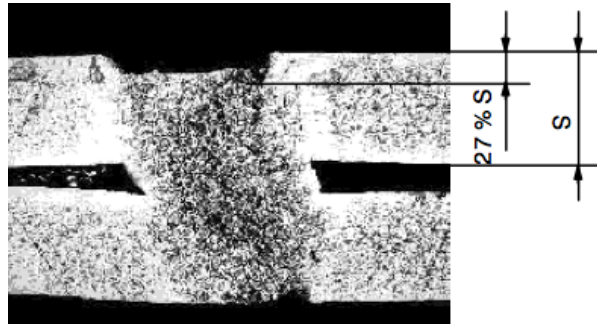


Figure 6.35: Marginal incision: non acceptable welding

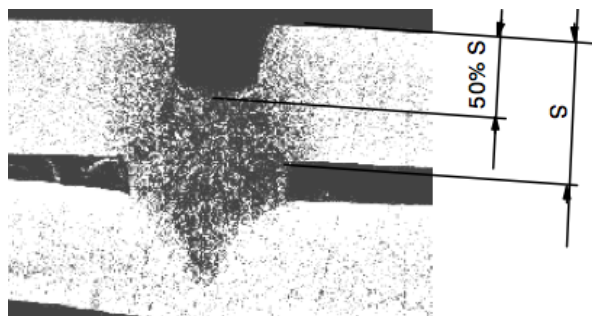


Figure 6.36: Non acceptable hollow welding

any interruption, otherwise if the unbottoming test fails, the test must be applied on the other produced parts from the last one until the last good tested part, because is a very dangerous situation and there is the risk of stopping the production and interrupt the production rate.

The most risking zone is the stripe between the inner frame and the waist reinforce, and often stitches are low quality. For this reason this parts will be analyzed in detail. Precisely, after the welding, three *planning points* in the welding zone are checked to built quality control charts to control the process of welding:

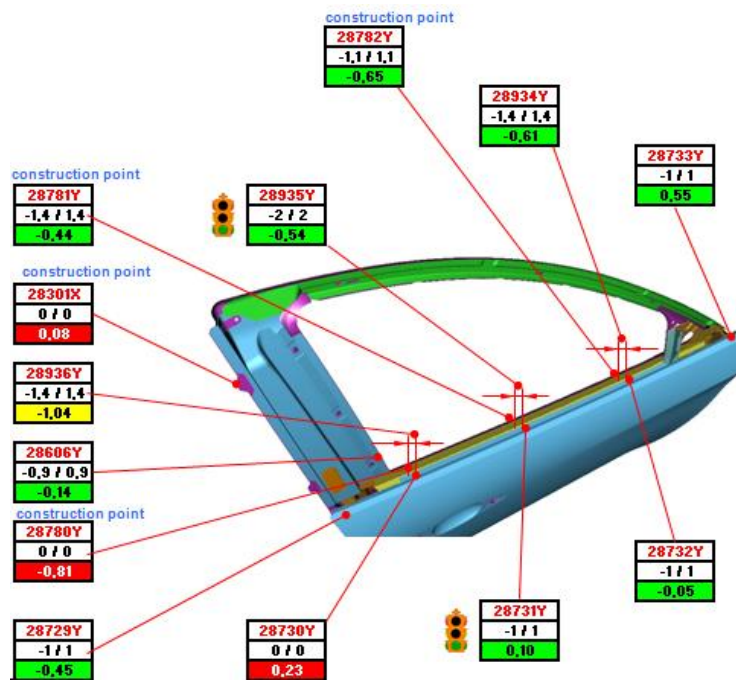


Figure 6.37: three planned quality checking points

For each control quality points tolerances are signed and the measure of CP(*Process Capability*) and CPK, two process capability indices. The first index is a *amplitude* index, because it summarizes the process potential to meet two-sided specification limits and indicates the process capacity of producing standard final parts. It's the ratio between the acceptable variability and the real variability (6σ).

Cpk is a *positioning* index and it is also a penalty factor for the process's being off nominal. It indicates the effective process capacity tackling into account the mean of the Normal curve respect the tolerance. Usually Cpk has negative value when the mean is out of tolerances, because it's calculated respect the closest tolerance. Usually Cpk

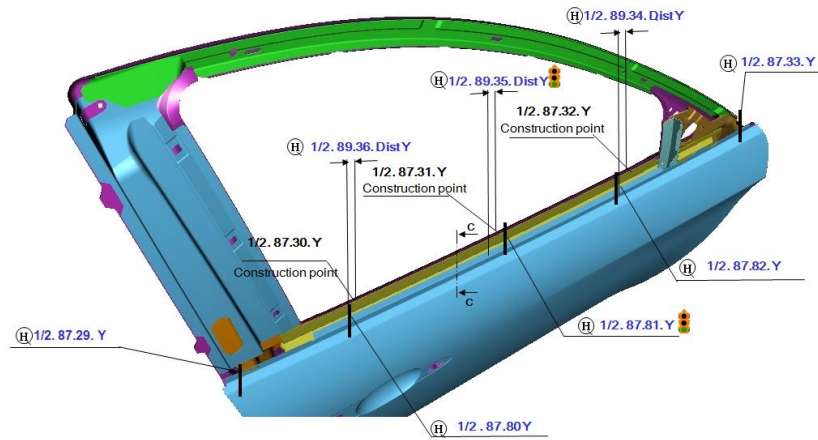


Figure 6.38: fixed coordinates of quality points

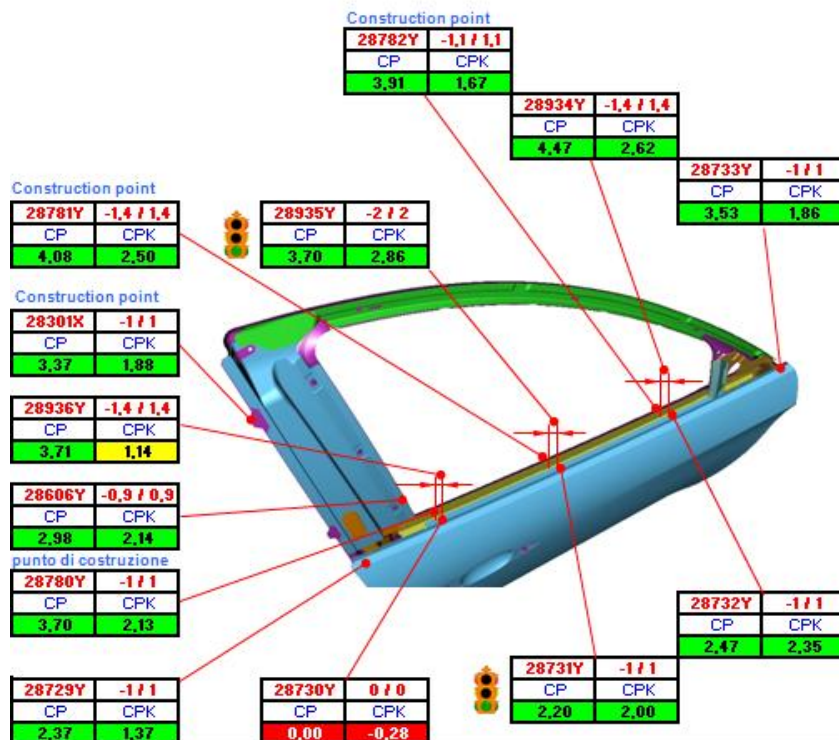


Figure 6.39: Distance tolerances and single quality points measures

value is lower than Cp value, in fact Cp is the superior limit for Cpk.

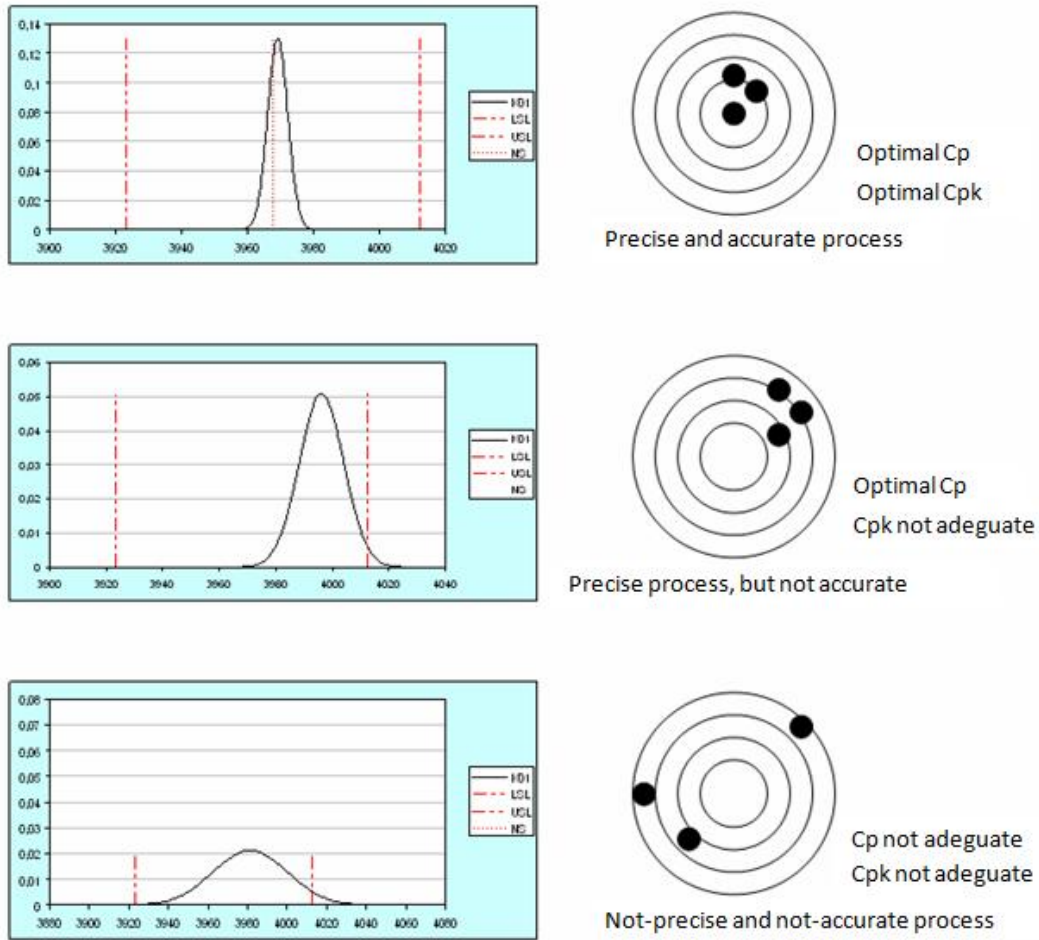


Figure 6.40: Process Capability

Periodically the planning points checking take place to keep the process in control and take some measures in case of problematic process.

6.8.4 Welding stitches locations

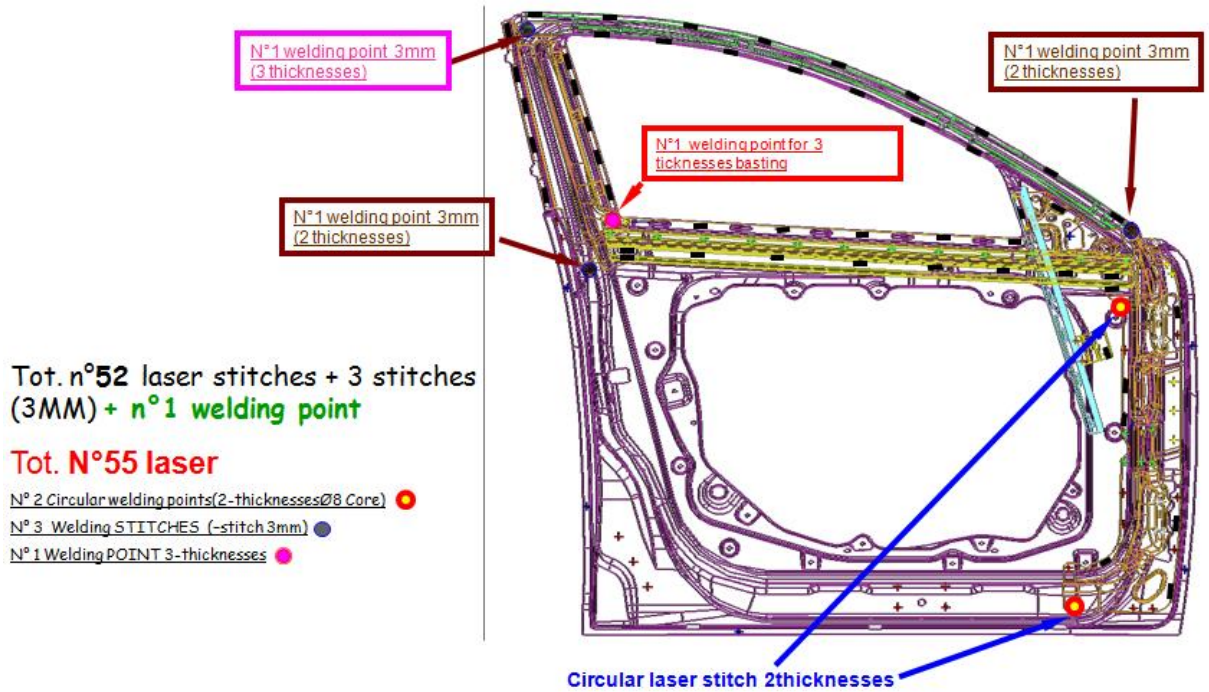


Figure 6.41: Total number of welding stitches on a car door

In figure 6.42 is represented the real positions of programmed welding points between inner points and the six subparts, everyone identified by an ID code, to obtain always the same reference positions during the welding process.

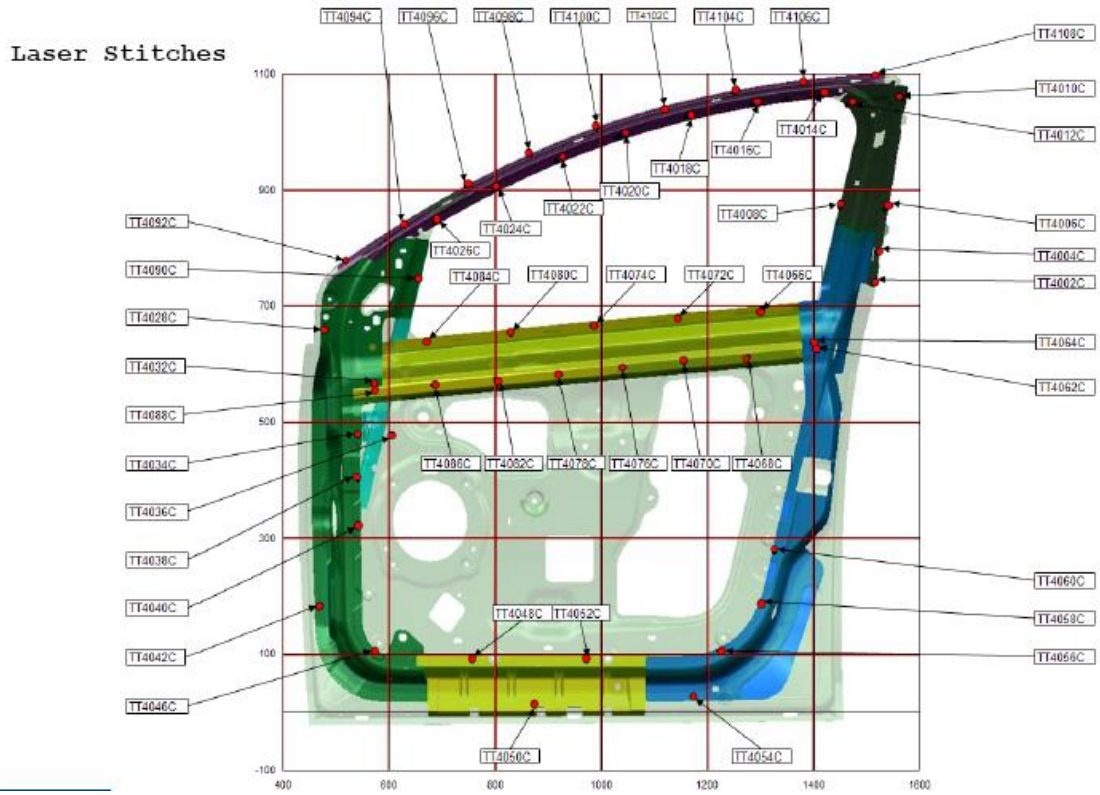


Figure 6.42: Welding stitches between inner frame and all reinforces

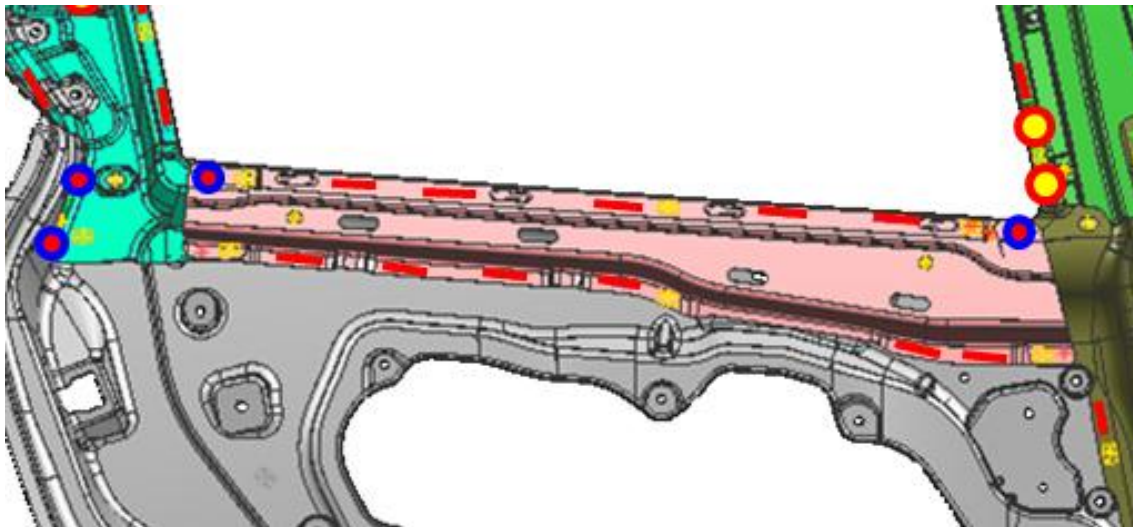


Figure 6.43: Welding stitches between inner frame and waist reinforce

6.9 Aim of the work

Because the problem of the gap is present, the idea to apply the SMA method and evaluate parts for an optimal matching is the aim of the work.

After the pressing manufacturing, parts arrive in line side and are collocated in buffers. During this phase our proposal is the introduction of a "scanner", which analyzes parts after pressing process and evaluate the error frequencies of the profile (in other terms, the deviation from the nominal value). After that, part is sent to a specific storage, which welcomes parts with the same error. In fact classes allocation is divided in the same number of groups as the modes partition for parts. Once established the kind of modes for each error group, parts can be addressed to a specific storage.

Each cluster welcomes two different parts : the inner frame and the waist reinforce. The other subgroups are not considered in this work, because not so critical.

Inner frame and waist reinforce enter in the scanner with an alternative arrival rate if only a scanner is available. The scanner analyzes the part and put it in the appropriate class, based on the representative mode defining the part.

When at least both parts are present in a class, parts are ready to be assembled and the assembly process starts. The inner frame is sent to the dimpling system, in which dimples are manufactured on it, meanwhile the waist reinforce is monted with the other subgropus on the gripper.

When inner frame is ready, parts are sent to the Remote Laser Welding Area, in which the components in geometry arrive to be mated with dimpled door, once fixtured all together, they will be welded.

For the welding process between the inner frame and waist reinforce, 13 stitches are required and for everyone the quality control will be done.

The validation of the quality improvement will be analyzed by the SMA index, that has been tested with experimental data and FEM analysis.

Based on the iterative classification from our research work and the presence of different parts, a quality control will be compared with the actual one.

Our objective function is to minimize the number of stitches with a gap upper the tolerance limit, that is an imperfection of the process, in order to reduce non perfect parts and improve the quality of the final product.

The quality control maintains the norm requirements, listed in the section 6.8.

6.9.1 Similarity Approach on COMAU System

The purpose of this section is to assess the opportunity of high quality welding achievement and to evaluate also the possibility of a fixture design simplification, in order to achieve costs advantages in the assembly line.

Parts with thickness greater than 1,5-2 mm cannot be controlled in their shape through fixture. They can only be positioned and referred correctly, but the usual impressed force by fixtures cannot constraint part to assume a tension state. Under these conditions, the perfect fitting between parts cannot be reached through clamping system. But also parts affected by different kinds of error, risk to return a non conforming final product as output, if pressed with a force able to deform it.

In this situation could be very meaningful a previous study of similarity between shapes of parts which will be involved in the welding process. The similarity analysis will interest only the stripes involved directly in the welding, not the whole zinc-covered part and its aim is to control the respect of the only upper limit defined by the requirements, because the lower limit is controlled by dimpling.

The similarity indicators proposed in chapter 3 are a meaningful support for this purpose.

6.9.2 Selected components for the case study

The typical application of RLW in automotive sector is the door assembly, which is a process standing for joining the inner frame with the six different subparts to obtain the final door.

In COMAU two fundamental door components were analyzed interested by welding joint (see figure 6.44):

- the inner frame door
- the Waist Reinforce

Nowadays all inner frame parts for every kind of door (both front and rear, both right and left) must be subjected to two manufacturing processes:

- Laser Dimples
- Laser Welding

A synthetic process description for each parts of the door is present in figure 6.47. Some important technical specifications are in table 6.1.

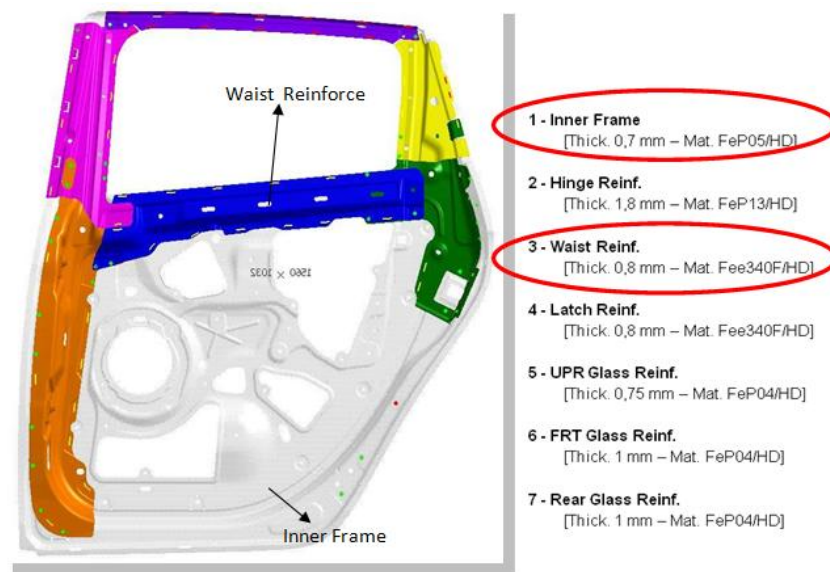


Figure 6.44: Car's door components

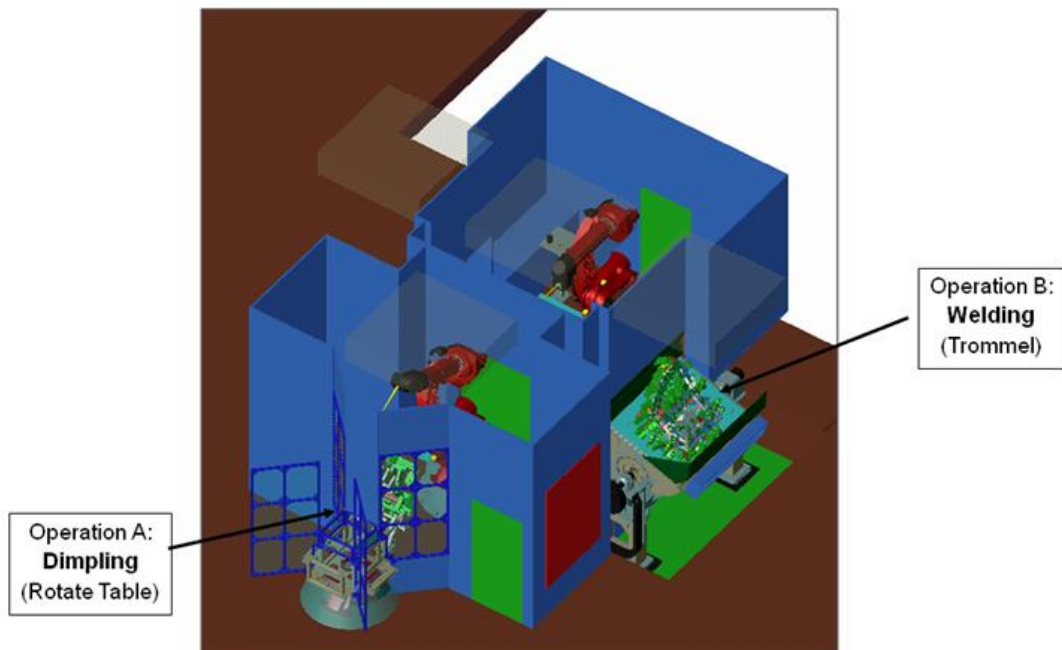


Figure 6.45: Laser Dimples and Laser Welding Process



Dimpling Station



Welding Station

Figure 6.46: Laser Dimples and Laser Welding Stations

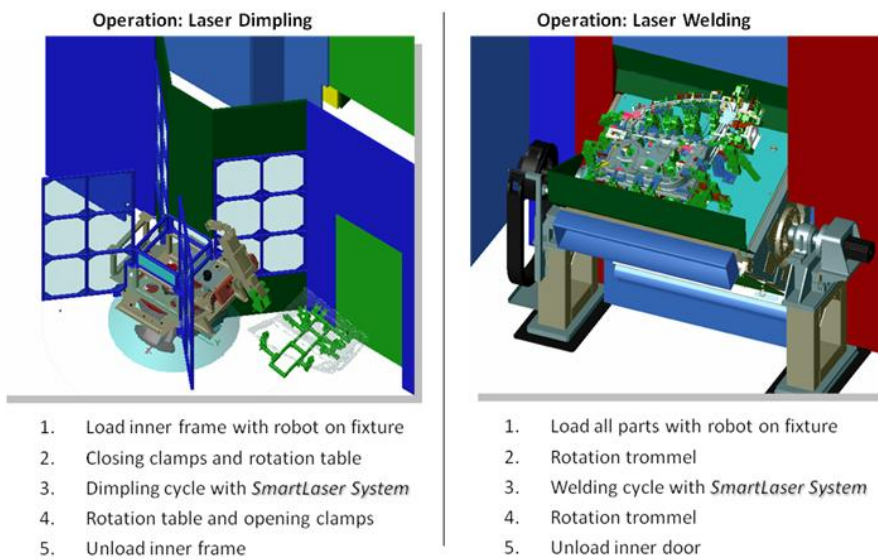


Figure 6.47: Synthetic description of part process

Table 6.1: Technical specifications of doors

REAR DOOR	FRONT DOOR
Cycle time= 78 s	Cycle time= 78 s
Efficiency= 90%	Efficiency= 90%
Laser Dimples:	Laser Dimples:
Dimples number for every stitch= 2	Dimples number for every stitch= 2
Total dimples number= 102 + 102	Total dimples number= 104 + 104
Operation time= 12s + 12s	Operation time= 12s + 12s
Laser Welding:	Laser Welding:
Length Single Stitches= 20 mm	Length Single Stitches= 20 mm
Stitches number= 51 + 51	Stitches number= 52 + 52
Total length of welding= 1020mm+1020mm	Total length of welding= 1040mm+1040mm
Welding time= 23s + 23s (incl. rapid move)	Welding time= 25s +25s (incl. rapid move)

The main idea is to quantify the similarity between the welding areas of the parts, which are interested in the welding process. Studying their shapes is evaluable the welding quality and is possible to determine, through the selective assembly theory, if parts will be located in the same class in order to be both catch by the moving laser and matched together.

Working in this way the probability of reaching low value of non-standard final parts will be very satisfying.

6.10 Similarity Analysis application on Comau parts

In collaboration with Fiat-COMAU Cassino, were measured and scanned 8 inner frames through an acquisition system. In figure 6.48 and figure 6.49 CAD file and standard part shapes are represented, they are the result coming out from the stamping process.

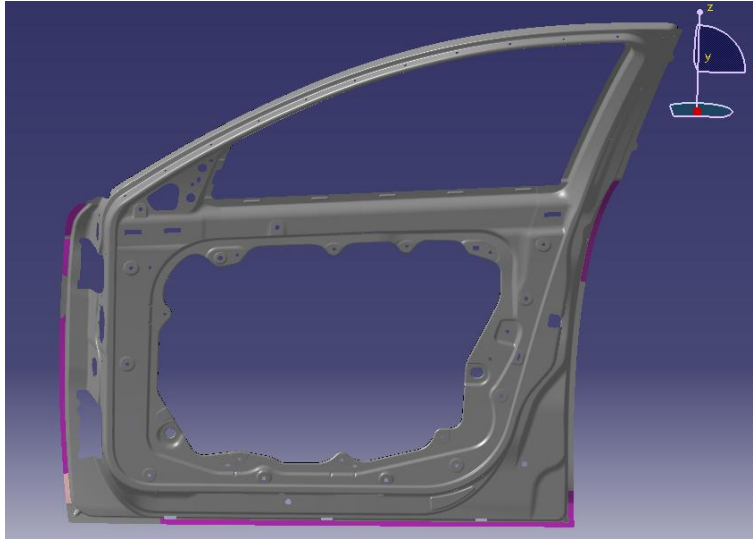


Figure 6.48: inner frame Internal view

Inner frames must be welded through two welding areas with the other selected components: the Waist Internal Reinforce, the box-shape element characterized by a very complex and peculiar movement and trend (figure 6.50, figure 6.51).

In figure 6.52 is possible to observe how two parts can be positioned and coupled before the welding (reciprocal position) taking into account also the other reinforces presence and setting.

In figure 6.53 all established positions of the welding stitches are reported, which maintain parts unified. Parts are welded only in this little stripes, but for the similarity analysis is more convenient the study of the whole welding area profiles, and evaluate the similarity couple by couple of all the welding stripes between all possible coupling between the two type of parts. The stitches position is considered fixed and planned first of all, and it will not change for the same car because it's memorized by the laser control processor.

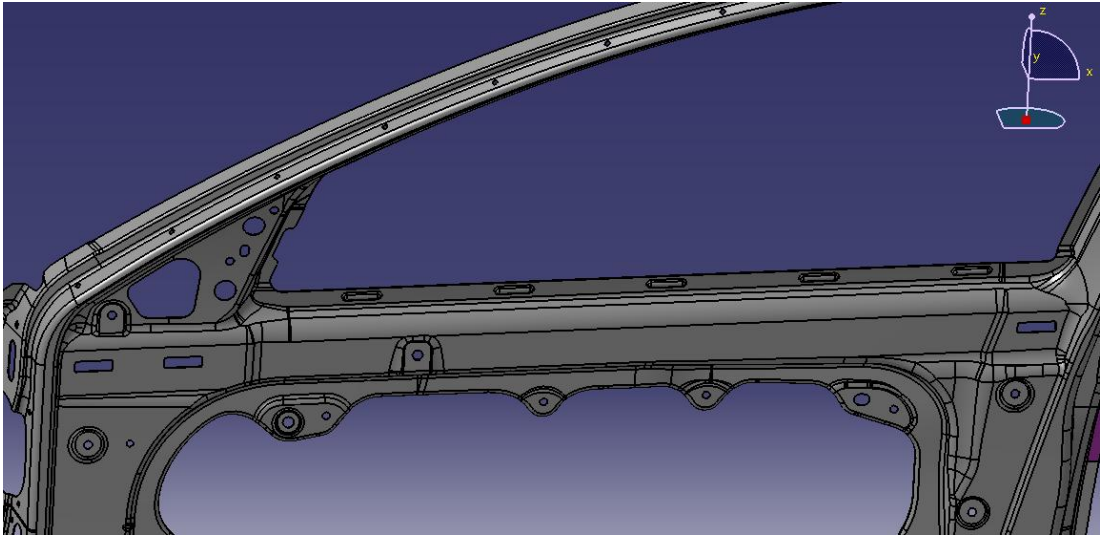


Figure 6.49: inner frame welding area view

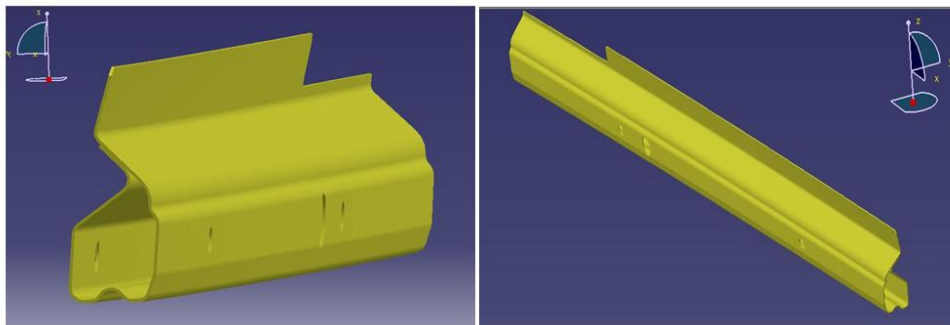


Figure 6.50: Waist Reinforce CAD

Obviously all these images are nominal reference shapes, while measurements provided by Cassino plant are real, so they present deformed surfaces, subjected to frequencies and typical modes of profile. The analysis stood for using the SMA indicator processing on all the welding areas of those mentioned parts. After the accurate selection of the correct joining areas, the fitting measures between couples was provided comparing all the frequencies of one typology of part (inner frame) with all the frequencies of all the other typology (waist reinforce). CAD were about 8 inner frame measurements and 8 reinforces, 100 coupling were possible. Analyzing all the couples was possible to assess best parts matchings for the welding process evaluating their similarity through

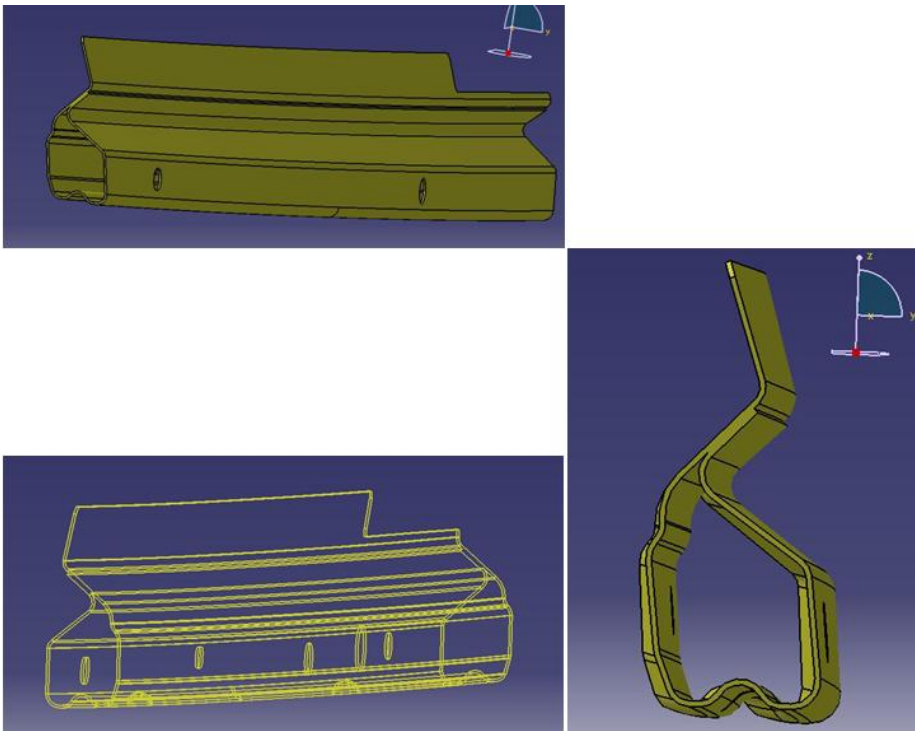


Figure 6.51: Waist Reinforce shape CAD

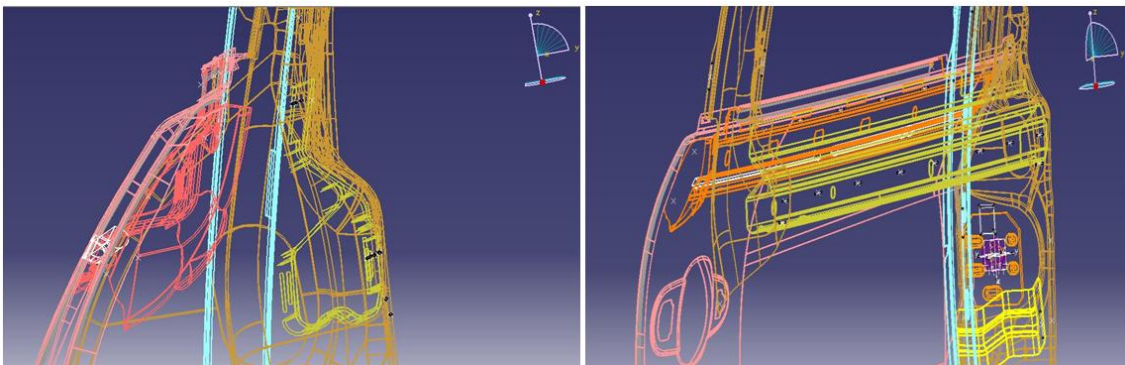


Figure 6.52: Matching view between reinforce and inner frame

the presence of some shared modes.

Comau case of study was necessary for this analysis to demonstrate that effectively real metallurgic car parts (automotive components) suffer distortion shape problems, so the study of the profile similarity can be an important way to improve the fitting

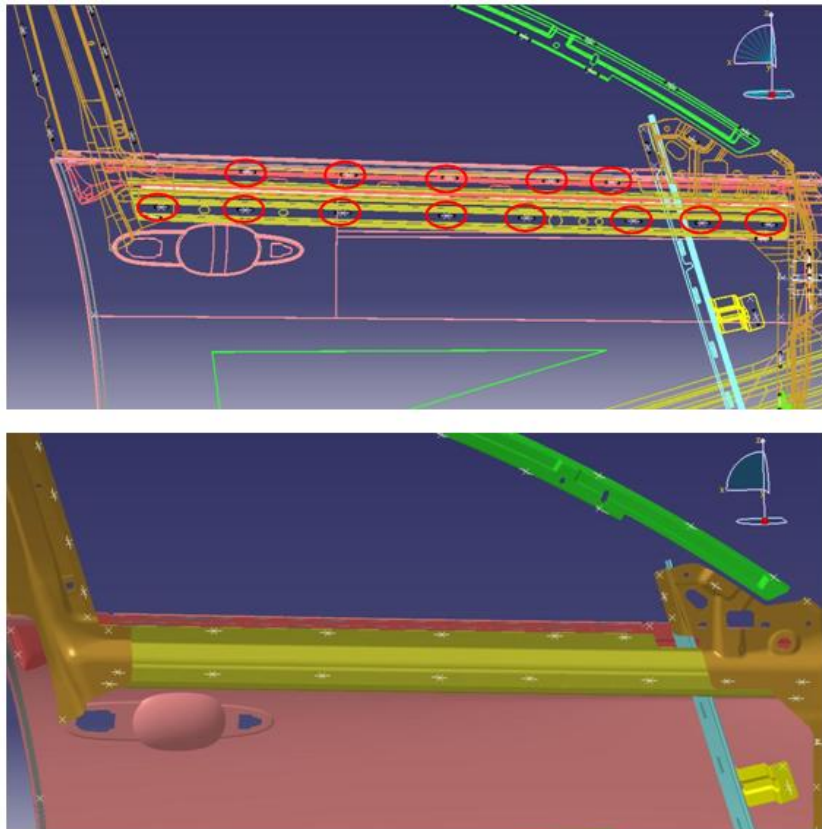


Figure 6.53: stitches position planning between the two considered parts

between them. Parts show decomposed frequencies modes, the SMA analysis finds can be a valid indicator to find the best combinations.

From this analysis, once obtained an indicator for quality welding assessment, is possible to reconfigure and modify COMAU assembly car door system in order to take into account the best/worst couples, and through simulation and various scenarios created later, evaluate system performance about quality improvement.

6.10.1 SMA results

The SMA index was applied to 8 real inner frames and 8 waist reinforces supplied by Fiat COMAU (To) in order to verify if deformation problems affect parts and then implement quality performances assessment on the assembly system.

On every parts' surfaces was selected the own specific area in which the welding takes place. Two welding areas for inner frames and reinforces, which are correspondent each

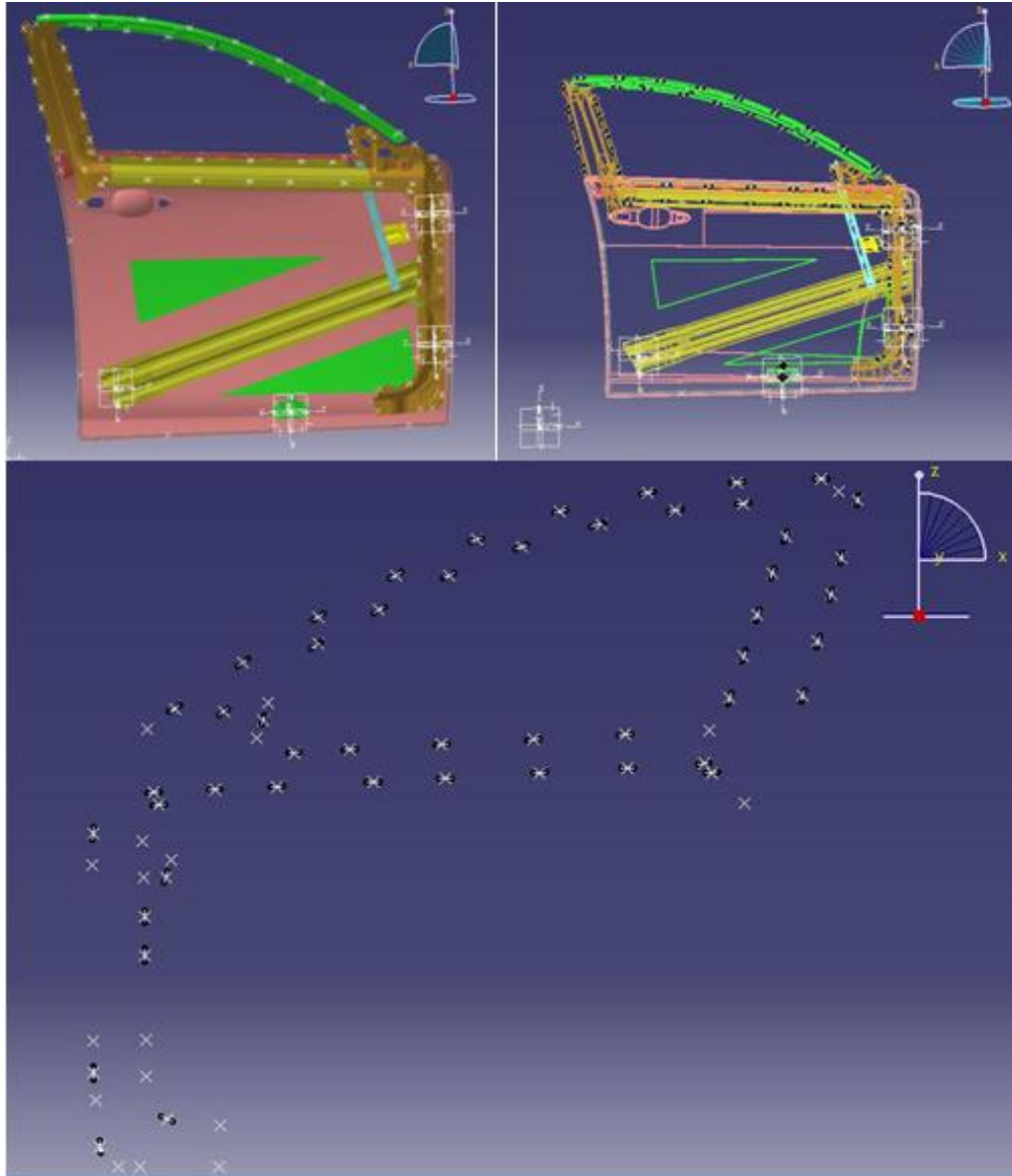


Figure 6.54: stitches position planning between the two considered parts

other, are shown in figures 6.55 and 6.56. In the real assembly cell a random reinforce will be joined with a random inner frame in selected area shown in figure 6.55. The SMA method will be applied on this small section.

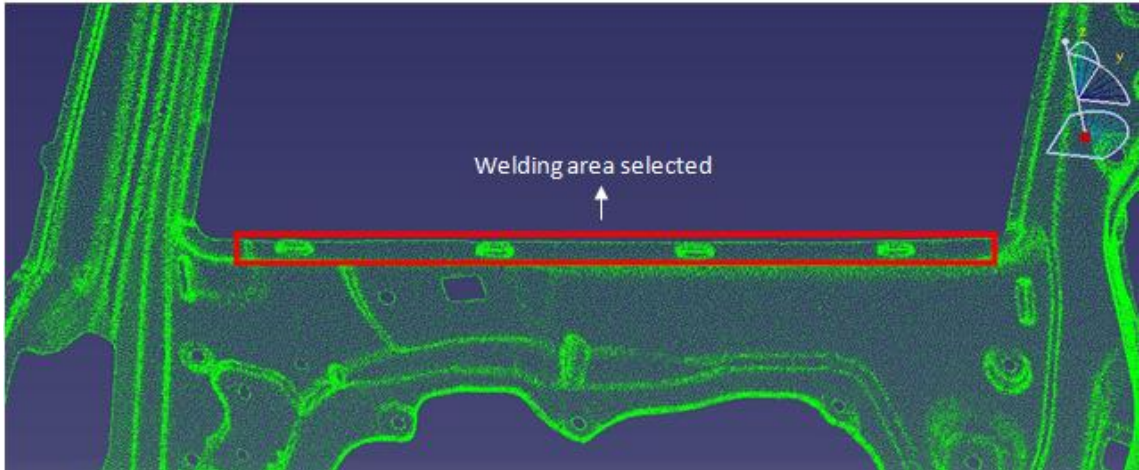


Figure 6.55: Inner Frame welding area

These 16 measurements are relative to parts stamped in different turns. Going more into details, the parts refer to two turns in Fiat. For each turn two batches were considered, for a total number of 4 batches. For each batch two reinforces were got, one at the beginning and one at the end of the batch, and for the inner frame was almost the same.

In figure 6.58 are linked the ID-names of the just mentioned components object of the analysis, with references to the turn and to the batch they belong to.

Basically every reinforce can be mated with every inner frame, creating 64 possible matings which can occur in the assembly system. The SMA can avoid bad couplings in order to increase quality welding ratio.

The SMA code was used for all the 16 parts producing their profile decompositions in several modes : table 6.57 is related to SMA analysis on available studied parts.

In SMA table in figure 6.57 are reported modes name, coefficient values and also magnitude sign, which correspond to phase sign : "+" phase values represent positive phase ($ph = 0$), "-" phase represent negative values with $ph = \pi$.

Highlighted modes in the table for each part represent the Dominant Modes of that parts, characterizing mostly their entire profiles. After using the SMA indicator on each part, a similarity study is necessary: if all inner frames would fit perfectly with every

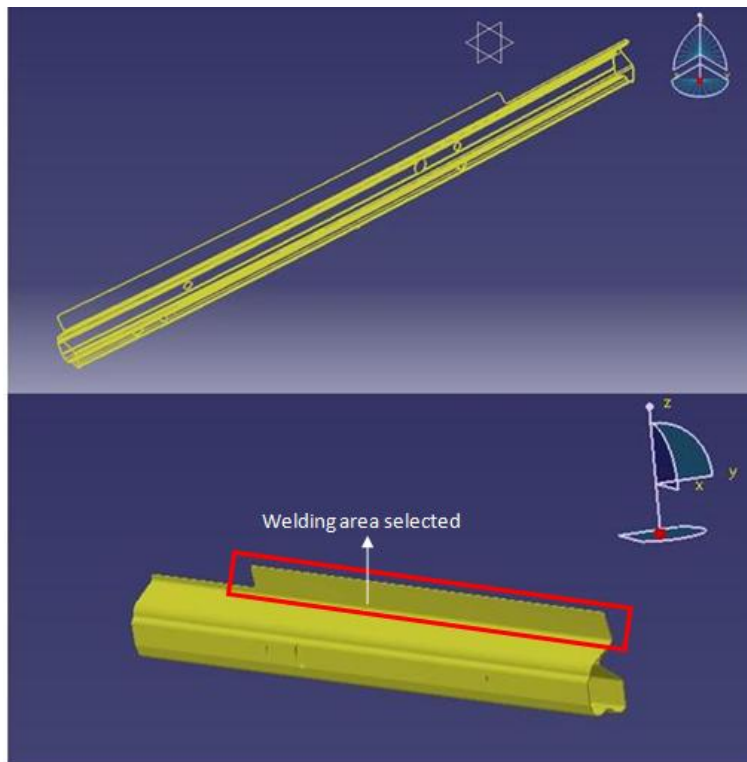


Figure 6.56: Waist Reinforce welding area

reinforce, the similarity study didn't make sense and the work cannot be applied on this case of study. But analyzing all the 64 total possible couples, a similarity study definitely make sense because there are present more situations in which reinforce and inner frame have completely different modes: thank to the SMA method they clearly won't never fit together.

All complete results of the case study are figured out in the appendix C.

Analyzing all 64 couples, a sum of best couplings is reported to see how two parts (example two reinforces) belonging to the same batch fit mostly equally with the same inner frame. Parts got from a unique batch usually are composed by very similar modes disposition and sorting.

It's reasonable they fit in the same way always with the same parts. This characteristic is always valid unless for the last batch : in fact, maybe because of a possible drift affecting the stamping process in last batch of last turn considered.

This aspect will be not discussed and faced in this thesis work because out of work, but it's necessary to take into account that some parts taken from same batches could

PART	RANK	MODE NAME	CONTRIBUTION %	PHASE
R1-A	MODE1	C(1,2)	82,1031	-
	MODE2	C(1,7)	5,6774	+
	MODE3	C(1,8)	3,552	+
	MODE4	C(1,9)	3,1428	-
	MODE5	C(1,6)	2,0839	+
	MODE6	C(1,3)	1,7206	+
R1-B	MODE1	C(1,2)	76,4886	-
	MODE2	C(1,7)	5,8791	+
	MODE3	C(1,8)	5,5307	-
	MODE4	C(1,9)	4,2367	+
	MODE5	C(1,6)	3,7915	-
	MODE6	C(1,10)	0,3164	-
R2-A	MODE1	C(1,2)	76,2435	-
	MODE2	C(1,7)	4,5941	+
	MODE3	C(1,8)	4,2171	-
	MODE4	C(1,6)	4,0601	-
	MODE5	C(1,9)	2,9064	+
	MODE6	C(1,5)	1,2452	+
R2-B	MODE1	C(1,2)	64,9419	-
	MODE2	C(1,3)	28,5603	+
	MODE3	C(1,4)	3,247	-
	MODE4	C(1,5)	2,1989	+
	MODE5	C(2,2)	0,49562	+
	MODE6	C(2,1)	0,45268	-
R3-A	MODE1	C(1,2)	60,3211	-
	MODE2	C(1,3)	21,7899	+
	MODE3	C(1,4)	7,5095	-
	MODE4	C(1,5)	4,2815	+
	MODE5	C(2,2)	3,52451	+
	MODE6	C(2,1)	1,41823	-
R3-B	MODE1	C(1,2)	64,7065	-
	MODE2	C(1,3)	20,7431	+
	MODE3	C(1,4)	7,8139	-
	MODE4	C(1,5)	5,289	+
	MODE5	C(2,2)	0,49601	-
	MODE6	C(2,1)	0,4462	+
R4-A	MODE1	C(1,3)	53,1441	+
	MODE2	C(1,5)	28,9196	+
	MODE3	C(1,2)	8,3761	-
	MODE4	C(1,4)	6,3876	-
	MODE5	C(1,6)	1,487	-
	MODE6	C(2,1)	0,47278	-
R4-B	MODE1	C(1,2)	55,7085	-
	MODE2	C(1,5)	25,4575	+
	MODE3	C(1,6)	4,5252	-
	MODE4	C(1,4)	3,9752	-
	MODE5	C(1,7)	2,6563	+
	MODE6	C(1,8)	1,6414	-
IF1-A	MODE1	C(1,2)	97,3395	-
	MODE2	C(1,3)	1,6796	+
	MODE3	C(1,4)	1,0493	-
IF1-B	MODE1	C(1,2)	95,1711	-
	MODE2	C(1,3)	2,8584	+
	MODE3	C(1,4)	1,0158	-
IF2-A	MODE1	C(1,2)	80,7347	-
	MODE2	C(1,3)	17,1985	+
	MODE3	C(1,4)	1,0977	-
IF2-B	MODE1	C(1,2)	78,9189	-
	MODE2	C(1,3)	18,8521	+
	MODE3	C(1,4)	1,1772	-
	MODE4	C(1,5)	0,4498	+
IF3-A	MODE1	C(1,2)	77,0033	-
	MODE2	C(1,3)	20,4402	+
	MODE3	C(1,7)	0,87241	+
	MODE4	C(2,1)	0,474	-
	MODE5	C(2,2)	0,3158	+
IF3-B	MODE1	C(1,3)	62,9303	+
	MODE2	C(1,5)	17,3511	+
	MODE3	C(1,6)	5,5594	-
	MODE4	C(1,2)	3,7646	-
	MODE5	C(1,4)	3,4194	+
	MODE6	C(1,7)	3,0595	+
IF4-A	MODE1	C(1,3)	44,5689	+
	MODE2	C(1,2)	42,4428	-
	MODE3	C(1,5)	5,8356	+
	MODE4	C(1,6)	3,4371	-
	MODE5	C(2,1)	1,3515	+
	MODE6	C(2,2)	0,6751	-
IF4-B	MODE1	C(1,3)	48,0537	+
	MODE2	C(1,2)	25,03	-
	MODE3	C(1,5)	23,65	+
	MODE4	C(1,6)	3,7374	-
	MODE5	C(1,7)	1,145	-
	MODE6	C(1,9)	0,9339	-

Figure 6.57: SMA analysis on Comau parts

also present some big differences in mode decompositions because of an hypothetical drift of the stamping process.

To see more clearly what explained before about the similar fitting properties char-

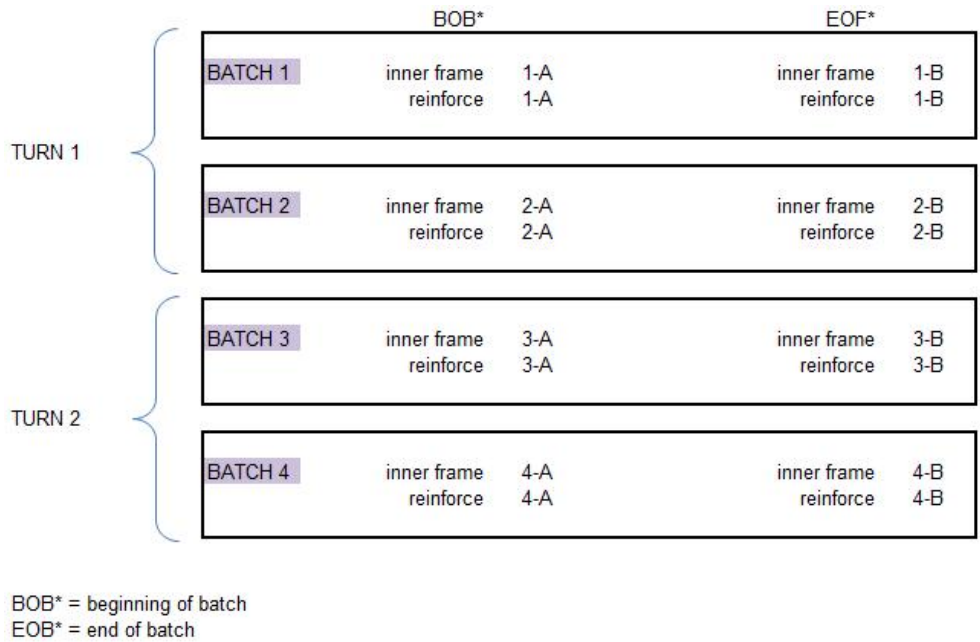


Figure 6.58: Reference batch, period batch and ID-name of COMAU parts

acterizing the same batch’s parts, an illustration is given by the following table 6.59, which describes only coupled reinforces with best fitting inner frames (the analysis is based on a discrimination through reinforces).

In *batch 1* and *batch 3* proper reinforces, belonging to them, fit equally with the same corresponding inner frames of the same batch; as reasonable two different batches are described by different deformations, so the number of best coupling will change batch by batch.

In *batch 2* only three inner frames commonly fit well both with the reinforces produced during the batch, probably for a possible little drift. Here the number of shared inner frame for their fitting properties is lower than the previous batch. WR2B, produced at the end of the process, starts losing good fitting properties, so a lower possible inner frames combinations will be present.

The mean drift can be observed in *batch 4*, where the reinforce produced at the beginning of stamping process has recognizable different characteristic modes, from the previous batch and at the end of the process the last reinforce of the last batch cannot be welded with any inner frame if high value of welding are required.

Checking the batch characteristics (referred to figure 6.59):

1. At the beginning both initial and final reinforces are good weldable with five inner frames (versus the total number of 8 parts);
2. The first reinforce of the second batch maintains the same characteristics of the parts belonging to the first one, but this last shows a decreasing number of good couplings;
3. The third batch presents the same condition of the last reinforce of the second one, and it remains constant along the batch;
4. The fourth buffer presents an additional loss of good mating till to arrive to the lost reinforce, not able to be coupled with any inner frame.

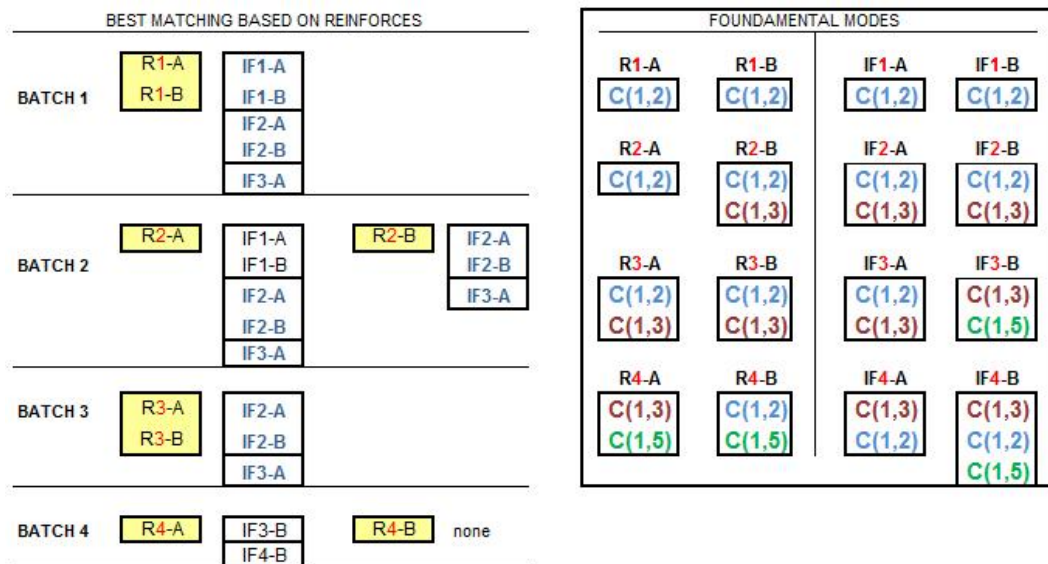


Figure 6.59: Best matching analysis based on reinforces belonging to the same batch

Near best matching table is shown a second table figuring dominant modes affecting each parts. Through this table is visible the community between dominant shared modes and best fitting. Inner frame and reinforces with the same dominant modes guarantee best coupling. If reinforces (or inner frames) belonging to the same batches have similar modes, they will fit equally with the same respective inner frames (reinforces).

COMAU parts classification

Exactly as it was done for parts set coming from the Warwick University, a parts classification in discriminating *cluster* must be done to group together in same bins parts having the same shared modes.

The entire process of classification is explained at the end of the chapter "Similarity Analysis" in section "Classification through SMA index", and here the same approach is implemented, but on a real industrial case of study.

From the modes analysis, two dominant modes are mainly affecting part profiles : **C(1,2)** and **C(1,3)**.

Some parts have C(1,2) as dominant mode present into the part for more than 70% like in figure 6.60. Couples composed by these reinforces and inner frames guarantee perfect coupling.

Some other parts, whose value is red-coloured, also have C(1,2) dominant, but if welded with Inner frames on the left, they are not able to guarantee an optimal welding quality only through the single C(1,2) mode, in fact the need for some other dominant secondary modes to be welded.

FOUNDAMENTAL MODE C(1,2) FOR INNER FRAMES				
IF2-A	MODE1	C(1,2)	80,7347	-
IF2-B	MODE1	C(1,2)	78,9189	-
IF3-A	MODE1	C(1,2)	77,0033	-
IF1-A	MODE1	C(1,2)	97,3395	-
IF1-B	MODE1	C(1,2)	95,1711	-

FOUNDAMENTAL MODE C(1,2) FOR REINFORCES				
R1-A	MODE1	C(1,2)	82,1031	-
R2-B	MODE1	C(1,2)	64,9419	-
R1-B	MODE1	C(1,2)	76,4886	-
R3-B	MODE1	C(1,2)	64,7065	-
R4-B	MODE1	C(1,2)	55,7085	-
R3-A	MODE1	C(1,2)	60,3211	-
R2-A	MODE1	C(1,2)	76,2435	-

Figure 6.60: Parts classified through fundamental *mode C(1,2)*

As it is visible, $C(1,2)$ is present into parts always with the same phase value (negative) equal to π , so they can be compared and clusterized together because all parts presents mostly similar shape trend.

CLASS 1 : Classification only through the dominant $C(2,1)$ greater than 70% guarantee 15/64 good quality coupling listed in figure 6.61. So the mode $C(2,1) > 70\%$ can build a valid factor for a first correct classification. So it's possible to create a first group in which will be sent all parts having $C(1,2)$ with a particular high value.

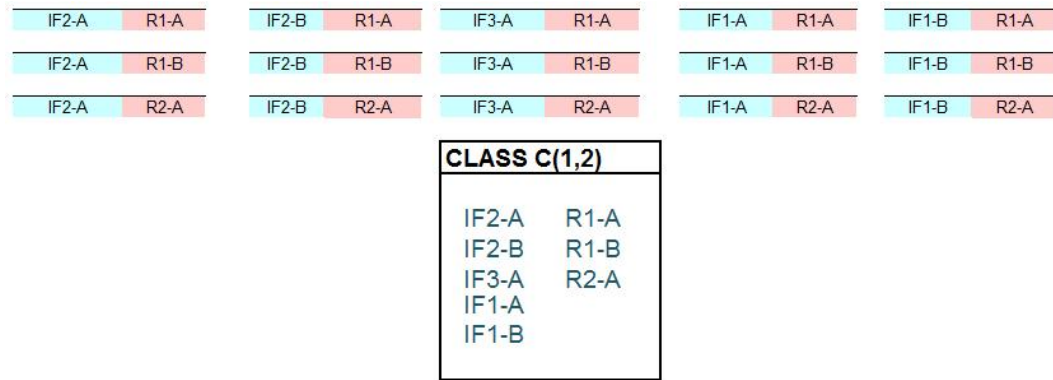


Figure 6.61: Composition of CLASS $C(1,2)$

CLASS 2 : The three couples with $C(1,2) \text{value} < 70\%$ must be analyzed and classified through their secondary modes too. In particular all of them are described by $C(1,3)$ as secondary mode. They will be welded, and so classified in the same cluster, with inner frame presenting the same peculiarity ($C(1,3)$ as dominant after $C(1,2)$). This classification through secondary $C(1,3)$ mode guarantees some other 9/64 good combinations.

In this way is possible to consider another class composed by all parts having:

- $C(1,2)$ as absolute dominant mode but with value less than 70%
- $C(1,3)$ as secondary relevant mode, with contribute percentage higher than 10%

Between couples with $C(1,2)$ as fundamental mode, instead of $C(3,1)$ there is also another secondary dominant modes at second position: **C(5,1)**. The only part described by $C(1,2)$ and $C(1,5)$ is Reinforce4-A illustrated in figure 6.63 , so there is no possible welding with this part, because the sum of percentage contribution of modes value with every other inner frame is not enough to achieve good welding requirement. All other inner frame having as dominant firsts mode $C(2,1)$ present $C(1,5)$ less than 2%, so it's

impossible to reach the 70% with a C(1,2) mode equal to 55% and a mode C(1,5) so low in its value.

For this reason WR4-A will not be considered during the classification.

SECONDARY MODE C(1,3) FOR REINFORCES				
IF2-A	MODE2	C(1,3)	17,1985	+
IF2-B	MODE2	C(1,3)	18,8521	+
IF3-A	MODE2	C(1,3)	20,4402	+

SECONDARY MODE C(1,3) FOR REINFORCES				
R2-B	MODE2	C(1,3)	28,5603	+
R3-B	MODE2	C(1,3)	20,7431	+
R3-A	MODE2	C(1,3)	21,7899	+

CLASS C(1,2)[dominant] & C(1,3)[secondary]	
IF2-A	R3-A
IF2-B	R3-B
IF3-A	R2-B

Figure 6.62: Composition of CLASS C(1,2) & C(1,3)

SECONDARY MODE C(1,5) FOR REINFORCES				
R4-B	MODE2	C(1,5)	25,458	+

Figure 6.63: R4-B, the reinforce without possible couplings

Another group can be created and it will include parts with C(3,1) as dominant mode instead of C(1,2). None of this coupling can guarantee alone a good matching as seen in figure 6.64 under the voice *min values* which consider the minimum value of percentage contribution between two parts, so it is necessary to analyze also secondary modes for all the three inner frames respect the reinforce to provide a good classification.

CLASS 3 : Analyzing the secondary existing modes after C(1,3) in available parts in figure 6.64, there are three inner frames with secondary dominant mode represented by C(1,5), and some others like in figure 6.66 which are affected by C(1,2).

The inner frames with C(1,5) as dominant secondary mode can be welded with the only reinforce having the same characteristic. They will represent a third cluster.

FOUNDAMENTAL MODE C(1,3) FOR INNER FRAMES				
IF4-A	MODE1	C(1,3)	44,5689	+
IF3-B	MODE1	C(1,3)	62,9303	+
IF4-B	MODE1	C(1,3)	48,0537	+

FOUNDAMENTAL MODE C(1,3) FOR REINFORCES				
R4-A	MODE1	C(1,3)	53,144	+

Figure 6.64: Composition of CLASS C(1,3)

SECONDARY MODE C(1,5) FOR INNER FRAMES				
IF3-B	MODE1	C(1,3)	62,9303	+
	MODE2	C(1,5)	17,3511	+
IF4-B	MODE1	C(1,3)	48,0537	+
	MODE2	C(1,2)	25,03	-
	MODE3	C(1,5)	23,65	+

SECONDARY MODE C(1,5) FOR Reinforces				
R4-A	MODE1	C(1,3)	53,1441	+
	MODE2	C(1,5)	28,9196	+

**CLASS C(1,3)[dominant]
& C(1,5)[secondary]**

IF3-B	R4-A
IF4-B	

Figure 6.65: Parts affected by C(1,3) as dominant and C(1,5) as secondary and composition of CLASS 3 C(1,3) & C(1,5)

CLASS 4 : The exception is represented by inner frame 4-A, which have dominant modes C(1,3) and C(1,2). There are no reinforces with the same mode disposition, in fact it cannot be welded with any part excluded R2-B affected by C(1,2) and C(1,3) in opposite position but with same phase.

This coupling in figure 6.66 represents a sporadic and rare case, explained by the

particularly high value of principal modes: for the inner frame the secondary mode is similar in value to the dominant one, so it's like this part is characterized by two modes at the same level.

For the reinforce the secondary mode C(1,3) is quite high value respect the typical secondary modes values, usually around the 17 – 20%.

This two parts represent the last cluster in which can be sent only these two specific parts in order to prevent bad-quality welding.

FOUNDAMENTAL MODE C(1,3)+ C(1,2) FOR IF				
IF4-A	MODE1	C(1,3)	44,5689	+
	MODE2	C(1,2)	42,4428	-
	MODE1	C(1,2)	64,942	-
	MODE2	C(1,3)	28,56	+

Figure 6.66: Exceptional coupling

Final classification configuration for COMAU components

<p>CLASS 1 : C(1,2)</p> <p>IF2-A R1-A IF2-B R1-B IF3-A R2-A IF1-A IF1-B</p>	<p>CLASS 2: C(1,2) [dominant]& C(1,3)[secondary]</p> <p>IF2-A R3-A IF2-B R3-B IF3-A R2-B</p>
<p>CLASS 3 : C(1,3)[dominant] & C(1,5)[secondary]</p> <p>IF3-B R4-A IF4-B</p>	

Figure 6.67: Final buffer creation

6.10.2 The iterative classification for COMAU components

As in the case of the experimental part, the iterative method can be applied to COMAU components. Differently from the research case, parts present a different main mode: there are C(1,2) and C(1,3). All results are present in appendix ??.

”As is” case

In the current case, all possible combinations are evaluated. With a 59% couples don't satisfies the requirement of gaining the 70% in energy compaction with common modes. The complete partition is shown in figure D.2.

First partition

As established in the schematic diagram flow 5.1 of chapter 5, the first step starts from the number of principal modes. In this case parts present 2 main modes: C(1,2) and C(1,3).

Classification is shown in appendix ?. The worst matings are present only in the group represented by the principal mode C(1,2). The next division splits this group.

Second partition

The need to explode classes in C(1,3) and C(1,2) leads to a deeper classification. the first class that have to be explored, is C(1,2) because presents worst coupling. The second partition is defined by the mode C(1,3), present in most of the worst parts of the precedent iteration in C(1,2) group. As visible from the table in appendix D.3, the number of non good combinations is reduced, because parts representing the current new class didn't reach the threshold of 70% of common energy compaction with only the principal shared mode, C(1,2), while the addition of the shared C(1,3) introduces a percentage, exceeding the lower limit. This is a representative case in which a second mode permits to avoid non perfect couplings.

Third partition

Because the group C(2,1), the most representative mode of every part in this case, is characterized by the biggest number of bad combinations too, it is useful to find another representative mode in this class and split it. In particular, all non perfect combinations have the R4B (and it is not random it is the last part of the batch), it is reasonable that this part is not good (coming from the drift process) in any coupling. This part is

characterized by a mode, C(1,5). However, it is the unique part which must be stored because presenting this mode. It will be stored alone, because there isn't any kind of inner frame with the same characteristic.

The waist reinforce R4B is automatically eliminated, because it has no possibility to have a good mating.

Fourth partition

The principal mode C(1,2) is completely arranged, the step is focused on C(1,3) division. It is characterized by few parts and only a mating is not good: C(1,3) will be subdivided in C(1,5), which contains all C(1,3) representative parts, except the inner frame IF4A. Being alone in a class, as the precedent case of the WR4B, this class is automatically deleted for the lack of the waist reinforce D.4.

In this situation the best classification is found.

CLASS1		CLASS2		MODE C(1,2)		CLASS3		MODE C(1,3)	
MODE C(1,2) MODE C(1,3)		MODE C(1,2) > 70%		MODE C(1,2) MODE C(1,5)		MODE C(1,3) MODE C(1,5)		MODE C(1,3) MODE C(1,2)	
High quality welding	Low quality	High quality	Low quality	High quality	Low quality	High quality	Low quality	High quality	Low quality
R2-B; IF2-A		R1-A; IF1-A		R4-B		R4-A; IF3-B		IF4-A	
R2-B; IF2-B		R1-A; IF1-B				R4-A; IF4-B			
R2-B; IF3-A		R1-A; IF2-A							
R3-A; IF2-A		R1-A; IF2-B							
R3-A; IF2-B		R1-A; IF3-A							
R3-A; IF3-A		R1-B; IF1-A							
R3-B; IF2-A		R1-B; IF1-B							
R3-B; IF2-B		R1-B; IF2-A							
R3-B; IF3-A		R1-B; IF2-B							
		R1-B; IF3-A							
		R2-A; IF1-A							
		R2-A; IF1-B							
		R2-A; IF2-A							
		R2-A; IF2-B							
		R2-A; IF3-A							

Figure 6.68: Step 4, Final buffer iteration

6.10.3 Conclusions

This classification is the result of the iterative classification, based on the SMA method.

Two parts are automatically removed from the production, because they don't satisfy a good grade of energy compaction, without any part. It is reasonable that consider two

flow rates as scraps it's onerous and cost effective, but it is as much true that non good final parts are most expensive.

Chapter 7

Conclusions

In this work a research study about the part-to-part control gap using Remote Laser Welding has been analyzed. To conclude the developed work is possible to affirm that the prefixed objectives have been reached.

Starting from the state of art of Remote Laser Welding, the problem of the distance between parts has been covered in the past by branches of research about the parameter selections of the beam and the fixture design. However, the problem is not strictly solved.

For this reason this work proposed an upstream resolution of this limit, before the fixture usage, in order to act previously on the welding process.

The first part of the work is addressed to the research of a good indicator, able to predict a good welding joint and able to classify parts in different groups in a selective assembly view. In particular the research of a method has brought the attention to the SMA one. The decomposition of the profile with Discrete Cosine Transformations permits to couple parts with a certain grade of common modes. The linkages between SMA outputs and experimental data are clear and evident.

This heuristic approach is confirmed by both experimental gap measurements and FEM analysis results.

After the validation of the method, its application to a real case study (COMAU) has been done, in order to apply the index on a set of data got through them. The collaboration with Comau allowed to analyze doors' components and to evaluate a possible classification based on DCT decomposition, with a consequent introduction to selective assembly approach in the assembly line.

End of proof, each part is described by a different modes set, adding value to the method, because the diversity of each part is present both in experimental data set and

in Fiat's doors.

Nevertheless, some limits are present in the work:

- A single data sample used during the research of the best indicator; however results are strengthened by results from the experimentation of the best fixture design and from the FEM analysis too;
- The heuristic approach, which defines an intuitive approach; the choice of the threshold is consequence of the comparison with real data set;
- The necessity to analyze parts; this classification requires a parts sampling, which must be representative of the assembly campaign.

Although presence of limits, results show a big improvement in the welding quality, thank to the best mating between parts, after its decomposition in modes.

The introduction of a selective assembly in the system, before the fixture design, is a good approach to take advantages of Remote Laser Welding.

Especially in automotive sector, in which the production rate is high thank to remote laser technology, the reduction of scrap ratio permits to be more competitive in market. In fact the realized work is mostly directed to the technician of automotive sector, and it represents a careful analysis of the welding quality characterizing car components to be joint together.

The collaboration with COMAU gave the opportunity to verify that deformation post-forming process are actually present in real car's door components. While the collaboration with CRF allowed to simulate the parts behaviour under the stress impressed by clamping forces and after the spot welding simulation.

7.1 Future works

This work opens other future works.

First of all, new indicators to evaluate the similarity between parts can be searched. For example, it could be interesting to specialized the similarity analysis indicator based on RLW, especially introducing the mass and weight of the part, in order to move the problem to a geometrical to physical one.

Then, an analytical solution for the classification of parts can be found. The problem of the heuristic threshold could be better solved and confirmed, in order to ensure the limit for

Bibliography

- [1] L. E. Izquierdo, D. Ceglarek, D. Kim, PKS Prakash, *Similarity-Based Part-to-Part Gap Characterization for Remote Laser Welding Assembly*, Technical Paper from International Digital Laboratory, IDL, 2010.
- [2] R.B.Durai and V.Duraisamy, *A generic approach to content based image retrieval using dct and classification techniques* International journal on Computer Science and Engineering, Vol. 2, n6, pp.2022-2024, 2010.
- [3] M. F. Zaeh, J. Moesl, J. Musiol, F. Oefele, *Material processing with remote technology: revolution or evolution?*, Physics Procedia, Vol. 5, n 1, pp.19-33, 2010.
- [4] Matsuurg, Shinozaki, *Optimal process design in selective assembly when components with smaller variance are manufactured at three shifted means*, International Journal of Production Research, 2010
- [5] H., W. Lilliefor, *On the Kolmogorov-Smirnov test for the exponential distribution with mean unknown*, Journal of the American Statistical Association, Vol. 64, No. 325, pp. 387- 389, 1969.
- [6] E. Capello, *Le lavorazioni industriali mediante laser di potenza-La tecnologia, le applicazioni e i sistemi*, Ed. Clup Library, pp 157-205.
- [7] S. Samper, P.A. Adragna, H. Favreliere and M.Pillet, *Modeling of 2D and 3D Assemblies Taking Into Account Forms Errors of Plane Surfaces*, Journal of Computing and Information Science in Engineering, Vol. 9, n4, pp.1-12, December 2009.
- [8] D. Ceglarek, W. Huang, *Mode-based Decomposition of Part Form Error by Discrete-Cosine-Transform with Implementation to Assembly and Stamping System with Compliant Parts*, CIRP Annals-Manufacturing Technology, Vol. 51, Issue 1, pp. 21-26, 2007.

- [9] Iyama, Mckay, *Optimal matching for inline resource selection when errors exist in error measurement*, Journal of Materials Processing Technology, Vol. 183, Issues 2-3, Pages 277-283, 23 March 2007.
- [10] X. Li, S. Lawson, Y. Zhou, *Novel technique for laser lap welding of zinc coated sheet steels*, Journal of laser applications, Vol. 19, Number 4, 2007.
- [11] S. Samper and F. Formosa, *Form defects tolerancing by natural modes*, Journal of Computing and Information Science in Engeneering, Vol. 7, n1, pp.44-51, March 2007.
- [12] R. Osada, T. Funkhouser, B. chazelle, D. Dobkin *Matching 3D Models with Shape Distributions*, ACM Transaction on Graphics, Vol. 21, n 4, p 807-832, October 2002.
- [13] Arnia, M. Fujiyoshi, H. Kiya, *The Use of DCT Coefficient Sign for Content-Based Copy Detection*, International Symposium on Communications and Information Technologies proceedings, p 1476-1481, 2007.
- [14] T.Tsai, T.W. Chiang, Y.P. Huang, *An efficient DCT-based image Retrieval Approach using Distance Threshold Pruning* journal of Advanced Computational Intelligence and Intelligent informations, Vol. 12, n 3, pp.268-276, 2008.
- [15] G. Tsoukantas and G. Chryssolouris, *Theoretical and experimental analysis of the remote welding process on thin, lap-joined AISI 304 sheets*, The International Journal of Advanced Manufacturing Technology, Vol. 35, Numbers 9-10, 880-894, 2006.
- [16] J. Epps, E. Ambikairajah, *Visualisation of Reduced-Dimension Microarray data using Gaussian Mixture Models*, Asia-Pacific symposium on information visualization, Vol. 45, 2005.
- [17] Tzeng Yih-fong, *Gap free welding of zinc coated steel using pulsed CO₂ laser*, The International Journal of Advanced Manufacturing Technology, Vol. 29, Numbers 3-4, 287-295, 2005.
- [18] Mease, Nair, *Selective assembly in manufacturing: statistical issues and optimal binning strategies*, Technometrics, Vol. 46, No. 2, pp. 165-175, May 2004.
- [19] S.Menghani, H.Zauhoani, *Characterization of the 3D waviness and roughness motifs* Wear, Vol. 257, n 12 SPEC.ISS, p 1250-1256, December 2004.

-
- [20] A. Iglesias, G. Echevarria, A. G. Ivez, *Functional networks for B-spline surface reconstruction*, Future Generation Computer System, Vol. 20, n 8, p 1337-1353, November 1, 2004.
- [21] G. Moroni, W. Polini, *Tolerance-based Variation in Solid Modeling*, Journal of Computing and Information Science in Engineering, Vol. 3, n 4, p 345-352, December 2003.
- [22] S.A.Khayam, *The Discrete Cosine Transformation (DCT): Theory and Application*, ECE 802-602 : Information Theory and Coding, March 2003.
- [23] S.A. Mehmood, I. Awan, *Towards a solution of laser welding of zinc coated steel sheets*, ICALEO, 2002.
- [24] B. Li, B.W. Shiu and K.J. Lau, *Fixture configuration design for sheet metal assembly with laser welding*, The International Journal of Advanced Manufacturing Technology Vol. 19, Number 7, 501-509, 2002.
- [25] J. Raia, B. Muralikrishnan, Fu Shengyu, *Recent advances in separation of roughness, waviness and form* Journal of International Societies for Precision Engineering and Nanotechnology, 222-235, April 2002.
- [26] B. Li, B.W. Shiu and K.J. Lau, *Fixture configuration design for sheet metal assembly with laser welding*, The International Journal of Advanced Manufacturing Technology Vol. 19, Number 7, 501-509, 2002.
- [27] D. Ceglarek, J. Camelio, S.J. Hu, *Impact of fixture design on sheet metal assembly variation*, Journal of Manufacturing Systems, Vol. 23, No. 3, pp. 182-193, 2004, 2001.
- [28] V. Jayabalan and SM. Kannan, *A New Grouping Method for Minimizing the Surplus Parts in selective Assembly*, International Journal on Quality Engineering, pp.67-75, Vol.14, No.1, 2001.
- [29] V. Jayabalan and SM. Kannan, *A New Grouping Method for Minimizing the Surplus Parts in selective Assembly*, International Journal on Quality Engineering, pp.67-75, Vol.14, No.1, 2001.
- [30] G.Giunta, *Appunti sulla DCT*, knows about DCT Numerical Signal Elaboration Course, n 1, 2000.

- [31] Tzeng Yih-fong, *Pulsed Nd:YAG laser seam welding of zinc coated steel*, Vol. 78, N 7, pp. 238.s-244.s, 1999.
- [32] Lin, Chan, *A grouping method for selective assembly of parts of dissimilar distributions*, Quality Engineering, Vol. 11, No. 2, pp. 221-234, December 2008.
- [33] E. Dimas and D. Briassoulis, *3D geometrical modelling based on NURBS : a review*, Advanced in engineering software, Vol. 30, n 9, p 741-751, September 1999.
- [34] J. Macken, *Remote Laser welding*, 1996.
- [35] Fang, Zhan, *New algorithm for minimizing the surplus part in selective assembly*, Computers & Industrial Engineering, Vol. 28, Issue 2, Pages 341-350, April 1995.
- [36] D.Ceglarek and J.Shi, *Dimentional Variation Reduction for Automotive Body Assembly* Manufacturing Review, Vol. 8, n 2, 1995.
- [37] H.J. Lamousin, N. Warren, Jr. Waggenspack, *NURBS-based free-form deformations*, IEEE Computer Graphics and Applications, Vol. 14, n 6, p 59-65, November 1994.
- [38] M. Mizuno, T. Iyama, K.N. Mckay, M. Ito, J. Tamaki, *The behaviour of machining-assembly automatic transfer line system adapting a matching method*, Japan Society of Mechanical Engineers, 243-248, 1992.
- [39] Allen G. Pugh, *Selective assembly with components of dissimilar variance*, Computers & Industrial Engineering Vol. 23, Issues 1-4, Pages 487-491, November 1992.
- [40] Akhter R, Steen WM, Cruciani D, *Laser welding of zinc-coated steel*, Proceedings of the 6th International Conference of Lasers in Manufacturing, pp 105?120, 1989.
- [41] A.D. Piane, F. Sartorio, M. Cantello,, and G. Ghiringhello, *Method of laser welding sheet metal protected by low-vaporizing-temper- ature materials*, U.S. Patent No. 4682002, 1987.
- [42] www.wikipedia.com
- [43] www.comau.com
- [44] www.cognitens.com

Appendix A

SMA code

```
%calculating DCT

Zval1=Welding_Area;
Zval1=Zval1-mean(mean(Zval1)); % CENTER THE PART

dctf=dct2(Zval1);      % CALCULATION OF THE 2D COSINE TRANSFORMATION

% code for identifying modes for defined energy compaction;

mat2vec=[];
dcts=size(dctf);
mat2vec(:,1)=dctf(:,1);
for i=2:dcts(2)
    mat2vec=[mat2vec; dctf(:,i)];
end

% Calculation of power
mul_val=mat2vec.*mat2vec;
[sdctval sdctind]=sort(abs(mat2vec), 'descend');
energy_comp=0.99;
compaction=0;
f2=sum(mul_val);
counter=1;
```

```
indices_column=[];
indices_row=[];
dummy=0;

while compaction<energy_comp
    compaction=compaction+(sdctval(counter)^2)/f2;
    valuecoeff(counter)=(compaction-dummy)*100;
    indices_row(counter)=sdctind(counter)-
        -floor(sdctind(counter)/dcts(1))*dcts(1);
    indices_column(counter)=floor(sdctind(counter)/dcts(1)) +1;
    indices_row(counter)=ceil(sdctind(counter)/dcts(2));
    indices_column(counter)=ceil( (sdctind(counter)-
        ((ceil(sdctind(counter)/dcts(2)))-1)*dcts(2))/dcts(1));
    dummy=compaction;
    counter=counter+1;
end

% Plot significant mode
no_modes=size(indices_column);
number_fig=6;
y=zeros(14,597);
struttura=struct('modes',[y]);
figure
for i=1:no_modes(2)
    pmode=zeros(size(dctf));
    pmode(sdctind(i))=dctf(sdctind(i));
    imode=idct2(pmode);
    struttura(i)=struct('modes',imode);
    if i<=number_fig
        subplot(3,2,i)
        surf(real(imode),imag(imode)),title(['Mode ',num2str(i),' ',
            Coef ('',num2str(indices_column(i)),'',num2str(indices_row(i)),' ')
            Contrib % = ',num2str(valuecoeff(i))])
        xlabel('X'),ylabel('Y'),zlabel('Z');
    else
        break;
    end
end
```

```

    end
end

%Memorize single modes
somma=0;
for i=1:no_modes(2)
    if i<=number_fig
        struttura(i).modes(1,1)
        somma=struttura(i).modes+somma;
    else
        break;
    end
end

kk = zeros(dcts);
for i=1:counter-1
    kk(indices_row(i),indices_column(i))=dctf(indices_row(i),indices_column(i));
end
recondata = idct2(kk);
error=Zval1-recondata;
RMS=sum(sum(error.^2))/(dcts(1)*dcts(2));

figure
subplot(311)
surf(Zval1), title('Original surface')
subplot(312)
surf(recondata),
title(['Reconstructed surface;
Compact. level= ', num2str(energy_comp*100),'])
subplot(313)
surf(error), title(['Error on surface reconstruction;
Error RMS = ',num2str(RMS)])

%Plot for cumulative chart showing percentage compaction and number of modes

Cumulative(1)=sdctval(1).^2

```

```
for k=2:length(sdctval)-1
    Cumulative(k)=Cumulative(k-1)+sdctval(k).^2;
end
Cumulative(1)=sdctval(1).^2./sum(sdctval.^2);
for k=2:length(sdctval)-1
    Cumulative(k)=Cumulative(k-1)+(sdctval(k).^2)./sum(sdctval.^2);
end

% Plot Pareto diagram
figure
subplot(211)
plot(Cumulative*100,'bo-'),xlabel('Number of modes'), ylabel ('% of compactation')
hold
plot(ones(1,length(Cumulative))*energy_comp*100,'r--')
subplot(212)
if length(Cumulative)>15
    plot(Cumulative(1:15)*100,'bo-'),xlabel('Numb of modes'),
        ylabel ('% compactation')
    hold
    plot(ones(1,length(Cumulative(1:15)))*energy_comp*100,'r--')
end

figure
subplot(311)
surf(dctf(1:14,1:20))
title('Modes of original shape'), xlabel('u'), ylabel('v'),
axis([1 20 1 14 min(min(dctf(1:14,1:20))) max(max(dctf(1:14,1:20)))]])
subplot(312)
surf(kk(1:14,1:20))
title(['Modes of approximated shape;
        Compaction level = ', num2str(energy_comp*100), '%'])
xlabel('u'), ylabel('v'),axis([1 20 1 14 min(min(dctf(1:14,1:20)))
        max(max(dctf(1:14,1:20)))]])
subplot(313)
surf(dctf(1:14,1:20)-kk(1:14,1:20))
xlabel('u'), ylabel('v'),title('Difference'),
```

```
axis([1 20 1 14 min(min(dctf(1:14,1:20))) max(max(dctf(1:14,1:20)))])

no_modes=size(indices_column);
number_fig=6;

% Plot the sum of modes with the surface of the part
figure
surf(somma)
hold on
surf(Zval1)

differenza=somma-Zval1;
assoluto=abs(differenza);
media=mean(mean(assoluto))
varianza=var(var(assoluto))

magnitudo=dctf(sdctind(1:counter-1))
```


Appendix B

Results correlation analysis

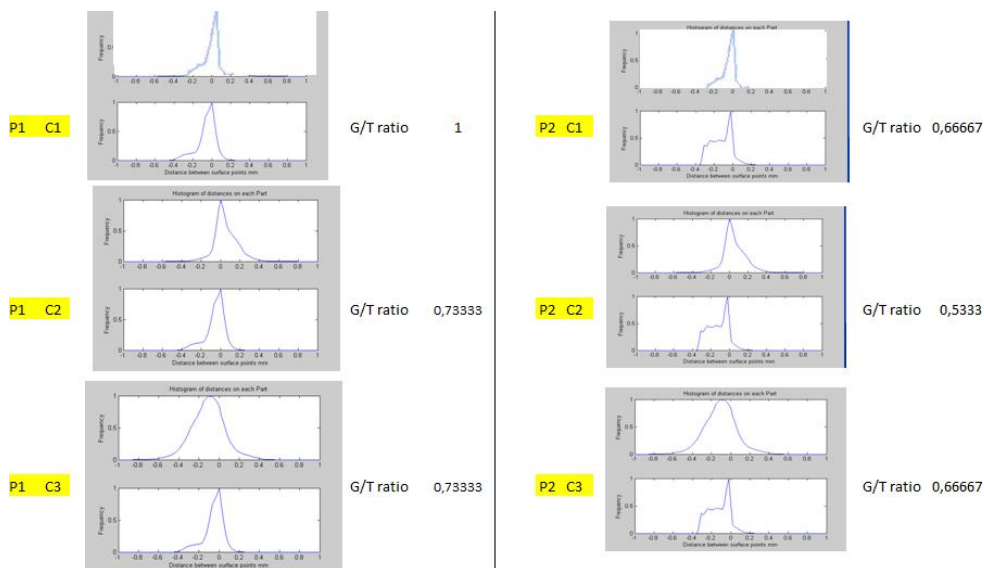
P1	P2	P3	P4	P5	P6	corr1	corr2	corr3	corr4	corr5	corr6	G/T r1	G/T r2	G/T r3	G/T r4	G/T r5	G/T r6
5	3	4	2	6	1	0,47	0,72	0,36	0,4	0,29	0,89	1	0,6667	0,6	0,8	1	0,867
5	3	2	6	1	4	0,47	0,72	0,12	0,2	0,31	0,6	1	0,6667	0,6	1	1	0,667
5	3	2	1	6	4	0,47	0,72	0,12	-0	0,29	0,6	1	0,6667	0,6	1	1	0,667
5	4	2	6	1	3	0,47	0,77	0,12	0,2	0,31	0,44	1	0,5333	0,6	1	1	0,8
5	4	2	1	6	3	0,47	0,77	0,12	-0	0,29	0,44	1	0,5333	0,6	1	1	0,8
5	2	4	6	1	3	0,47	-0,4	0,36	0,2	0,31	0,44	1	0,5333	0,6	1	1	0,8
5	2	4	1	6	3	0,47	-0,4	0,36	-0	0,29	0,44	1	0,5333	0,6	1	1	0,8
5	3	4	6	1	2	0,47	0,72	0,36	0,2	0,31	-0,6	1	0,6667	0,6	1	1	0,6
5	3	4	1	6	2	0,47	0,72	0,36	-0	0,29	-0,6	1	0,6667	0,6	1	1	0,6
5	3	2	4	6	1	0,47	0,72	0,12	0,3	0,29	0,89	1	0,6667	0,6	0,7333	1	0,867
4	5	2	6	1	3	0,68	0,05	0,12	0,2	0,31	0,44	0,8	0,6667	0,6	1	1	0,8
4	5	2	1	6	3	0,68	0,05	0,12	-0	0,29	0,44	0,8	0,6667	0,6	1	1	0,8
4	3	5	2	6	1	0,68	0,72	0,11	0,4	0,29	0,89	0,8	0,6667	0,7333	0,8	1	0,867
1	5	4	2	6	3	0,55	0,05	0,36	0,4	0,29	0,44	1	0,6667	0,6	0,8	1	0,8
1	3	5	2	6	4	0,55	0,72	0,11	0,4	0,29	0,6	1	0,6667	0,7333	0,8	1	0,667
4	2	5	6	1	3	0,68	-0,4	0,11	0,2	0,31	0,44	0,8	0,5333	0,7333	1	1	0,8
4	2	5	1	6	3	0,68	-0,4	0,11	-0	0,29	0,44	0,8	0,5333	0,7333	1	1	0,8
1	4	5	2	6	3	0,55	0,77	0,11	0,4	0,29	0,44	1	0,5333	0,7333	0,8	1	0,8
4	3	2	5	6	1	0,68	0,72	0,12	0,4	0,29	0,89	0,8	0,6667	0,6	0,8667	1	0,867
1	3	2	5	6	4	0,55	0,72	0,12	0,4	0,29	0,6	1	0,6667	0,6	0,8667	1	0,667
5	4	3	2	6	1	0,47	0,77	0,07	0,4	0,29	0,89	1	0,5333	0,6	0,8	1	0,867
5	2	3	6	1	4	0,47	-0,4	0,07	0,2	0,31	0,6	1	0,5333	0,6	1	1	0,667
5	2	3	1	6	4	0,47	-0,4	0,07	-0	0,29	0,6	1	0,5333	0,6	1	1	0,667
5	1	4	2	6	3	0,47	0,93	0,36	0,4	0,29	0,44	1	0,6	0,6	0,8	1	0,8

correlation 0,085

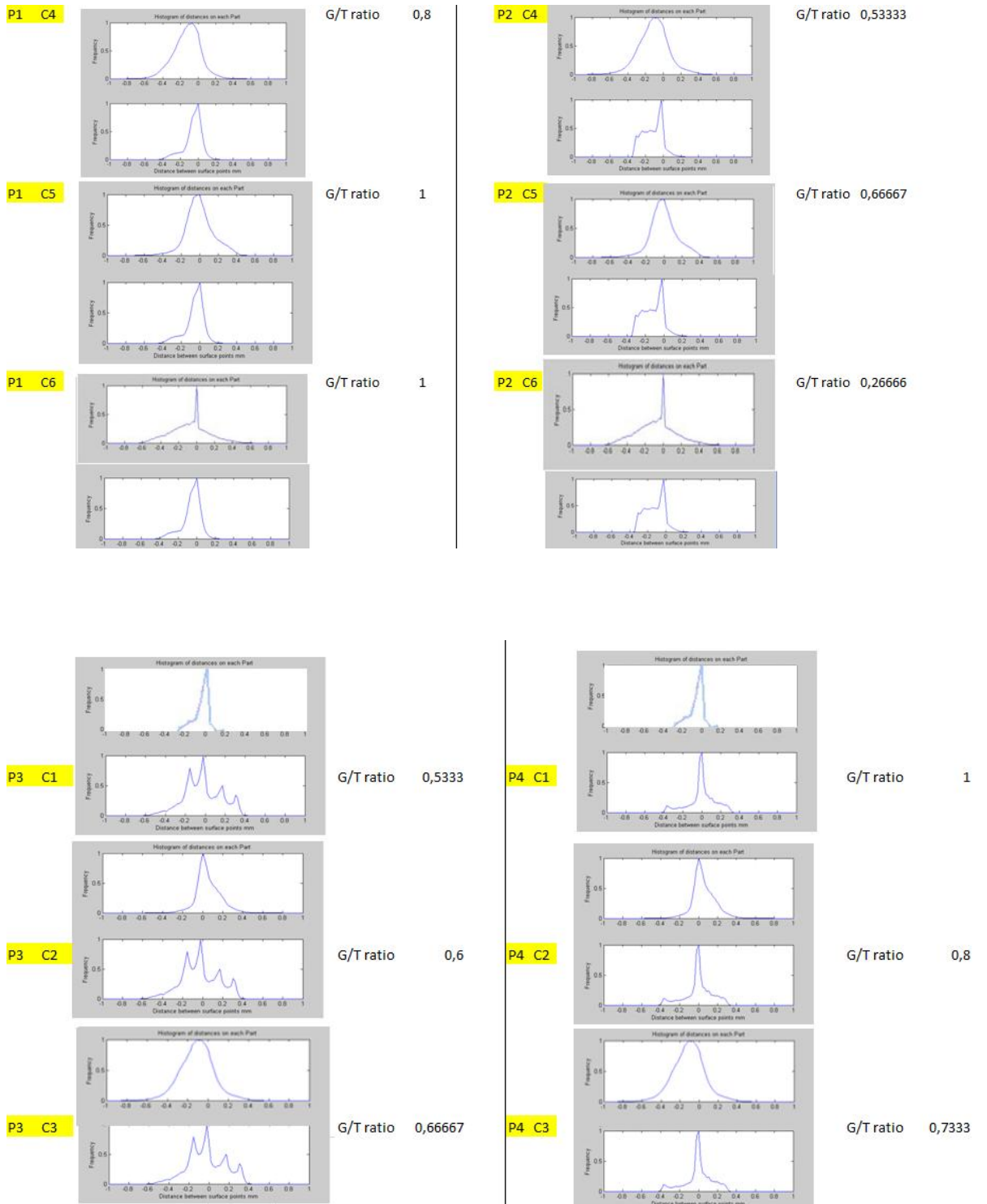
Figure B.1: Link or Recurrences between correlation index and Gap Measurements

Appendix C

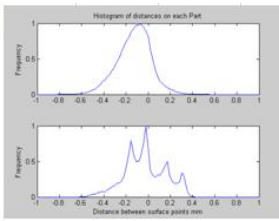
Results from shape distribution analysis



RESULTS FROM SHAPE DISTRIBUTION ANALYSIS

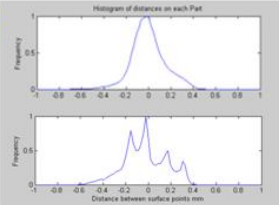


P3 C4



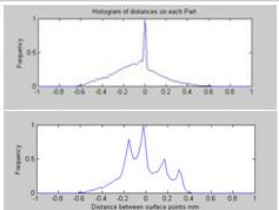
G/T ratio 0,6

P3 C5



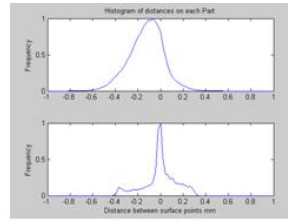
G/T ratio 0,66667

P3 C6



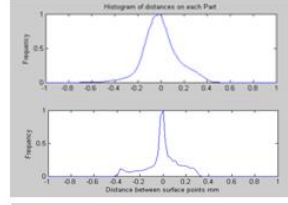
G/T ratio 0,46667

P4 C4



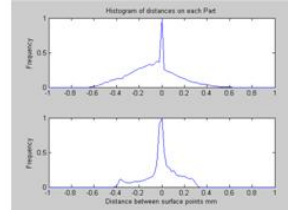
G/T ratio 0,7333

P4 C5



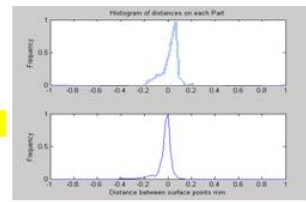
G/T ratio 0,8667

P4 C6



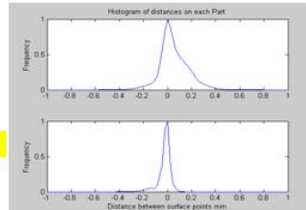
G/T ratio 1

P5 C1



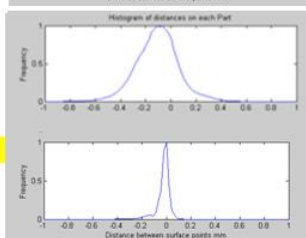
G/T ratio 1

P5 C2



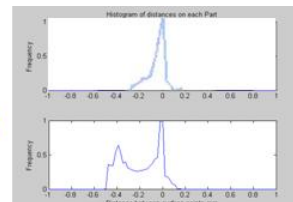
G/T ratio 0,6

P5 C3



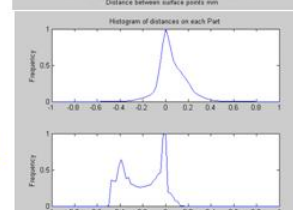
G/T ratio 0,733

P6 C1



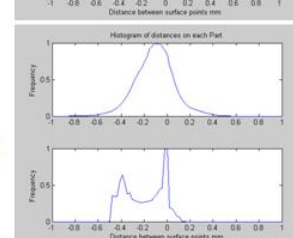
G/T ratio 0,8667

P6 C2



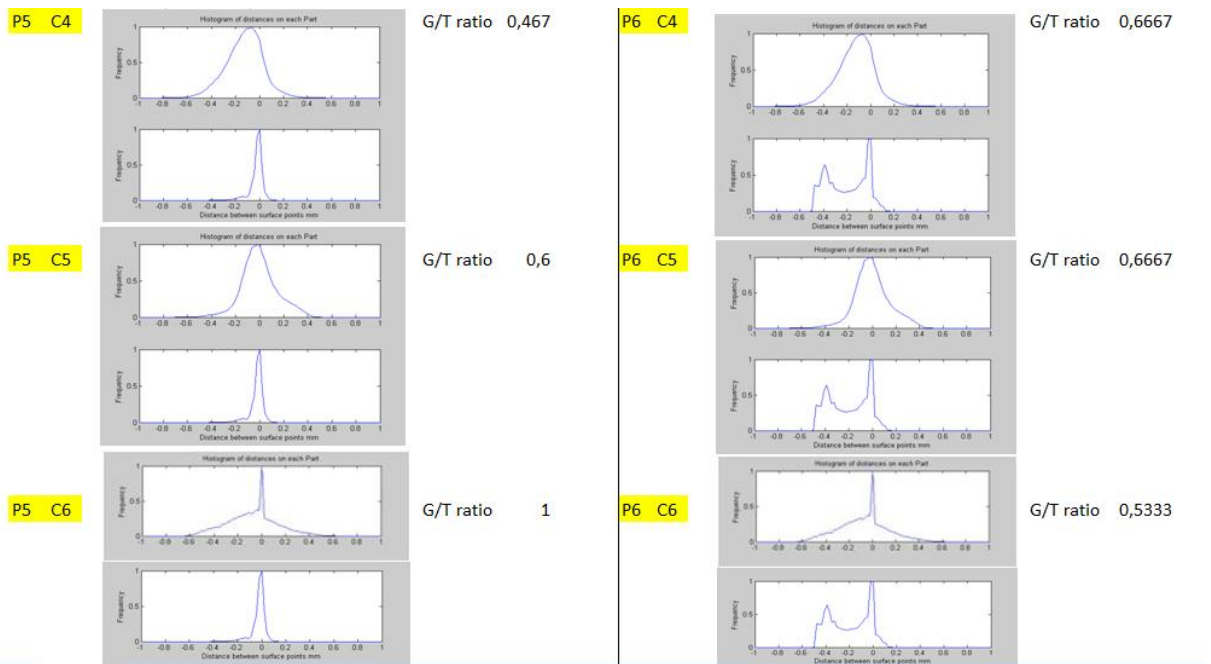
G/T ratio 0,6

P6 C3



G/T ratio 0,8

RESULTS FROM SHAPE DISTRIBUTION ANALYSIS



Appendix D

COMAU iterative classification

AS-IS case	
High quality	Low quality
R1-A; IF1-A R1-A; IF1-B R1-A; IF2-A R1-A; IF2-B R1-A; IF3-A	R1-A; IF3-B R1-A; IF4-A R1-A; IF4-B
R1-B; IF1-A R1-B; IF1-B R1-B; IF2-A R1-B; IF2-B R1-B; IF3-A	R1-B; IF3-B R1-B; IF4-A R1-B; IF4-B
R2-A; IF1-A R2-A; IF1-B R2-A; IF2-A R2-A; IF2-B R2-A; IF3-A	R1-A; IF3-B R1-A; IF4-A R1-A; IF4-B
R2-B; IF2-A R2-B; IF2-B R2-B; IF3-A	R2-B; IF1-A R2-B; IF1-B R2-B; IF3-B R2-B; IF4-A R2-B; IF4-B
R3-A; IF2-A R3-A; IF2-B R3-A; IF3-A	R3-A; IF1-A R3-A; IF1-B R3-A; IF3-B R3-A; IF4-B R3-A; IF4-A

R3-B; IF2-A R3-B; IF2-B R3-B; IF3-A	R3-B; IF1-A R3-B; IF1-B R3-B; IF3-B R3-B; IF4-A R3-B; IF4-B
R4-A; IF3-B R4-A; IF4-B	R4-A; IF1-A R4-A; IF1-B R4-A; IF2-A R4-A; IF2-B R4-A; IF3-A R4-A; IF4-A
	R4-B; IF1-A R4-B; IF1-B R4-B; IF2-A R4-B; IF2-B R4-B; IF3-A R4-B; IF3-B R4-B; IF4-A R4-B; IF4-B

Figure D.1: "As is" case car's components

MODE C(1,2)		C(1,3)	
High quality	Low quality	High quality	Low quality
R1-A; IF1-A R1-A; IF1-B R1-A; IF2-A R1-A; IF2-B R1-A; IF3-A	0	R4-A; IF3-B R4-A; IF4-B	R4-A; IF4-A
R1-B; IF1-A R1-B; IF1-B R1-B; IF2-A R1-B; IF2-B R1-B; IF3-A	0		
R2-A; IF1-A R2-A; IF1-B R2-A; IF2-A R2-A; IF2-B R2-A; IF3-A	0		
R2-B; IF2-A R2-B; IF2-B R2-B; IF3-A	R2-B; IF1-A R2-B; IF1-B		
R3-A; IF2-A R3-A; IF2-B R3-A; IF3-A	R3-A; IF1-A R3-A; IF1-B		
R3-B; IF2-A R3-B; IF2-B R3-B; IF3-A	R3-B; IF1-A R3-B; IF1-B		
	R4-B; IF1-A R4-B; IF1-B R4-B; IF2-A R4-B; IF2-B R4-B; IF3-A		

Figure D.2: Step 1 of the iterative classification

MODE C(1,2)		MODE C(1,2)		C(1,3)	
MODE C(1,3)					
High quality WELDING	Low quality w.	High quality	Low quality w.	High quality	Low quality w.
R2-B; IF2-A		R1-A; IF1-A	R4-B; IF1-A	R4-A; IF3-B	R4-A; IF4-A
R2-B; IF2-B		R1-A; IF1-B	R4-B; IF1-B	R4-A; IF4-B	
R2-B; IF3-A		R1-A; IF2-A	R4-B; IF2-A		
R3-A; IF2-A		R1-A; IF2-B	R4-B; IF2-B		
R3-A; IF2-B		R1-A; IF3-A	R4-B; IF3-A		
R3-A; IF3-A		R1-B; IF1-A			
R3-B; IF2-A		R1-B; IF1-B			
R3-B; IF2-B		R1-B; IF2-A			
R3-B; IF3-A		R1-B; IF2-B			
		R1-B; IF3-A			
		R2-A; IF1-A			
		R2-A; IF1-B			
		R2-A; IF2-A			
		R2-A; IF2-B			
		R2-A; IF3-A			

Figure D.3: Step 2 of the iterative classification

MODE C(1,2)		MODE C(1,2)		MODE C(1,2)		C(1,3)	
MODE C(1,3)		> 70%		MODE C(1,5)			
High quality welding	Low quality	High quality	Low quality	High quality	Low quality	High quality	Low quality
R2-B; IF2-A		R1-A; IF1-A		R4-B ALONE		R4-A; IF3-B	R4-A; IF4-A
R2-B; IF2-B		R1-A; IF1-B				R4-A; IF4-B	
R2-B; IF3-A		R1-A; IF2-A					
R3-A; IF2-A		R1-A; IF2-B					
R3-A; IF2-B		R1-A; IF3-A					
R3-A; IF3-A		R1-B; IF1-A					
R3-B; IF2-A		R1-B; IF1-B					
R3-B; IF2-B		R1-B; IF2-A					
R3-B; IF3-A		R1-B; IF2-B					
		R1-B; IF3-A					
		R2-A; IF1-A					
		R2-A; IF1-B					
		R2-A; IF2-A					
		R2-A; IF2-B					
		R2-A; IF3-A					

Figure D.4: Step 3 of the iterative classification

Appendix E

Results from FEM analysis by CRF

In following figures E.1, E.2, E.3 and E.4 are illustrated good coupling characterized by few tensional release. In particular figure E.1, showing P1 and C1, present a sort of regular tension affecting the channel's welding area, around -0,22 mm respect the nominal. For the Plate the spring-back is around 0,3 mm, completely uniform along the welding area.

In figure E.2 the considered welding area of Plate 4 - Channel 1 presents tension inside tolerances, in fact the "blue areas" characterized by high deviation value from nominal. The two metallic parts are similar in the selected welding area because their deviations are similar in color. The blue areas belong to the other welding area not studied in this thesis work. So it's possible to sustain the idea of close similarity considering the only welding area in analysis.

Figure E.3 Plate 5 and Channel 6 show similarity in the right welding area because of the low tensional state present in that. The maximum value of tensional value is lower than the limit of 0,8. The blue area out of the lower limit is present only on the top of the channel, in a section not used for the welding process.

Lastly figure E.4 presents one of the best coupling of Plate 6, which is weldable only with Channel 1 and 3. For this couple, the tensional global value for the whole parts is very low, so parts are very similar in welding area shape profile.

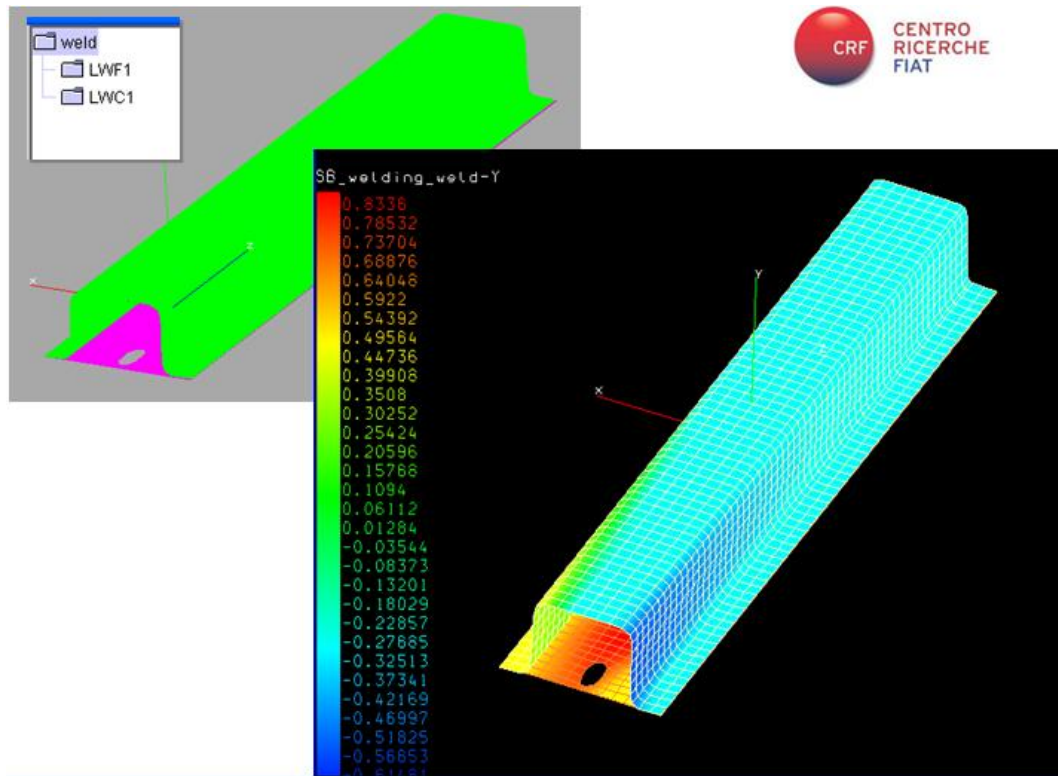


Figure E.1: Plate 1 - Channel 1, spring-back range [0,8336;-0,611]

Worst coupling characterized by evident springback due to different shape profile matched together are mostly characterized by tensional spring-back values higher than $\pm 0,8$ as the following sample couples in image E.5, E.6, ??P3-C2crf and E.8.

In particular the first figure E.5 showing Plate 6 and Channel 6 presents an high tensional residual state value (respect the upper limit) in the welding area. This means that it's likely the two welding areas mated have different shapes profiles, so their reciprocal tension will be greater. All the light blue area characterizing both plate and channel it's around -1,4 tensional value, so the whole parts will be not inside the tensional tolerances.

Clear is the situation displayed in figure E.6, where the yellow welding area section is characterized by quite high tensional value, as the last small blue section otherwise presenting very low value. This not uniformity in tensional distribution along this area could figure out a possible straining of the welding surfaces with two different shapes.

In the same way image E.7 presents higher and lower spring-back values respect limits at the extremities of welding areas, exactly like the situation of the welding between Plate

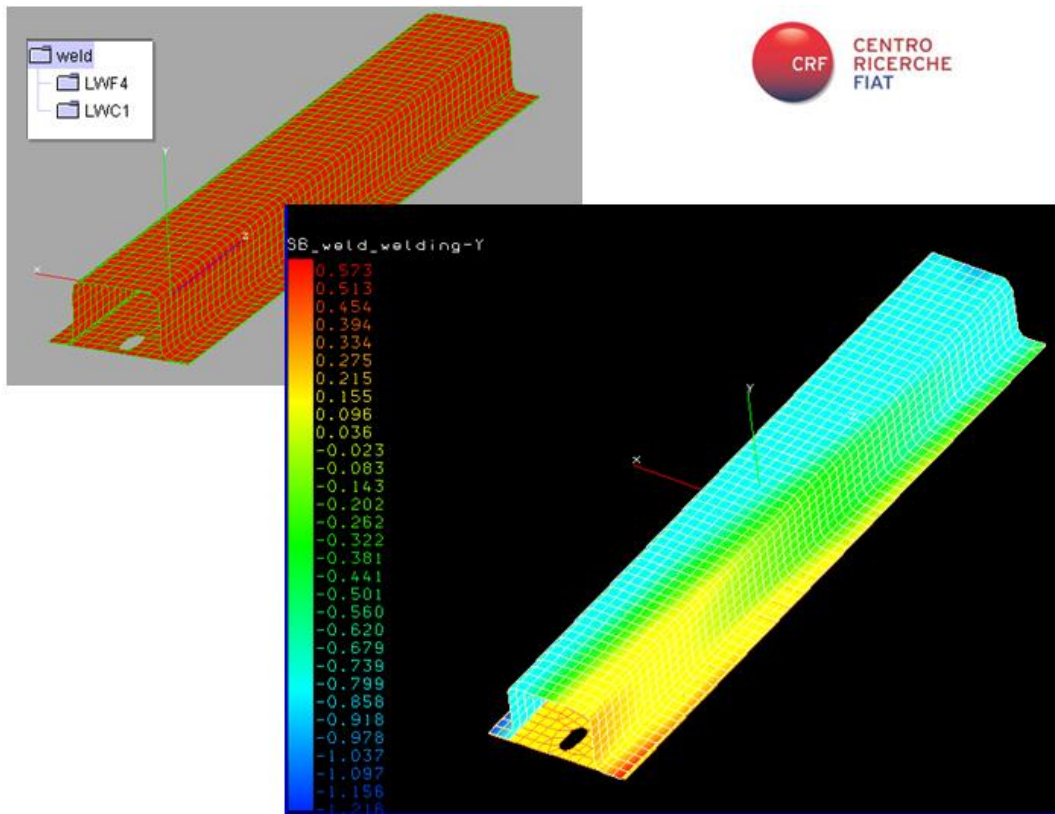


Figure E.2: Plate 4 - Channel 1, spring-back range [0,573;-1,215]

2 and Channel 2 in figureP2-C2crf. This last case shows a huge tensional spring-back mostly on the plate, probably completely deformed in its shape in order to make it follows the channel's profile.

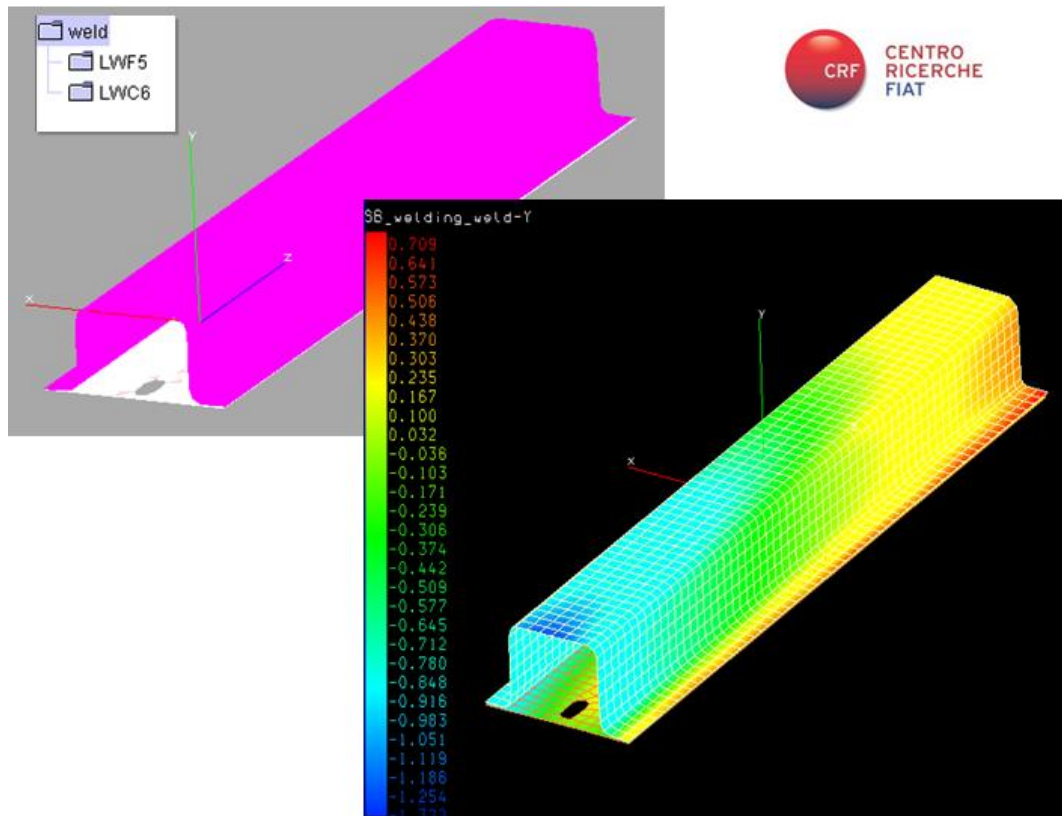


Figure E.3: Plate 5 - Channel 6, spring-back range [0,709;-1,333]

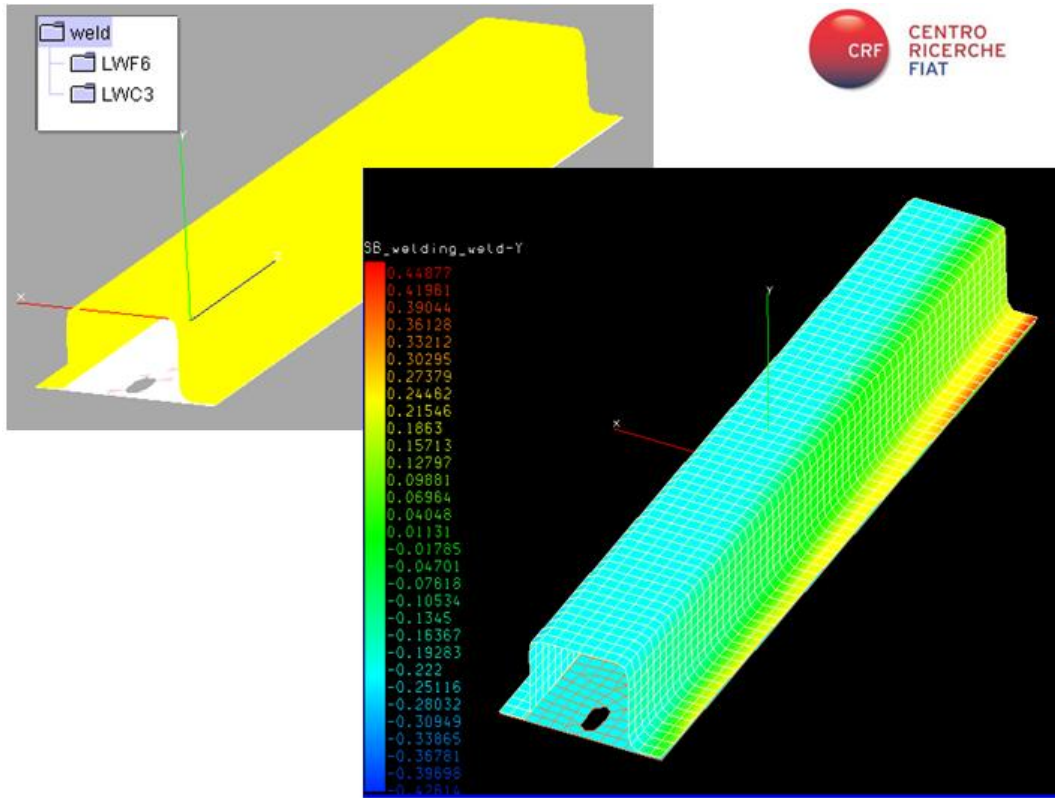


Figure E.4: Plate 6 - Channel 3, spring-back range [0,448;-0,428]

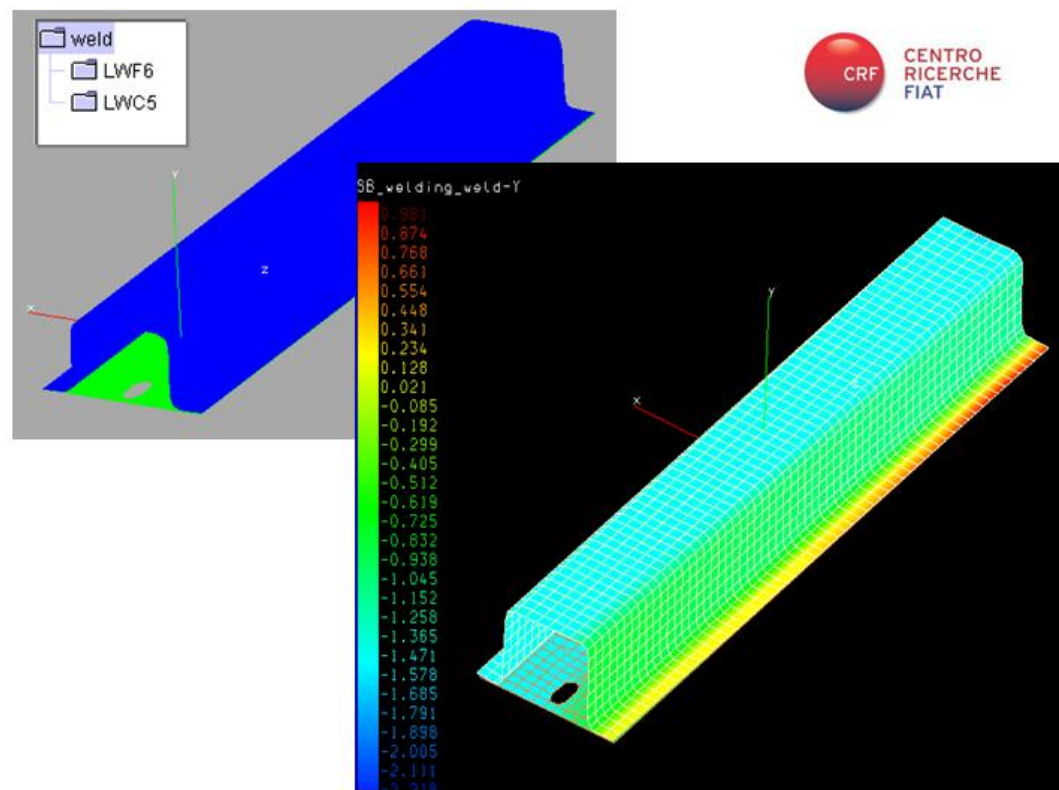


Figure E.5: Plate 6 - Channel 6, spring-back range [0,981;-0,913]

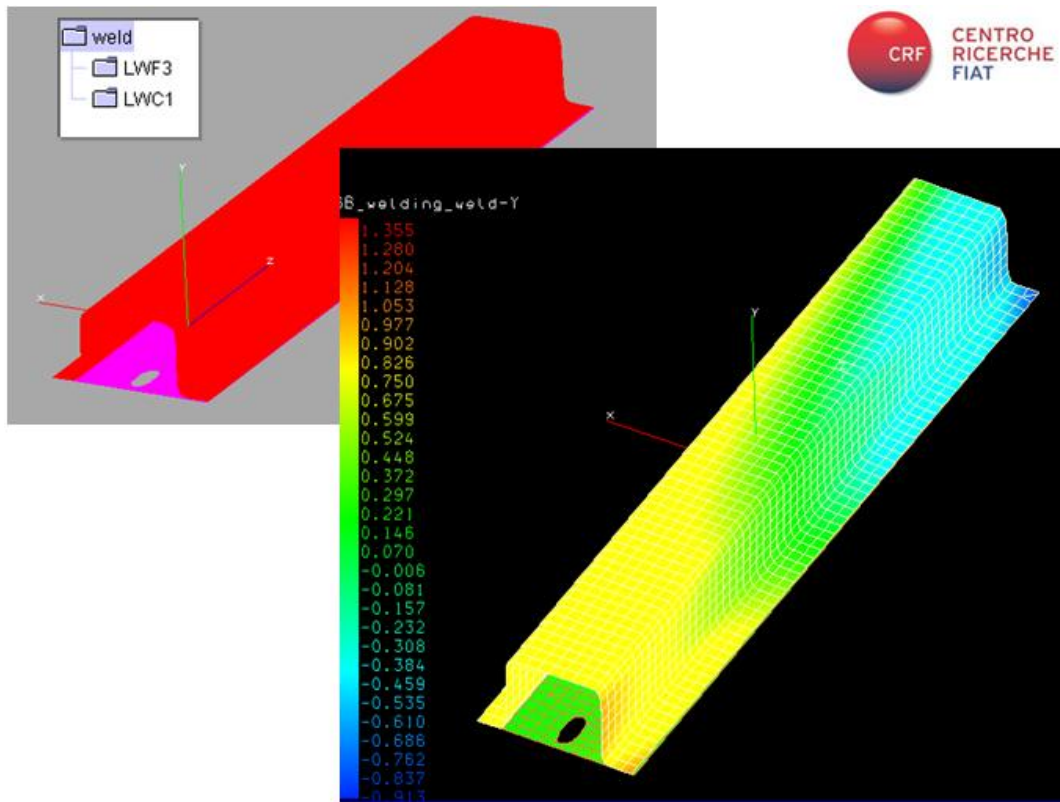


Figure E.6: Plate 3 - Channel 1, spring-back range [1,355;-2,385]

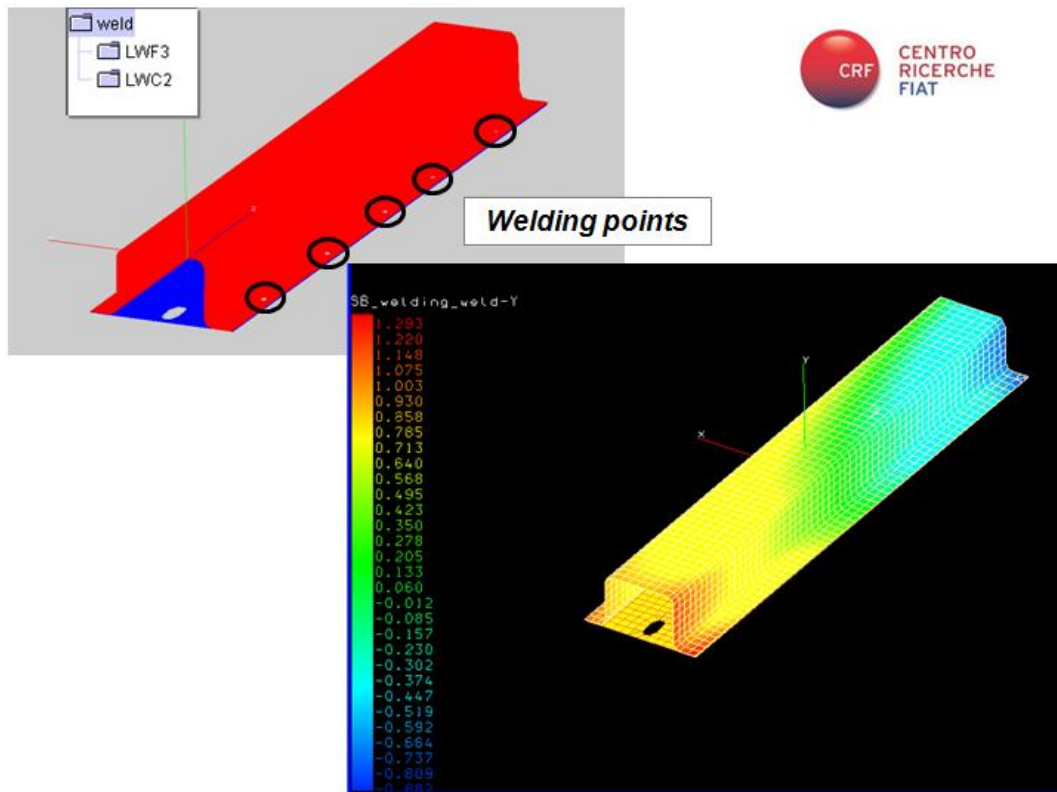


Figure E.7: Plate 3 - Channel 2, spring-back range [1,293;-0,882]

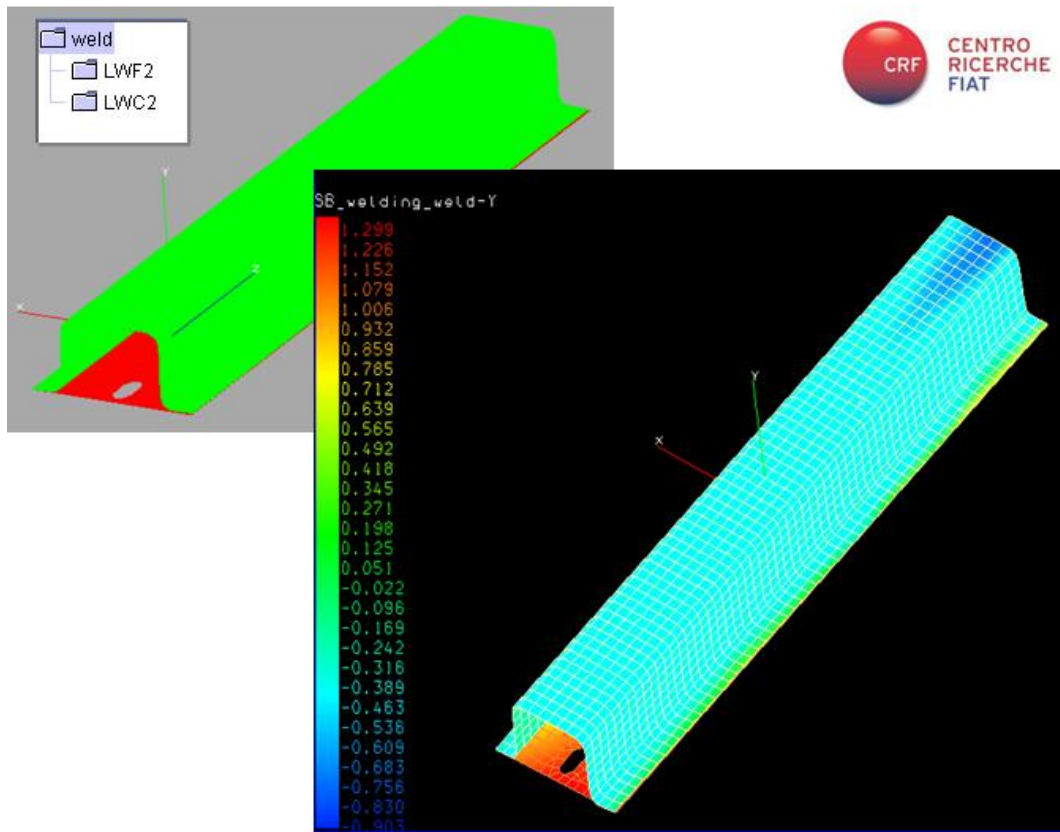


Figure E.8: Plate 2 - Channel 2, spring-back range [1,299;-0,903

Acknowledgements

This research project would not have been possible without support of many people.

First of all, we wish to express our gratitude to supervisor Prof. Tullio Tolio, who was abundantly helpful and offered invaluable assistance, support and guidance.

This thesis would not have gained these results without Eng. Nunzio Magnano, Welding Technologies Manager at COMAU Robotics. He showed his support many times and he was fundamental for the real case of study informations and close examinations. A big thankful to the whole staff of Fiat-COMAU Robotics in Cassino and Torino.

Special thanks also to Marcello Colledani, Barbara Previtali and Giacomo Bianchi, for their advices, for their criticism towards, for drawing us to a deeper analysis of the problem.

We would also like to convey thanks to some CRF members, mainly Antonella Turi, so willing and available to conduce FEM analysis for our work.

It's a pleasure to thank who made this thesis possible, professors Darek Ceglarek and Eduardo Izquierdo, without whose approval the experience at International Digital Laboratory in England would not have been done. A special thank to Prakash, our supporter.

We are heartily thankful to our families, whose encouragement and support let us go on this work, both in England and Italy.

Lastly, we offer our regards and blessing to all of those who, directly or not, supported us in any respect during the thesis work.